

Improvement of Solid Tumor Therapy by Changing the Tumor Pathophysiology

Saske Hoving

The described research in this thesis was performed at the Department of Experimental Surgical Oncology at the Erasmus MC, Rotterdam, the Netherlands

This thesis was financially supported by:
Dutch Cancer Society, Boehringer Ingelheim Pharma GmbH, J.E. Jurriaanse Stichting,
Harlan Nederland and Becton Dickinson

ISBN 9090198229

Improvement of Solid Tumor Therapy by Changing the Tumor Pathophysiology

Verbetering van de Behandeling van Solide Tumoren door het
Veranderen van de Tumor Pathofysiologie

PROEFSCHRIFT

ter verkrijging van de graad van doctor aan de
Erasmus Universiteit Rotterdam
op gezag van de rector magnificus
Prof.dr. S.W.J. Lamberts
en volgens besluit van het College voor Promoties.

De openbare verdediging zal plaatsvinden op
donderdag 15 september 2005 om 13.30 uur

door

Saske Hoving

geboren te Stadskanaal

Promotiecommissie

Promotor: Prof.dr. A.M.M. Eggermont

Overige leden: Prof.dr. J. Verweij
Prof.dr. B.B.R. Kroon
Prof.dr. G. Storm

Copromotor: Dr. T.L.M. ten Hagen

Contents

Part I	General introduction	
	1 General introduction and aim of the thesis	11
Part II	Isolated limb perfusion	
	2 Synergistic antitumor response of IL-2 with melphalan in isolated limb perfusion in soft-tissue sarcoma-bearing rats	25
	3 Synergistic antitumor activity of histamine plus melphalan in isolated limb perfusion: preclinical studies	45
	4 Lack of synergy between histamine and IL-2 in the melphalan-based isolated limb perfusion	63
	5 Early changes in tumor pathophysiology during TNF-based isolated limb perfusion determines response	75
	6 Lack of efficacy of Doxil [®] in TNF- α -based isolated limb perfusion in sarcoma-bearing rats	97
Part III	Liposomal systemic treatment	
	7 Effect of low-dose tumor necrosis factor- α in combination with Stealth [®] liposomal cisplatin (SPI-077) on soft-tissue- and osteosarcoma-bearing rats	105
	8 Addition of low dose tumor necrosis factor- α to systemic treatment with Stealth [®] liposomal doxorubicin (Doxil [®]) improved anti-tumor activity in osteosarcoma-bearing rats	121
	9 <i>In vivo</i> evaluation of drug delivery improvement by tumor vascular manipulation with TNF: an intravital microscopy study	135
	10 Tumor vessel permeability rather than vessel size and density correlates with liposomal uptake and anti-tumor response in B16BL6 melanoma compared to Lewis lung carcinoma	153

Part IV	General discussion and summary	
	11 General discussion: Current status and future perspective of isolated limb perfusion: role for vasoactive drugs	173
	12 General discussion: Bringing liposomal therapy to a new level	185
	13 Summary and conclusions/samenvatting en conclusies	197
	Dankwoord	206
	Curriculum vitae	208
	List of publications	209
	Abbreviations	211

Part I

General introduction

Chapter 1

General introduction and aim of the thesis

In 2000, 69,000 cases of cancer were diagnosed in the Netherlands. Over 85% of human cancers are solid tumors and a common type of solid tumors is melanoma with 2418 new cases in 2000, while sarcomas are relatively rare with an incidence of 448 in soft tissues and 65 in bones and joints. Over 50% of these patients will eventually die of the disease (1). Soft-tissue sarcomas (STS) can occur in any anatomic region of the body because of the ubiquitous nature of connective tissue, but about half of the sarcomas develop in the extremities and the lower limb is approximately two to three times more affected than the upper limb (2,3).

To eradicate tumors with chemotherapy, lethal concentration of anticancer drugs must reach the tumor cells. Inadequate drug delivery would lead to regrowth of tumors and possible development of resistant cells. There are several reasons why treatment of solid tumors with anticancer drugs is not sufficient. The first reason is the metabolism and clearance of drugs in the body, resulting in low drug concentrations at the tumor site. Secondly, heterogeneous tumor perfusion and increased interstitial fluid pressure (IFP) may limit the penetration of drugs into the tumor and impair drug accumulation in tumor cells distant from blood vessels. Last reason is the toxicity of most anticancer drugs for both tumor and normal cells. Hence, the dose of administered drugs is limited by normal tissue tolerance (4-8). Methods for improving drug delivery and penetration in tumor tissues are therefore of great clinical interest.

This thesis describes two strategies for improving solid tumor therapy. The first strategy is based on the addition of vasoactive drugs, like Tumor Necrosis Factor- α (TNF), Interleukin-2 (IL-2) and histamine to melphalan-based isolated limb perfusion (ILP). The second approach is based on vascular targeting with TNF in combination with chemotherapeutic drugs, encapsulated in Stealth[®] liposomes in a systemic treatment setting.

Tumor Necrosis Factor- α

In 1893 Coley observed that patients with concurrent bacterial infections sometimes developed spontaneous regression of tumors (9). In 1944 bacterial lipopolysaccharide (LPS) was demonstrated as the active factor that induced haemorrhagic necrosis of transplantable tumors in mice (10). It was not until 1975 that the serum factor TNF was found to be responsible for the haemorrhagic necrosis (11).

Cytokine TNF is member of the TNF ligand superfamily and its family consists of nearly 20 different homologues including TNF- β , CD27, CD30, CD40, Fas ligand, OX40, RANK and TRAIL (12,13). Monocytes/macrophages are the main producers of TNF, but other cells such as T-lymphocytes, natural killer (NK) cells, smooth muscle cells, endothelial cells and some tumor cells also produce TNF (14,15). The circulation half-life of TNF is 15-30 min (16-18) and clearance predominantly takes place in the kidney, followed by the liver (14). TNF binds as a trimer of 17 kDa subunits to two distinct cell-surface receptors,

TNF-R1 (55 kDa) and TNF-R2 (75 kDa), present in great numbers on most cells. TNF-R1 signals for cell survival and the death domain of the receptor induces cell death. TNF-R2 lacks a death domain and primarily mediates cell survival signals (19-23). The proteolytic cleavage of membrane-bound TNF-receptors results in soluble TNF-receptors. These soluble TNF-receptors compete with membrane receptors for binding of free TNF and may therefore have physiologic importance in the regulation of TNF-activity (24). The primary role of TNF is the regulation of immune cells, but TNF is also known to be involved in disorders such as rheumatoid arthritis, asthma, septic shock, inflammatory bowel disease, haemorrhagic fever and cachexia (13,14,25-27).

TNF showed antitumor activity in some murine and human tumors *in vitro* (28) and induced haemorrhagic necrosis in certain transplanted animal tumors. The majority of the antitumor effects are indirectly mediated through damage of the tumor associated vasculature (11,29-31). Low doses of TNF (0.01-1 ng) induced angiogenesis, whereas high doses (1-5 µg) caused inhibition of angiogenesis and can even induce destruction of newly formed bloodvessels (32). TNF-induced endothelial damage leads to release of von Willebrand factor (VWF) (33), followed by platelet aggregation and erythrostasis, which results in an impaired blood flow. Impaired blood flow leads to edema, vascular congestion, extravasation of erythrocytes, infiltration of polymorphonuclear neutrophils and haemorrhagic necrosis (29,31,34-37).

Impressive antitumor activity observed in animal models raised high expectations for the results of clinical trials. However, systemic TNF therapy proved ineffective with a lack of objective tumor response and severe side effects (hypotension and organ failure). The maximum tolerated dose was 10-50 times lower than the estimated effective dose (38-42).

Interleukin-2

Since its identification by Morgan *et al.* in 1976 (43), T cell growth factor or IL-2 has been studied extensively as a molecule of central importance in the long-term culture of T lymphocytes. IL-2 is a 15 kDa glycoprotein produced by antigen-activated T lymphocytes that plays a varied and critical role in immuno-regulation. It activates other cells in the immune system such as NK cells and B-lymphocytes. IL-2 binds to the IL-2 receptor and this receptor has been demonstrated on all classes of lymphocytes, i.e. T-, B-, and NK- cells and their precursors and on macrophages/monocytes (44). IL-2R is composed of three different receptor subunits; alpha chain (α), common beta chain (β_c) and common gamma chain (γ_c). It is clear that the IL-2R is expressed not only on hematopoietic cells, but also on non-hematopoietic cells. Different reports have indicated the presence of IL-2 receptors on cells in head and neck squamous cell carcinoma (45) and different human melanomas (46). IL-2, as a single agent, has been shown to have antitumor activity in animal models (47,48). Clinical studies have been carried out mainly in patients with renal cell cancer and

melanomas and trials with high-doses of IL-2 have achieved response rates approaching 20% without significant differences according to route, schedule and dosage (49-52).

Due to the rapid clearance of IL-2, high and frequent doses must be administered to achieve significant antitumor activity, leading to serious side effects, including fever, nausea, diarrhea, cardiac toxicity, hypotension, hepatic dysfunction, capillary leakage and in some instances death. Capillary leak syndrome is characterized by retention of extravascular fluid, severe hypotension, and multiple organ system dysfunction (44,49-54).

Many authors have investigated the effects of combined immunotherapy with IL-2 and other cytokines like Interferon (IFN) and TNF, traditional cytotoxic antineoplastic drugs or lymphokine-activated killer cells (LAK cells). Response rates and survival benefits of current treatment options remain disappointing and future studies of newer agents or treatment protocols are needed (44,53,55-59).

Histamine

Histamine, or β -aminoethylimidazole, is one of the most important mediators involved in various physiological and pathological conditions, including neurotransmission, secretion of pituitary hormones, regulation of gastrointestinal functions and inflammatory reactions and histamine has been shown to influence the immune response. Histamine is synthesized by decarboxylation of histidine by L-histidine decarboxylase (HDC). Mast cells and basophils are the major sources of granule-stored histamine. Histamine is released when these cells degranulate in response to various immunologic and non-immunologic stimuli. Several myeloid and lymphoid cell types (dendritic cells and T-cells), which do not store histamine, show high HDC activity and are capable of producing high amounts of histamine. Histamine exerts its effects by activating histamine receptors (HR) of which 4 subtypes (H_1 -R, H_2 -R, H_3 -R and H_4 -R) are found. H_1 -R and H_2 -R are expressed on many cell types, including nerve cells, vascular smooth muscle cells, endothelial cells, neutrophils, monocytes and T- and B- cells. H_3 -R is expressed on histaminergic neurons in the brain and on some peripheral tissues. H_4 -R is found mainly on neutrophils, eosinophils and T-helper cells, but also on mast cells (reviewed in (60-62)).

The interest in histamine as a potential anti-neoplastic agent originated in the late 1970s from mouse studies in which passive induction of local anaphylaxis reduced the size of established, chemically induced fibrosarcomas (63). Most investigators have administered histamine systemically by subcutaneous or intravenous injection and some antitumor effects have been observed in fibrosarcoma (64), Leydig cell sarcoma (65), chemically induced gut tumor (66), colorectal carcinoma (67) and melanoma (68). The mechanisms for the antitumoral effects of histamine are largely unknown, but both H_1 (64) and H_2 (67,68) receptors have been suggested to mediate the protective effects.

Experimental data indicate that histamine in combination with IL-2 act synergistically to activate NK- and T-cells and restore their antineoplastic cytotoxic capabilities (69,70). Clinical studies with IL-2 plus histamine showed favorable clinical results in melanoma patients with liver metastases (71,72).

Isolated limb perfusion

The technique of isolated limb perfusion (ILP) was first described in 1958 by Creech *et al.* (73). Isolation of the blood circuit of a limb is achieved by clamping and cannulation of the artery and vein, connection to an oxygenated extracorporeal circuit, ligating of collateral vessels and application of a tourniquet around the base of the limb to compress the remaining minor vessels. Once isolation is secured, drugs can be added to the perfusion circuit. Temperature of the limb and systemic leakage are monitored throughout the procedure. After 1-1.5 hours of perfusion, the limb is rinsed with an electrolyte solution, cannulas are removed and the vessels are repaired (74-76).

The advantage of ILP is the high dose of cytostatic drug that can be delivered to the tumor-bearing extremity. Cytostatic drug concentrations of 15-20 times higher than with systemic administration can be reached without systemic toxicity (77). With ILP using the standard drug melphalan (L-phenyl-alaninemustard), a mean complete remission rate of about 54% can be obtained in patients with advanced extremity melanoma (reviewed in (78)). Soft tissue sarcomas are large and bulky in contrast to relatively small melanomas and results have been quite poor (79,80).

The successful application of TNF for the treatment of soft tissue sarcomas is seriously hampered by its severe toxicity. Lienard *et al.* were the first who pioneered the use of high-dose TNF in combination with melphalan in the isolated limb perfusion setting and they reported impressive results (81). TNF-based ILP with melphalan has been reported in a European multicenter trial with response rates greater than 80% and limb salvage rates above 70% in advanced soft tissue sarcoma (76,82) and advanced extremity melanoma (81,83,84). These studies led to the approval of TNF by the European Medicine Evaluation Agency (EMA) (85). Currently, TNF-based ILP has become the standard treatment for patients with multiple in transit melanoma metastases or non-resectable extremity sarcomas.

In the clinical setting, the tumor vascular bed appears to be the selective target of TNF. The effects seen after TNF-based ILP are described as early endothelium activation, upregulation of adhesion molecules and invasion of polymorphonuclear cells, leading to coagulative necrosis with haemorrhagic necrosis (86-88). Angiographic studies revealed that 1 or 2 weeks after TNF-based ILP all tumor associated vessels had disappeared, indicating that TNF only targets tumor vasculature and not normal vessels (82,89,90).

Liposomal therapy

Liposomes were discovered in 1965 (91) and ten years later their potential as vehicles for the delivery of cytotoxic drugs to tumors was explored (92-94). Early studies however, demonstrated rapid recognition and removal of liposomes from the circulation by the reticulo-endothelial system (RES). The primary organs associated with the RES are the liver, spleen and lung. A major breakthrough in prolonging circulation time was the coating of liposomes with polyethylene glycol (PEG), a synthetic hydrophilic polymer. The PEG headgroup serves as a barrier preventing interactions with plasma opsonins as a result of the concentration of highly hydrated groups that sterically inhibit hydrophobic and electrostatic interactions of a variety of blood components with the liposome surface. These PEG-coated liposomes are referred to as sterically stabilized or Stealth[®] liposomes (95-97). The use of Stealth[®] liposomes as drug carriers for chemotherapeutic agents offers a potential means of manipulating drug distribution to improve antitumor efficacy and reduce toxicity (96,98-100). Because of their small size, long circulation time, and reduced interaction with formed elements of the blood, these liposomes tend to accumulate in tumors, presumably due to leakage through the often-compromised tumor vasculature. Furthermore, they can target the tumor with high selectivity by taking advantage of the enhanced permeability and retention effect (EPR) (5,96-99,101-105).

A well known liposomal formulation is Doxil[®] (Stealth[®] liposomal doxorubicin). Doxil[®] is effective in the treatment of several tumor types, including advanced or metastatic soft tissue sarcoma (106), AIDS-related Kaposi's sarcoma (107), metastatic breast cancer (108) and epithelial ovarian cancer (109).

We showed in previous studies that co-administration of Doxil[®] and low-dose TNF resulted in a pronounced tumor response in both rat and murine tumor models. The augmented accumulation of the chemotherapeutic drug found in tumor tissue presumably explains the enhanced tumor regression (110,111). A possible explanation for the augmented accumulation is that TNF likely increases the leakiness of the vasculature by increasing the gaps between the endothelial lining in the tumor (34,112).

Stealth[®] liposomes offer an attractive tool for delivery of anticancer drugs to tumors. Combining the tumor localizing properties with appropriate vascular targeting may enable a further step of improvement.

Aim of the thesis

The aim of this thesis is to improve local and systemic chemotherapy by changing the pathophysiology of solid tumors. Several studies were performed to identify ways to further improve efficacy of existing local and systemic therapies, to elucidate mechanisms of TNF and test new therapies.

ILP with TNF and melphalan is associated with synergistic antitumor effects against melanoma, large soft tissue sarcoma and various other tumors in the clinical setting. We showed that the basis for the synergy is the enhancement of tumor-selective melphalan uptake and the complete destruction of the tumor vasculature. The enhanced tumor uptake of different cytotoxic agents prompted us to investigate a number of vasoactive drugs for similar effects. In **chapter 2** the effects of IL-2 in a melphalan-based ILP in soft-tissue sarcoma bearing rats were investigated and in **chapter 3** the combination therapy of histamine and melphalan is described. Based on the potential synergistic effects of IL-2 and histamine in the systemic setting we evaluated whether this combination could improve response rates in melphalan-based ILP (**chapter 4**).

In **chapter 5** we focused on early effects inflicted by TNF during and shortly after ILP, which could explain the improved tumor response when used in a melphalan-based ILP.

The advantage of Doxil[®] liposomes over free doxorubicin is the prolonged circulation time, decreased toxicity and augmented tumor localization. In **chapter 6** we examined the efficacy of Doxil[®] in a TNF-based ILP in sarcoma-bearing rats.

In previous studies we showed that the addition of low-dose TNF to Doxil[®] treatment resulted in a pronounced tumor response in soft tissue sarcoma-bearing rats with most of the rats showing tumor regression and comparable results were seen in B16BL6 melanoma-bearing mice. In **chapter 7** we evaluated the antitumor activity and side effects of low dose TNF and liposomal cisplatin (SPI-077) in soft tissue- and osteosarcoma-bearing rats.

In **chapter 8** experiments are described whether the use of low-dose TNF in combination with Doxil[®] not only results in synergistic antitumor response in the highly vascularized soft-tissue sarcoma but also in the less vascularized osteosarcoma.

In **chapter 9** the B16BL6 mouse tumor model was used to investigate the biodistribution of Stealth[®] liposomes of different sizes in combination with low-dose TNF. Intravital observations are performed to evaluate tumor distribution of free and liposomal drugs in B16BL6 melanoma implanted in the mouse dorsal skin-fold chamber. In **chapter 10** is investigated whether or not addition of low-dose TNF to Doxil[®] treatment would have a similar effect in two very different tumor systems in terms of tumor vasculature: the Lewis Lung Carcinoma and the B16BL6 melanoma model.

References

1. Visser O, Siesling S, Dijk JAAM. Incidence of cancer in the Netherlands 1999/2000. Utrecht: Vereniging van Integrale Kankercentra. 2003.
2. Moley JF, Eberlein TJ. Soft-tissue sarcomas. *Surg Clin North Am.* 2000;80(2):687-708.
3. Brennan M, Alektiar K, and Maki R Soft tissue sarcoma. *In* DeVita VT, Hellman SA, and Rosenberg SA (eds.), *Cancer: Principles and Practice of Oncology*, edn 6, pp. 1841-1883. Philadelphia, PA: Lippincott Williams and Wilkins, 2001.
4. Yuan F. Transvascular drug delivery in solid tumors. *Semin Radiat Oncol.* 1998;8(3):164-175.
5. Jang SH, Wientjes MG, Lu D, Au JL. Drug delivery and transport to solid tumors. *Pharm Res.* 2003;20(9):1337-1350.
6. Jain RK. Barriers to drug delivery in solid tumors. *Sci Am.* 1994;271(1):58-65.

7. Jain RK. Delivery of molecular and cellular medicine to solid tumors. *Adv Drug Deliv Rev.* 2001;46(1-3):149-168.
8. Dvorak HF, Nagy JA, Dvorak JT, Dvorak AM. Identification and characterization of the blood vessels of solid tumors that are leaky to circulating macromolecules. *Am J Pathol.* 1988;133(1):95-109.
9. Coley WB. The treatment of malignant tumors by repeated inoculations of erysipelas; with a report of ten original cases. *Am J Med Sci.* 1893;105:487-490.
10. Shear MJ. Chemical treatment of tumors. IX. Reactions of mice with primary subcutaneous tumors to injection of a hemorrhage-producing bacterial polysaccharide. *J Natl Cancer Inst.* 1944;4:461-467.
11. Carswell EA, Old LJ, Kassel RL, Green S, Fiore N, Williamson B. An endotoxin-induced serum factor that causes necrosis of tumors. *Proc Natl Acad Sci U S A.* 1975;72(9):3666-3670.
12. Bodmer JL, Schneider P, Tschopp J. The molecular architecture of the TNF superfamily. *Trends Biochem Sci.* 2002;27(1):19-26.
13. Locksley RM, Killeen N, Lenardo MJ. The TNF and TNF receptor superfamilies: integrating mammalian biology. *Cell.* 2001;104(4):487-501.
14. Bemelmans MH, van Tits LJ, Buurman WA. Tumor necrosis factor: function, release and clearance. *Crit Rev Immunol.* 1996;16(1):1-11.
15. Fiers W. Tumor necrosis factor. Characterization at the molecular, cellular and in vivo level. *FEBS Lett.* 1991;285(2):199-212.
16. Gamm H, Lindemann A, Mertelsmann R, Herrmann F. Phase I trial of recombinant human tumour necrosis factor alpha in patients with advanced malignancy. *Eur J Cancer.* 1991;27(7):856-863.
17. Saks S, Rosenblum M. Recombinant human TNF-alpha: preclinical studies and results from early clinical trials. *Immunol Ser.* 1992;56:567-87.:567-587.
18. Selby P, Hobbs S, Viner C, et al. Tumour necrosis factor in man: clinical and biological observations. *Br J Cancer.* 1987;56(6):803-808.
19. Gupta S. A decision between life and death during TNF-alpha-induced signaling. *J Clin Immunol.* 2002;22(4):185-194.
20. MacEwan DJ. TNF ligands and receptors--a matter of life and death. *Br J Pharmacol.* 2002;135(4):855-875.
21. Idriss HT, Naismith JH. TNF alpha and the TNF receptor superfamily: structure-function relationship(s). *Microsc Res Tech.* 2000;50(3):184-195.
22. Tartaglia LA, Weber RF, Figari IS, Reynolds C, Palladino MA, Jr., Goeddel DV. The two different receptors for tumor necrosis factor mediate distinct cellular responses. *Proc Natl Acad Sci U S A.* 1991;88(20):9292-9296.
23. Tartaglia LA, Goeddel DV. Two TNF receptors. *Immunol Today.* 1992;13(5):151-153.
24. Aderka D. The potential biological and clinical significance of the soluble tumor necrosis factor receptors. *Cytokine Growth Factor Rev.* 1996;7(3):231-240.
25. Kips JC, Tavernier JH, Joos GF, Peleman RA, Pauwels RA. The potential role of tumour necrosis factor alpha in asthma. *Clin Exp Allergy.* 1993;23(4):247-250.
26. Maini RN, Taylor PC. Anti-cytokine therapy for rheumatoid arthritis. *Annu Rev Med.* 2000;51:207-29.:207-229.
27. Maeda M, Watanabe N, Neda H, et al. Serum tumor necrosis factor activity in inflammatory bowel disease. *Immunopharmacol Immunotoxicol.* 1992;14(3):451-461.
28. Nakano K, Abe S, Sohmura Y. Recombinant human tumor necrosis factor--I. Cytotoxic activity in vitro. *Int J Immunopharmacol.* 1986;8(3):347-355.
29. Palladino MA, Jr., Shalaby MR, Kramer SM, et al. Characterization of the antitumor activities of human tumor necrosis factor-alpha and the comparison with other cytokines: induction of tumor-specific immunity. *J Immunol.* 1987;138(11):4023-4032.
30. Sohmura Y, Nakata K, Yoshida H, Kashimoto S, Matsui Y, Furuichi H. Recombinant human tumor necrosis factor--II. Antitumor effect on murine and human tumors transplanted in mice. *Int J Immunopharmacol.* 1986;8(3):357-368.
31. Watanabe N, Niitsu Y, Umeno H, et al. Toxic effect of tumor necrosis factor on tumor vasculature in mice. *Cancer Res.* 1988;48(8):2179-2183.
32. Fajardo LF, Kwan HH, Kowalski J, Prionas SD, Allison AC. Dual role of tumor necrosis factor-alpha in angiogenesis. *Am J Pathol.* 1992;140(3):539-544.
33. Renard N, Nooijen PT, Schalkwijk L, et al. VWF release and platelet aggregation in human melanoma after perfusion with TNF alpha. *J Pathol.* 1995;176(3):279-287.
34. Brett J, Gerlach H, Nawroth P, Steinberg S, Godman G, Stern D. Tumor necrosis factor/cachectin increases permeability of endothelial cell monolayers by a mechanism involving regulatory G proteins. *J Exp Med.* 1989;169(6):1977-1991.
35. Manusama ER, Nooijen PT, Stavast J, de Wilt JH, Marquet RL, Eggermont AM. Assessment of the role of neutrophils on the antitumor effect of TNFalpha in an in vivo isolated limb perfusion model in sarcoma-bearing brown Norway rats. *J Surg Res.* 1998;78(2):169-175.

36. Nooijen PT, Manusama ER, Eggermont AM, et al. Synergistic effects of TNF-alpha and melphalan in an isolated limb perfusion model of rat sarcoma: a histopathological, immunohistochemical and electron microscopical study. *Br J Cancer*. 1996;74(12):1908-1915.
37. Shimomura K, Manda T, Mukumoto S, Kobayashi K, Nakano K, Mori J. Recombinant human tumor necrosis factor-alpha: thrombus formation is a cause of anti-tumor activity. *Int J Cancer*. 1988;41(2):243-247.
38. Spriggs DR, Sherman ML, Michie H, et al. Recombinant human tumor necrosis factor administered as a 24-hour intravenous infusion. A phase I and pharmacologic study. *J Natl Cancer Inst*. 1988;80(13):1039-1044.
39. Blick M, Sherwin SA, Rosenblum M, Gutterman J. Phase I study of recombinant tumor necrosis factor in cancer patients. *Cancer Res*. 1987;47(11):2986-2989.
40. Feinberg B, Kurzrock R, Talpaz M, Blick M, Saks S, Gutterman JU. A phase I trial of intravenously-administered recombinant tumor necrosis factor-alpha in cancer patients. *J Clin Oncol*. 1988;6(8):1328-1334.
41. Chapman PB, Lester TJ, Casper ES, et al. Clinical pharmacology of recombinant human tumor necrosis factor in patients with advanced cancer. *J Clin Oncol*. 1987;5(12):1942-1951.
42. Sherman ML, Spriggs DR, Arthur KA, Imamura K, Frei E, III, Kufe DW. Recombinant human tumor necrosis factor administered as a five-day continuous infusion in cancer patients: phase I toxicity and effects on lipid metabolism. *J Clin Oncol*. 1988;6(2):344-350.
43. Morgan DA, Ruscetti FW, Gallo R. Selective in vitro growth of T lymphocytes from normal human bone marrows. *Science*. 1976;193(4257):1007-1008.
44. Winkelhake JL, Gauny SS. Human recombinant interleukin-2 as an experimental therapeutic. *Pharmacol Rev*. 1990;42(1):1-28.
45. Weidmann E, Sacchi M, Plaisance S, et al. Receptors for interleukin 2 on human squamous cell carcinoma cell lines and tumor in situ. *Cancer Res*. 1992;52(21):5963-5970.
46. Rimoldi D, Salvi S, Hartmann F, et al. Expression of IL-2 receptors in human melanoma cells. *Anticancer Res*. 1993;13(3):555-564.
47. Baselmans AH, Koten JW, Battermann JJ, Van Dijk JE, Den Otter W. The mechanism of regression of solid SL2 lymphosarcoma after local IL-2 therapy. *Cancer Immunol Immunother*. 2002;51(9):492-498.
48. Den Otter W, De Groot JW, Bernsen MR, et al. Optimal regimes for local IL-2 tumour therapy. *Int J Cancer*. 1996;66(3):400-403.
49. Eton O, Rosenblum MG, Legha SS, et al. Phase I trial of subcutaneous recombinant human interleukin-2 in patients with metastatic melanoma. *Cancer*. 2002;95(1):127-134.
50. Negrier S, Escudier B, Lasset C, et al. Recombinant human interleukin-2, recombinant human interferon alfa-2a, or both in metastatic renal-cell carcinoma. *Groupe Francais d'Immunotherapie*. *N Engl J Med*. 1998;338(18):1272-1278.
51. Yang JC, Sherry RM, Steinberg SM, et al. Randomized study of high-dose and low-dose interleukin-2 in patients with metastatic renal cancer. *J Clin Oncol*. 2003;21(16):3127-3132.
52. Atkins MB, Lotze MT, Dutcher JP, et al. High-dose recombinant interleukin 2 therapy for patients with metastatic melanoma: analysis of 270 patients treated between 1985 and 1993. *J Clin Oncol*. 1999;17(7):2105-2116.
53. Atkins MB. Interleukin-2: clinical applications. *Semin Oncol*. 2002;29(3 Suppl 7):12-17.
54. Kruit WH, Stoter G. The role of adoptive immunotherapy in solid cancers. *Neth J Med*. 1997;50(2):47-68.
55. Atkins MB, Regan M, McDermott D. Update on the role of interleukin 2 and other cytokines in the treatment of patients with stage IV renal carcinoma. *Clin Cancer Res*. 2004;10(18 Pt 2):6342S-6346S.
56. Le Cesne A, Vassal G, Farace F, et al. Combination interleukin-2 and doxorubicin in advanced adult solid tumors: circumvention of doxorubicin resistance in soft-tissue sarcoma? *J Immunother*. 1999;22(3):268-277.
57. Legha SS, Ring S, Eton O, et al. Development of a biochemotherapy regimen with concurrent administration of cisplatin, vinblastine, dacarbazine, interferon alfa, and interleukin-2 for patients with metastatic melanoma. *J Clin Oncol*. 1998;16(5):1752-1759.
58. Naglieri E, Gebbia V, Durini E, et al. Standard interleukin-2 (IL-2) and interferon-alpha immunotherapy versus an IL-2 and 4-epirubicin immuno-chemotherapeutic association in metastatic renal cell carcinoma. *Anticancer Res*. 1998;18(3B):2021-2026.
59. Oppenheim MH, Lotze MT. Interleukin-2: solid-tumor therapy. *Oncology*. 1994;51(2):154-169.
60. Akdis CA, Blaser K. Histamine in the immune regulation of allergic inflammation. *J Allergy Clin Immunol*. 2003;112(1):15-22.
61. Jutel M, Watanabe T, Akdis M, Blaser K, Akdis CA. Immune regulation by histamine. *Curr Opin Immunol*. 2002;14(6):735-740.
62. Leurs R, Smit MJ, Timmerman H. Molecular pharmacological aspects of histamine receptors. *Pharmacol Ther*. 1995;66(3):413-463.

63. Lynch NR, Salomon JC. Passive local anaphylaxis: demonstration of antitumor activity and complementation of intratumor BCG. *J Natl Cancer Inst.* 1977;58(4):1093-1098.
64. Burtin C, Scheinmann P, Salomon JC, Lespinats G, Canu P. Decrease in tumour growth by injections of histamine or serotonin in fibrosarcoma-bearing mice: influence of H1 and H2 histamine receptors. *Br J Cancer.* 1982;45(1):54-60.
65. Rizell M, Hellstrand K, Lindner P, Naredi P. Monotherapy with histamine dihydrochloride suppresses *in vivo* growth of a rat sarcoma in liver and subcutis. *Anticancer Res.* 2002;22(4):1943-1948.
66. Tatsuta M, Iishi H, Ichii M, Noguchi S, Yamamura H, Taniguchi H. Inhibitory effects of tetragastrin and histamine on carcinogenesis in the small intestines of W rats by N-methyl-N'-nitro-N-nitrosoguanidine. *J Natl Cancer Inst.* 1986;76(2):277-281.
67. Suonio E, Tuomisto L, Alhava E. Effects of histamine, H1, H2 and Hic receptor antagonists and alpha-fluoromethylhistidine on the growth of human colorectal cancer in the subrenal capsule assay. *Agents Actions.* 1994;41 Spec No:C118-20.:C118-C120.
68. Hellstrand K, Asea A, Hermodsson S. Role of histamine in natural killer cell-mediated resistance against tumor cells. *J Immunol.* 1990;145(12):4365-4370.
69. Hellstrand K, Hermodsson S. Synergistic activation of human natural killer cell cytotoxicity by histamine and interleukin-2. *Int Arch Allergy Appl Immunol.* 1990;92(4):379-389.
70. Agarwala SS, Sabbagh MH. Histamine dihydrochloride: inhibiting oxidants and synergising IL-2-mediated immune activation in the tumour microenvironment. *Expert Opin Biol Ther.* 2001;1(5):869-879.
71. Asemissen AM, Scheibenbogen C, Letsch A, et al. Addition of histamine to interleukin 2 treatment augments type 1 T-cell responses in patients with melanoma *in vivo*: immunologic results from a randomized clinical trial of interleukin 2 with or without histamine (MP 104). *Clin Cancer Res.* 2005;11(1):290-297.
72. Agarwala SS, Glaspy J, O'Day SJ, et al. Results from a randomized phase III study comparing combined treatment with histamine dihydrochloride plus interleukin-2 versus interleukin-2 alone in patients with metastatic melanoma. *J Clin Oncol.* 2002;20(1):125-133.
73. Creech O, Kremenz ET, Ryan RF, Winblad JN. Chemotherapy of cancer: regional perfusion utilizing an extracorporeal circuit. *Ann Surg.* 1958;148(4):616-632.
74. Noorda EM, Vrouenraets BC, Nieweg OE, van Coevorden F, van Slooten GW, Kroon BB. Isolated limb perfusion with tumor necrosis factor-alpha and melphalan for patients with unresectable soft tissue sarcoma of the extremities. *Cancer.* 2003;98(7):1483-1490.
75. Bickels J, Manusama ER, Gutman M, et al. Isolated limb perfusion with tumour necrosis factor-alpha and melphalan for unresectable bone sarcomas of the lower extremity. *Eur J Surg Oncol.* 1999;25(5):509-514.
76. Eggermont AM, Schraffordt KH, Klausner JM, et al. Isolated limb perfusion with tumor necrosis factor and melphalan for limb salvage in 186 patients with locally advanced soft tissue extremity sarcomas. The cumulative multicenter European experience. *Ann Surg.* 1996;224(6):756-764.
77. Benckhuijsen C, Kroon BB, van Geel AN, Wieberdink J. Regional perfusion treatment with melphalan for melanoma in a limb: an evaluation of drug kinetics. *Eur J Surg Oncol.* 1988;14(2):157-163.
78. Vrouenraets BC, Nieweg OE, Kroon BB. Thirty-five years of isolated limb perfusion for melanoma: indications and results. *Br J Surg.* 1996;83(10):1319-1328.
79. Hoekstra HJ, van Ginkel RJ. Hyperthermic isolated limb perfusion in the management of extremity sarcoma. *Curr Opin Oncol.* 2003;15(4):300-303.
80. Schraffordt KH, Eggermont AM, Lienard D, et al. Hyperthermic isolated limb perfusion for the treatment of soft tissue sarcomas. *Semin Surg Oncol.* 1998;14(3):210-214.
81. Lienard D, Ewalenko P, Delmotte JJ, Renard N, Lejeune FJ. High-dose recombinant tumor necrosis factor alpha in combination with interferon gamma and melphalan in isolation perfusion of the limbs for melanoma and sarcoma. *J Clin Oncol.* 1992;10(1):52-60.
82. Eggermont AM, Schraffordt KH, Lienard D, et al. Isolated limb perfusion with high-dose tumor necrosis factor-alpha in combination with interferon-gamma and melphalan for nonresectable extremity soft tissue sarcomas: a multicenter trial. *J Clin Oncol.* 1996;14(10):2653-2665.
83. Olieman AF, Lienard D, Eggermont AM, et al. Hyperthermic isolated limb perfusion with tumor necrosis factor alpha, interferon gamma, and melphalan for locally advanced nonmelanoma skin tumors of the extremities: a multicenter study. *Arch Surg.* 1999;134(3):303-307.
84. Vrouenraets BC, Eggermont AM, Hart AA, et al. Regional toxicity after isolated limb perfusion with melphalan and tumour necrosis factor- alpha versus toxicity after melphalan alone. *Eur J Surg Oncol.* 2001;27(4):390-395.
85. Eggermont AM, Koops HS, Klausner JM, et al. Limb salvage by isolation limb perfusion with tumor necrosis factor alpha and melphalan for locally advanced extremity soft tissue sarcomas: results of 279 perfusions in 246 patients. *Proc Am Soc Clin Oncol.* 1999;11:497.

86. Renard N, Lienard D, Lespagnard L, Eggermont A, Heimann R, Lejeune F. Early endothelium activation and polymorphonuclear cell invasion precede specific necrosis of human melanoma and sarcoma treated by intravascular high-dose tumour necrosis factor alpha (rTNF alpha). *Int J Cancer*. 1994;57(5):656-663.
87. Renard N, Nooijen PT, Schalkwijk L, et al. VWF release and platelet aggregation in human melanoma after perfusion with TNF alpha. *J Pathol*. 1995;176(3):279-287.
88. Nooijen PT, Eggermont AM, Schalkwijk L, Henzen-Logmans S, De Waal RM, Ruiter DJ. Complete response of melanoma-in-transit metastasis after isolated limb perfusion with tumor necrosis factor alpha and melphalan without massive tumor necrosis: a clinical and histopathological study of the delayed-type reaction pattern. *Cancer Res*. 1998;58(21):4880-4887.
89. Eggermont AM, Schraffordt KH, Klausner JM, et al. Isolation limb perfusion with tumor necrosis factor alpha and chemotherapy for advanced extremity soft tissue sarcomas. *Semin Oncol*. 1997;24(5):547-555.
90. Eggermont AM, de Wilt JH, ten Hagen TL. Current uses of isolated limb perfusion in the clinic and a model system for new strategies. *Lancet Oncol*. 2003;4(7):429-437.
91. Bangham AD, Standish MM, Watkins JC. Diffusion of univalent ions across the lamellae of swollen phospholipids. *J Mol Biol*. 1965;13(1):238-252.
92. Gregoriadis G. The carrier potential of liposomes in biology and medicine (second of two parts). *N Engl J Med*. 1976;295(14):765-770.
93. Gregoriadis G. The carrier potential of liposomes in biology and medicine (first of two parts). *N Engl J Med*. 1976;295(13):704-710.
94. Gregoriadis G, Wills EJ, Swain CP, Tavill AS. Drug-carrier potential of liposomes in cancer chemotherapy. *Lancet*. 1974;1(7870):1313-1316.
95. Lasic DD, Martin FJ, Gabizon A, Huang SK, Papahadjopoulos D. Sterically stabilized liposomes: a hypothesis on the molecular origin of the extended circulation times. *Biochim Biophys Acta*. 1991;1070(1):187-192.
96. Papahadjopoulos D, Allen TM, Gabizon A, et al. Sterically stabilized liposomes: improvements in pharmacokinetics and antitumor therapeutic efficacy. *Proc Natl Acad Sci U S A*. 1991;88(24):11460-11464.
97. Mayer LD, Cullis PR, and Bally MB Designing therapeutically optimized liposomal anticancer delivery systems: lessons from conventional liposomes. *In* Lasic DD and Papahadjopoulos D (eds.), *Medical Applications of Liposomes*, pp. 231-257. 2002.
98. Allen TM, Newman MS, Woodle MC, Mayhew E, Uster PS. Pharmacokinetics and anti-tumor activity of vincristine encapsulated in sterically stabilized liposomes. *Int J Cancer*. 1995;62(2):199-204.
99. Lasic DD. Doxorubicin in sterically stabilized liposomes. *Nature*. 1996;380(6574):561-562.
100. Sparano JA, Winer EP. Liposomal anthracyclines for breast cancer. *Semin Oncol*. 2001;28(4 Suppl 12):32-40.
101. Gabizon A, Papahadjopoulos D. Liposome formulations with prolonged circulation time in blood and enhanced uptake by tumors. *Proc Natl Acad Sci U S A*. 1988;85(18):6949-6953.
102. Gabizon A, Martin F. Polyethylene glycol-coated (pegylated) liposomal doxorubicin. Rationale for use in solid tumours. *Drugs*. 1997;54 Suppl 4:15-21.
103. Maeda H, Fang J, Inutsuka T, Kitamoto Y. Vascular permeability enhancement in solid tumor: various factors, mechanisms involved and its implications. *Int Immunopharmacol*. 2003;3(3):319-328.
104. Wu NZ, Da D, Rudoll TL, Needham D, Whorton AR, Dewhirst MW. Increased microvascular permeability contributes to preferential accumulation of Stealth liposomes in tumor tissue. *Cancer Res*. 1993;53(16):3765-70.
105. Gabizon AA. Liposomal drug carrier systems in cancer chemotherapy: current status and future prospects. *J Drug Target*. 2002;10(7):535-538.
106. Judson I, Radford JA, Harris M, et al. Randomised phase II trial of pegylated liposomal doxorubicin (DOXIL/CAELYX) versus doxorubicin in the treatment of advanced or metastatic soft tissue sarcoma: a study by the EORTC Soft Tissue and Bone Sarcoma Group. *Eur J Cancer*. 2001;37(7):870-877.
107. Northfelt DW, Dezube BJ, Thommes JA, et al. Pegylated-liposomal doxorubicin versus doxorubicin, bleomycin, and vincristine in the treatment of AIDS-related Kaposi's sarcoma: results of a randomized phase III clinical trial. *J Clin Oncol*. 1998;16(7):2445-2451.
108. O'Brien ME, Wigler N, Inbar M, et al. Reduced cardiotoxicity and comparable efficacy in a phase III trial of pegylated liposomal doxorubicin HCl (CAELYX/Doxil) versus conventional doxorubicin for first-line treatment of metastatic breast cancer. *Ann Oncol*. 2004;15(3):440-449.
109. Stebbing J, Gaya A. Pegylated liposomal doxorubicin (Caelyx) in recurrent ovarian cancer. *Cancer Treat Rev*. 2002;28(2):121-125.
110. Brouckaert P, Takahashi N, van Tiel ST, et al. Tumor necrosis factor-alpha augmented tumor response in B16BL6 melanoma-bearing mice treated with stealth liposomal doxorubicin (Doxil) correlates with altered Doxil pharmacokinetics. *Int J Cancer*. 2004;109(3):442-448.

111. ten Hagen TL, van Der Veen AH, Nooijen PT, van Tiel ST, Seynhaeve AL, Eggermont AM. Low-dose tumor necrosis factor-alpha augments antitumor activity of stealth liposomal doxorubicin (DOXIL) in soft tissue sarcoma-bearing rats. *Int J Cancer*. 2000;87(6):829-37.
112. Partridge CA, Horvath CJ, Del Vecchio PJ, Phillips PG, Malik AB. Influence of extracellular matrix in tumor necrosis factor-induced increase in endothelial permeability. *Am J Physiol*. 1992;263(6 Pt 1):L627-L633.

Part II

Isolated limb perfusion

Chapter 2

Synergistic antitumor response of IL-2 with melphalan in isolated limb perfusion in soft-tissue sarcoma bearing rats

Saske Hoving¹, Flavia Brunstein¹, Gisela aan de Wiel-Ambagtsheer¹, Sandra T van Tiel¹, Gert de Boeck², Ernst A de Bruijn², Alexander MM Eggermont¹, Timo LM ten Hagen¹

¹Department of Surgical Oncology, Erasmus MC-Daniel den Hoed Cancer Center, Rotterdam, the Netherlands

²Department of Experimental Oncology, University of Leuven, Leuven, Belgium

Abstract

The cytokine interleukin-2 (IL-2) is a mediator of immune cell activation with some antitumor activity, mainly in renal cell cancer and melanoma. We have previously demonstrated that Tumor Necrosis Factor-alpha (TNF) has strong synergistic antitumor activity in combination with chemotherapeutics in the isolated limb perfusion (ILP) setting based on a TNF-mediated enhanced tumor-selective uptake of the chemotherapeutic drug followed by a selective destruction of the tumor vasculature. IL-2 can cause vascular leakage and edema and for this reason we examined the antitumor activity of a combined treatment with IL-2 and melphalan in our well-established ILP in soft tissue sarcoma-bearing rats (BN175). ILP with either IL-2 or melphalan alone has no antitumor effect, but the combination of IL-2 and melphalan resulted in a strong synergistic tumor response, without any local or systemic toxicity. IL-2 significantly enhanced melphalan uptake in tumor tissue. No signs of significant vascular damage were detected to account for this observation, although the tumor sections of the IL-2 and IL-2 plus melphalan treated animals revealed scattered extravasation of erythrocytes compared to the untreated animals. Clear differences were seen in the localization of ED-1 cells, with an even distribution in the sham, IL-2 and melphalan treatments, while in the IL-2 plus melphalan treated tumors clustered ED-1 cells were found. Additionally, increased levels of TNF mRNA were found in tumors treated with IL-2 and IL-2 plus melphalan. These observations indicate a potentially important role for macrophages in the IL-2-based perfusion. The results in our study indicate that the novel combination of IL-2 and melphalan in ILP has synergistic antitumor activity and may be an alternative for ILP with TNF and melphalan.

Introduction

We have demonstrated that isolated limb perfusion with TNF α and melphalan is associated with excellent antitumor effects against melanoma (1), large soft tissue sarcomas (2,3) and various other tumors in the clinical setting (4-6). We have previously shown that the basis for the synergy is, on one hand a significant enhancement of tumor selective melphalan uptake and on the other hand the subsequent complete destruction of tumor vasculature (2,7). The enhanced uptake of different cytotoxic agents shown in various limb and liver tumor models in our laboratory prompted us to investigate a number of vasoactive substances for similar potential effects (7-12).

One of these agents is the cytokine IL-2 that is known to cause significant changes in vascular permeability and to cause a vascular leakage syndrome when administered at high concentrations (13-15). IL-2 is a pleiotropic cytokine that is mainly known as a molecule of central importance in the long-term culture of T lymphocytes and as a mediator of immune cells (16). IL-2, as a single agent, has been shown to have antitumor activity in both animal

models (17,18) and some antitumor activity in mainly renal cell cancer or melanoma patients (19-21).

Here we report on the evaluation of the effects of high concentrations of IL-2 in combination with melphalan in the ILP setting.

Materials and methods

Chemicals

Human recombinant interleukin 2 (IL-2) was kindly provided by Chiron (Amsterdam, the Netherlands). The content of one vial of lyophilized IL-2 (1 mg per vial, specific activity 18×10^6 IU/mg) was diluted in 1 ml sterile water for injections according to the manufacturer's instructions. Melphalan (Alkeran, 50 mg per vial, Wellcom, Beckenham, UK) was dissolved in 10 ml diluent solvent. Further dilutions were made in phosphate buffered saline to a concentration of 2 mg/ml. Fluorescein and fluorescein isothiocyanate conjugated to bovine serum albumin (FITC-BSA) were purchased from Sigma (Zwijndrecht, the Netherlands) and dissolved in phosphate buffered saline to a concentration of 10 mg/ml.

Animals and tumor model

Male inbred Brown Norway rats were used for the soft tissue sarcoma model (BN175). Rats were obtained from Harlan-CPB, (Austerlitz, the Netherlands), weighing 250-300 grams, and were fed a standard laboratory diet *ad libitum* (Hope Farms Woerden, the Netherlands). Small fragments (3 mm) of the syngeneic BN175 sarcoma were implanted subcutaneously in the right hind leg just above the ankle as previously described (8,10). Tumor growth was recorded by caliper measurement and tumor volume calculated using the formula $0.4(A^2 \times B)$ (where B represents the largest diameter and A the diameter perpendicular to B). Rats were sacrificed if tumor diameter exceeded 25 mm or at the end of the experiment. All animal studies were done in accordance with protocols approved by the committee on Animal Research of the Erasmus MC, Rotterdam, the Netherlands.

Isolated limb perfusion

The perfusion technique was performed as described previously (8,10). Perfusions were performed at a tumor diameter of 12-15 mm at least 7 days after implantation. During perfusion animals were anaesthetized with Hypnorm and Ketamine (Janssen Pharmaceutica, Tilburg, the Netherlands). The femoral vessels were approached through an incision parallel to the inguinal ligament after systemic heparin administration of 50 IU (Leo Pharmaceutical Products, Weesp, the Netherlands) to prevent coagulation in the collateral circulation and in the perfusion circuit. The femoral artery and vein were cannulated with silastic tubing (0.30 mm inner diameter, 0.64 mm outer diameter; 0.64 mm

inner diameter, 1.19 mm outer diameter, respectively; Dow Corning, Ann Arbor, MI). Collaterals were temporarily occluded by applying a tourniquet around the groin. An oxygenation reservoir filled with 5 ml Haemaccel (Behring Pharma, Amsterdam, the Netherlands) and a low-flow roller pump (Watson Marlow type 505 U, Falmouth, UK) were included into the circuit. Drugs, 50 µg IL-2 and/or 40 µg melphalan, were added to the Haemaccel reservoir. The roller pump circulated the perfusate at a flow rate of 2.4 ml/min for 30 minutes. A washout with 5 ml oxygenated Haemaccel was performed at the end of the perfusion. During ILP and washout, the hind leg was kept at a constant temperature of 38-39°C by a warm-water mattress applied around the leg. The pH of the perfusate was monitored during ILP with a pH probe in the perfusion reservoir (pH meter HI 8424, Hanna Instruments, Inc, Ann Arbor, USA).

Assessment of tumor response

Tumor size was recorded by daily caliper measurements. The classification of tumor response was: progressive disease (PD) = increase of tumor volume (>25%); no change (NC) = tumor volume equal to volume during perfusion (in a range of -25% and + 25%); partial remission (PR) = decrease of tumor volume (-25% and -90%); complete remission (CR) = tumor volume less than 10% of initial volume (10). To test synergy of IL-2 and melphalan, the tumor response ratio is calculated by dividing the tumor volume at day 0 with the volume at day 8. The ratio of IL-2 alone plus melphalan alone was compared with the ratio of IL-2 plus melphalan (Mann Whitney U test).

In vitro response of endothelial and tumor cells to IL-2

Cells isolated from the BN175 soft tissue sarcoma were maintained in cell culture in RPMI 1640 supplemented with 10% fetal calf serum and 0.1% penicilline-streptomycine. Media and supplements were obtained from Life Technologies (Breda, the Netherlands).

Human Umbilical Vein Endothelial Cells (HUVEC) were isolated from normal human umbilical cords by the method of Jaffe *et. al.* (22). Cells were cultured in fibronectin coated tissue culture flasks in culture medium (Human Endothelial-SFM (GIBCO-BRL, Life Technologies, Breda, the Netherlands), with 20% Newborn Calf Serum, 10% Human Serum (Cambrex, Verviers, Belgium), 20 ng/ml bFGF and 100 ng/ml EGF (Peprotech, London, UK). Passages 5-7 were used for the experiments.

BN175 cells were added in 100 µl aliquots to 96-well flat-bottomed microtiter plates (Costar, Cambridge, MA, USA) at a final concentration of 1×10^4 cells per well and allowed to grow as a monolayer. HUVECs were plated in fibronectine coated 96-well plates at a final concentration of 6×10^3 cells per well. Cells were incubated at 37°C in 5% CO₂ for 72 hours in the presence of various concentrations of IL-2 and melphalan with or without leukocytes in a total volume of 150 µl.

Growth of tumor cells was measured using the Sulphorhodamine-B (SRB) assay according to the method of Skehan (23). In short, cells were washed twice with phosphate buffered saline, incubated with 10% trichloric acetic acid (1 hour, 4°C) and washed again. Cells were stained with 0.4% SRB (Sigma, Zwijndrecht, the Netherlands) for 15-30 min, washed with 1% acetic acid and were allowed to dry. Protein bound SRB was dissolved in TRIS (10 mM, pH 9.4). The optical density was read at 540 nm. Tumor growth was calculated using the formula: tumor growth = (test well/control) x 100 percent. The drug concentration reducing the absorbance to 50% of the control (IC₅₀) was determined from the growth curves. The experiments were repeated at least 5 times.

Preparation of leukocytes

Venous blood from healthy adult volunteers was collected in Na-heparin tubes (Becton Dickinson, Alphen aan den Rijn, the Netherlands). After centrifuging for 20 min (1500 g, room temperature), total white blood cell fraction was collected and remaining red blood cells were lysed with lysis buffer (0.83% NH₄Cl, 10 mM Hepes, pH = 7.0) for 30 min at room temperature. After centrifuging for 30 min (1500 rpm, room temperature), the leukocytes were dissolved in HUVEC medium at a concentration of 120.10⁴ cells/ml.

Measurement of melphalan in tissue

At the end of the perfusion directly after the washout, the tumor and part of the hind limb muscle were excised. The tissues were immediately frozen in liquid nitrogen to stop metabolism of melphalan and stored at -80°C. Tumor and muscle tissues were homogenized in 2 ml acetonitrile (Pro 200 homogenizer, Pro Scientific, CT, USA) and centrifuged at 2500 g. Melphalan was measured in the supernatant by gas chromatography-mass spectrometry (GC-MS). p-[Bis(2-chloroethyl)amino]-phenylacetic methyl ester was used as an internal standard. Samples were extracted over trifunctional C18 silica columns. After elution with methanol and evaporation, the compounds were derived with trifluoroacetic anhydride and diazomethane in ether. The stable derivates were separated on a methyl phenyl siloxane GC capillary column and measured selectively by single-ion monitoring GC-MS in the positive EI mode described earlier by Tjaden and de Bruijn (24).

Vascular permeability

During ILP 400 µl FITC BSA was added to the perfusate. After perfusion the tumor was excised and frozen in liquid nitrogen. Acetone-fixed frozen sections were fixed for 30 min with 4% formaldehyde. After washing with PBS, the slides were incubated for 1 hour with mouse-anti-rat-CD31PE (Becton Dickinson, Alphen aan den Rijn, the Netherlands) diluted 1:50 in PBS with 5% rat serum. Thereafter, the sections were rinsed with PBS and counterstained with 300 µg/ml Hoechst (Molecular Probes, Leiden, the Netherlands) and

mounted with mounting medium containing polyvinyl alcohol (Mowiol 4-88, Fluka, Zwijndrecht, the Netherlands). The sections were examined on a Leica DM-RXA and photographed using a Sony 3CCD DXC 950 camera.

HUVEC permeability assays

To study the effect of IL-2 on transendothelial monolayer permeability a transwell device (Costar, Cambridge, MA, USA) consisting of an upper chamber with a polycarbonate membrane (6.5 mm diameter, 0.4 μm pore size), placed inside a 24-well plate (lower chamber) was used. Confluent HUVECs were trypsinized and 1.2×10^4 cells were seeded on the fibronectin coated upper chamber. In the lower compartment 1 ml of HUVEC medium was added. Two days after seeding, non-adhering cells were removed and the medium was replaced with 250 μl of 10 $\mu\text{g/ml}$ IL-2 together with 50 μl FITC-BSA or fluorescein (1 mg/ml). The medium in the lower chamber was replaced with 700 μl of HUVEC medium. At 0.25, 0.5, 1, 2, 4, 8 and 24 hours, 50 μl medium of the lower chamber was taken and fluorescence activity was measured under excitation at 490 nm and emission at 530 nm. A standard curve was prepared with known concentrations of FITC-BSA or fluorescein. Induction of permeability was indicated by a higher concentration of FITC-BSA or fluorescein in the lower chamber of the transwell, relative to untreated controls.

HE staining

Directly after ILP tumors were excised, stored in formalin and embedded in paraffin. The 4 μm sections were stained with hematoxylin and eosin using standard procedures. Three or four different tumors in each experimental group were subjected to blind evaluation. At least 6 slides were examined from each tumor. The sections were examined on a Leica DM-RXA and photographed using a Sony 3CCD DXC 950 camera.

Apoptosis Assays: TUNEL/CD31PE double staining

Apoptotic cell death was detected using the technique of 3'hydroxy end labeling. A commercially available end-labeling kit (In Situ Cell Death detection Kit, Fluorescein labeled, Roche, Almere, the Netherlands) was used. Tumor tissues were also stained for endothelial cells to differentiate between apoptosis of the endothelium and apoptosis of tumor cells. Aceton-fixed frozen sections were fixed in 4% paraformaldehyde for 30 minutes and incubated for 1 hour with mouse-anti-rat CD31PE (Becton Dickinson) diluted 1:50 in PBS with 5% rat serum. After washing with PBS the sections were again fixed in 4% paraformaldehyde for 10 minutes and incubated in 0.1% Triton X-100 in 0.1% sodium citrate for 2 minutes on ice to allow permeabilization. The slides were incubated with the TUNEL mixture for 60 min at 37°C. After incubation, the slides were rinsed three times in PBS and counterstained with 300 $\mu\text{g/ml}$ Hoechst (Molecular Probes) for 10 min. After

washing with PBS the slides were mounted with mounting medium containing polyvinyl alcohol (Mowiol 4-88, Fluka). The slides were examined on a Leica DM-RXA and photographed using a Sony 3CCD DXC 950 camera.

Immunohistochemistry

After ILP the tumor was excised and immediately frozen in liquid nitrogen. Immunohistochemical studies were performed on acetone-fixed 7 μm cryostat sections. The tumor sections were fixed for 30 min with 4% paraformaldehyde and after rinsing with PBS the endogenous peroxidase activity was blocked by incubation for 5 minutes in methanol/3% H_2O_2 . The slides were incubated for 1 hour with 1:50 mouse-anti-rat-CD31, CD4, CD8, antibodies to granulocytes (clone HIS48) (Becton Dickinson, Alphen aan den Rijn, the Netherlands) or macrophages (ED-1) (Serotec, Breda, the Netherlands) diluted in 5% rat serum/PBS. Thereafter, sections were washed with PBS and incubated for 1 h with goat-anti-mouse peroxidase-labeled antibody (DAKO, ITK Diagnostics BV, Uithoorn, the Netherlands) diluted 1:100 in PBS with 5% rat serum. After rinsing with PBS, positive cells were revealed by immunoperoxidase reaction with DAB solution (DAB-kit, DAKO) and counterstained lightly with haematoxylin (Sigma).

For quantification of macrophage, CD4+ cell, CD8+ cell and granulocyte infiltration and microvessel density two independent persons performed blinded analysis. Six representative fields (magnification 16x) in each slide and three tumors per treatment were evaluated. The sections were examined on a Leica DM-RXA and photographed using a Sony 3CCD DXC 950 camera. For macrophage, T cell and granulocyte infiltration the total number of positive cells per field of interest were counted. For the microvessel quantification, the area of vessels per field of interest was measured in calibrated digital images (Research Assistant 3.0, RVC, Hilversum, the Netherlands) and number of vessels counted.

RT-PCR

Total RNA was extracted from frozen tumor tissue using the guanidine isothiocyanate based TRIzol reagent (Life Technologies, Breda, the Netherlands) according to the manufacturer's specifications. BN175 cells *in vitro* were treated with medium, 10 $\mu\text{g}/\text{ml}$ IL-2, 8 $\mu\text{g}/\text{ml}$ melphalan or IL-2 plus melphalan and after 30 min of incubation total RNA was extracted. All procedures were carried out with sterile, RNase-free solutions, reagents and disposables. Total RNA was quantified by spectrophotometric analysis at wavelengths of 260 and 280 nm. To assure the quality of the RNA isolates, samples were analyzed by electrophoresis in agarose gel.

Table 1. RT-PCR primers for the immune related genes and for β -actin, which was used as a housekeeping gene.

Gene	Primers	Annealings temp.	Product size (bp)
β -actin	f: 5'-ATGGATGACGATATCGCTG-3' r: 5'-ATGAGGTAGTCTGTCAGGT-3'	60°C	569
IL-6	f: 5'-GACTTCACAGAGGATAACC-3' r: 5'-TAAGTTGTTCTTCACAAACTCC-3'	55°C	294
GRO/ CINC-A	f: 5'-GAAGATAGATTGCACCGATG-3' r: 5'-CATAGCCTCTCACACATTTTC-3'	57°C	367
IL-10	f: 5'-TGACAATAACTGCACCCACTT-3' r: 5'-TCATTCATGGCCTTGTAGACA-3'	60°C	402
IL-12	f: 5'-TCATCAGGGACATCATCAAACC-3' r: 5'-CGAGGAACGCACCTTTCTG-3'	65°C	210
TNF- α	f: 5'-TACTGAACTTCGGGGTGATCGGTCC-3' r: 5'-CAGCCTTGTCCTTGAAGAGAACC-3'	60°C	295
IFN- γ	f: 5'-GCCTCCTCTTGGATATCTGG-3' r: 5'-GTGCTGGATCTGTGGGTTG-3'	60°C	239
MCP-1	f: 5'-ATGCAGGTCTCTCTGTCACG-3' r: 5'-CTAGTTCTCTGTCATACT-3'	57°C	446
MIP-2	f: 5'-GGCACAATCGGTACGATCCAG-3' r: 5'-ACCCTGCCAAGGGTTGACTTC-3'	55°C	287
TGF- β 1	f: 5'-TGGAAGTGGATCCACGAGCCCAAG-3' r: 5'-GCAGGAGCGCACGATCATGTTGGAC-3'	55°C	240

f: forward primer, r: reverse primer

A volume of 20 μ l containing 1.0 μ g of total RNA of each sample was used for generation of cDNA with Omniscript Reverse Transcriptase (Qiagen, Leusden, the Netherlands) and oligo d(T)₁₆ (Life Technologies, Breda, the Netherlands). After incubation at 42°C for 1 hour, the samples were heated for 5 min at 93°C to terminate the reaction. Titanium Taq DNA polymerase (Becton Dickinson, Alphen aan den Rijn, the Netherlands) was used for the PCRs and 1.5 μ l of cDNA per 37.5 μ l of reaction mixture was used. The primers were purchased from Life Technologies (Breda, the Netherlands) and primer sequences are shown in table 1. β -actin was used as an internal standard. PCRs were performed on a Biometra T-gradient PCR machine using the following parameters: initial denaturation at 94°C for 5 min followed by a maximum of 40 cycles of 94°C for 45 sec, annealing for 45 sec (temperatures see table 1) and extension 72°C for 1 min and a final extension step at

72°C for 7 min. The resulting DNA fragments were electrophoretically separated on a 1.5% agarose gel, stained with ethidium bromide and photographed under UV light. A 100-bp ladder was used as the standard.

Semi-quantitative RT-PCR

Total RNA isolation, cDNA preparation and RT-PCR were performed as described above (see RT-PCR). Semi-quantification of cytokine expression was carried out as followed, every 2 cycles, 5 µl of PCR product was collected and the samples were electrophoretically separated on a 1.5% agarose gel, stained with ethidium bromide and photographed under UV light. The threshold cycle was determined as the cycle where the visible band of a specific PCR product first appeared on the gel. Intensities of the PCR product bands were determined by ImageJ v1.34 software (W. Rasband, Research Services Branch, National Institute of Mental Health, Bethesda, Maryland, USA) and normalized for b-actin.

Statistical analysis

Results were evaluated for statistical significance with the Mann Whitney U test. P-values below 0.05 were considered statistically significant. Calculations were performed on a personal computer using GraphPad Prism v3.0 and SPSS v11.0 for Windows 2000.

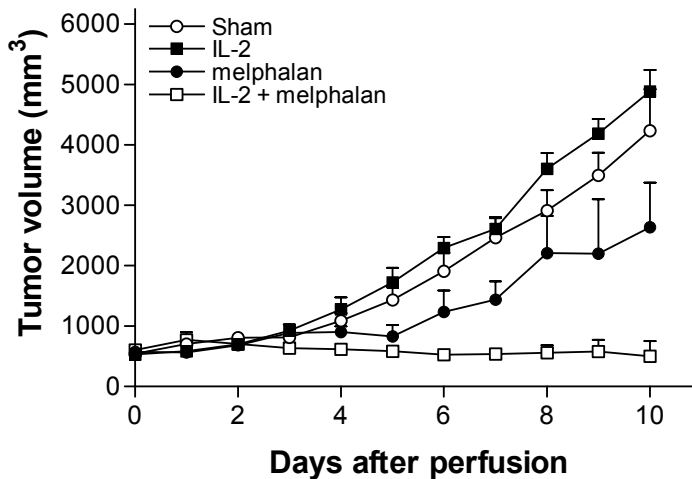


Figure 1. Tumor volumes of the subcutaneously implanted soft-tissue sarcoma BN175 after isolated limb perfusion with perfusate alone, 50 µg IL-2, 40 µg melphalan, or a combination of IL-2 and melphalan. Mean tumor volumes are shown ± SE. Number of rats per group is shown in Table 2.

Results

Tumor response in IL-2 based ILP

To evaluate the antitumor activity of melphalan when combined with IL-2 in an isolated limb perfusion, soft tissue sarcoma-bearing rats were perfused with the agents alone or combined. Sham perfusion with haemaccel alone resulted in progressive disease in all animals (Figure 1 and Table 2), whereas application of melphalan resulted in a slight inhibition of the tumor growth, with a tumor response rate of 17% (PR and CR combined). Progressive disease was also seen in all animals perfused with 50 µg IL-2. Perfusion with IL-2 plus melphalan resulted in a strong synergistic antitumor response and tumor response reaching 67% ($p < 0.05$ compared with melphalan alone). We statistically proved the IL-2 plus melphalan synergy ($p < 0.02$). No obvious regional or systemic toxicity was observed in any of the treatments.

Table 2. Tumor response in soft tissue sarcoma-bearing rats after isolated limb perfusion with IL-2 and melphalan over a total period of 10 days.

Treatment	Response rate ^a				
	PD ^b	NC	PR	CR	RR
sham (n=8)	100%	-	-	-	0
IL-2 (n=9)	100%	-	-	-	0
melphalan (n=6)	66%	17%	17%	-	17%
IL-2 + melphalan (n=8)	22%	11%	56%	11%	67% *

^a responses were scored as described in Materials and Methods, ^b PD: progressive disease, NC: no change, PR: partial remission, CR: complete remission, RR: response rate (PR plus CR), * $p < 0.05$ compared to melphalan alone.

Direct effect of IL-2 and melphalan on BN175 and endothelial cells

In vitro experiments were performed to define whether direct cytotoxicity contributed to the improved tumor response. Because the target can be tumor vascular endothelial cells as well as tumor cells, both HUVECs and BN175 cells were tested. No direct cytotoxicity could be observed when BN175 cells or HUVECs were exposed to concentrations of IL-2 up to 10 µg/ml. Exposure of BN175 cells or HUVECs to melphalan resulted in a response curve with an IC_{50} of 0.25 and 11.4 µg/ml respectively. Addition of IL-2 to melphalan did not alter the IC_{50} of melphalan in both cell types. Incubation of HUVEC with IL-2 did not change the typical cobblestone-shape of these cells. IL-2 had also no additive effect on HUVECs when co-incubated with leukocytes (data not shown).

Tissue concentrations of melphalan

Accumulation of melphalan in tumor and normal muscle tissue was determined. A highly significant tumor-selective increase of melphalan uptake was observed in the rats treated by an ILP with IL-2 and melphalan in comparison to rats treated with an ILP with melphalan alone. Figure 2 demonstrates a 3.7-fold increase in melphalan concentration in tumor tissue after perfusion with IL-2 plus melphalan (n=4) in comparison with perfusion with melphalan alone (n=4) ($p < 0.01$). Importantly, IL-2 had no effect on the uptake of melphalan by muscle tissue.

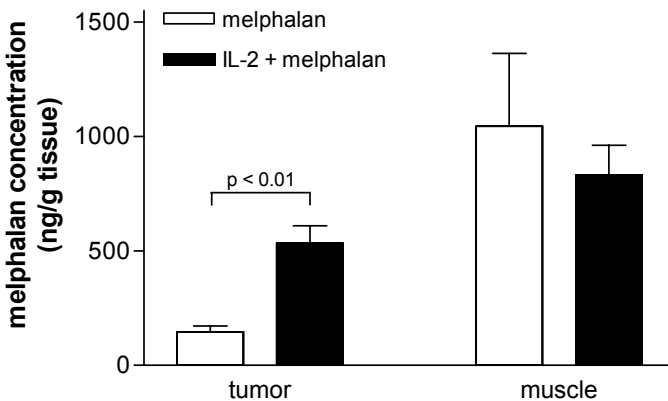


Figure 2. Accumulation of melphalan in soft tissue sarcoma BN175 and muscle during isolated limb perfusion. Rats were perfused with 40 μg melphalan or 50 μg IL-2 plus 40 μg melphalan, after which tumor and muscle were excised and total melphalan content determined as described in Materials and Methods. The mean of six rats is shown \pm SD.

Vascular permeability and damage by IL-2

Since we observed an increased accumulation of melphalan especially in tumor tissue after ILP with IL-2 and melphalan, we investigated the effect of IL-2 on the tumor vascular lining in more detail. First, we looked at extravasation of a larger tracer molecule (FITC-BSA) into the tumor tissue. During the perfusion, FITC-BSA was added to the perfusate and after ILP tumors were excised and frozen sections were stained with CD31PE to visualize blood vessels. We saw no increased vascular permeability for this molecule in the IL-2 plus melphalan group compared to the sham group (data not shown). Most of the FITC-BSA was still present in the blood vessels and hardly any extravasation of the albumin had taken place. For this we hypothesized that permeability of the relatively small melphalan (0.3 kD) molecule is differently affected as compared to FITC-BSA (66.4 kD).

These results were confirmed *in vitro* in which we assessed the capacity of IL-2 to induce permeability in endothelial cell monolayers. A transwell insert with only fibronectin coating and no cells was used to determine the maximum passage of FITC-BSA or fluorescein across the membrane. Incubation of HUVECs with 10 $\mu\text{g}/\text{ml}$ IL-2 did not cause an increase in monolayer permeability for FITC-BSA in a period of 24 hours (data not

shown). These experiments were repeated with fluorescein, a smaller molecule. Incubation with IL-2 resulted in a 1.6-fold increased permeability compared to untreated cells after 15 min of exposure and incubation times of 1 hour or longer showed no increased permeability anymore (Figure 3). In conclusion, there was a transient effect of IL-2 on the permeability of endothelial cells *in vitro* for small molecules like fluorescein and not for proteins like BSA. This could explain why an increased melphalan uptake *in vivo* directly after ILP was seen and no increased permeability of FITC-BSA *in vivo*.

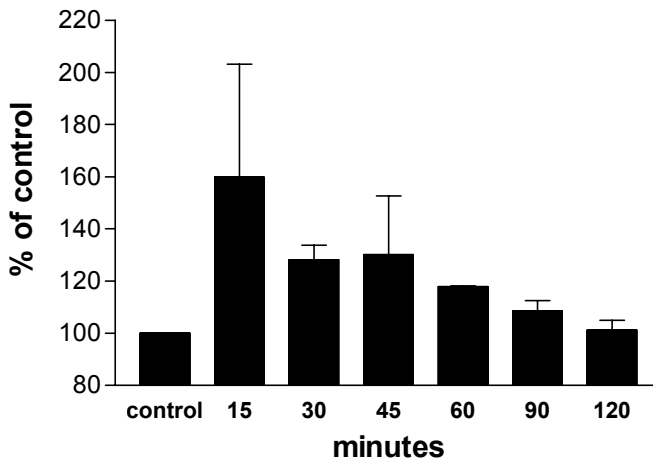


Figure 3. Effect of IL-2 on HUVEC monolayer permeability. HUVECs were cultured on the filter of a transwell unit for 48 hours before the addition of fluorescein containing medium (control) or IL-2 (see Material and Methods). The amount of fluorescein in the lower compartment was measured for period of 2 hours. Values are from two experiments, each done in duplicate. The mean is shown \pm SD.

pH measurement in perfusate

Before and during perfusion the pH of the perfusate was measured. The pH of Haemaccel is 6.9 and oxygenation lowered the pH to 6.2. Directly after start of the perfusion the pH increased up to 6.5 ± 0.3 . Different treatments did not have an effect on the pH of the perfusate and the pH at the end of the perfusion was 6.9 ± 0.1 for all four treatments.

HE staining and apoptosis in vivo

Histopathological examination was performed on the tumors from animals treated with sham, IL-2, melphalan or IL-2 plus melphalan to evaluate damage to the endothelial lining of tumor vessels. The animals were autopsied directly after ILP and the tumor slides were stained with hematoxylin. The tumor sections of the IL-2 and IL-2 plus melphalan treated animals revealed scattered extravasation of erythrocytes compared to the sham and melphalan treated animals, although the endothelial lining seemed mostly to be intact (Figure 4). In the IL-2 and the IL-2 plus melphalan treatment there was a small increase in edema in the tumor in comparison with the other two groups. Because the BN175 tumor is a fast growing tumor, necrotic areas were seen in all four treatments (data not shown). At

this immediate post-ILP time-point there seemed to be no difference in the number and size of the necrotic areas between the treatments.

The subtle changes in vascular leakage and damage to the tumor vessels evoked by IL-2 were further confirmed by double staining of tumor sections for apoptosis and for CD31 expression. Only a few apoptotic tumor and endothelial cells were detected in both the sham and the IL-2 treated rats, without differences between the two groups (data not shown). These results indicate that IL-2 has a much less pronounced effect on the tumor vasculature when compared to TNF, which inflicts massive haemorrhagic necrosis when used in ILP (25).

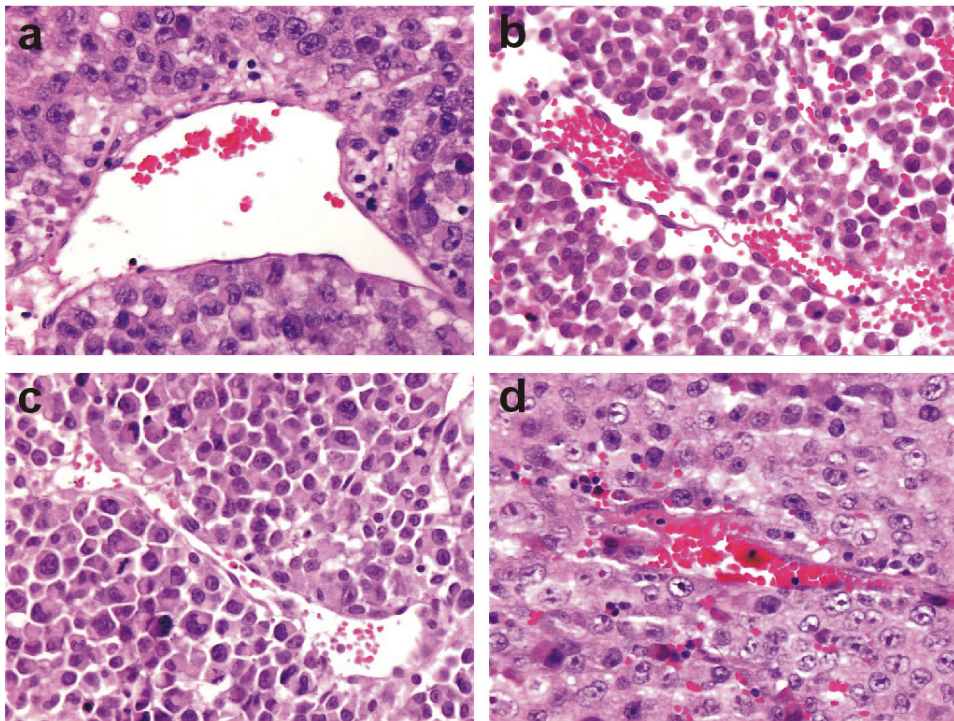


Figure 4. Paraffin sections of BN175 tumor tissue after isolated limb perfusion, haematoxylin-eosin stained. Sham (a), 50 µg IL-2 (b), 40 µg melphalan (c) and IL-2 plus melphalan (d). Original magnification x40.

Assessment of tumor vascular functionality

The increased uptake of melphalan might correlate with the functionality of the tumor-associated vasculature. Quantification of the microvessel density and functionality was performed by immunohistochemical staining of endothelial cells. The number of vessels as well as vessel area was measured. The area per vessel is computed by dividing the total area of vessels by the number of vessels. There was no significant difference between the treatments in the number of vessels, area endothelium or the area per vessel (Table 3).

Table 3. Microvessel density, area of the vessels and tumor infiltration after isolated perfusion with sham, IL-2, melphalan or IL-2 plus melphalan.

	sham	IL-2	melphalan	IL-2 + melphalan
number of vessels ^a	33 ± 9	64 ± 24	22 ± 2	29 ± 5
area endothelium ^b	6.8 ± 0.6	9.2 ± 1.3	5.9 ± 0.9	6.4 ± 0.8
area endothelium/vessel ^c	0.30 ± 0.09	0.16 ± 0.04	0.28 ± 0.03	0.24 ± 0.02
CD4 ^d	0.4 ± 0.2	2.4 ± 0.2	0.2 ± 0.2	0.1 ± 0.1
CD8 ^d	51 ± 7	36 ± 10	67 ± 47	37 ± 10
granulocytes ^d	60 ± 4	79 ± 4*	48 ± 3*	63 ± 4 [#]
macrophages ^d	210 ± 7	222 ± 52	201 ± 20	189 ± 20

Note: Directly after ILP the tumors were excised and frozen sections were stained for granulocytes, macrophages and CD31, CD4 and CD8 positive cells. At least 2 animals per group and 6 fields of interest per tumor were evaluated. Average ± SEM is shown. ^a number of vessels per field of interest, ^b % of total vessel area per field of interest, ^c area per vessel, ^d amount of positive cells per field of interest, * p=0.05 compared with sham treatment, [#] p=0.05 compared to melphalan treatment

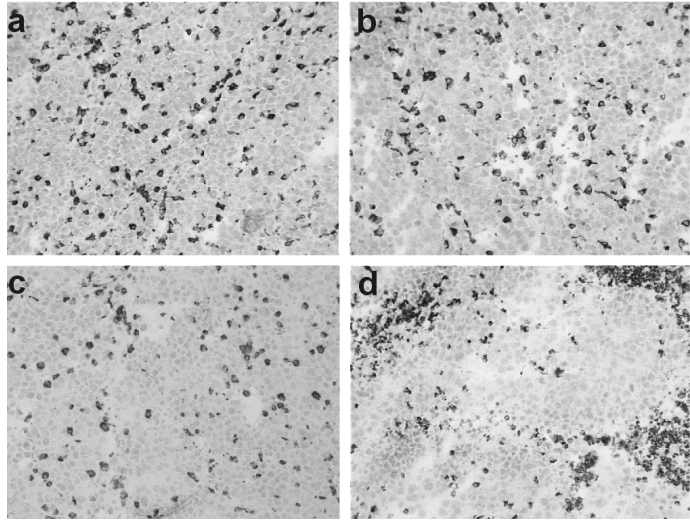
Tumor infiltration of leukocytes and macrophages

In vitro IL-2 seems to have a small and transient effect on endothelial cells and no effect on tumor cells, which is also seen with TNF. We hypothesized that IL-2 stimulates immune-cells to contribute to the increased vascular leakage. To see if there is an increased infiltration of leukocytes into the tumor tissue, tumors were excised directly after isolated perfusion with sham, IL-2, melphalan or IL-2 plus melphalan. Immunohistochemical staining for CD4 and CD8 was performed on frozen sections. There were hardly any CD4 positive cells present in all four treatments (Table 3). The number of infiltrating CD8 cells was much higher compared to the number of CD4 cells. However, no clear differences in the amount of infiltrating CD8 cells were seen between the four groups.

Infiltrated granulocytes were detected in tumor tissue in slightly larger numbers than CD8 cells. ILP with melphalan resulted in a decreased number of granulocytes compared to sham perfusions (p=0.05). Addition of IL-2 to the sham perfusion increased the number of infiltrating cells and addition of IL-2 to melphalan ILP also resulted in an increase in infiltrating granulocytes (p=0.05). However, no increased infiltration of granulocytes in the IL-2 plus melphalan group compared to sham perfusions was found. In none of the treatments a difference in distribution pattern of granulocytes was found.

Macrophages were present in all treated and untreated tumors in larger proportions than T cells and granulocytes, without differences between the treatments. But, clear differences were seen in the localization of ED-1 cells, with an even distribution in the treatments sham, IL-2 and melphalan, while in the IL-2 plus melphalan group clustered ED-1 cells were found (Figure 5).

Figure 5. Representative pictures of macrophage localization in BN175 tumor. Rats were perfused with sham (a), 50 μg IL-2 (b), 40 μg melphalan (c) and IL-2 plus melphalan (d), after which tumors were excised and an immunohistochemical staining for ED-1 positive cells was performed on frozen tumor section. Treatment with IL-2 plus melphalan resulted in a redistribution of macrophages and clustered ED-1 cells were found. Original magnification 16X.



Cytokine expression in tumor tissue and tumor cells in vitro

The different macrophage distribution after perfusion with IL-2 and melphalan indicates possible macrophage activation. These activated macrophages could produce non-specific effector molecules like cytokines and reactive oxygen and nitrogen intermediates, all of which exhibit potent antitumor properties. Tumor biopsies were obtained directly after ILP and RNA extracted from these samples was amplified in order to create an overview of cytokine-profile in the tumor microenvironment and the effect of treatment on this profile.

All cytokines tested were expressed in sham treated tumors (data not shown). In these tumors, TGF- β 1 showed to have the highest expression level followed by MCP-1 and expression of TNF was the lowest compared to the other cytokines tested. Strikingly, only for TNF expression a response to IL-2 treatment was observed. The threshold cycle of TNF expression in IL-2 and IL-2 plus melphalan treated tumors was 5 cycles lower than that of sham treated tumors ($p < 0.05$). Integrated density was measured and TNF mRNA levels were expressed as a ratio of TNF to b-actin (Figure 6). A 5.7-fold increase in TNF mRNA expression was found in tumor tissue treated with IL-2 plus melphalan compared to sham treatment ($p < 0.05$). IL-2 ILP caused a 3.2-fold increased TNF mRNA expression compared to sham ($p < 0.05$), whereas melphalan ILP had no effect on TNF mRNA expression.

To investigate which cytokines the tumor cells produced, RNA was isolated from BN175 tumor cells *in vitro*. Cells were also incubated with 10 $\mu\text{g}/\text{ml}$ IL-2 and 8 $\mu\text{g}/\text{ml}$ melphalan or the combination for 30 minutes. Clear differences were seen between cytokine expression levels *in vivo* and *in vitro*. mRNA expression in tumors showed higher levels of IL-12, MCP-1 and TGF- β 1 than tumor cells *in vitro*. Levels of the other cytokines tested were comparable. Treatment with IL-2 and/or melphalan had no effect on the cytokine expression of tumor cells *in vitro* (data not shown).

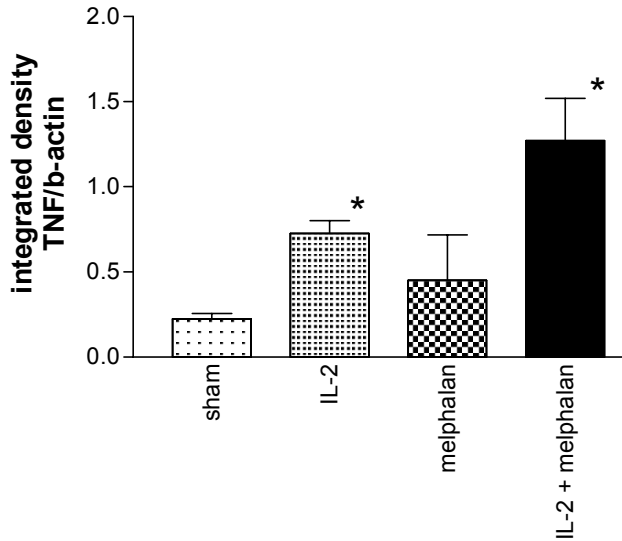


Figure 6. Semi-quantitative RT-PCR. BN175-bearing rats were treated with buffer alone, 50 μ g IL-2, 40 μ g melphalan or a combination of IL-2 and melphalan and directly after ILP the tumors were excised. RNA was isolated and RT-PCR with TNF primers was carried out. Integrated density of the PCR bands was measured and TNF mRNA levels are presented as a ratio of TNF to b-actin. The mean of 3 animals per group is shown \pm SEM. * $p < 0.05$ compared to sham (Mann Whitney U test).

Discussion

In this study we have examined the antitumor activity of a combined treatment with IL-2 and melphalan in an isolated limb perfusion in soft tissue sarcoma-bearing rats. We demonstrate for the first time that ILP with the combination of IL-2 and melphalan in the BN175 tumor resulted in a strong synergistic tumor response. The tumor response (PR and CR combined) of 67% was much higher than the tumor response of melphalan alone (17%), while progressive disease was seen in all animals treated with IL-2 alone. These results are comparable with those of our previous study with TNF and melphalan where we found similar synergy for the combination of TNF and melphalan (8,10). Importantly, the application of high dose IL-2 in ILP was without any local or systemic toxicity indicating possible translation of this cytokine to loco-regional settings in the clinic.

In different animal models IL-2, as a single agent, has been shown to have antitumor activity (17,18). In the systemic setting this requires high doses and multiple dosing, which is associated with serious systemic toxicity with hypotension, massive vascular leakage syndrome and multiple organ failure leading to death (13-15,26). The advantage of a loco-regional application, i.e. an ILP, is the minimal systemic exposure while maintaining a high therapeutic dose locally. For this reason we hypothesized that IL-2 could be a good candidate to be used in a melphalan-based ILP. IL-2 is known not to have direct antitumor effects and thus seems to be an unlikely candidate to be used in the isolated limb perfusion setting. However, we speculated that IL-2 with its multiple effects, could well impact on the pathophysiology of large tumors in a similar way as TNF and might thus significantly potentiate the distribution and uptake of melphalan throughout the tumor. A critical step for

TNF-based ILP is the accurate and real-time monitoring of systemic leakage with the aim of avoiding severe systemic TNF mediated toxicity. Because IL-2 is used in a systemic clinical setting, we hypothesized that IL-2 is a potentially safer drug than TNF and therefore a useful alternative for ILP with TNF. Moreover, the lack of toxicity warrants exploration of IL-2 in loco-regional treatment of liver cancer, in which TNF cannot be used effectively due to its inherent dose limiting liver toxicity.

Here we demonstrate that IL-2 alone in the ILP-setting had no effect on tumor growth, in spite of the high dosage we were using. A strong synergistic tumor response was observed when IL-2 was combined with melphalan. A set of experiments to investigate potential mechanisms behind the observed synergy between IL-2 and melphalan was performed both *in vitro* and *in vivo*. We showed that IL-2 did not have an effect on the proliferation or morphology of HUVECs or BN175 tumor cells *in vitro*. We speculate that the improved antitumor effect shown *in vivo* is probably not caused by a direct cytotoxic effect on tumor or endothelial cells.

IL-2 is a 15 kD glycoprotein produced by antigen-activated T lymphocytes that plays a varied and critical role in immunoregulation. IL-2 binds to the IL-2 receptor and the IL-2R is expressed not only on hematopoietic cells, but also on non-hematopoietic cells. Different reports have indicated the presence of IL-2 receptors on cells in head and neck squamous cell carcinoma (27) and different human melanomas (28). We evaluated the direct effect of IL-2 on endothelial cells. We did not see an effect on the proliferation of HUVECs, nor morphologic changes. Holzinger *et al.* showed that HUVECs possess low numbers of IL-2 receptor, although IL-2 had no effect on the proliferation of the endothelial cells neither on the typical cobblestone-shape morphology of the cells (29). This in contrast with the study of Hicks *et al.* where they showed that HUVECs do proliferate in response to IL-2 (30). To test whether IL-2 had an indirect effect on HUVECs we co-cultured leukocytes with HUVECs and treated them with different concentrations of IL-2. We showed that there was no effect on proliferation of endothelial cells nor did we observe morphologic changes.

Systemic IL-2 administration is often complicated by significant capillary leakage, with consequent extravasation of interstitial fluid and plasma proteins (14,15,26). In this study we evaluated whether IL-2 could cause capillary leakage in the tumor and therefore enhance the delivery of melphalan at the tumor site. We showed that IL-2 caused a 3.7-fold augmented accumulation of melphalan specifically in tumor tissue, which correlated closely with the enhanced tumor responses. This increase could very well explain the improved efficacy, as ILP with IL-2 alone did not induce any tumor response. The 3.7-fold increase in local melphalan results in a shift from a hardly effective dose of 0.14 $\mu\text{g/ml}$ to an effective dose of 0.53 $\mu\text{g/ml}$, when translated to the *in vitro* cytotoxicity profile of melphalan on BN175 tumor cells. Taken into account that we expect a heterogeneous distribution of melphalan especially around the tumor vessels in the well-perfused region of

the tumor, actual local drug levels are likely to be even higher. Further more, IL-2 did not have an effect on the accumulation of melphalan in muscle tissue, indicating that IL-2 works specifically on the tumor-associated vessels.

The mildly acidic condition of the perfusate (pH 6.2) might enhance the antitumor effect of melphalan as suggested by a study of Kelley *et al.* (31). Others showed that hypoxia and acidosis both *in vitro* and *in vivo* are able to augment the cytotoxicity of melphalan (32,33). Addition of IL-2 did not have an effect on the pH of the perfusate. The final pH for all treatments was 6.9.

We showed in a previous study that TNF comparably augmented the accumulation of chemotherapeutic drugs specifically in tumor tissue 4- to 6-fold (7,11). As the augmented melphalan accumulation in tumor tissue induced by IL-2 correspond with our observations in TNF-based ILP we expected comparable histological changes. However, the HE slides of tumor tissue after IL-2-based ILP showed a much less pronounced extravasation of erythrocytes when compared to TNF-based ILP (25). However, in IL-2 and IL-2 plus melphalan treated tumors, although the endothelial lining seemed to be intact, scattered extravasation of erythrocytes was observed next to locally increased edema. These findings indicate that IL-2 has a much more subtle effect on the endothelial lining, compared to TNF. Moreover, IL-2 did not increase the permeability to FITC-BSA *in vivo*. Also *in vitro* endothelial permeability for FITC-BSA was not increased when HUVECs were treated with IL-2, while an enhanced permeability of 1.6-fold for fluorescein was seen after 15 minutes of incubation with IL-2. An explanation can be that FITC-BSA is a much larger molecule than fluorescein (molecular weight 66.400 D and 332 D, respectively) and the molecular weight of melphalan (305 D) is comparable with fluorescein. The lack of a strong tumor-vascular effect was confirmed by staining of tumor section for apoptosis. We could only detect few apoptotic tumor and endothelial cells and no differences between sham and IL-2-based ILP were noted. The increased tumor accumulation of melphalan might be correlated with the vessel functionality of the tumors. However, we did not see any differences between the treatments in the vessel area.

As IL-2 did not seem to have an effect on endothelial or tumor cells directly we hypothesized that immune cells are involved. We performed immunohistochemical stainings on tumor tissue collected directly after ILP. We did not see an effect on the number of infiltrating CD4 or CD8 cells. A reason why we do not see more pronounced differences in the amount of infiltrating cells between the treatments could be explained by the time-point at which tissues were collected, after only 30 minutes of treatment. None of the perfusions had an effect on the number of infiltrating macrophages, but clear differences were seen in the localization of macrophages. After ILP with IL-2 and melphalan clustered macrophages were present, while in the other treatments macrophages were evenly distributed. LPS, IFN γ and IL-2 are established as activating agents for

monocytes/macrophages. Activated monocytes/macrophages produce cytokines (such as TNF) and free radicals (superoxide and nitric oxide) that have cytotoxic effects on tumor cells (34-37). We showed in tumor tissue treated with IL-2 alone or IL-2 plus melphalan a 5.7-fold increased expression of TNF, while *in vitro* stimulation of tumor cells did not result in an increased TNF expression. These results indicate that activated macrophages could play a role in the antitumor response of IL-2-based ILP. Additional studies are ongoing to further elucidate the mechanism.

In conclusion, IL-2 in a melphalan-based ILP is causing a strong synergistic antitumor response in soft-tissue sarcoma BN175. Importantly, the addition of IL-2 inflicted no toxicity locally or systemically. The results in our study indicate that the novel combination of IL-2 and melphalan in an ILP can be of value and therefore possibly a useful alternative for ILP with TNF and melphalan, or as a novel candidate for isolated hepatic perfusion.

Acknowledgements

We would like to thank Chiron for the generous supply of IL-2. This study was supported by grant DDHK 2000-2224 of the Dutch Cancer Society.

References

1. Lienard D, Lejeune FJ, Ewalenko P. In transit metastases of malignant melanoma treated by high dose rTNF alpha in combination with interferon-gamma and melphalan in isolation perfusion. *World J Surg.* 1992;16(2):234-240.
2. Eggermont AM, Schraffordt KH, Lienard D, et al. Isolated limb perfusion with high-dose tumor necrosis factor-alpha in combination with interferon-gamma and melphalan for nonresectable extremity soft tissue sarcomas: a multicenter trial. *J Clin Oncol.* 1996;14(10):2653-2665.
3. Eggermont AM, Schraffordt KH, Klausner JM, et al. Isolated limb perfusion with tumor necrosis factor and melphalan for limb salvage in 186 patients with locally advanced soft tissue extremity sarcomas. The cumulative multicenter European experience. *Ann Surg.* 1996;224(6):756-764.
4. Bickels J, Manusama ER, Gutman M, et al. Isolated limb perfusion with tumour necrosis factor-alpha and melphalan for unresectable bone sarcomas of the lower extremity. *Eur J Surg Oncol.* 1999;25(5):509-514.
5. Eggermont AM, de Wilt JH, ten Hagen TL. Current uses of isolated limb perfusion in the clinic and a model system for new strategies. *Lancet Oncol.* 2003;4(7):429-437.
6. Olieman AF, Lienard D, Eggermont AM, et al. Hyperthermic isolated limb perfusion with tumor necrosis factor alpha, interferon gamma, and melphalan for locally advanced nonmelanoma skin tumors of the extremities: a multicenter study. *Arch Surg.* 1999;134(3):303-307.
7. de Wilt JH, ten Hagen TL, de Boeck G, van Tiel ST, de Bruijn EA, Eggermont AM. Tumor necrosis factor alpha increases melphalan concentration in tumour tissue after isolated limb perfusion. *Br J Cancer.* 2000;82(5):1000-1003.
8. de Wilt JH, Manusama ER, van Tiel ST, van Ijken MG, ten Hagen TL, Eggermont AM. Prerequisites for effective isolated limb perfusion using tumour necrosis factor alpha and melphalan in rats. *Br J Cancer.* 1999;80(1-2):161-166.
9. Manusama ER, Stavast J, Durante NM, Marquet RL, Eggermont AM. Isolated limb perfusion with TNF alpha and melphalan in a rat osteosarcoma model: a new anti-tumour approach. *Eur J Surg Oncol.* 1996;22(2):152-157.
10. Manusama ER, Nooijen PT, Stavast J, Durante NM, Marquet RL, Eggermont AM. Synergistic antitumor effect of recombinant human tumour necrosis factor alpha with melphalan in isolated limb perfusion in the rat. *Br J Surg.* 1996;83(4):551-555.
11. van Der Veen AH, de Wilt JH, Eggermont AM, van Tiel ST, Seynhaeve AL, ten Hagen TL. TNF-alpha augments intratumoural concentrations of doxorubicin in TNF-alpha-based isolated limb perfusion in rat sarcoma models and enhances anti-tumour effects. *Br J Cancer.* 2000;82(4):973-980.

12. van Etten B, de Vries MR, van Ijken MG, et al. Degree of tumour vascularity correlates with drug accumulation and tumour response upon TNF-alpha-based isolated hepatic perfusion. *Br J Cancer*. 2003;88(2):314-319.
13. Epstein AL, Mizokami MM, Li J, Hu P, Khawli LA. Identification of a protein fragment of interleukin 2 responsible for vasopermeability. *J Natl Cancer Inst*. 2003;95(10):741-749.
14. Siegel JP, Puri RK. Interleukin-2 toxicity. *J Clin Oncol*. 1991;9(4):694-704.
15. Winkelhake JL, Gauny SS. Human recombinant interleukin-2 as an experimental therapeutic. *Pharmacol Rev*. 1990;42(1):1-28.
16. Morgan DA, Ruscetti FW, Gallo R. Selective in vitro growth of T lymphocytes from normal human bone marrows. *Science*. 1976;193(4257):1007-1008.
17. Baselmans AH, Koten JW, Battermann JJ, Van Dijk JE, Den Otter W. The mechanism of regression of solid SL2 lymphosarcoma after local IL-2 therapy. *Cancer Immunol Immunother*. 2002;51(9):492-498.
18. Den Otter W, De Groot JW, Bernsen MR, et al. Optimal regimes for local IL-2 tumour therapy. *Int J Cancer*. 1996;66(3):400-403.
19. Eton O, Rosenblum MG, Legha SS, et al. Phase I trial of subcutaneous recombinant human interleukin-2 in patients with metastatic melanoma. *Cancer*. 2002;95(1):127-134.
20. Negrier S, Escudier B, Lasset C, et al. Recombinant human interleukin-2, recombinant human interferon alfa-2a, or both in metastatic renal-cell carcinoma. Groupe Francais d'Immunotherapie. *N Engl J Med*. 1998;338(18):1272-1278.
21. Yang JC, Sherry RM, Rosenberg SM, et al. Randomized study of high-dose and low-dose interleukin-2 in patients with metastatic renal cancer. *J Clin Oncol*. 2003;21(16):3127-3132.
22. Jaffe EA, Nachman RL, Becker CG, Minick CR. Culture of human endothelial cells derived from umbilical veins. Identification by morphologic and immunologic criteria. *J Clin Invest*. 1973;52(11):2745-2756.
23. Skehan P, Storeng R, Scudiero D, et al. New colorimetric cytotoxicity assay for anticancer-drug screening. *J Natl Cancer Inst*. 1990;82(13):1107-1112.
24. Tjaden UR, de Bruijn EA. Chromatographic analysis of anticancer drugs. *J Chromatogr*. 1990;531:235-294.
25. Nooijen PT, Manusama ER, Eggermont AM, et al. Synergistic effects of TNF-alpha and melphalan in an isolated limb perfusion model of rat sarcoma: a histopathological, immunohistochemical and electron microscopical study. *Br J Cancer*. 1996;74(12):1908-1915.
26. Atkins MB. Interleukin-2: clinical applications. *Semin Oncol*. 2002;29(3 Suppl 7):12-17.
27. Weidmann E, Sacchi M, Plaisance S, et al. Receptors for interleukin 2 on human squamous cell carcinoma cell lines and tumor in situ. *Cancer Res*. 1992;52(21):5963-5970.
28. Rimoldi D, Salvi S, Hartmann F, et al. Expression of IL-2 receptors in human melanoma cells. *Anticancer Res*. 1993;13(3):555-564.
29. Holzinger C, Weissinger E, Zuckermann A, et al. Effects of interleukin-1, -2, -4, -6, interferon-gamma and granulocyte/macrophage colony stimulating factor on human vascular endothelial cells. *Immunol Lett*. 1993;35(2):109-117.
30. Hicks C, Cooley MA, Penny R. Investigation of interleukin 2 receptors on human endothelial cells. *Growth Factors*. 1991;5(3):201-208.
31. Kelley ST, Menon C, Buerk DG, Bauer TW, Fraker DL. Acidosis plus melphalan induces nitric oxide-mediated tumor regression in an isolated limb perfusion human melanoma xenograft model. *Surgery*. 2002;132(2):252-258.
32. Skarsgard LD, Skwarchuk MW, Vinczan A, Kristl J, Chaplin DJ. The cytotoxicity of melphalan and its relationship to pH, hypoxia and drug uptake. *Anticancer Res*. 1995;15(1):219-223.
33. Chaplin DJ, Acker B, Olive PL. Potentiation of the tumor cytotoxicity of melphalan by vasodilating drugs. *Int J Radiat Oncol Biol Phys*. 1989;16(5):1131-1135.
34. Economou JS, McBride WH, Essner R, et al. Tumour necrosis factor production by IL-2-activated macrophages in vitro and in vivo. *Immunology*. 1989;67(4):514-519.
35. Maekawa H, Iwabuchi K, Nagaoka I, Watanabe H, Kamano T, Tsurumaru M. Activated peritoneal macrophages inhibit the proliferation of rat ascites hepatoma AH-130 cells via the production of tumor necrosis factor-alpha and nitric oxide. *Inflamm Res*. 2000;49(10):541-547.
36. Albina JE, Reichner JS. Role of nitric oxide in mediation of macrophage cytotoxicity and apoptosis. *Cancer Metastasis Rev*. 1998;17(1):39-53.
37. Bonnotte B, Larmonier N, Favre N, et al. Identification of tumor-infiltrating macrophages as the killers of tumor cells after immunization in a rat model system. *J Immunol*. 2001;167(9):5077-5083.

Chapter 3

Synergistic antitumor activity of histamine plus melphalan in isolated limb perfusion: preclinical studies

Flavia Brunstein¹, Saske Hoving¹, Ann LB Seynhaeve¹, Sandra T van Tiel¹, Gunther Guetens², Ernst A de Bruijn², Alexander MM Eggermont¹, Timo LM ten Hagen¹

¹Department of Surgical Oncology, Erasmus MC-Daniel den Hoed Cancer Center, Rotterdam, the Netherlands

²Department of Experimental Oncology, University of Leuven, Leuven, Belgium

Abstract

We have previously shown how tumor response of isolated limb perfusion (ILP) with melphalan was improved when tumor necrosis factor alpha (TNF- α) was added. Taking into account that other vasoactive drugs could also improve tumor response to ILP, we evaluated histamine (Hi) as an alternative to TNF- α . We used a rat ILP model to assess the combined effects of Hi and melphalan (n=6) on tumor regression, melphalan uptake (n=6), and tissue histology (n=2) compared with Hi or melphalan alone. We also evaluated the growth of BN175 tumor cells as well as apoptosis, necrosis, cell morphology, and paracellular permeability of human umbilical vein endothelial cells (HUVECs) after Hi treatment alone and in combination with melphalan. The antitumor effect of the combination of Hi and melphalan *in vivo* was synergistic, and Hi-dependent reduction in tumor volume was blocked by H₁ and H₂ receptor inhibitors. Tumor regression was observed in 66% of the animals treated with Hi and melphalan, compared with 17% after treatment with Hi or melphalan alone. Tumor melphalan uptake increased and vascular integrity in the surrounding tissue was reduced after ILP treatment with Hi and melphalan compared with melphalan alone. *In vitro* results paralleled *in vivo* results. BN175 tumor cells were more sensitive to the cytotoxicity of combined treatment than HUVECs, and Hi treatment increased the permeability of HUVECs. In conclusion, Hi in combination with melphalan in ILP improved response to that of melphalan alone through direct and indirect mechanisms. These results warrant further evaluation in the clinical ILP setting and, importantly, in organ perfusion.

Introduction

Isolated limb perfusion (ILP) is a treatment method in which high concentrations of drugs are administered to a limb containing an unresectable tumor that is temporarily isolated from the rest of the body's circulatory system by the use of an extracorporeal perfusion circuit and a tourniquet placed at the root of the limb. ILP with tumor necrosis factor alpha (TNF- α) and melphalan is associated with synergistic antitumor effects against melanoma (1), large soft-tissue sarcomas (2,3), and various other tumors in the clinical setting (4-6). We have previously shown that the basis for the synergy is both a substantial enhancement of tumor-selective melphalan uptake (7) and the complete destruction of the tumor vasculature (2). The enhanced tissue uptake of different cytotoxic agents, when combined with TNF- α , shown in various limb and liver tumor models in our laboratory (7-12), prompted us to investigate a number of vasoactive substances for similar effects.

Histamine (Hi) is an obvious candidate to enhance tissue uptake of cytotoxic agents during ILP. It is an inflammatory mediator that is formed and stored mainly in the granules of mast cells and basophils, but it has also been identified in epidermal cells, gastric mucosa, neurons of the central nervous system, and in cells in regenerating or rapidly growing

tissues. Its effect on fine vessels is to cause edema by increasing the flow of lymph and lymph proteins into the extracellular space and also by promoting the formation of gaps between endothelial cells, thus increasing transcapillary vesicular transport (13). The same mechanism that causes edema in fine vessels could potentially be used to increase drug concentrations in tumor tissues.

In this study, we performed ILP in a rat model by using combinations of Hi and melphalan to determine if Hi would increase the effects of melphalan. To determine the *in vivo* mechanisms involved, we measured melphalan uptake and performed histologic analysis after treatment. In addition, cultured sarcoma (14) and normal endothelial cells were treated *in vitro* with Hi, melphalan, or a combination of the two, and cytotoxicity, necrosis, apoptosis, and paracellular permeability were assayed.

Materials and Methods

ILP

Male inbred Brown Norway rats weighing 250–300 g were obtained from Harlan-CPB (Austerlitz, the Netherlands) and were fed a standard laboratory diet *ad libitum* (Hope Farms, Woerden, the Netherlands). The studies were done in accordance with protocols approved by the Animal Care Committee of the Erasmus University Rotterdam (Rotterdam, the Netherlands). Small fragments (diameter = 3 mm) of the spontaneous, nonimmunogenic, syngeneic BN175 sarcoma (14) were inserted subcutaneously in the right hind legs of the rats, as previously described (8). Tumor growth was measured daily with a caliper, and tumor volume was calculated using the formula $0.4(A^2 \times B)$ (where B represents the largest tumor diameter and A is the diameter perpendicular to it). When tumor diameter exceeded 25 mm or at the end of the experiment, rats were anesthetized and killed by cervical dislocation.

The treatment consisted of the experimental ILP previously described (8,11). In brief, 7–10 days after tumor fragments were inserted (when they reached a diameter of 12–15 mm) rats were anesthetized by intraperitoneal ketamine and intramuscular hypnomidate. An incision parallel to the inguinal ligament was made, and the inguinal vessels were cannulated and connected by way of a low-flow roller pump (Watson Marlow, Falmouth, U.K.) to an oxygenated reservoir where drugs were added, in bolus, to the perfusate (total volume = 5 mL). A groin tourniquet was used to occlude collateral vessels, allowing a proper isolation of the limb. The temperature of the limb was maintained at 38°C using a warm-water blanket.

The perfusate consisted of Haemaccel alone (sham) (Boehring Pharma, Amsterdam, the Netherlands), Haemaccel plus μ 40 g of melphalan (Alkeran Wellcome, Beckenham, UK), Haemaccel plus 40 μ g of melphalan and 1000 μ g of Hi (kindly provided by Maxim Pharmaceuticals, San Diego, CA), or Haemaccel plus 1000 μ g of Hi.

To evaluate the role of the different Hi receptors in the Hi-based ILP, the Hi receptor blockers promethazine (H₁-R) (Centrafarm, Etten-Leur, the Netherlands) and famotidine (H₂-R) (Sigma, Zwijndrecht, the Netherlands) were added to the perfusate (200 and 50 µg/mL, respectively) and allowed to circulate into the limb for 5 minutes before melphalan and Hi were added.

Tumor dimensions were measured every day and used to monitor tumor volume. Volume on day 9 was compared with that on day 0, and response was classified as follows: progressive disease, increase of more than +25%; no change, volume between -25% and +25%; partial remission, decrease between -25% and -90%; or complete response, tumor volume less than 10% of initial volume.

Limb function was clinically observed as the ability to walk and stand on the perfused limb after ILP. On a scale from grade 0 to 2, grade 0 is severely impaired function in which the rat drags its hind limb, grade 1 is slightly impaired function (cannot use it in a normal way but can stand on it), and grade 2 is an intact function (normal walking and standing pattern) (8).

In vivo melphalan uptake

To evaluate melphalan distribution, we killed 11 rats (six treated with Hi plus melphalan and five treated with melphalan alone) immediately after ILP was performed. Tumors and muscle from the limb were removed, snap-frozen in liquid nitrogen, and stored at -80°C. Tissues were homogenized in 2 mL of acetonitrile with a PRO 200 homogenizer (Pro Scientific, Oxford, CT) and centrifuged at 2500g and 4°C. Melphalan concentration (reported as nanograms of melphalan per gram of tissue) was measured by gas chromatography–mass spectrometry on at least three different pieces of similar final weight per sample, as described previously (7,15). Given the tumor and muscle values for melphalan uptake, the tumor-to-muscle ratio was calculated, considering the amount of melphalan measured in muscle as 100% and calculating the tumor value in comparison with it.

Histologic evaluation

Two animals from each treatment group were killed by cervical dislocation directly after ILP; tumors and a piece of muscle from the limb were excised and cut in half. One half was fixed in 4% formaldehyde solution, embedded in paraffin, and stained with hematoxylin and eosin. Images of stained samples were taken on a Leica DM-RXA microscope (Leica Microsystems, Rijswijk, the Netherlands) with a Sony 3CCD DXC camera (Sony Netherlands, Badhoevedorp, the Netherlands).

Cell culture

BN175 cells (spontaneous rapidly growing and metastasizing soft-tissue sarcoma) (14) were grown in RPMI 1640 medium (Life Technologies, Leiden, the Netherlands) supplemented with 10% fetal calf serum (FCS) and 0.1% penicillin–streptomycin (Life Technologies). For growth assays, BN175 cells were plated in 96-well flat-bottomed microtiter plates (Costar, Cambridge, MA) at 10^5 cells per well (in 100 μ L) 24 hours before treatment and allowed to grow to confluence. Next, the cells were incubated at 37°C in 5% CO₂ for 72 hours in the presence of medium alone or medium plus various concentrations of melphalan and Hi. Hi concentrations ranged from 0 to 200 μ g/mL. Melphalan concentration ranged from 0 to 8 μ g/mL.

HUVECs were prepared by collagenase treatment of freshly obtained human umbilical veins and cultured in human endothelial serum-free medium–RPMI medium (Cambrex Bioscience, Verviers, Belgium) supplemented with 10% heat inactivated human serum (Invitrogen Life Technologies, Breda, the Netherlands), 20% FCS, human epidermal growth factor, human basic fibroblast growth factor, and 0.1% penicillin–streptomycin (Life Technologies). For growth assays, HUVECs were plated 24 hours before treatment at 6×10^4 cells per well and cultured for 48 hours with various concentrations of Hi (0 to 200 μ g/mL) and melphalan (0 to 200 μ g/mL).

Cell growth

Growth of BN175 cells and HUVECs was measured using the Sulforhodamine-B (SRB) assay (16). In brief, cells were washed with phosphate-buffered saline, incubated with 10% trichloroacetic acid for 1 hour at 4°C, and washed again with phosphate-buffered saline. Cells were stained with SRB (0.5% SRB in 1% acetic acid) for 15 to 30 minutes, washed with 1% acetic acid, and air-dried. Protein-bound SRB was dissolved in Tris base (10 mM, pH 9.4). Absorbance at 540 nm was measured for each well, and tumor cell growth was calculated according to the following formula: percentage of tumor cell growth = (absorbance of test well/absorbance of control well) x 100%. The Hi concentration leading to 50% reduction in absorbance compared with control (i.e., 50% inhibitory concentration [IC₅₀]) was determined from the growth curve. Each experiment was performed four times in duplicate. The mean of all values and the 95% confidence intervals (CIs) were determined and reported.

HUVEC morphology and necrosis–apoptosis assays

HUVECs were plated 24 hours before treatment at 6×10^4 cells per well in flat-bottomed 12-well plates (Costar) in a volume of 900 μ L per well and grown to confluence. Cells were then incubated at 37°C in 5% CO₂ with various concentrations of Hi for various times. At each time point, medium was discarded and replaced with 500 μ L of HUVEC medium plus

0.05% YO-PRO for detection of apoptotic cells (Molecular Probes) or with propidium iodide to detect necrotic cells (Sigma). Cells were incubated for 30 minutes in the dark at 37°C, and pictures were taken with a Zeiss AxioVert 100M inverted microscope with an AxioCam camera (Carl Zeiss, Sliedrecht, the Netherlands).

Cells were cultured and treated using the time points above with the Vybrant Apoptosis assay kit #3 (Molecular Probes) for both adherent and detached cells. In brief, cells were treated with various concentrations of Hi alone (0 to 200 µg/ml), melphalan alone (0 or 8 µg/ml), or with combinations of the drugs for 15 or 30 minutes. Culture medium containing floating cells was removed from the wells and transferred to 5-mL tubes. Adherent cells were washed with RPMI medium, trypsinized with 300 µL of trypsin-EDTA (Biowhitaker), neutralized with 100 µL of HUVEC medium containing 20% FCS, and added to the 5-mL tubes. Tubes were centrifuged for 5 minutes at 250g, and the supernatant was discarded. Cells were then incubated in 200 µL of annexin binding buffer and propidium iodide, with or without annexin V (both reagents from the Vybrant Apoptosis assay kit) at room temperature for 15 minutes in the dark and evaluated by flow cytometry with a FACScan (Becton Dickinson, Alphen aan den Rijn, the Netherlands) flow cytometer. Data were processed with Winmidi software version 2.7 (J. Trotter; Salk Institute, San Diego, CA). Experiments were done three times in duplicate, and the mean and 95% CIs of the percentage of living, apoptotic, and necrotic cells were reported.

Endothelial cell monolayer permeability assay

HUVECs were plated 48 hours before treatment at 6×10^4 cells per well in a monolayer on a fibronectin-coated polycarbonate membrane (diameter = 6.5 mm; pore size = 0.4 µm) in a transwell device (Costar). HUVEC medium (1 mL) was added to the lower compartment. Approximately 24 hours after the cells reached confluence, medium in the upper chamber was replaced with 50 µL of fluorescein isothiocyanate-bovine serum albumin (FITC-BSA) (1 mg/mL; Sigma) plus 250 µL of HUVEC medium containing various concentrations of Hi. At the same time, medium in the lower chamber was replaced with 700 µL of HUVEC medium. Fifty-microliter samples were taken from the lower chamber at various times, and FITC fluorescence was measured with a fluorescence photospectrometer (Victor² FSR; Perkin Elmer, Bucks, U.K.) at 490 nm excitation and 530 nm emission. Values were compared with a standard curve based on known concentrations of FITC-BSA.

Next, to evaluate whether melphalan would have any effect on endothelial cell permeability, directly or in conjunction with Hi, the HUVEC monolayer was exposed to 250 µL of HUVEC medium alone (control), melphalan at 8 µg/mL, or Hi at 100 µg/mL with or without melphalan (8 µg/mL). Permeability was assayed as described above. Experiments were done three times in duplicate. The data were reported as the mean and 95% CIs of all values.

Statistical analysis

Tumor growth curves were plotted as means and 95% CIs of the data from all animals. We used repeated-measure analyses of variance on the three most representative days, taken from the growth curve patterns 4, 8, and 10 using SAS Software release 8.2 for Windows 2000 (SAS institute, Cary, NC) using PROC MIXED. Main effects of treatment and day (three levels: days 4, 8, and 10) were included in the models, as was the interaction between treatment and day. For days in which response was statistically significant, interaction terms were further investigated by testing for differences following treatment on that day.

The data from HUVEC monolayer permeability assays was also analyzed as described above. The effects of treatment and time (5 levels: 0, 15, 30, 45, and 60 minutes) were evaluated. Viability of HUVECs after Hi incubation data was presented and analyzed using the Kruskal-Wallis test with SPSS version 10.0 for Windows 2000.

Melphalan accumulation was shown both as mean values (with 95% CIs) of three measurements performed using different tumor areas and as a ratio between tumor and muscle values, expressed in percentages of tumor versus muscle melphalan uptake. Data were analyzed using the Mann-Whitney U test with SPSS version 10.0 for Windows 2000.

Synergism between Hi and melphalan was evaluated by determining whether tumor response after Hi alone or melphalan alone added together was different from the tumor response after Hi plus melphalan. First, the tumor response index was calculated by dividing the initial tumor volume by the tumor volume on a given day after treatment; then, the tumor response index of a rat from the Hi-treated group was randomly added to the tumor response index of a rat from the melphalan-treated group and compared with the tumor response index from the Hi-plus-melphalan group. Next, the data were analyzed with the Mann-Whitney U test (exact significance [2x(one-tailed significance)]) using SPSS version 10.0 for Windows 2000. All statistical tests were two-sided. For all statistical tests, a P value less than .05 was considered statistically significant.

Results

Tumor response after Hi-based ILP

We previously showed that TNF- α improves the response to ILP by increasing the amount of melphalan delivered to tumor tissues (7). In this study, we used a similar model to test whether another vasoactive molecule, Hi, could also enhance melphalan uptake. A range of Hi concentrations were tested (20 to 200 $\mu\text{g}/\text{mL}$), and the concentration that led to optimal tumor regression was determined to be 200 $\mu\text{g}/\text{mL}$. Tumors grew exponentially in the Brown Norway rats after control ILP. However, the response to Hi plus melphalan ILP was striking, with a regression (more than a 25% decrease in tumor volume) in four (66%) of the six treated animals, including two (33%) with no palpable tumors approximately 10 days after treatment ($p < 0.001$). Perfusion with Hi or melphalan alone reduced or stabilized

tumor growth—three stable (50%) and one regression (17%) (Figure 1A and Table 1). The combination of Hi plus melphalan showed a synergistic effect because the response index of the combination group was statistically significantly greater than that when the response index from the Hi and melphalan alone groups was randomly added ($p=0.043$, Mann-Whitney U test {exact significance [$2 \times$ (one-tailed significance)]}). Perfusion with Hi, either alone or combined with melphalan, did not cause systemic toxicity. Only a transient, mild edema after Hi ILP, both with and without melphalan, was observed, leading to a temporary grade 1 toxicity in two rats for each group. After 2 days, the edema disappeared and limb function returned to normal.

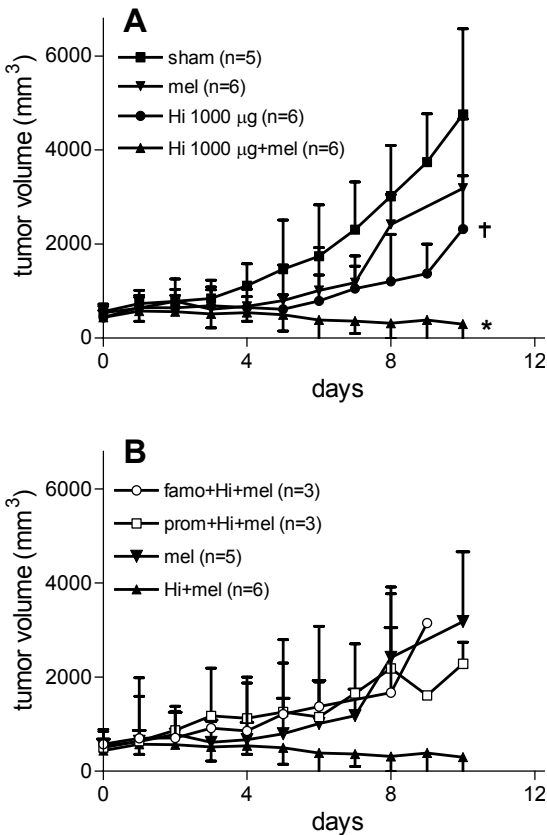


Figure 1 A) Tumor response after histamine-based isolated limb perfusion (ILP): small fragments of BN175 soft-tissue sarcoma were inserted in the right hind limb of Brown Norway rats (see “Materials and Methods”). After 7 to 10 days when tumors reached 12 to 15 mm in diameter, they were randomly submitted to ILP with perfusate alone (sham), 8 µg/mL melphalan (mel), 200 µg/mL histamine (Hi), or 200 µg/mL Hi plus 8 µg/mL melphalan. Tumors were measured daily with a caliper, and tumor volumes were calculated. When tumor diameter exceeded 25 mm, rats were killed. * $p<0.001$ on day 8 and 10 compared with sham; † $p=0.003$ on day 8 and $p<0.001$ on day 10 compared with sham (repeated-measure analyses of variance; two-sided).

B) Involvement of histamine receptors in histamine-based ILP. Promethazine (H_1 receptor inhibitor, 200 µg/mL) or famotidine (H_2 receptor inhibitor, 50 µg/mL) were added in bolus to the perfusate and allowed to circulate for 5 minutes before Hi and melphalan were added. Mean tumor volumes and upper 95% confidence intervals are depicted in both graphs. The number of in-independent experiments (rats) for each treatment is shown in parentheses.

Involvement of Hi receptors in Hi-based ILP

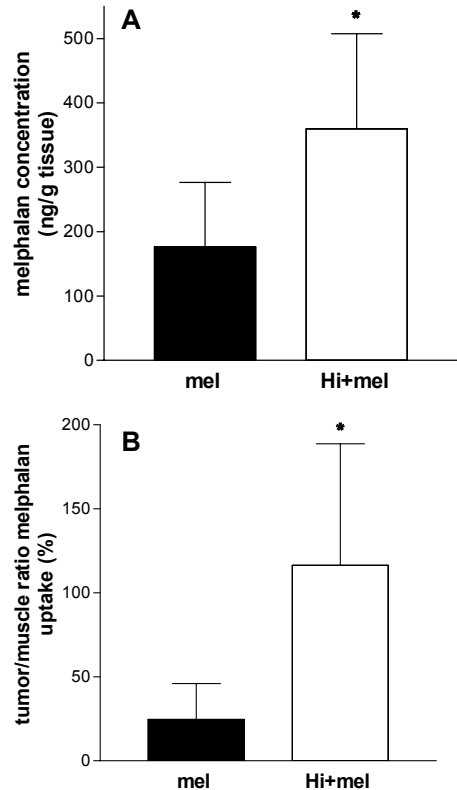
To determine which Hi receptor (H_1 -R or H_2 -R) is involved in the effects observed above, specific Hi inhibitors were used during the treatment. Both pyrillamine, an H_1 -R blocker, and famotidine, an H_2 -R blocker, could block the effect of Hi in the ILP setting, which means that either H_1 or H_2 receptors are involved (Figure 1B).

Table 1. Tumor response after histamine-based ILP

Treatment	CR (%)	PR (%)	NC (%)	PD (%)
Sham (n=5)	-	-	-	100
Melphalan (n=6)	-	17	17	66
Hi (n=6)	-	-	50	50
Hi + melphalan (n=6)	33	33	33	-

Volume on day 9 was compared with that on day 0, and response was classified as follows: PD = progressive disease, increase of more than 25%; NC = no change, volume between -25% and 25%; PR = partial remission, decrease between -25% and -99%; CR = complete response, no palpable tumor. Values are expressed in percentage of animals per response per group.

Figure 2. Indirect effect of Hi on the accumulation of melphalan in tumors treated with isolated limb perfusion (ILP). Both tumor and adjacent muscle were excised immediately after ILP and snapfrozen in liquid nitrogen. Melphalan was measured by gas chromatography–mass spectrometry on at least three different pieces per sample as described in “Materials and Methods”. A) Tumor melphalan concentration. Closed bar, melphalan alone; open bar, Hi plus melphalan. * $p=0.024$ (Mann-Whitney U test, two-tailed). B) Ratio between tumor and muscle melphalan uptake. Closed bar, melphalan alone; open bar, Hi plus melphalan. * $p=0.02$ (Mann-Whitney U test, two-tailed). Mean values with upper 95% confidence intervals are shown.



Indirect effect of Hi on tumor melphalan uptake

We next evaluated whether Hi treatment could indirectly affect tumor-associated vasculature by increasing vascular permeability, which could cause more melphalan to accumulate in tumors than in normal tissue, as we previously showed using TNF combined with melphalan in ILP (7). To compare melphalan uptake in tumors and adjacent muscle, we excised tumors and muscle immediately after ILP with melphalan alone or melphalan combined with Hi and measured melphalan concentration. Hi addition not only led to a

twofold increase in the amount of melphalan in tumor tissue ($p=0.024$) but also reduced melphalan concentration in the muscle. As a result, adding Hi increased the ratio of melphalan in the tumor to that in the adjacent muscle by four ($p=0.02$) (Figure 2).

Histology

To evaluate both the direct and indirect effects of Hi-based ILP on the tumor and the tumor-associated vasculature, we histologically examined tissue sections taken right after ILP was performed. After ILP with 200 $\mu\text{g}/\text{mL}$ Hi alone, scattered vascular damage was observed (Figure 3). After ILP with 200 $\mu\text{g}/\text{L}$ Hi and 8 $\mu\text{g}/\text{L}$ melphalan, vascular damage became more pronounced. Perfusion with Hi alone resulted in vasodilatation of the tumor vasculature, extravasation of red blood cells into the tumor, and damage to the endothelial cell lining of tumor vessels. After ILP with Hi and melphalan, most of the tumor vessels were severely damaged and massive haemorrhage was observed. Tumor vessels showed loss of integrity and extensive gap formation, indicating edema. Red and white blood cells observed in the tissue suggested extravasation.

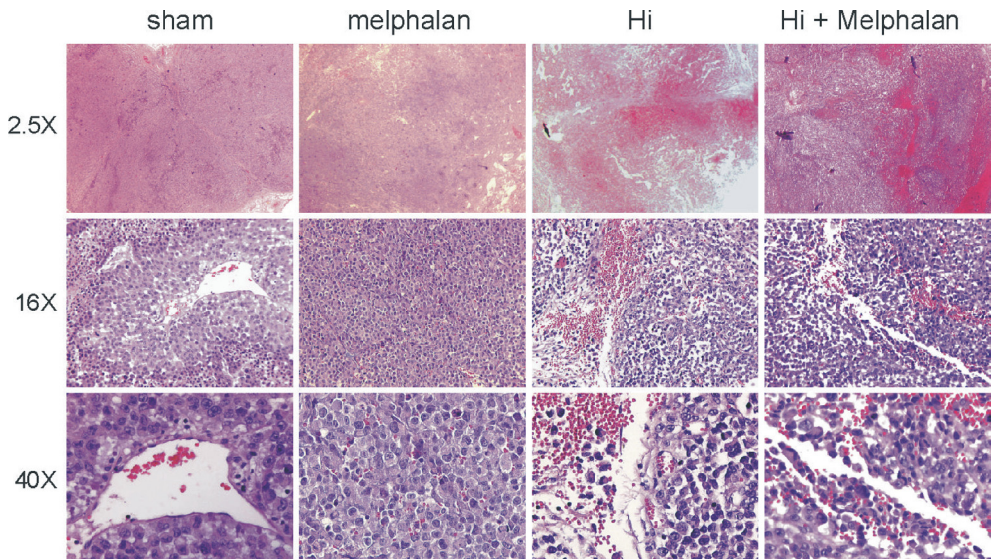


Figure 3. Histology of tumor and adjacent muscle after isolated limb perfusion (ILP). Tumors and muscle were excised immediately after and 24 hours after ILP for each treatment, fixed in 4% formaldehyde solution, and embedded in paraffin for hematoxylin-eosin staining. Perfusate alone (sham) ILP with intact vessels and normal tumor tissue; melphalan 8 $\mu\text{g}/\text{mL}$ ILP with some spots of necrosis on tumor tissue but no vascular damage; Hi-alone 200 $\mu\text{g}/\text{mL}$ ILP showing vascular vasodilatation, extravasation of red blood cells into the tumor and damage to the endothelial cell lining of tumor vessels; Hi plus melphalan (200 $\mu\text{g}/\text{mL}$ and 8 $\mu\text{g}/\text{mL}$, respectively) ILP showing the damage to tumor vessels and massive hemorrhage. Pictures illustrate representative examples of each treatment.

We hypothesize that the edema observed in tumor tissue may indicate an augmented influx of melphalan from the blood stream into the tumor. In the muscle, however, no apparent changes in terms of hemorrhage, vasodilatation, or infiltrates after treatment, as above, were observed (data not shown).

These vascular effects were not observed when rats received sham ILP or melphalan via ILP (Figure 3). After sham ILP, vessels were intact and tumor tissue was unaffected. When tumors were perfused with melphalan alone, some necrosis of the tumor tissue could be observed, but no vascular damage was seen. Together, these results indicate that Hi has tumor vascular-selective activity against the endothelial lining. This vascular effect was even more pronounced when Hi was combined with melphalan.

Cytotoxicity of Hi

The direct cytotoxic effects of Hi on BN175 tumor cells and HUVEC endothelial cells were evaluated by means of *in vitro* cytotoxicity assays. Cell growth was inhibited in a concentration-dependent manner for both cell lines evaluated. BN175 tumor cells were more sensitive to Hi, with an IC_{50} of 30 $\mu\text{g}/\text{mL}$. HUVEC appeared less sensitive to Hi with an IC_{50} of approximately 100 $\mu\text{g}/\text{mL}$ (Figure 4). The cytotoxic effect of Hi combined with melphalan *in vitro* was not synergistic, it was only additive.

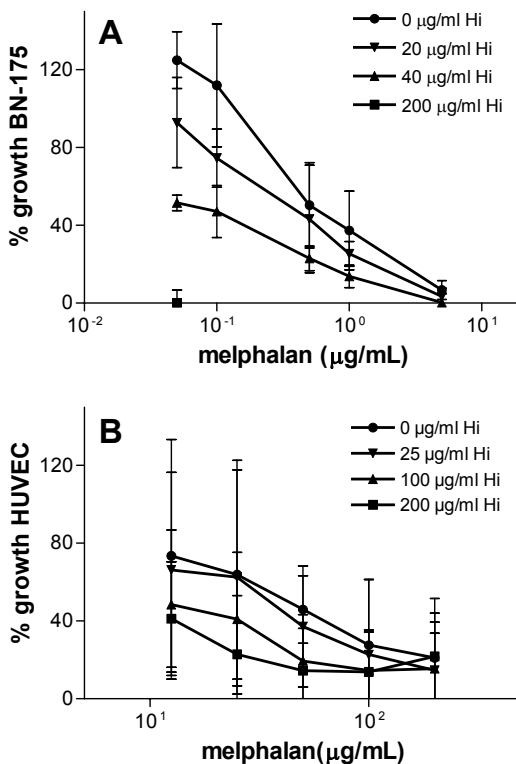


Figure 4. *In vitro* cytotoxicity of Hi according to percentage of tumor growth inhibition. Cells were incubated for 72 hours with different concentrations of Hi with or without melphalan, and cell growth was evaluated using the Sulphorhodamine B assay as described in “Materials and Methods”. A) BN175 sarcoma (Hi 50% inhibitory concentration [IC_{50}] of 30 $\mu\text{g}/\text{mL}$); B) Human umbilical vascular endothelial cells (HUVECs) (Hi IC_{50} of 100 $\mu\text{g}/\text{mL}$). Each point represents an average of four independent experiments. Error bars show 95% confidence intervals of the mean.

Direct effect on HUVEC: morphology and apoptosis assay

In vitro, Hi was only slightly cytotoxic to HUVEC cells after long-term treatment (Figure 4B). Moreover, addition of Hi to melphalan did not enhance the sensitivity of HUVEC toward melphalan (Figure 4B). However, after ILP, a strong effect of Hi on the endothelial lining of tumor vessels was observed (Figure 3). Therefore, we examined the morphology of HUVECs after short incubations (no longer than 60 minutes) with Hi plus melphalan. We observed a dose- and time-dependent effect of Hi on HUVEC, starting with the appearance of gaps between the cells. As time progressed, some cells became rounded and others became extended. In the higher concentration range or after prolonged incubation, cell fragments were seen in the medium (Figure 5). Cells exposed to medium alone did not show these morphologic changes.

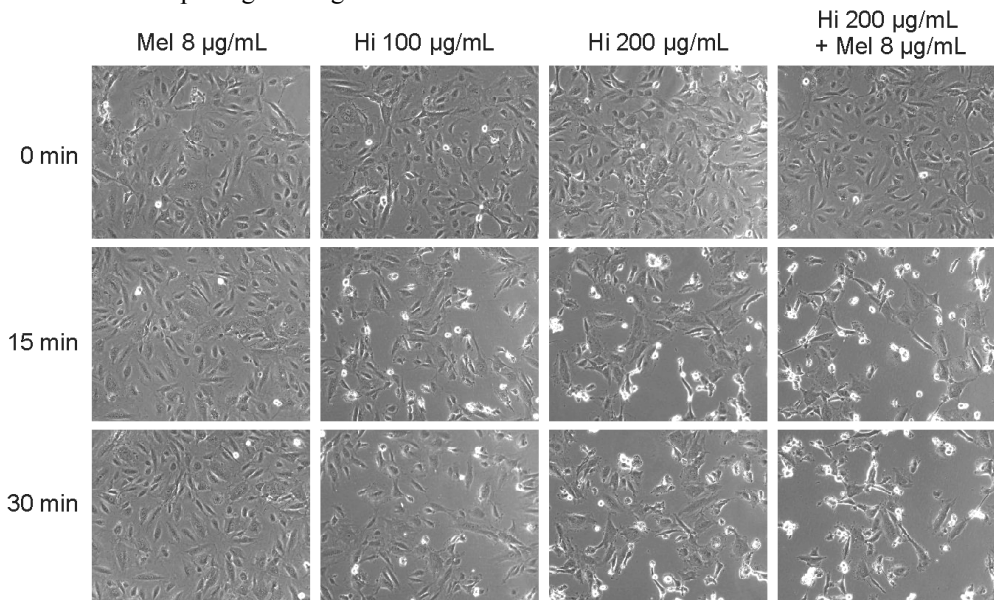


Figure 5. Direct effect of Hi on endothelial cells. Human umbilical vascular endothelial cells (HUVECs) were incubated with medium alone, melphalan (8 µg/mL) alone, Hi (100 µg/mL or 200 µg/mL) alone or in combination for 15 and 30 minutes. Gap formation and morphologic changes can be observed already after 15 minutes incubation both with 100 and 200 µg/mL (a more pronounced effect for 200 µg/mL).

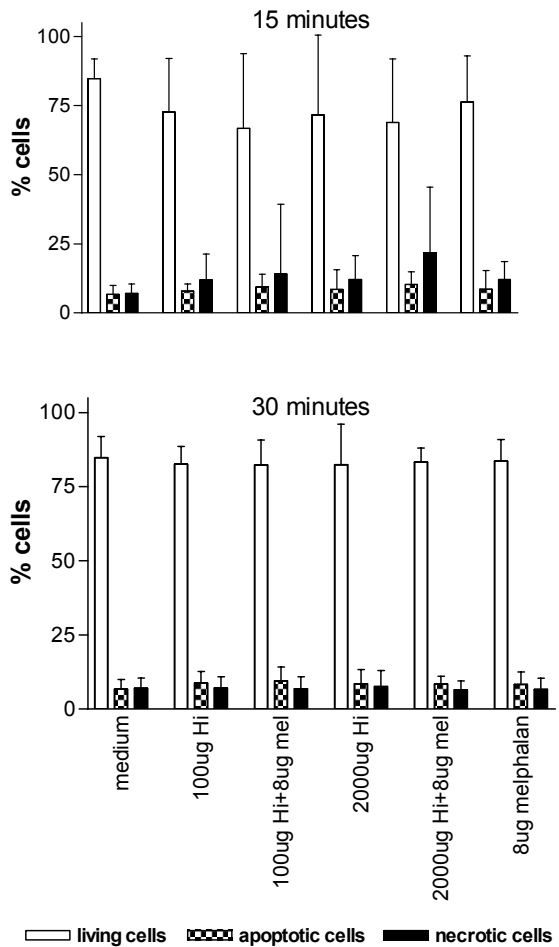
The observed differences in HUVEC morphology after Hi treatment prompted us to investigate whether these changes were irreversible, that is, whether they could lead to apoptosis or necrosis. With YO-PRO and propidium iodide to detect apoptosis and necrosis of adherent cells, respectively, we found no differences in the number of apoptotic or necrotic cells after exposure of HUVECs to Hi compared with exposure to medium alone (data not shown). When all cells, adherent as well as detached, were examined using the Vybrant apoptosis assay, no increase in the number of apoptotic cells or the number of necrotic cells was observed when Hi was added compared with medium alone ($p=0.4$ and

p=0.5, respectively) (Figure 6). Moreover, when Hi was combined with melphalan, still no increase in the number of apoptotic or necrotic cells was seen.

Hi and paracellular permeability in vitro

We observed an increase in melphalan concentration in tumors treated with both drugs, which was accompanied by strong effect of Hi on the tumor associated vasculature after ILP (Figure 2 and 3). Histopathologic examination revealed the Hi-induced formation of gaps *in vivo* in a concentration-dependent manner, requiring a minimum concentration of 200 µg/mL (data not shown). Andriopoulou *et al.* (17) reported that incubation of microvascular endothelial cells for 25 minutes with a relatively low Hi concentration (11 µg/mL) resulted in a 120% and 45% increase in permeability for long- and recently confluent cultures, respectively.

Figure 6. Viability of human umbilical vascular endothelial cells (HUVECs) after short incubation with Hi. HUVECs were plated 24 hours before treatment at 6×10^4 cells per well and grown to confluence. Cells were cultured at 37°C in 5% CO₂ with different concentrations of Hi (0 to 200 µg/mL) and melphalan (0 or 8 µg/mL) for 15 or 30 minutes. The Vybrant Apoptosis assay kit was used to detect apoptosis and necrosis of adherent and detached cells prior to flow cytometric evaluation of the cells. Experiments were done three times in duplicate. The mean percentage, per group of cells, and upper 95% confidence intervals are shown.



We investigated the pattern of permeability using Hi concentrations 10-fold higher than in that study. In line with the findings of Andriopoulou *et al.* (17), we found a concentration- and time-related effect of Hi on HUVEC monolayer permeability as well as a sharper increase in permeability in the first 15 minutes. The results presented in Figure 7A show that exposure of HUVEC to 200 $\mu\text{g}/\text{mL}$ Hi alone resulted in an increase in permeability of fivefold (5.6, 95% CI=3.5 to 7.7) compared with the control, and 100 $\mu\text{g}/\text{mL}$ Hi alone resulted in a two- to threefold (2.8, 95% CI=1.5 to 4.1) increase compared with the control. Incubation with 50 $\mu\text{g}/\text{mL}$ Hi caused only a very slight increase of about 1.5-fold (1.5, 95% CI=1.0 to 2.0). Interestingly, when HUVECs were exposed to 50 $\mu\text{g}/\text{mL}$ or 100 $\mu\text{g}/\text{mL}$ Hi, no additional effect on permeability was observed after 15 and 30 minutes of incubation (curves start to parallel the control), respectively. Exposure of HUVECs to 200 $\mu\text{g}/\text{mL}$ Hi resulted in an ongoing response of HUVECs as shown by the continuing permeability increase compared with control. Even at 60 minutes, the response of HUVECs to Hi did not parallel the control curve. Incubation with melphalan had no effect on the permeability of HUVEC monolayer, neither alone nor in combination with Hi (Figure 7B). The ongoing permeability increase might be essential to the observations *in vivo*.

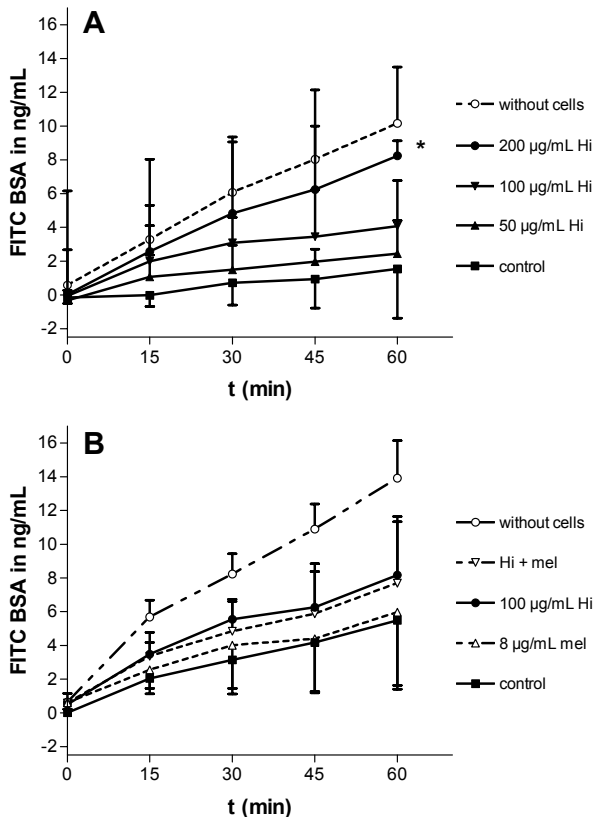


Figure 7. Effect of Hi on human umbilical vascular endothelial cell (HUVEC) monolayer permeability. HUVECs were cultured on the filter of a transwell unit for 48 hours before the addition of fluorescein isothiocyanate and bovine serum albumin (FITC-BSA)-containing medium (control) or A) Hi in different concentrations, B) plus or minus melphalan to the upper compartment (see “Material and Methods”). The amount of FITC-BSA in the lower compartment was measured every 15 minutes for an hour. Values are from three experiments, each done in duplicate. Error bars show 95% confidence intervals of the mean. * p-values using repeated-measure analysis of variance test $p=0.001$ for 200 $\mu\text{g}/\text{mL}$ Hi at 15, 30, 45, and 60 minutes compared with control.

Discussion

This study shows for the first time, to our knowledge, the activity of Hi plus melphalan in ILP for the treatment of soft-tissue sarcomas. The strong effect of Hi-based ILP with melphalan was explained by three mechanisms: 1) direct cytotoxicity to the tumor cells, 2) direct cytotoxicity to the tumor-associated vasculature, and 3) an indirect effect through Hi-mediated, increased melphalan concentration in the tumor.

The direct inhibitory effect of Hi on tumor cells is in accordance with previous reports on Hi receptor expression on different cell lines and human neoplasias, suggesting that it might regulate tumor cell growth (18,19). This growth-inhibitory effect on the tumor cells, combined with the observed direct effect on the endothelial cells, seen by us both *in vitro* and *in vivo*, might be an explanation for the antitumor effect of Hi alone (50% of the tumors stopped growing), compared with control perfusions (all tumors continued to grow). Nevertheless, chemotherapeutic drugs, such as melphalan, for example, must be added to the ILP to achieve a good antitumor response, which coincides with our observations in TNF- α -based ILP (8).

The direct effect of Hi on endothelial cells *in vitro* is more pronounced than that of TNF- α , the current drug of choice for ILP, which we believe adds to the observed tumor response *in vivo*. Hi alone is capable of changing the morphology of endothelial cells after a short incubation period, resulting in gap formation and rounded cells, as shown in Figure 5. When combined with melphalan *in vivo*, the effect on the vasculature is much more evident, with diffuse gap formation and destruction of endothelial cell lining observed immediately after the ILP. In the standard treatment using TNF- α plus melphalan, destruction of the endothelial lining is a secondary effect and takes a couple of days to become evident (20). Therefore, ILP with Hi would likely enhance drug uptake more quickly and effectively than ILP with TNF- α .

The *in vitro* permeability results were in accordance with the *in vivo* findings of an augmented uptake of melphalan in the tumor as well as a decrease in the muscular concentration, reducing regional toxicity. It is remarkable that the Hi concentration used in the ILP (200 $\mu\text{g}/\text{mL}$) led to a continuous increase in the permeability of endothelial cells, which is different from the standard described short-term effect of Hi that occurs only for the first 15 minutes of exposure (18). We speculate that with the Hi concentration used in the ILP, a threshold is reached that triggers a prolonged cellular response, a supposition that is currently under investigation.

Another potential advantage of Hi over TNF- α is its pharmacokinetics. Hi has a very short half-life in serum - 0.35 minutes versus 20 minutes for TNF- α (21). Hi is metabolized through two major pathways in humans; the main pathway involves ring methylation and is catalyzed by the enzyme histamine-*N*-methyltransferase, which is widely distributed in the tissues. Most of the product, *N*-methylhistamine, is converted by monoamine oxidase to *N*-

methyl imidazole acetic acid. Alternatively, Hi can undergo oxidative deamination, catalyzed mainly by the nonspecific enzyme diamine oxidase. The products are imidazole acetic acid and its riboside, which have little or no activity and are excreted in the urine (13). Although these data come from studies with lower dosages or endogenous Hi, the wide distribution of and fast action of the enzymes that metabolize Hi means that Hi is a potentially safer drug than TNF- α in case of leakage into the systemic circulation during ILP. Furthermore, these properties of Hi pharmacokinetics open new possibilities of application in, for example, isolated liver perfusion. More studies on the pharmacokinetics of higher doses and evaluation in the clinical setting are, however, essential for the clinical translation of Hi.

Our findings support a tumor endothelial cell-specific targeting effect of Hi resulting in dramatic hemorrhage and destruction of the endothelial cell lining of tumor vessels (confirmed with CD-31 staining [data not shown]) *in vivo*. We hypothesize that the pronounced direct effect of Hi on the endothelial cell lining is fundamental for the better response than that achieved by melphalan alone in the ILP model discussed here.

H₁ and H₂ receptors were involved in Hi-induced tumor regression in our model. Each receptor inhibitor alone blocked the Hi effect *in vivo*. The two receptors are located in different cell types and have independent mechanisms of action: H₁-R has a higher affinity, a rapid but short-lived effect, and is located in the endothelial cells; H₂-R has a lower affinity, a slower but more sustained effect, and is located in the vascular smooth muscle cells.

Toxicity would be unlikely to be a limiting factor for the use of Hi in ILP in humans because no systemic toxicity was observed, and the regional toxicity, affecting 33% of the rats receiving Hi either alone or combined with melphalan, was very mild and completely reversible after 2 days of recovery. Accordingly, ILP with TNF- α and melphalan in the clinical setting, as Hi plus melphalan did in the animal model, also results in erythema and edema, which sometimes slightly impairs motility (grades II and III of Wieberdink, respectively) in most of the patients (6,22).

In conclusion, Hi combined with melphalan had a striking effect in the ILP for the treatment of soft-tissue sarcomas in rats. The mechanism of action involved both direct and indirect effects - cytotoxicity on the tumor and endothelial cells and tumor-associated vasculature with a twofold increase in the tumoral uptake of melphalan combined with a reduction in the uptake in the adjacent muscle. Therefore, Hi plus melphalan in ILP seems to be a promising alternative to TNF- α , to be evaluated in the clinical setting.

Acknowledgements

F. Brunstein was supported by a grant from CAPES-MEC Brazil, process number 1237/01-2. A. Eggermont was supported by a grant from Maxim Pharmaceuticals.

We thank Maxim Pharmaceuticals, Inc., San Diego, CA, for kindly providing histamine dihydrochloride injections for the studies. We thank Gerard J. J. M. Borsboom from the Department of Public Health, Erasmus MC, University Medical Center Rotterdam, Rotterdam, the Netherlands, for expert assistance with statistical evaluation of the manuscript.

References

1. Lienard D, Lejeune FJ, Ewalenko P. In transit metastases of malignant melanoma treated by high dose rTNF alpha in combination with interferon-gamma and melphalan in isolation perfusion. *World J Surg.* 1992;16(2):234-240.
2. Eggermont AM, Schraffordt KH, Lienard D, et al. Isolated limb perfusion with high-dose tumor necrosis factor-alpha in combination with interferon-gamma and melphalan for nonresectable extremity soft tissue sarcomas: a multicenter trial. *J Clin Oncol.* 1996;14(10):2653-2665.
3. Eggermont AM, Schraffordt KH, Klausner JM, et al. Isolated limb perfusion with tumor necrosis factor and melphalan for limb salvage in 186 patients with locally advanced soft tissue extremity sarcomas. The cumulative multicenter European experience. *Ann Surg.* 1996;224(6):756-764.
4. Olieman AF, Lienard D, Eggermont AM, et al. Hyperthermic isolated limb perfusion with tumor necrosis factor alpha, interferon gamma, and melphalan for locally advanced nonmelanoma skin tumors of the extremities: a multicenter study. *Arch Surg.* 1999;134(3):303-307.
5. Bickels J, Manusama ER, Gutman M, et al. Isolated limb perfusion with tumour necrosis factor-alpha and melphalan for unresectable bone sarcomas of the lower extremity. *Eur J Surg Oncol.* 1999;25(5):509-514.
6. Eggermont AM, de Wilt JH, ten Hagen TL. Current uses of isolated limb perfusion in the clinic and a model system for new strategies. *Lancet Oncol.* 2003;4(7):429-437.
7. de Wilt JH, ten Hagen TL, de Boeck G, van Tiel ST, de Bruijn EA, Eggermont AM. Tumour necrosis factor alpha increases melphalan concentration in tumour tissue after isolated limb perfusion. *Br J Cancer.* 2000;82(5):1000-1003.
8. de Wilt JH, Manusama ER, van Tiel ST, van Ijken MG, ten Hagen TL, Eggermont AM. Prerequisites for effective isolated limb perfusion using tumour necrosis factor alpha and melphalan in rats. *Br J Cancer.* 1999;80(1-2):161-166.
9. Manusama ER, Nooijen PT, Stavast J, Durante NM, Marquet RL, Eggermont AM. Synergistic antitumour effect of recombinant human tumour necrosis factor alpha with melphalan in isolated limb perfusion in the rat. *Br J Surg.* 1996;83(4):551-555.
10. Manusama ER, Stavast J, Durante NM, Marquet RL, Eggermont AM. Isolated limb perfusion with TNF alpha and melphalan in a rat osteosarcoma model: a new anti-tumour approach. *Eur J Surg Oncol.* 1996;22(2):152-157.
11. van Der Veen AH, de Wilt JH, Eggermont AM, van Tiel ST, Seynhaeve AL, ten Hagen TL. TNF-alpha augments intratumoural concentrations of doxorubicin in TNF-alpha-based isolated limb perfusion in rat sarcoma models and enhances anti-tumour effects. *Br J Cancer.* 2000;82(4):973-980.
12. van Etten B, de Vries MR, van Ijken MG, et al. Degree of tumour vascularity correlates with drug accumulation and tumour response upon TNF-alpha-based isolated hepatic perfusion. *Br J Cancer.* 2003;88(2):314-319.
13. Garison JC Histamine, bradykinin, 5-hydroxytryptamine and their antagonists. *In Goodman Gilman A, Rall TW, Nie AS, and Taylor P (eds.), The pharmacological basis of therapeutics, 8th ed, pp. 575-599. Elmsford (NY): Pergamon Press, 1990.*
14. Kort WJ, Zondervan PE, Hulsman LO, Weijma IM, Westbroek DL. Incidence of spontaneous tumors in a group of retired breeder female brown Norway rats. *J Natl Cancer Inst.* 1984;72(3):709-713.
15. de Boeck G, van Cauwenberghe K, Eggermont AM, Van Oosterom AT, de Bruijn EA. Determination of melphalan and hydrolysis products in body fluids by GC-MS. *J High Resolut Chromatogr.* 1997;20:697-700.
16. Skehan P, Storeng R, Scudiero D, et al. New colorimetric cytotoxicity assay for anticancer-drug screening. *J Natl Cancer Inst.* 1990;82(13):1107-1112.
17. Andriopoulou P, Navarro P, Zanetti A, Lampugnani MG, Dejana E. Histamine induces tyrosine phosphorylation of endothelial cell-to-cell adherens junctions. *Arterioscler Thromb Vasc Biol.* 1999;19(10):2286-2297.
18. Cricco G, Martin G, Labombarda F, Cocca C, Bergoc R, Rivera E. Human pancreatic carcinoma cell line Panc-I and the role of histamine in growth regulation. *Inflamm Res.* 2000;49 Suppl 1:S68-9.:S68-S69.

19. Valencia S, Hernandez-Angeles A, Soria-Jasso LE, Arias-Montano JA. Histamine H(1) receptor activation inhibits the proliferation of human prostatic adenocarcinoma DU-145 cells. *Prostate*. 2001;48(3):179-187.
20. Nooijen PT, Manusama ER, Eggermont AM, et al. Synergistic effects of TNF-alpha and melphalan in an isolated limb perfusion model of rat sarcoma: a histopathological, immunohistochemical and electron microscopical study. *Br J Cancer*. 1996;74(12):1908-1915.
21. Rizell M, Naredi P, Lindner P, Hellstrand K, Sarno M, Jansson PA. Histamine pharmacokinetics in tumor and host tissues after bolus-dose administration in the rat. *Life Sci*. 2002;70(8):969-976.
22. Wieberdink J, Benckhuysen C, Braat RP, van Slooten EA, Olthuis GA. Dosimetry in isolation perfusion of the limbs by assessment of perfused tissue volume and grading of toxic tissue reactions. *Eur J Cancer Clin Oncol*. 1982;18(10):905-910.

Chapter 4

Lack of synergy between histamine and IL-2 in the melphalan-based isolated limb perfusion

Flavia Brunstein¹, Saske Hoving¹, Gisela aan de Wiel-Ambagtsheer¹, Gert de Boeck², Alexander MM Eggermont¹, Timo LM ten Hagen¹

¹Department of Surgical Oncology, Erasmus MC-Daniel den Hoed Cancer Center, Rotterdam, the Netherlands

²Department of Experimental Oncology, University of Leuven, Leuven, Belgium

Abstract

Histamine (Hi) combined to melphalan in isolated limb perfusion (ILP) resulted in overall response rates (OR) of 66%. Likewise, Interleukin-2 (IL-2) resulted in OR of 67%, when combined to melphalan in ILP. In systemic immunotherapy the combination of IL-2 and Hi has been used on solid tumors based on immunomodulatory effects. In this study we used our well-established ILP experimental rat model to evaluate whether the synergistic effect between the two drugs seen in the systemic setting, could further improve response rates in a loco-regional setting. Histological evaluation was done directly and 24 hours after ILP. Melphalan uptake by tumor and muscle was measured. Hi and IL-2 together, combined to melphalan ILP led to OR of only 28%. Histology of tumors demonstrated partial loss of Hi-induced haemorrhagic effect when IL-2 was present. Melphalan accumulation in the tumor when both Hi and IL-2 were added (3.1 fold) was very similar to accumulation with Hi only (2.8 fold), or IL-2 only (3.5 fold) combined to melphalan. *In vitro* there was no synergy between the drugs. In conclusion, the positive synergistic effect between IL-2 and Hi is lost in the regional setting.

Introduction

We have demonstrated that isolated limb perfusion with TNF and melphalan leads to excellent antitumor effects against melanoma (1), large soft tissue sarcomas (2,3) and various other tumors in the clinical setting (4-6). The basis for the synergy being primarily a significant enhancement of tumor-specific melphalan accumulation and secondarily the complete destruction of tumor associated vasculature (2,7). The enhanced uptake of different cytotoxic agents shown in various limb and liver tumor models in our laboratory with the combination of TNF and melphalan, prompted us to investigate a number of vasoactive drugs for similar potential effects (7-12). The inflammatory mediator histamine (Hi) was an almost obvious candidate due to its effects on fine vessels with the formation of edema and also the formation of gaps between endothelial cells (13). Indeed, it strongly augmented tumor response in melphalan-based ILP with OR of 66% (14). Similarly we found that the cytokine IL-2, known to cause significant changes in vascular permeability and the vascular leakage syndrome when administered at high concentrations (15-17), dramatically improved tumor response in melphalan-based ILP (18).

Interleukin-2 (IL-2) has been widely used in the systemic immunotherapy of solid tumors and leukemias (19) based on immunomodulatory effects which can be further enhanced by combining histamine (20).

Based on this synergistic effects of IL-2 and Hi seen in the systemic setting we evaluated whether this could be also present in the loco-regional setting further improving the good response rates observed with Hi or IL-2 alone in melphalan-based ILP.

Materials and Methods

Animals and tumor cell line

Male inbred Brown Norway (BN) rats were obtained from Harlan-CPB (Austerlitz, the Netherlands), weighing 250-300g. Animals were housed at the Central Animal Facility of the Erasmus MC Rotterdam and fed a standard laboratory diet *ad libitum* (Hope Farms Woerden, the Netherlands).

The syngeneic spontaneous rapidly growing and metastasizing BN175 soft tissue sarcoma (21) was kept in liquid nitrogen and implanted on the dorsum of a BN rat for further growth before being inserted in the right hind limb of the experimental animals.

All animal studies were done in accordance with protocols approved by the Animal Care Committee of the Erasmus University Rotterdam, the Netherlands.

Isolated limb perfusion protocol

Small fragments (3 mm) of the syngeneic BN175 sarcoma were inserted subcutaneously in the right hind leg of the animals as previously described (7,9). Tumor growth was measured daily with a caliper and the volume was calculated using the formula $0.4(A^2 \times B)$ (where B represents the largest tumor diameter and A is the diameter perpendicular to B). When tumor diameter exceeded 25 mm or at the end of the experiment rats were killed by cervical dislocation, under anesthesia.

The treatment consisted of the experimental ILP, previously described (7,9). Briefly, 7-10 days after inserting tumor fragments they reached a diameter between 12-15 mm and were amenable to the procedure. Under anesthesia (intraperitoneal ketamine and intramuscular hypnomidate), the inguinal vessels were reached through an incision parallel to the inguinal ligament, cannulated and connected via a roller pump to an oxygenated reservoir where drugs were added in boluses. A groin tourniquet occluded collateral vessels, warranting a proper isolation of the limbs.

Drugs, 40 µg melphalan (Alkeran® Wellcome, Beckenham, United Kingdom), 50 µg IL-2 (kindly provided by Chiron Amsterdam, the Netherlands) and/or 1000 µg of Hi (kindly provided by Maxim Pharmaceuticals Inc., San Diego, CA) were added to the reservoir containing 5 ml Haemaccel (Boehring Pharma, Amsterdam, the Netherlands). Between six and nine rats were included in each group.

Tumor dimensions were measured every day and response was classified, according to the lowest value obtained, as progressive disease (PD) volume increase of more than 25%; no change (NC) volume kept in the range of -25% to +25%; partial remission (PR) decrease between -25% and -90% or complete response (CR), tumor volume less than 10% of initial volume (22)

Limb function was a clinical observation in which the rat's ability to walk and stand on the perfused limb was scored after ILP. On this scale grade 0 means a severe impaired function

where the rat drags its hindlimb without any function; grade 1 indicates a slightly impaired function, meaning the hindlimb is not used in a normal way but the rat stands on it when rising; finally grade 2 indicates an intact hindlimb function and normal walking and standing pattern is observed.

Histologic evaluation after ILP

Two animals for each group were killed right after ILP, tumors were excised, fixed in 4% formaldehyde solution and embedded in paraffin before staining with hematoxylin and eosin. Images were taken on a Leica microscope supplied with a Sony 3CCD DXC camera.

In vivo melphalan uptake

Right after ILP with either melphalan alone; melphalan plus Hi; melphalan plus IL-2 or melphalan plus Hi and IL-2, rats were killed by cervical dislocation. Tumors and muscle were removed and quickly frozen in liquid nitrogen and stored at -80°C. Next, they were homogenized in 2 ml acetonitrile (PRO 200 homogenizer, Pro Scientific, CT, USA) and centrifuged before melphalan was measured by gas chromatography-mass spectrometry (GC-MS), as previously described (7,23). Between five and six rats were included in each group.

Cytotoxicity assay

BN175 tumor cells were first grown in RPMI-1640 medium (Life Technologies, the Netherlands) supplemented with 10% fetal calf serum and 0.1% penicillin-streptomycin (Life Technologies, the Netherlands).

Cells were plated 24 hours before treatment in 96-wells, flat-bottomed, microtiter plates (Costar, Cambridge, MA, USA) at 10^5 cells per well (100 μ l) and allowed to grow as a monolayer. Next, they were incubated at 37°C in 5% CO₂ for 72 hours in the presence of medium alone or medium plus different concentrations of IL-2 and Hi. Hi ranged from 0 to 200 μ g/ml and IL-2 from 0 to 20 μ g/ml.

Growth of tumor cells was measured using the Sulphorhodamine-B (SRB) assay (24). In brief, cells were washed with phosphate buffered saline, incubated with 10% trichloric acetic acid for one hour at a temperature of 4°C and washed again. Cells were then stained with SRB for about 15 to 30 minutes, washed with 1% acetic acid and allowed to dry. Protein-bound SRB was dissolved in TRIS (10mM, pH 9.4). Extinction was measured at 540 nm and the percentage of growth inhibition was calculated according to the formula: percentage of tumor cell growth = (test well/control well) x 100%. The drug concentration leading to 50% reduction in the absorbance, as compared to control (IC₅₀), was determined from the growth curve. The experiments were repeated four times.

Human umbilical vein endothelial cells (HUVEC) were prepared by collagenase treatment of freshly obtained human umbilical veins and cultured in Human endothelial SFM/RPMI medium (Biotechnologies, the Netherlands) supplemented with heat inactivated human serum (Biowhitaker, the Netherlands), new born calf serum, human EGF, human bFGF and 0.1% penicillin-streptomycin (Life Technologies, the Netherlands).

HUVEC were plated 24 hours before treatment at 6×10^4 cells per well and cultured as described above. Growth inhibition and IC_{50} were determined as for the BN175.

Statistical analysis

Kruskal-Wallis and Mann-Whitney U tests were used to evaluate statistical significance of the results. All statistical tests were two-sided and P values less than 0.05 were considered as statistical significant. Calculations were performed on a personal computer using Prism v3.0 software (GraphPad Software Inc.) and SPSS v10.0 for Windows 2000.

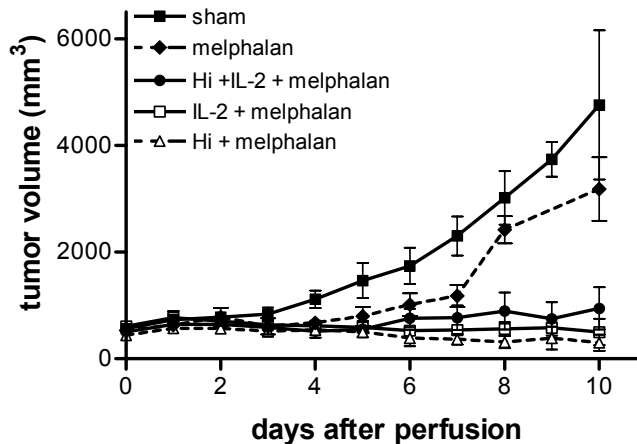


Figure 1. Tumor response after isolated limb perfusions. Small fragments of BN175 soft tissue sarcomas were inserted in the right hind limb of brown Norway rats (see Material and methods). When tumors reached 12-15 mm (7-10 days), rats were randomly submitted to ILP with perfusate alone (sham); 8 $\mu\text{g}/\text{mL}$ melphalan; 200 $\mu\text{g}/\text{mL}$ Hi plus 50 $\mu\text{g}/\text{mL}$ IL-2 plus 8 $\mu\text{g}/\text{mL}$ melphalan; 50 $\mu\text{g}/\text{mL}$ IL-2 plus 8 $\mu\text{g}/\text{mL}$ melphalan or 200 $\mu\text{g}/\text{mL}$ Hi plus 8 $\mu\text{g}/\text{mL}$ melphalan. Tumors were measured daily with a caliper and volumes were calculated. Mean tumor volume are shown \pm SEM.

Results

Tumor response study

Sham perfusion and IL-2 alone perfusions did not inhibit tumor growth, whereas ILP with Hi alone resulted in tumor growth stabilization in 50% of the rats. Melphalan ILP arrested tumor growth in 2 rats for at least 4 days. As expected from the previous studies, Hi plus melphalan and IL-2 plus melphalan had both 66% OR.

ILP with the triple combination of IL-2, Hi and melphalan resulted in a tumor growth inhibition apparently slightly less pronounced as observed after ILP with IL-2 or Hi combined with melphalan. With the triple combination an OR of only 28% was obtained, accounting for 2 rats out of 7 with a PR. As for the other 5 rats there was 2 NC (29%) and 3 PD (42%) (Figure 1, Table 1).

No serious regional toxicity was observed in any of the treatments. There was only some edema associated with the use of Hi but without any implication on limb function.

Table 1. Response in BN175 soft tissue sarcoma-bearing rats after melphalan-based ILP in combination with histamine and IL-2.

Treatment ^a	CR (%) ^b	PR (%)	NC (%)	PD (%)
Sham (n=5)	-	-	-	100%
Melphalan (n=6)	-	17%	17%	66%
Hi+IL-2+Melphalan (n=7)	-	29%	29%	42%
IL-2+Melphalan (n=9)	11%	56%	11%	22%
Hi+melphalan (n=6)	33%	33%	33%	-

^a) Melphalan (40 µg), histamine (Hi, 1000 µg) and IL-2 (50 µg) were added as boluses to the perfusate (5 mL), ^b) responses were scored as described in materials and methods. CR complete response, PR Partical response, NC no change, and PD progressive disease.

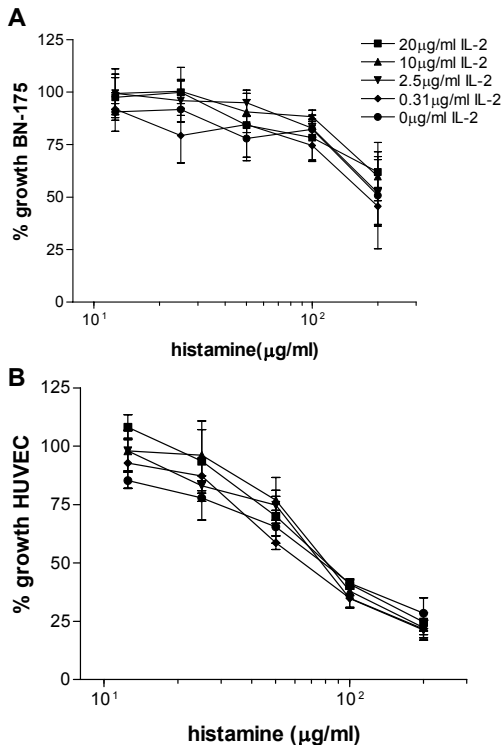


Figure 2. *In vitro* cytotoxicity of Hi and IL-2 according to percentage of tumor growth inhibition on. Cells were incubated for 72h with different concentrations of Hi plus IL-2 and cell growth was evaluated by the sulphorhodamine assay as described in materials and methods section. (A) BN175 soft tissue sarcoma cells and (B) Human umbilical vein endothelial cells. Each point represents an average of four independent experiments. Error bars show Standard Deviations.

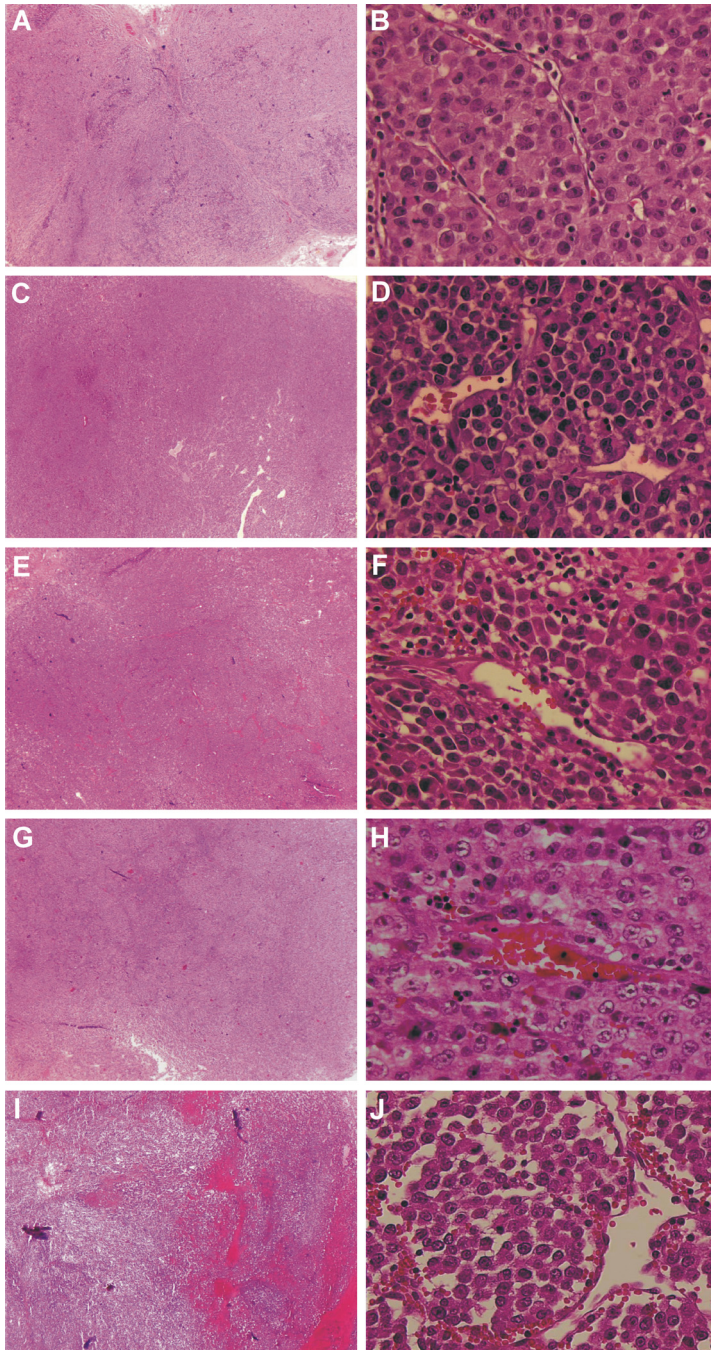


Figure 3. Histology of tumors after isolated limb perfusion (ILP). Tumors were excised immediately after and 24 hours after ILP for each treatment and fixed in 4% formaldehyde solution and embedded in paraffin for hematoxylin-eosin staining. Pictures illustrate the most representative example for each treatment, right after ILP. Sham (A,B), melphalan (C,D), IL-2 + Hi + melphalan (E,F), IL-2 + melphalan (G,H), Hi + melphalan (I,J). Original magnification 2.5X (A,C,E,G,I) and 40X (B,D,F,H,J).

In vitro synergy between Hi and IL-2

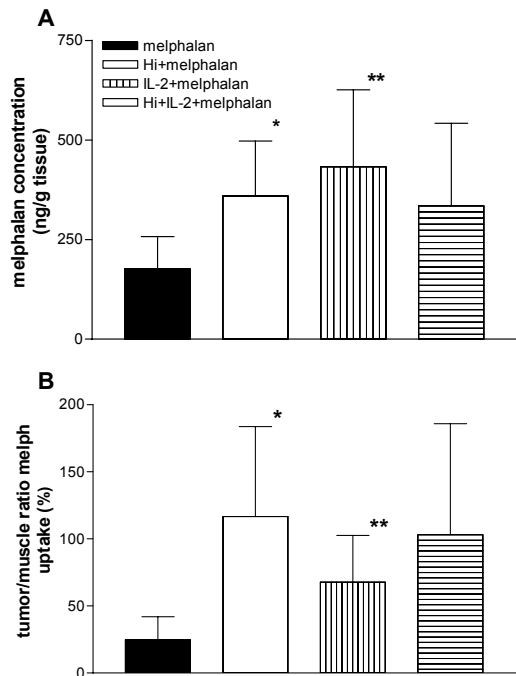
Searching for an explanation for the decrease in the response rates observed when IL-2 was combined to Hi, we first used *in vitro* cytotoxicity assays.

We knew from previous studies that IL-2 had no direct cytotoxic effect on BN175 nor HUVEC (18) whereas with Hi we observed an IC₅₀ of respectively 30 µg/ml (BN175) and 100 µg/ml (HUVEC) (14). We tested the hypothesis whether IL-2 could decrease the direct effect of Hi on the cells. The addition of IL-2 was however ineffective with all curves overlapping each other (Figure 2).

Direct effects on tumor cells and tumor associated vasculature (TAV)

Next we evaluated tumor histology right after ILP, searching for difference in the patterns previously seen. Observations right after ILP and 24 hours after were very similar with a striking loss in the haemorrhagic effect related to Hi. Although we still found some extravasation of red blood cells, the diffuse pattern seen after Hi plus melphalan was gone. Moreover, the massive destruction of the endothelial cell lining characteristic of Hi plus melphalan ILP is softened. The edema between tumor cells is also reduced and the vessels look less dilated than expected after a Hi ILP (Figure 3).

Figure 4. Melphalan accumulation in tumor tissue during melphalan-based ILP. Tumors and muscle were excised right after ILP and quickly frozen in liquid nitrogen. Melphalan was measured by gas chromatography-mass spectrometry (GC-MS) as described material and methods. A) Values obtained in the tumor. * p=0.03 (Hi + melphalan as compared to melphalan); ** p=0.006 (IL-2 + melphalan as compared to melphalan). B) Ratio between tumor and muscle melphalan uptake. * p=0.02 (Hi + melphalan as compared to melphalan); ** p=0.01 (IL-2 + melphalan as compared to melphalan).



Indirect effect on TAV

Finally we evaluated melphalan accumulation in tumor and muscle and compared these values to those previously reported for Hi and IL-2. Accumulation of melphalan after ILP with the triple combination of Hi, IL-2 and melphalan is very similar to the levels obtained after ILP with Hi or IL-2. An increase in melphalan accumulation in tumor of 3.1 fold Hi plus IL-2 against 2.8 fold for Hi and 3.5 fold with IL-2 (Figure 4).

Discussion

We have shown in this study that the synergy between Hi and IL-2 seen in the systemic treatment is lost in the regional setting, with a 30% decrease in OR rate, as compared to each drug alone plus melphalan.

A possible explanation might be the dose used in the regional setting, which is in the order of 6 to 8 times higher than those reported for the systemic treatment (14,25), or the much shorter exposure time in the ILP. In this different pharmacokinetic scenario the combination of two inflammatory agents could lead to a down regulation of their action and consequently to the lost in efficacy. A similar effect was previously reported with the combination of histamine and TNF- α (26,27).

Besides, we hypothesize that the mechanism of action of Hi in the regional setting is quite different from the systemic one. Instead of the immunological effect involved in the systemic setting effect, we propose a triplet action of Hi in the ILP: a direct cytotoxic effect on TAV, a direct cytotoxic effect on tumor cells and an indirect effect on tumor vasculature, increasing drug accumulation in the tumor (14).

The reduction on haemorrhagic effect seen when IL-2 is combined to ILP with Hi and melphalan is surprising, as IL-2 apparently had no direct effect on endothelial cells nor on the activity of Hi towards endothelial cells. Still, IL-2 also increased melphalan accumulation in the tumor after ILP. According to our findings, there was a very similar melphalan accumulation in the tumor, whether or not IL-2 and Hi were combined. Based on these findings, we speculate that the lost in Hi-induced haemorrhage and vascular destruction would be responsible for the reduced OR (from 66% to only 28%), when IL-2 was combined.

In conclusion the association of Hi and IL-2 in the Melphalan-based ILP setting does not improve response, far the opposite, it diminishes response rates observed with either drug alone plus melphalan in the ILP.

Acknowledgments

We thank Maxim Pharmaceuticals Inc., San Diego, CA for kindly providing Histamine Dihydrochloride for the studies. We thank Chiron, Amsterdam, the Netherlands for kindly providing IL-2.

References

1. Lienard D, Lejeune FJ, Ewalenko P. In transit metastases of malignant melanoma treated by high dose rTNF alpha in combination with interferon-gamma and melphalan in isolation perfusion. *World J Surg.* 1992;16(2):234-240.
2. Eggermont AM, Schraffordt KH, Lienard D, et al. Isolated limb perfusion with high-dose tumor necrosis factor-alpha in combination with interferon-gamma and melphalan for nonresectable extremity soft tissue sarcomas: a multicenter trial. *J Clin Oncol.* 1996;14(10):2653-2665.
3. Eggermont AM, Schraffordt KH, Klausner JM, et al. Isolated limb perfusion with tumor necrosis factor and melphalan for limb salvage in 186 patients with locally advanced soft tissue extremity sarcomas. The cumulative multicenter European experience. *Ann Surg.* 1996;224(6):756-764.
4. Bickels J, Manusama ER, Gutman M, et al. Isolated limb perfusion with tumour necrosis factor-alpha and melphalan for unresectable bone sarcomas of the lower extremity. *Eur J Surg Oncol.* 1999;25(5):509-514.
5. Olieman AF, Lienard D, Eggermont AM, et al. Hyperthermic isolated limb perfusion with tumor necrosis factor alpha, interferon gamma, and melphalan for locally advanced nonmelanoma skin tumors of the extremities: a multicenter study. *Arch Surg.* 1999;134(3):303-307.
6. Eggermont AM, de Wilt JH, ten Hagen TL. Current uses of isolated limb perfusion in the clinic and a model system for new strategies. *Lancet Oncol.* 2003;4(7):429-437.
7. de Wilt JH, ten Hagen TL, de Boeck G, van Tiel ST, de Bruijn EA, Eggermont AM. Tumor necrosis factor alpha increases melphalan concentration in tumour tissue after isolated limb perfusion. *Br J Cancer.* 2000;82(5):1000-1003.
8. de Wilt JH, Manusama ER, van Tiel ST, van Ijken MG, ten Hagen TL, Eggermont AM. Prerequisites for effective isolated limb perfusion using tumour necrosis factor alpha and melphalan in rats. *Br J Cancer.* 1999;80(1-2):161-166.
9. Manusama ER, Stavast J, Durante NM, Marquet RL, Eggermont AM. Isolated limb perfusion with TNF alpha and melphalan in a rat osteosarcoma model: a new anti-tumour approach. *Eur J Surg Oncol.* 1996;22(2):152-157.
10. Manusama ER, Nooijen PT, Stavast J, Durante NM, Marquet RL, Eggermont AM. Synergistic antitumour effect of recombinant human tumour necrosis factor alpha with melphalan in isolated limb perfusion in the rat. *Br J Surg.* 1996;83(4):551-555.
11. van Der Veen AH, de Wilt JH, Eggermont AM, van Tiel ST, Seynhaeve AL, ten Hagen TL. TNF-alpha augments intratumoural concentrations of doxorubicin in TNF-alpha-based isolated limb perfusion in rat sarcoma models and enhances anti-tumour effects. *Br J Cancer.* 2000;82(4):973-980.
12. van Etten B, de Vries MR, van Ijken MG, et al. Degree of tumour vascularity correlates with drug accumulation and tumour response upon TNF-alpha-based isolated hepatic perfusion. *Br J Cancer.* 2003;88(2):314-319.
13. Garison JC Histamine, bradykinin, 5-hydroxytryptamine and their antagonists. *In Goodman Gilman A, Rall TW, Nie AS, and Taylor P (eds.), The pharmacological basis of therapeutics, 8th ed, pp. 575-599. Elmsford (NY): Pergamon Press, 1990.*
14. Brunstein F, Hoving S, Seynhaeve AL, et al. Synergistic antitumor activity of histamine plus melphalan in isolated limb perfusion: preclinical studies. *J Natl Cancer Inst.* 2004;96(21):1603-1610.
15. Epstein AL, Mizokami MM, Li J, Hu P, Khawli LA. Identification of a protein fragment of interleukin 2 responsible for vasopermeability. *J Natl Cancer Inst.* 2003;95(10):741-749.
16. Siegel JP, Puri RK. Interleukin-2 toxicity. *J Clin Oncol.* 1991;9(4):694-704.
17. Winkelhake JL, Gauny SS. Human recombinant interleukin-2 as an experimental therapeutic. *Pharmacol Rev.* 1990;42(1):1-28.
18. Hoving S, Brunstein F, aan de Wiel-Ambagtsheer G, et al. Synergistic antitumor response of IL-2 with melphalan in isolated limb perfusion in soft-tissue sarcoma bearing rats. *Cancer Res.* 2005;65(10):4300-4308.
19. Naredi P. Histamine as an adjunct to immunotherapy. *Semin Oncol.* 2002;29(3 Suppl 7):31-34.
20. Hellstrand K. Histamine in cancer immunotherapy: a preclinical background. *Semin Oncol.* 2002;29(3 Suppl 7):35-40.
21. Kort WJ, Zondervan PE, Hulsman LO, Weijma IM, Westbroek DL. Incidence of spontaneous tumors in a group of retired breeder female brown Norway rats. *J Natl Cancer Inst.* 1984;72(3):709-713.
22. Manusama ER, Nooijen PT, Stavast J, Durante NM, Marquet RL, Eggermont AM. Synergistic antitumour effect of recombinant human tumour necrosis factor alpha with melphalan in isolated limb perfusion in the rat. *Br J Surg.* 1996;83(4):551-555.
23. de Boeck G, van Cauwenbergh K, Eggermont AM, Van Oosterom AT, de Bruijn EA. Determination of melphalan and hydrolysis products in body fluids by GC-MS. *J High Resolut Chromatogr.* 1997;20:697-700.
24. Skehan P, Storeng R, Scudiero D, et al. New colorimetric cytotoxicity assay for anticancer-drug screening. *J Natl Cancer Inst.* 1990;82(13):1107-1112.

25. Asea A, Hermodsson S, Hellstrand K. Histaminergic regulation of natural killer cell-mediated clearance of tumour cells in mice. *Scand J Immunol.* 1996;43(1):9-15.
26. Azuma Y, Shinohara M, Wang PL, Hidaka A, Ohura K. Histamine inhibits chemotaxis, phagocytosis, superoxide anion production, and the production of TNF α and IL-12 by macrophages via H2-receptors. *Int Immunopharmacol.* 2001;1(9-10):1867-1875.
27. Hayley S, Kelly O, Anisman H. Murine tumor necrosis factor- α sensitizes plasma corticosterone activity and the manifestation of shock: modulation by histamine. *J Neuroimmunol.* 2002;131(1-2):60-69.

Chapter 5

Early changes in tumor pathophysiology during TNF-based isolated limb perfusion determines response

Saske Hoving¹, Ann LB Seynhaeve¹, Sandra T van Tiel¹, Gisela aan de Wiel-Ambagtsheer¹, Ernst A de Bruijn², Alexander MM Eggermont¹, Timo LM ten Hagen¹

¹Department of Surgical Oncology, Erasmus MC-Daniel den Hoed Cancer Center, Rotterdam, the Netherlands

²Department of Experimental Oncology, University of Leuven, Leuven, Belgium

Abstract

Addition of high-dose TNF to melphalan-based isolated limb perfusion (ILP) enhances anti-tumor effects impressively. The mechanism of action of TNF is still under debate. Here we investigate the effects of TNF on the tumor microenvironment and on secondary immunological events during and shortly after ILP in soft-tissue sarcoma-bearing rats.

Already during ILP softening of the tumor was observed. At the end of the ILP a six-fold enhanced drug uptake of melphalan in the tumor could be demonstrated. Directly after perfusion with TNF plus melphalan a slight increase in vascular destruction, erythrocyte extravasation and necrosis were detected. Strikingly, interstitial fluid pressure (IFP) and pH in the tumor were not altered by TNF. No clear immune effects, cellular infiltration and cytokine expression were observed, although we identified PMNs as key effector cells in TNF-mediated permeability of the endothelial lining.

Taken together, these results indicate that the TNF-induced augmentation of drug accumulation is the key explanation for the observed synergistic anti-tumor response, whereas it is too early for an immune response related to TNF to be detected. Importantly, the augmented accumulation of melphalan is not due to an altered IFP, but most likely results from an increased permeability of the tumor vasculature.

Introduction

Isolated limb perfusion (ILP) with tumor necrosis factor- α (TNF) and melphalan is currently one of the therapies available for the treatment of patients with advanced bulky melanoma and sarcoma of the limbs. Addition of high-dose TNF to the melphalan-based ILP results in impressive enhancement of the response rates of over 80% in a great variety of tumors (reviewed in (1)). Angiographic studies revealed that 1 or 2 weeks after ILP all tumor-associated vessels had disappeared, indicating that TNF only targets tumor vasculature and not normal vessels (2). At the histopathological level at 3 hours after ILP we have shown that the effects of TNF in a melphalan-based ILP starts with intratumoral endothelial cell activation followed by over-expression of adhesion molecules, which in turn leads to polymorphonuclear leukocyte (PMN) homing, endothelium injury and finally coagulative and haemorrhagic necrosis (3,4). Ruegg *et al.* demonstrated that TNF in combination with interferon- γ (IFN) induced downregulation of $\alpha_v\beta_3$ resulting in detachment and subsequent apoptosis of endothelial cells after ILP (5). Yet, ILP with TNF alone does not cause tumor regression without the combination with a chemotherapeutic agent (6).

We developed TNF-based isolated limb perfusion models in rats, with similar results compared to the clinical setting, to gain further insight in the mechanisms underlying the observed synergy. Directly after perfusion with TNF and melphalan or doxorubicin softening of the tumor tissue and significantly enhanced drug uptake were observed (7,8).

Subsequent events were haemorrhagic necrosis, edema, extravasation of erythrocytes, infiltration of polymorphonuclear neutrophils and destruction of tumor vasculature (7,9). Inadequate blood supply in necrotic areas will result in hypoxic and acidic tumor regions and acidic products will accumulate (10,11). Although others showed direct cytotoxic effects of TNF on several different cell lines *in vitro* (12,13) and tumors *in vivo*, like Met A sarcoma, B16BL6 melanoma and Lewis lung carcinoma (13-15), we observed in our tumor models that TNF alone had no anti-tumor activity (12-15). Besides a direct cytotoxic effect of TNF, a reduction in the interstitial fluid pressure (IFP), as shown by others, could lead to enhanced uptake of large molecules (16).

It is also known that TNF induces the production of other cytokines (e.g. IL-1, IL-6 and IL-8) as well as cytotoxic factors (e.g. nitric oxide) by T lymphocytes, granulocytes and macrophages, which could mediate tumor suppression. The complexity of the interaction of TNF with various immune modulators within the tumor microenvironment is yet not well defined (17-19).

Here we focus on early effects inflicted by TNF during and shortly after ILP, which could explain the improved tumor response when used in a melphalan-based ILP.

Materials and methods

Animals and tumor model

Male inbred Brown Norway rats, obtained from Harlan-CPB (Austerlitz, the Netherlands), were used. Small fragments (3 mm) of the syngeneic BN175 soft tissue sarcoma were implanted subcutaneously in the right hind leg just above the ankle as previously described (7,8). Tumor growth was recorded daily by caliper measurement and tumor volume was calculated using the formula $0.4(A^2 \times B)$ (where B represents the largest diameter and A the diameter perpendicular to B). Rats were sacrificed if tumor diameter exceeded 25 mm or at the end of the experiments. All animal studies were done in accordance with protocols approved by the committee on Animal Research of the Erasmus MC, Rotterdam, the Netherlands.

Isolated limb perfusion

The perfusion technique was performed as described previously in detail (7,8). Briefly, perfusions were performed at a tumor diameter of 12-15 mm at least 7 days after implantation. During perfusion animals were anaesthetized with Hypnorm and Ketamine (Janssen Pharmaceutica, Tilburg, the Netherlands). The femoral artery and vein were cannulated and connected to an extracorporeal circuit including an oxygenation reservoir and a low-flow roller pump. Drugs, 50 μ g TNF (Boehringer Ingelheim GmbH, Austria) and/or 40 μ g melphalan (Alkeran, 50 mg per vial, Wellcom, Beckenham, UK), were added as

bolus to the reservoir. A washout was performed at the end of the perfusion. During ILP and washout, the hind leg was kept at a constant temperature of 38-39°C.

The classification of tumor response was: progressive disease (PD) = increase of tumor volume (>25%); no change (NC) = tumor volume equal to volume during perfusion (in a range of -25% and + 25%); partial remission (PR) = decrease of tumor volume (-25% and -90%); complete remission (CR) = tumor volume less than 10% of initial volume.

Interstitial fluid pressure (IFP)

IFP was measured in tumor and muscle during ILP with the Wick-in-Needle technique (20). A 23-gauge needle (Venisystems, Abbott Ireland LTD) with a 2-3 mm side hole 5 mm from the tip was filled with five surgical sutures 6/0 (Braun Medical B.V., Oss) and connected to a pressure transducer (DTX™ Plus Transducer, Becton Dickinson, Alphen aan den Rijn, the Netherlands). Pressure was recorded on an analog-digital converter (AS/3 DATEX). After cannulating the femoral artery and vein, but before applying the tourniquet, the needle was inserted in the tumor and in the muscle of the same leg. The IFP was recorded until the end of the perfusion.

pH measurements

To measure the pH of the tumor during ILP a pH electrode in 20 Gauge Needle (Harvard Apparatus, Inc, Holliston, MA, USA) was used. The calibrated pH electrode was inserted in the tumor just before the roller pump was started and the pH was measured throughout the perfusion. At the mean time the pH of the perfusate was measured (pH meter HI 8424, Hanna Instruments, Inc, Ann Arbor, USA).

HE staining

Directly or 6 hours after perfusion tumors were excised cut in two equal parts. Both parts were divided into a peripheral part and a central part. The tissues were stored in formalin and embedded in paraffin. 4 µm sections were stained with haematoxylin and eosin using standard procedures. Three or four different tumors in each experimental group were subjected to blind evaluation. At least 6 slides were examined from each tumor. All slides were examined on a Leica DM-RXA and photographed using a Sony 3CCD DXC 950 camera.

Apoptosis assay: TUNEL/CD31PE double staining

Apoptotic cell death was detected using the technique of 3'hydroxy end labeling (In Situ Cell Death detection Kit, Fluorescein labelled, Roche, Almere, the Netherlands). Tumor tissues were also stained for endothelial cells (CD31) to differentiate between apoptosis of the endothelium and of tumor cells.

After ILP the tumors were excised and immediately frozen in liquid nitrogen. Stainings were performed on acetone-fixed 7 μm cryostat sections. The tumor sections were fixed in 4% paraformaldehyde for 30 minutes and incubated for 1 hour with mouse-anti-rat CD31PE (1:50, Becton Dickinson, Alphen aan den Rijn, the Netherlands). After washing with PBS the sections were again fixed in 4% paraformaldehyde for 10 minutes and incubated in 0.1% Triton X-100 in 0.1% sodium citrate for 2 minutes on ice to allow permeabilization. The slides were incubated with the TUNEL mixture for 60 min at 37°C and after that the slides were rinsed three times in PBS and counterstained with 300 $\mu\text{g}/\text{ml}$ Hoechst (Molecular Probes, Leiden, the Netherlands) for 10 min. After washing with PBS the slides were mounted with mounting medium containing polyvinyl alcohol (Mowiol 4-88, Fluka, Zwijndrecht, the Netherlands).

Measurement of melphalan in tissue

At the end of the perfusion directly after the washout the tumor and part of the hind limb muscle were excised. The tissues were immediately frozen in liquid nitrogen to stop metabolism of melphalan and stored at -80°C. Tumor and muscle tissues were homogenized in 2 ml acetonitrile (Pro 200 homogenizer, Pro Scientific, CT, USA) and centrifuged at 2500 g. Melphalan was measured in the supernatant by gas chromatography-mass spectrometry (GC-MS). p-[Bis(2-chloroethyl)amino]-phenyl-acetic methyl ester was used as an internal standard. Samples were extracted over trifunctional C18 silica columns. After elution with methanol and evaporation, the compounds were derived with trifluoroacetic anhydride and diazomethane in ether. The stable derivatives were separated on a methyl phenyl siloxane GC capillary column and measured selectively by single-ion monitoring GC-MS in the positive EI mode described earlier by Tjaden and de Bruijn (21).

Immunohistochemistry

Directly or 6 hours after ILP immunohistochemical studies were performed on acetone-fixed 7 μm cryostat sections. The tumor sections were fixed for 30 min with 4% formaldehyde and after rinsing with PBS, the endogenous peroxidase activity was blocked by incubation for 5 minutes in methanol/3% H_2O_2 . The slides were incubated for 1 hour with 1:50 mouse-anti-rat-CD31, -CD4, -CD8, -granulocytes (clone HIS48) (Becton Dickinson, Alphen aan den Rijn, the Netherlands) and -macrophages (ED-1) (Serotec, Breda, the Netherlands). Thereafter, sections were washed with PBS and incubated for 1 h with goat-anti-mouse peroxidase-labeled antibody (1:100, DAKO, ITK Diagnostics BV, Uithoorn, the Netherlands). After rinsing with PBS, positive cells were revealed by immunoperoxidase reaction with DAB solution (DAKO, ITK Diagnostics BV, Uithoorn, the Netherlands) and counterstained lightly with haematoxylin (Sigma, Zwijndrecht, the Netherlands).

For quantification of ED-1, CD4, CD8 and granulocyte infiltration and microvessel density two independent persons performed blinded analysis. Six representative fields (magnification 16x) in each slide and three tumors per treatment were evaluated. The sections were examined on a Leica DM-RXA and photographed using a Sony DXC950 camera. For macrophage, T cell and granulocyte infiltration the total amount of positive cells were counted per field of interest. For the microvessel quantification, the number of tumor blood vessels and the area of vessels per field of interest were measured in calibrated digital images (Research Assistant 3.0, RVC, Hilversum, the Netherlands).

RT-PCR

Total RNA was extracted from frozen tumor tissue using TRIzol reagent (Invitrogen, Breda, the Netherlands). BN175 cells *in vitro* were treated with medium, 10 µg/ml TNF, 8 µg/ml melphalan or TNF plus melphalan and after 30 min of incubation total RNA was extracted. Total RNA was quantified by spectrophotometric analysis and quality of the RNA isolates was assured by electrophoresis in agarose gel.

A volume of 20 µl containing 1.0 µg of total RNA of each sample was used for generation of cDNA with Omniscript Reverse Transcriptase (Qiagen, Leusden, the Netherlands) and oligo d(T)₁₆ (Invitrogen, Breda, the Netherlands). After incubation at 42°C for 1 hour, the samples were heated for 5 min at 93°C to terminate the reaction. Titanium Taq DNA polymerase (Becton Dickinson, Alphen aan den Rijn, the Netherlands) was used for the PCRs and 1.5 µl of cDNA per 37.5 µl of reaction mixture was used. The primers were purchased from Invitrogen (Breda, the Netherlands) and primer sequences are shown in table 1. β-actin was used as an internal standard. PCRs were performed at a Biometra T-gradient PCR machine using the following parameters: initial denaturation at 94°C for 5 min followed by a maximum of 40 cycles of 94°C for 45 sec, annealing for 45 sec (temperatures see Table 1) and extension 72°C for 1 min and a final extension step at 72°C for 7 min. The resulting DNA fragments were electrophoretically separated on a 1.5% agarose gel, stained with ethidium bromide and photographed under UV light. A 100-bp ladder was used as the standard.

Semi-quantitative RT-PCR

Total RNA isolation, cDNA preparation and RT-PCR were performed as described above (see RT-PCR). Semi-quantification of cytokine expression was carried out as followed, every 2 cycles, 5 µl of PCR product was collected and the samples were electrophoretically separated on a 1.5% agarose gel, stained with ethidium bromide and photographed under UV light. The threshold cycle was determined as the cycle where the visible band of a specific PCR product first appeared on the gel. Intensities of the PCR product bands were

determined by ImageJ v1.34 software (W. Rasband, Research Services Branch, National Institute of Mental Health, Bethesda, Maryland, USA) and normalized for β -actin.

Table 1. RT-PCR primers for the immune related genes and for β -actin, which was used as a housekeeping gene.

Gene	Primers	Annealings temperature	Product size (bp)
β -actin	f: 5'-ATGGATGACGATATCGCTG-3' r: 5'-ATGAGGTAGTCTGTCTCAGGT-3'	60°C	569
IL-6	f: 5'-GACTTCACAGAGGATACC-3' r: 5'-TAAGTTGTTCTTCACAACTCC-3'	55°C	294
GRO/ CINC-A	f: 5'-GAAGATAGATTGCACCGATG-3' r: 5'-CATAGCCTCTCACACATTTTC-3'	57°C	367
IL-10	f: 5'-TGACAATAACTGCACCCACTT-3' r: 5'-TCATTCATGGCCTTG TAGACA-3'	60°C	402
IL-12	f: 5'-TCATCAGGGACATCATCAAACC-3' r: 5'-CGAGGAACGCACCTTTCTG-3'	65°C	210
TNF- α	f: 5'-TACTGAACTTCGGGGTGATCGGTCC-3' r: 5'-CAGCCTTGTCCCTGAAGAGAACC-3'	60°C	295
IFN- γ	f: 5'-GCCTCCTCTTGGATATCTGG-3' r: 5'-GTGCTGGATCTGTGGGTTG-3'	60°C	239
MCP-1	f: 5'-ATGCAGGTCTCTCTGTCACG-3' r: 5'-CTAGTTCTCTGTCATACT-3'	57°C	446
MIP-2	f: 5'-GGCACAATCGGTACGATCCAG-3' r: 5'-ACCCTGCCAAGGGTTGACTTC-3'	55°C	287
TGF- β 1	f: 5'-TGGAAGTGGATCCACGAGCCCAAG-3' r: 5'-GCAGGAGCGCACGATCATGTTGGAC-3'	55°C	240

f: forward primer, r: reverse primer

Cell culture

Cells isolated from the BN175 soft tissue sarcoma were maintained in culture in RPMI 1640 supplemented with 10% fetal calf serum and 0.1% penicilline-streptomycine (all Cambrex, Verviers, Belgium). Human Umbilical Vein Endothelial Cells (HUVEC) were isolated from normal human umbilical cords by the method of Jaffe *et al.* (22). Cells were cultured in fibronectin coated tissue culture flasks containing Human Endothelial-serum free medium (GIBCO-BRL, Invitrogen, Breda, the Netherlands), with 20% heat inactivated newborn calf serum, 10% heat inactivated human serum (Cambrex, Verviers, Belgium), 20

ng/ml human recombinant Basic Fibroblast Growth Factor (Peprotech EC Ltd, London, United Kingdom) and 100 ng/ml human recombinant Epidermal Growth Factor (Peprotech EC Ltd, London, United Kingdom). Passages 5-7 were used for the experiments.

Preparation of polymorphonuclear leukocytes (PMN)

Venous blood from healthy adult volunteers was collected in Na-heparin tubes (Becton Dickinson, Alphen aan den Rijn, the Netherlands). After centrifuging for 20 min (1500 g, room temperature), total white blood cell fraction was collected and remaining red blood cells were lysed with lysis buffer (0.15 M NH_4Cl , 10 mM Hepes, pH = 7.0) for 30 min at room temperature. After centrifuging for 30 min (1500 rpm, room temperature), the pellet was resuspended in 4 ml diluent (0.15 M NaCl, 10 mM EDTA, 20 mM Hepes, pH = 7.4) in a 15 ml tube. A density gradient was created by sequentially adding to the bottom of the tube 4 ml of Optiprep at 1.077 g/ml followed by 4 ml of 1.095 g/ml Optiprep. The tube was then centrifuged at 800 g for 20 min at room temperature. The layer at 4 ml, containing PMN was removed and washed in diluent and then centrifuged at 1500 rpm for 5 min. The PMN were dissolved in HUVEC medium at a concentration of $120 \cdot 10^4$ cells/ml.

HUVEC permeability assays

To study the effect of TNF on transendothelial monolayer permeability, a transwell device (Costar, Cambridge, MA, USA) consisting of an upper chamber with a polycarbonate membrane (6.5 mm diameter, 0.4 μm pore size), placed inside a 24-well plate (lower chamber) was used. HUVEC were plated on the fibronectin coated upper chamber, at a density of $1.2 \cdot 10^4$ cells. In the lower compartment 1 ml of HUVEC medium was added. Two days after seeding, non-adhering cells were removed and the medium was replaced with 250 μl medium containing 10 $\mu\text{g/ml}$ TNF, 8 $\mu\text{g/ml}$ melphalan and/or PMN together with 50 μl FITC-BSA or fluorescein (1 mg/ml, Sigma). The medium in the lower chamber was replaced with 700 μl of HUVEC medium. At 5, 15, 30, 60 and 90 min, 50 μl medium of the lower chamber was taken and fluorescence activity was measured under excitation at 490 nm and emission at 530 nm. A standard curve was prepared with known concentrations of FITC-BSA or fluorescein. Induction of permeability was indicated by a higher concentration of FITC-BSA or fluorescein in the lower chamber of the transwell, relative to untreated controls.

Nitrite measurement

Nitrite concentrations were measured using the Griess reaction. Cells were trypsinized and seeded on fibronectin-coated 24 well plates (HUVEC, $3.6 \cdot 10^4$ cells/well) or on non-coated plates (BN175, $6 \cdot 10^4$ cells/well). 24 hours after seeding, non-adhering cells were removed and the medium was replaced with 250 μl of 0.1, 1 or 10 $\mu\text{g/ml}$ TNF. After incubation for

72 hours, culture supernatant was collected and spun down to remove cell debris. 50 μ l of supernatant was incubated with equal volumes of 1% (w/v) sulfanilamide in 5% phosphoric acid and 0.1% (w/v) N-1-naphthylethylene-diamine dihydrochloride. After 10 min of incubation at room temperature, absorbance of the chromophore so-formed was measured at 545 nm using a microtiter plate reader. Nitrite concentrations were calculated by comparison with a standard calibration curve with sodium nitrite (NaNO_2 : 1.25 – 20 μ M).

Measurement of ROS production by dichlorofluorescein fluorescence

Reactive oxygen species (ROS) generation in cells was assessed using the probe 2,7-dichlorofluorescein diacetate (DCFH-DA, 10 μ M; Molecular Probes, Leiden, the Netherlands). Within the cell esterases cleave the acetate group, thereby trapping the nonfluorescent DCFH probe intracellularly. Subsequent oxidation by ROS, particularly H_2O_2 or the hydroxyl radical ($\text{OH}\cdot$), yields the fluorescent product dichlorofluorescein (DCF). DCF fluorescence was measured with excitation wavelength of 490 nm and emission at 530 nm using a microtiter plate reader.

HUVECs were trypsinised and 6×10^3 cells/well were seeded on fibronectin-coated black 96 well plates with clear bottom (Costar, Cambridge, MA, USA). One day after seeding DCFH-DA was added at a final concentration of 10 μ M and incubated for 60 min at 37°C. The cells were washed once with medium without FCS and then incubated with 0, 0.1, 1 or 10 μ g/ml TNF with or without PMN (6×10^4 cells/well) for 30 min. Also ROS production by PMN alone was measured. PMN ($120 \cdot 10^4$ cells/ml) were incubated with 10 μ M DCFH-DA for 60 min at 37°C. The cells were washed once with medium without FCS, plated on black 96 well plates with clear bottom (6×10^4 cells/well), incubated with 0, 0.1, 1 or 10 μ g/ml TNF for 30 min and DCF fluorescence measured.

Statistical analysis

Results were evaluated for statistical significance with the Mann Whitney U test. P-values below 0.05 were considered statistically significant. Calculations were performed on a personal computer using GraphPad Prism v3.0 and SPSS v11.0 for Windows 2000.

Results

TNF based ILP with melphalan results in strong tumor response, which is caused by augmented drug accumulation.

In vivo response to melphalan and TNF

Typically, the combination of TNF and melphalan resulted in increased anti-tumor activity with a response rate of 75% (PR and CR) ($p < 0.001$ compared with melphalan alone) (Table 2). Progressive disease was found in all animals treated with buffer or TNF alone. Although

ILP with melphalan alone resulted in a slight inhibition of the tumor growth when compared with the sham control, none of the rats showed a tumor response. In tumors treated with TNF and melphalan softening of tumor tissue was observed.

Table 2. Tumor response and drug accumulation after TNF-based ILP with melphalan

Treatment	Tumor volume at day 8 (mm ³) ^a	Response rates ^b				Melphalan (ng/g tissue) ^d
		PD ^c	NC	PR	CR	
Sham	> 5000	100%				-
TNF	4570 ± 511	100%				-
Mel	1918 ± 293	38%	38%	23%	-	136 ± 24
TNF + mel	491 ± 245	19%	6%	44%	31%*	831 ± 293**

^a average ± SEM, ^b responses were scored as described in Materials and Methods, ^c PD: progressive disease, NC: no change, PR: partial remission, CR: complete remission, RR: response rate (PR plus CR), ^d average ± SD, * p < 0.001 compared to melphalan alone, ** p = 0.01 compared to melphalan alone

Histological analysis

Previously we demonstrated TNF-induced vascular damage days after ILP, although TNF alone had no effect on tumor progression (4). Directly after perfusion with TNF plus melphalan a slight increase in the number and size of necrotic areas was observed accompanied by scattered extravasation of erythrocytes (Figure 1). Tumors showed a few areas with complete destruction of the vasculature, something that was not seen in other treatments. Extravasation of erythrocytes was also seen in TNF-treated animals, but to a smaller extent and endothelial linings seemed to be mostly intact. Treatment with melphalan caused a mild increase in oedema. No clear differences were seen between central and peripheral part of the tumors and comparable results were seen 6 hours after ILP, except that after 6 hours slightly more necrotic areas were detected (data not shown). In all four treatments apoptotic tumor cells were observed and sporadically apoptotic endothelial cells (Figure 2). In the TNF and TNF plus melphalan treated rats an increased number of apoptotic endothelial cells were detected directly after ILP. No differences were seen between 0 and 6 hours after perfusion (data not shown).

Melphalan uptake in tumor and muscle tissue

Importantly, a six-fold increased melphalan uptake in tumor tissue directly after ILP with TNF and melphalan was observed in comparison with perfusions with melphalan alone (p=0.01) (Table 2). In contrast in the normal tissues skin and muscle no effect of TNF is found on the uptake of melphalan (data not shown).

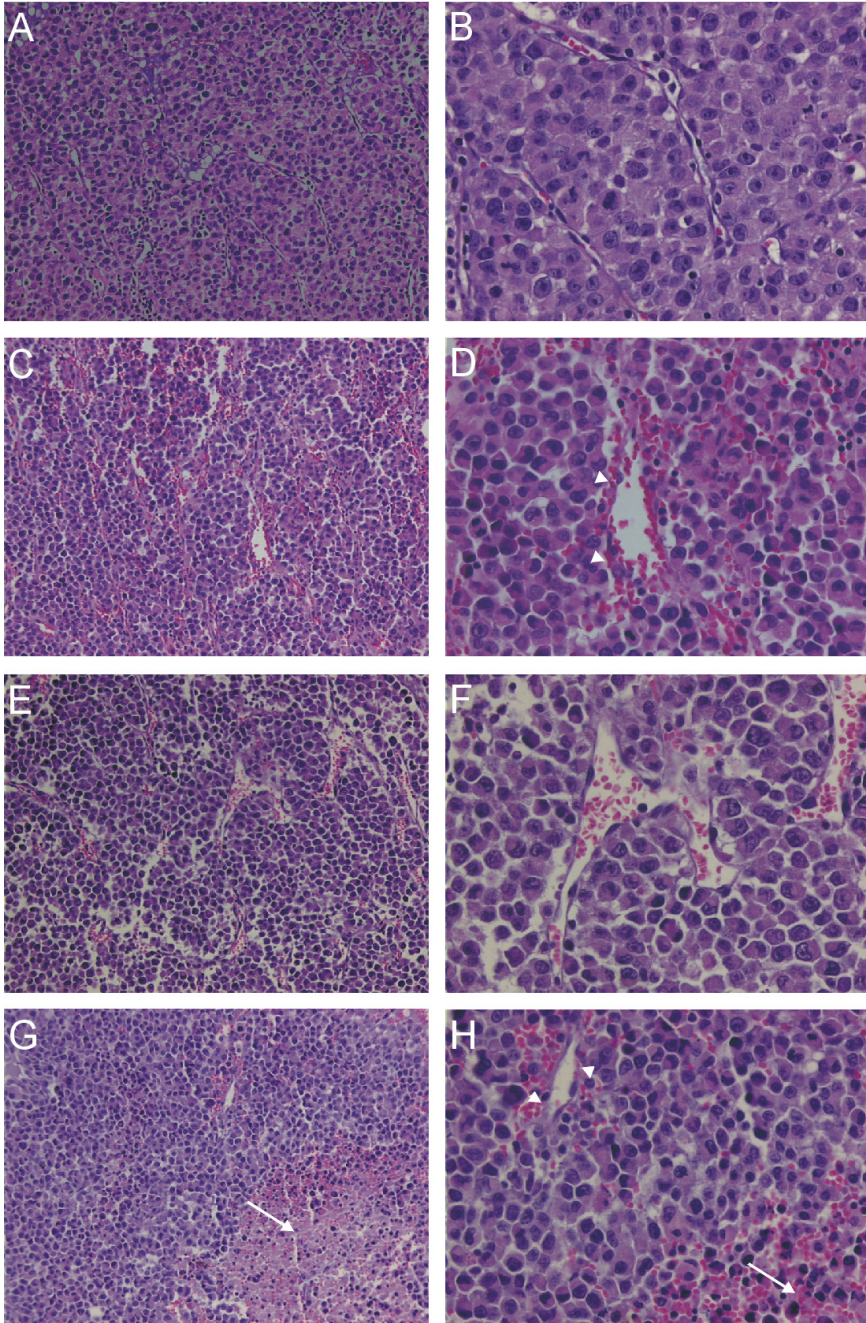


Figure 1. Paraffin sections of BN175 tumor tissue directly after isolated limb perfusion, haema-toxylin-eosin stained. (A and B) Intact blood vessel lining in periphery of sham-treated tumor. (C and D) ILP with 50 µg TNF, central part of tumor. Arrowheads: extravasated erythrocytes. (E and F) Central part of tumor treated with 40 µg of melphalan. (G and H) Periphery of TNF plus melphalan-treated tumor. Arrow-head: extravasated erythrocytes, arrows: necrotic area. Original magnification 16X (A,C,E,G) and 40X (B,D,F,H).

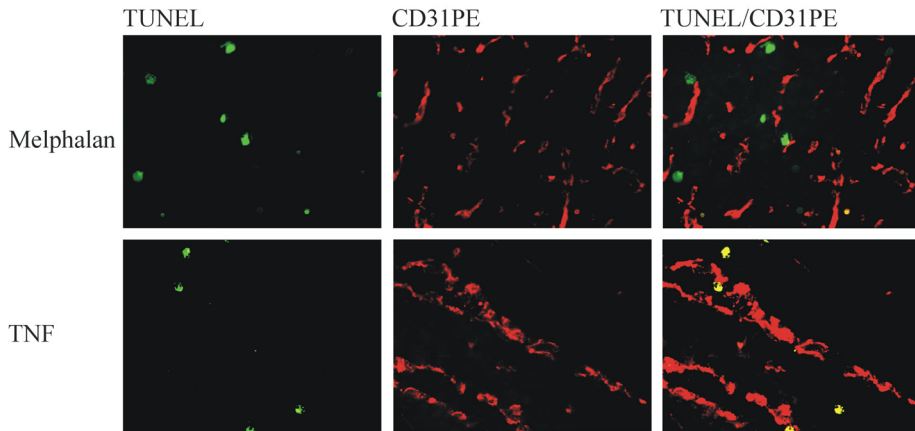


Figure 2. Double staining with CD31PE and TUNEL. Photographs demonstrating apoptotic tumor cells (green), endothelial cells (red) and apoptotic endothelial cells (yellow). Frozen section of BN175 tumor biopsies collected directly after isolated limb perfusion with melphalan (A) or TNF (B). Original magnification 40X.

Vascular permeability in vitro

The observed increased drug accumulation *in vivo* was confirmed *in vitro*. Incubation of HUVEC with 10 $\mu\text{g/ml}$ TNF resulted in an increased permeability to fluorescein in 15 minutes (Figure 3). Also incubation with 8 $\mu\text{g/ml}$ melphalan or PMN resulted in an increased permeability. TNF in combination with melphalan and PMN increased permeability 4.7-fold. Longer incubation times had no additional effect. TNF however, did not increase monolayer permeability to FITC-BSA in 30 minutes nor in 24 h perfusion timeframe.

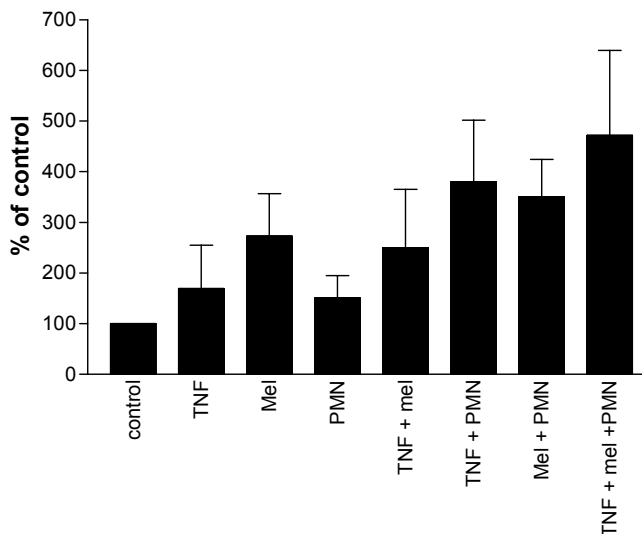


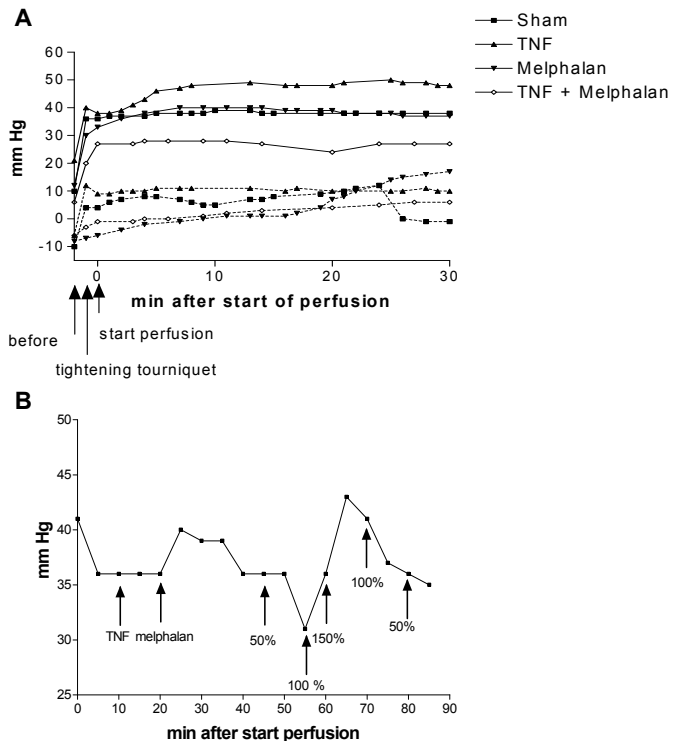
Figure 3. Effect of TNF, melphalan and PMNs on HUVEC monolayer permeability. HUVECs were cultured on the filter of a transwell unit for 48 hours before the addition of fluorescein-containing medium (=control) with 10 $\mu\text{g/ml}$ TNF, 8 $\mu\text{g/ml}$ melphalan (mel) and/or $120 \cdot 10^4$ cells/ml PMN (see Material and Methods). The amount of fluorescein in the lower compartment was measured after 15 min of incubation. Values are from two experiments, each done in duplicate. The mean is shown \pm SD.

In another experiment we showed that IFN- γ influences HUVEC permeability for proteins. We found a 4.1-fold increased permeability for FITC-BSA after 15 minutes of incubation with 10 $\mu\text{g/ml}$ TNF, 0.1 $\mu\text{g/ml}$ IFN- γ and PMN (data not shown).

IFP measurements in tumor and muscle tissue

As TNF was shown to reduce IFP in tumor tissue (16), IFP measurements were performed in both tumor and muscle tissue to investigate if in our experimental setting TNF-induced lowering of the IFP could be an explanation for the enhanced drug accumulation and softening of the tumor. Under normal conditions the IFP of tumor tissue is much higher than of muscle tissue (11 ± 5 and -5 ± 8 mm Hg, respectively) ($p < 0.0001$) (Figure 4). Tightening of the tourniquet resulted in a 2.4-fold increased IFP in tumor tissue with an average of 26 ± 11 mm Hg ($p < 0.0001$) and start of the perfusion pump did not further increase the IFP. None of the treatments had an effect on the IFP. Also IFP in muscle tissue increased after tightening of the tourniquet (1 ± 9 mm Hg), and further increase was only seen in the melphalan treated group after 20 and 30 min (14 ± 5 and 20 ± 4 mm Hg, respectively) ($p = 0.02$) (Figure 4A).

Figure 4. Interstitial fluid pressure during ILP. IFP was continuously recorded as described in Material and Methods. A. BN175-bearing rats were treated with buffer alone (■), 50 μg TNF (▲), 40 μg melphalan (▼) or a combination of TNF and melphalan (◇). IFP in tumor (continuous line) and muscle tissue (dotted line) are measured (in mm Hg) and representative curves are shown. At least three animals per group were measured. B. Interstitial fluid pressure in a patient. Decreasing perfusion pump rate resulted in a lower IFP and vice versa indicating that in an ILP the IFP is dictated by the pump pressure.



We speculated that pressure inflicted by the pump in the extracorporeal circuit might have a major impact on the IFP. Indeed, when we increased the pump rate, tumor IFP increased and decreased again when the pump rate was reduced (data not shown). The effect of the pump rate on the IFP was confirmed in the clinical setting in which comparable results were obtained (figure 4B). No effect of TNF or melphalan on the IFP was seen throughout the ILP (data not shown).

pH measurements in tumor and perfusate

It is thought that TNF causes damage to the tumor vasculature inducing hypoxia in tumor regions with inadequate blood supply (4,11). In our experiments we tested the hypothesis whether treatment with TNF could cause a lower pH in tumor tissue because of early effects on the tumor vasculature.

The pH of Haemaccel is 6.9 and oxygenation lowered the pH to 6.2. Directly after start of the perfusion the pH increased to 6.5 ± 0.3 . Different treatments did not have an effect on the pH of the perfusate and the pH at the end of the perfusion was 6.9 ± 0.1 for all four treatments. The pH of the tumor at the beginning of the perfusion was slightly acidic (6.9 ± 0.1). At the end of the ILP the pH in the tumor was somewhat lower (6.6 ± 0.3) and stayed at the same level till after the washout. None of the treatments had an effect on the pH of the tumor.

Assessment of tumor vascular functionality

The increased uptake of melphalan might be correlated with the functionality of the tumor-associated vasculature. Quantification of the microvessel density and functionality was performed by immunohistochemical staining of endothelial cells. The number of vessels as well as vessel area was measured. The area per vessel was computed by dividing the total area of vessels by the number of vessels. There were no differences found between the treatments and the sham perfusions (Table 3). The area endothelium in center and/or periphery was significantly decreased six hours after ILP compared to the area measured directly after perfusion with sham, TNF or melphalan. In the central part of the tumor of the sham and TNF treated tumors a decrease in area endothelium per vessels was measured.

NO and reactive oxygen species production in vitro

Only after 72 h incubation HUVEC produced NO above the detection limit of 1 μM , a 1.3-fold increased NO production was found in HUVEC exposed to 0.1 $\mu\text{g/ml}$ TNF compared to untreated cells (respectively 4.2 and 3.2 μM NO). Treatment with 10 $\mu\text{g/ml}$ TNF resulted in a reduction of the NO production (2.2 μM). Exposure of BN175 to TNF (0.1 $\mu\text{g/ml}$) resulted in a 1.7-fold increased NO production (4.0 μM), whereas exposure to 10 $\mu\text{g/ml}$ TNF resulted in the same production as untreated cells (6.8 μM).

Table 3. Microvessel density and area of the tumor vessels after isolated perfusion with sham, TNF, melphalan or TNF plus melphalan.

	sham	TNF	melphalan	TNF + melphalan
number of vessels ^a				
center 0 hours	19 ± 6	21 ± 7	22 ± 2	34 ± 25
periphery 0 hours	43 ± 12	32 ± 9	34 ± 6	19 ± 5
center 6 hours	46 ± 31	34 ± 13	32 ± 14	18 ± 7
periphery 6 hours	36 ± 15	29 ± 5	38 ± 26	25 ± 6
area endothelium ^b				
center 0 hours	7.6 ± 0.7	10.7 ± 2.7	5.9 ± 0.9	5.7 ± 1.0
periphery 0 hours	7.6 ± 0.3	7.2 ± 0.4	7.2 ± 0.1	5.0 ± 1.1
center 6 hours	4.0 ± 1.1*	4.0 ± 0.7*	6.1 ± 1.4	7.2 ± 2.4
periphery 6 hours	3.8 ± 0.5*	3.5 ± 0.4*	3.9 ± 1.5*	3.6 ± 0.5
area endothelium/vessel ^c				
center 0 hours	0.44 ± 0.09	0.59 ± 0.25	0.27 ± 0.03	0.41 ± 0.17
periphery 0 hours	0.22 ± 0.08	0.28 ± 0.10	0.23 ± 0.03	0.30 ± 0.08
center 6 hours	0.16 ± 0.05*	0.14 ± 0.0*	0.22 ± 0.03	0.48 ± 0.16
periphery 6 hours	0.14 ± 0.04	0.13 ± 0.02	0.18 ± 0.08	0.18 ± 0.07

Note: directly after ILP or 6 hours later the tumors were excised and frozen sections were stained for CD31 positive cells. 6 fields of interest per tumor and 3 animals per group were quantified. Average ± SEM are shown.

^a number of vessels per field of interest, ^b % of total vessel area per field of interest, ^c area per vessel, * p=0.05 compared with 0 hours and the same tumor region

Oxygen radicals are released by various cell types in response to stimulation with factors such as TNF and can cause DNA and membrane damage (23,24). Incubation of HUVEC with 0.1 µg/ml TNF for 30 min resulted in a 1.9-fold increased ROS production compared to medium alone, although this increase was not significant. On the other hand, incubation with the highest concentration of 10 µg/ml TNF did not change the ROS production compared to the control. Addition of PMN to the HUVEC monolayer caused an enhanced ROS production of 1.6 fold (not significant) and co-incubation with TNF did not further change the ROS production. Incubation of TNF and PMN did not have any effect on the ROS generation by PMN.

Secondary immunological effect of TNF

Tumor infiltration of leukocytes and macrophages

Directly or 6 h after ILP no evident alterations in number nor in localization of the tumor infiltrating cells was observed in all treatment groups (Table 4).

Table 4. Tumor infiltration after isolated perfusion with sham, TNF, melphalan or TNF plus melphalan.

	sham	TNF	melphalan	TNF + mel
CD4^a				
center 0 hours	0.3 ± 0.1	0.5 ± 0.3	0.2 ± 0.1	13.5 ± 13.0
periphery 0 hours	1.0 ± 0.5	1.4 ± 0.4	0.7 ± 0.5	0.5 ± 0.3
center 6 hours	1.0 ± 0.5	0.9 ± 0.4	1.2 ± 0.4	0.4 ± 0.1
periphery 6 hours	0.5 ± 0.3	0.6 ± 0.2	0.8 ± 0.3	1.6 ± 0.4
CD8^a				
center 0 hours	34 ± 21	27 ± 21	67 ± 47	56 ± 55
periphery 0 hours	64 ± 26	35 ± 7	75 ± 27	139 ± 25
center 6 hours	22 ± 12	51 ± 16	41 ± 13	48 ± 29
periphery 6 hours	62 ± 20	33 ± 3 [*]	51 ± 7	42 ± 8 [#]
Granulocytes^a				
center 0 hours	60 ± 4	89 ± 18	48 ± 3 [*]	88 ± 12
periphery 0 hours	74 ± 19	81 ± 25	62 ± 10	37 ± 5
center 6 hours	69 ± 10	72 ± 18	79 ± 14	47 ± 6 ^{*#}
periphery 6 hours	109 ± 39	71 ± 12	50 ± 13	81 ± 12 [#]
ED-1^a				
center 0 hours	189 ± 5	192 ± 33	201 ± 20	172 ± 34
periphery 0 hours	221 ± 42	165 ± 11	207 ± 23	239 ± 11
center 6 hours	171 ± 34	174 ± 18	230 ± 29	147 ± 10
periphery 6 hours	246 ± 39	214 ± 34	180 ± 16	189 ± 2 [#]

Note: directly after ILP or 6 hours later the tumors were excised and frozen sections were stained for CD4, CD8, granulocytes and ED-1 positive cells. 6 fields of interest per tumor and 3 animals per group were quantified. Average ± SEM are shown. ^a number of positive cells per field of interest, * p=0.05 compared with sham treatment at same timepoint and region of the tumor, [#] p=0.05 compared with 0 hours and the same tumor region.

Cytokine expression in tumor tissue and tumor cells in vitro

As the number of infiltrating cells was not affected by TNF, we hypothesized that TNF could probably activate macrophages and T lymphocytes resulting in the production of non-specific effector molecules. Increased expression levels of TNF and IFN were found in tumor tissue collected directly after ILP with TNF plus melphalan compared to sham ILP (p=0.05) (Figure 5). Obviously, sham perfusions did affect cytokine expression in the tumor microenvironment. Increased expression of IL-6, GRO/CINC-A, TNF and IL-12 and decreased expression of IFN and TGF-β1 were detected in tumor tissue 6 hours after ILP compared to expression levels in tumor tissue taken out directly after perfusion (p=0.05).

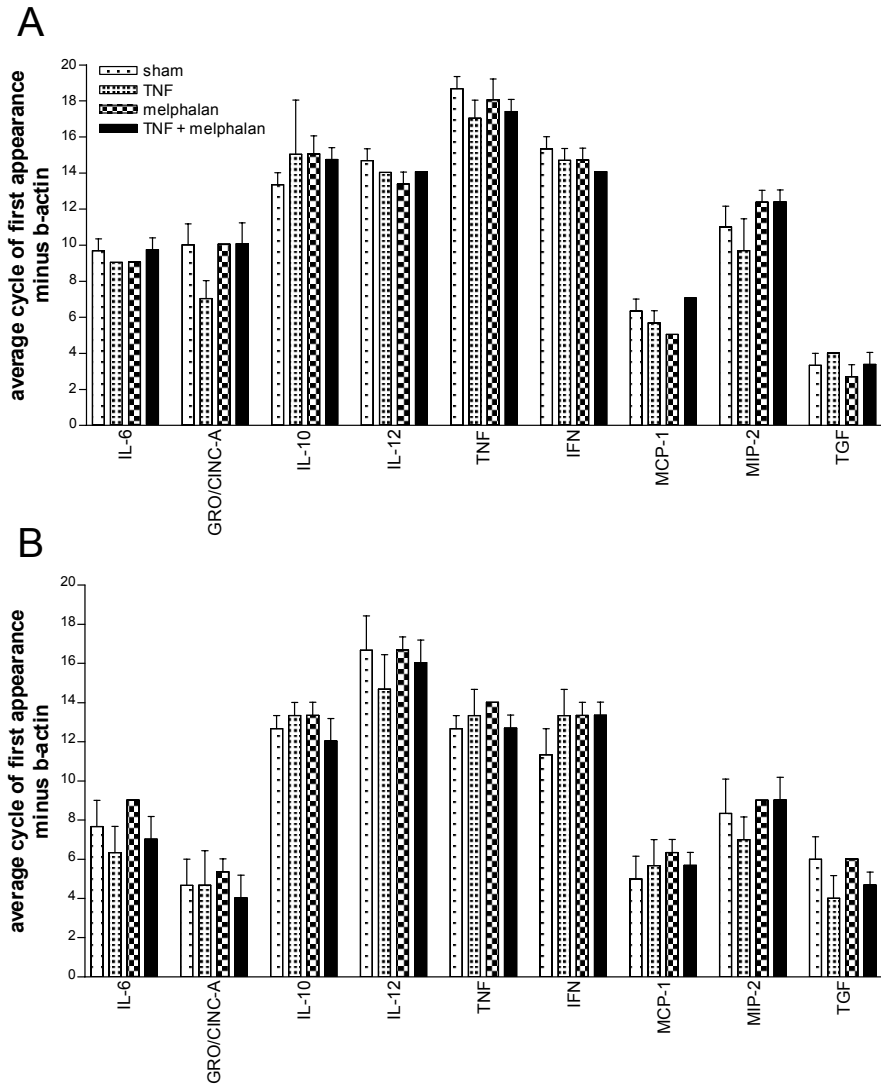


Figure 5. Semi-quantitative RT-PCR. BN175-bearing rats were treated with buffer alone, 50 μg TNF, 40 μg melphalan or a combination of TNF and melphalan directly after ILP (A) or 6 hours later (B) the tumor were excised. RNA was isolated and RT-PCR was carried out with various cycles of PCR reactions. Numbers given in the figures are the cycles where first band of each cytokine appeared minus the first band of b-actin of the same cDNA sample (cycle 18-20). The average of each cytokine is shown \pm SEM.

To investigate which cytokines are produced by the tumor cells alone, RNA was isolated from BN175 tumor cells *in vitro*. Cells were also incubated with 10 $\mu\text{g}/\text{ml}$ TNF, 8 $\mu\text{g}/\text{ml}$ melphalan or the combination for 30 minutes. Clear differences were seen between expression levels *in vivo* and *in vitro*. mRNA expression in tumors showed higher IL-6,

MCP-1 and TGF- β 1 and lower IL-10 and MIP-2 levels than tumor cells *in vitro*. Levels of GRO/CINC-A, IL-12, TNF and IFN- γ expression were comparable. Treatment of tumor cells *in vitro* with TNF and TNF resulted in higher expression of all cytokines tested, with the exception of TGF- β 1. Most clear differences were seen for GRO/CINC-A, MCP-1 and MIP-2 mRNA expression (data not shown).

Discussion

Clinical studies showed impressive improvement of the anti-tumor activity of melphalan in local treatment of different tumor types when TNF was co-administered (reviewed in (1)). We demonstrated that the basis for the synergy is a significant enhancement of tumor drug uptake (7,8). Subsequent events were haemorrhagic necrosis and destruction of tumor vasculature (7,9). Although TNF alone already inflicts these effects in rodent tumor models, no significant tumor regression occurs in the clinic nor in the animal models after ILP with TNF alone (11-15). Here we focus on the direct effects of TNF on the tumor microenvironment and on secondary immunological effects during and shortly after perfusion. Already during perfusion with TNF and melphalan softening of the tumor was observed and some vascular damage was detected. Perfusion with TNF alone showed extravasation of erythrocytes, but the endothelial linings seemed to be mostly intact. ILP with TNF and melphalan resulted in slight increase of the necrotic areas and sections revealed scattered extravasation of erythrocytes. The tumors showed some areas with complete destruction of the vasculature.

In the present study we demonstrate that isolated limb perfusion in soft-tissue sarcoma bearing rats with melphalan in combination with TNF results in high response rates. We previously showed that the combination therapy is also very effective for the rat osteosarcoma and with another chemotherapeutical agent, namely doxorubicin. In both tumor types TNF caused an augmented drug uptake and a synergistic anti-tumor response (8,25). Several studies showed that TNF was able to enhance the uptake of macromolecules (26,27). In the present study a six-fold increased melphalan uptake in tumor tissue was found and no increased drug uptake in skin and muscle tissue. There was a transient effect of TNF in combination with melphalan and PMN on the permeability of endothelial cells *in vitro* for small molecules like fluorescein (0.33 kD) and melphalan (0.3 kD) and not for proteins like BSA (66.4 kD) explaining the improved melphalan accumulation. The permeability *in vitro* was not enhanced to larger molecules, (e.g. BSA) which might be explained by the absence of IFN- γ . We hypothesize that endogenous IFN- γ is a critical component in the synergistic anti-tumor activity of TNF and chemotherapy (28). We showed that IFN- γ in combination with TNF and PMN is needed for an increased permeability to proteins.

Destruction of the vasculature was detected only at some areas accompanied by extravasation of erythrocytes after perfusion with TNF and melphalan. However, no destruction of vessels was seen after treatment with TNF alone. The slightly increased amount of apoptotic cells found directly after ILP, only partly explain the vascular damage caused by TNF in combination with melphalan. Ruegg *et al.* showed that inhibition of the $\alpha_v\beta_3$ -mediated endothelial cell adhesion results in apoptosis and finally disruption of the tumor vasculature induced by TNF and IFN- γ , but in this study tumor biopsies were examined 24 hours after ILP (5), which might therefore be a secondary effect.

Several studies have suggested that increased delivery of macromolecules can be achieved by lowering the interstitial fluid pressure (29,30). The IFP in nearly all normal tissues is close to atmospheric pressure, but is significantly elevated in most solid malignant tumors (31,32). The capillaries in tumors are structurally and functionally abnormal and some are hyperpermeable to fluid and serum proteins. Poor uptake of drugs into tumor interstitium is thought to, at least in part, be responsible for the low efficiency in pharmacological treatment of solid malignancies (33). Kristensen *et al.* showed that TNF caused a reduction in the IFP in human melanoma xenografts, what could lead to enhanced uptake of large molecules (16). In our experiments we did not see an effect of TNF on the IFP, but the perfusion procedure itself caused a 2.4-fold increase in IFP. We concluded that the enhanced drug uptake in the ILP setting was not due to a lowering of IFP.

Besides an increased IFP in tumor tissue, the microenvironment of most solid tumors is acidic. The origins of this extracellular acidity are thought to lie in the chaotic nature of tumor vasculature, increased glycolytic flux in tumor cells and diminished buffering capacity of tumor interstitial fluid (10,11). In our study we also found that the pH of the BN175 tumor is slightly acidic and none of the treatments had an effect on the pH of the tumor during ILP. Mildly acidic condition of the perfusate might enhance the antitumor effect of melphalan as suggested by a study of Kelley *et al.* (34). Others showed that hypoxia and acidosis both *in vitro* and *in vivo* are able to potentiate the cytotoxicity of melphalan (35,36). In TNF-based ILP this seems not to play a role of importance.

Mocellin *et al.* found significantly higher levels of eNOS mRNA in complete responders than in partial/minimal responders after TNF-based ILP (37). Higher levels of NO will result in vasodilatation, a higher blood flow and could therefore have a beneficial effect on drug uptake (38). This is in contrast with results of de Wilt *et al.* where in the BN175 tumor model an additional antitumor effect was demonstrated when the NO inhibitor L-NAME was added to the synergistic combination of melphalan and TNF response rate increased up to 100% (39).

Some studies showed that administration of TNF resulted in a reduced blood flow, whereas others saw no effect of TNF on tumor blood flow (26,40). To obtain further insight into the mechanism underlying the effect of TNF experiments are currently conducted.

Although TNF is able to upregulate the expression of some cytokines *in vitro*, BN175 cells are not sensitive to TNF both *in vitro* and *in vivo*. Mocellin *et al.* found 24 hours after ILP with TNF and doxorubicin a Th1 type shift in the tumor microenvironment compared with tumor tissue before treatment (41). An increased TIA-1 gene expression in tumor biopsies 24 hours after TNF-ILP compared to the patients treated with doxorubicin alone was found. These experiments indicate that TNF-induced TIA-1 overexpression might sensitize endothelial cells to proapoptotic stimuli present in the tumor microenvironment and enhance NK cell cytotoxic activity against cancer cells (42). We found no clear shift toward a Th1 or a Th2 type response, but these data do not exclude up- or down-regulation of cytokines locally. Imbalance in the cytokine profile within the tumor microenvironment more than the absolute level of an individual cytokine may be responsible for an effective versus ineffective immune response (18).

In conclusion, application of TNF in combination with melphalan in an isolated limb perfusion strongly improves response rates, which is due to an augmented melphalan accumulation in the tumor during ILP. We have recently reported on a similar and crucial activity of histamine and interleukin-2 in this setting (43,44), further identifying that enhancement of cytotoxic drug uptake in the tumor is key. This increased drug accumulation is not explained by a lowering of the IFP. Most likely TNF induces at short term, in conjunction with PMN-derived factors and IFN, permeability of the endothelial lining facilitating better tumor penetration of small molecules.

Acknowledgements

The authors thank Joost Rens for his assistance with the IFP measurements, Cindy van Velthoven for the immunohistochemical studies and Boehringer Ingelheim GmbH for the generous supply of TNF. This study was supported by grant DDHK 2000-2224 of the Dutch Cancer Society and a grant of the Foundation “Stichting Erasmus Heelkundig Kankeronderzoek”.

References

1. Eggermont AM, de Wilt JH, ten Hagen TL. Current uses of isolated limb perfusion in the clinic and a model system for new strategies. *Lancet Oncol.* 2003;4(7):429-437.
2. Eggermont AM, Schraffordt KH, Klausner JM, et al. Isolation limb perfusion with tumor necrosis factor alpha and chemotherapy for advanced extremity soft tissue sarcomas. *Semin Oncol.* 1997;24(5):547-555.
3. Nooijen PT, Eggermont AM, Schalkwijk L, Henzen-Logmans S, De Waal RM, Ruiter DJ. Complete response of melanoma-in-transit metastasis after isolated limb perfusion with tumor necrosis factor alpha and melphalan without massive tumor necrosis: a clinical and histopathological study of the delayed-type reaction pattern. *Cancer Res.* 1998;58(21):4880-4887.
4. Renard N, Lienard D, Lespagnard L, Eggermont A, Heimann R, Lejeune F. Early endothelium activation and polymorphonuclear cell invasion precede specific necrosis of human melanoma and sarcoma treated by intravascular high-dose tumour necrosis factor alpha (rTNF alpha). *Int J Cancer.* 1994;57(5):656-663.
5. Ruegg C, Yilmaz A, Bieler G, Bamat J, Chaubert P, Lejeune FJ. Evidence for the involvement of endothelial cell integrin alphaVbeta3 in the disruption of the tumor vasculature induced by TNF and IFN-gamma [see comments]. *Nat Med.* 1998;4(4):408-14.

6. Posner MC, Lienard D, Lejeune FJ, Rosenfelder D, Kirkwood J. Hyperthermic Isolated Limb Perfusion With Tumor Necrosis Factor Alone for Melanoma. *Cancer J Sci Am.* 1995;1(4):274.
7. de Wilt JH, ten Hagen TL, de Boeck G, van Tiel ST, de Bruijn EA, Eggermont AM. Tumour necrosis factor alpha increases melphalan concentration in tumour tissue after isolated limb perfusion. *Br J Cancer.* 2000;82(5):1000-1003.
8. van Der Veen AH, de Wilt JH, Eggermont AM, van Tiel ST, Seynhaeve AL, ten Hagen TL. TNF-alpha augments intratumoural concentrations of doxorubicin in TNF-alpha-based isolated limb perfusion in rat sarcoma models and enhances anti-tumour effects. *Br J Cancer.* 2000;82(4):973-980.
9. Nooijen PT, Manusama ER, Eggermont AM, et al. Synergistic effects of TNF-alpha and melphalan in an isolated limb perfusion model of rat sarcoma: a histopathological, immunohistochemical and electron microscopical study. *Br J Cancer.* 1996;74(12):1908-1915.
10. Stubbs M, McSheehy PM, Griffiths JR, Bashford CL. Causes and consequences of tumour acidity and implications for treatment. *Mol Med Today.* 2000;6(1):15-19.
11. Vaupel P, Kallinowski F, Okunieff P. Blood flow, oxygen and nutrient supply, and metabolic microenvironment of human tumors: a review. *Cancer Res.* 1989;49(23):6449-6465.
12. Nakano K, Abe S, Sohmura Y. Recombinant human tumor necrosis factor--I. Cytotoxic activity in vitro. *Int J Immunopharmacol.* 1986;8(3):347-355.
13. Carswell EA, Old LJ, Kassel RL, Green S, Fiore N, Williamson B. An endotoxin-induced serum factor that causes necrosis of tumors. *Proc Natl Acad Sci U S A.* 1975;72(9):3666-3670.
14. Sohmura Y, Nakata K, Yoshida H, Kashimoto S, Matsui Y, Furuichi H. Recombinant human tumor necrosis factor--II. Antitumor effect on murine and human tumors transplanted in mice. *Int J Immunopharmacol.* 1986;8(3):357-368.
15. Watanabe N, Niitsu Y, Umeno H, et al. Toxic effect of tumor necrosis factor on tumor vasculature in mice. *Cancer Res.* 1988;48(8):2179-2183.
16. Kristensen CA, Nozue M, Boucher Y, Jain RK. Reduction of interstitial fluid pressure after TNF-alpha treatment of three human melanoma xenografts. *Br J Cancer.* 1996;74(4):533-6.
17. Klimp AH, de Vries EG, Scherphof GL, Daemen T. A potential role of macrophage activation in the treatment of cancer. *Crit Rev Oncol Hematol.* 2002;44(2):143-161.
18. Mocellin S, Wang E, Marincola FM. Cytokines and immune response in the tumor microenvironment. *J Immunother.* 2001;24(5):392-407.
19. Cassatella MA. The production of cytokines by polymorphonuclear neutrophils. *Immunol Today.* 1995;16(1):21-26.
20. Fadnes HO, Reed RK, Aukland K. Interstitial fluid pressure in rats measured with a modified wick technique. *Microvasc Res.* 1977;14(1):27-36.
21. Tjaden UR, de Bruijn EA. Chromatographic analysis of anticancer drugs. *J Chromatogr.* 1990;531:235-294.
22. Jaffe EA, Nachman RL, Becker CG, Minick CR. Culture of human endothelial cells derived from umbilical veins. Identification by morphologic and immunologic criteria. *J Clin Invest.* 1973;52(11):2745-2756.
23. Schulze-Osthoff K, Fiers W. Oxygen radicals as second messengers. *Trends Cell Biol.* 1991;1(6):150.
24. Maeda H, Akaike T. Nitric oxide and oxygen radicals in infection, inflammation, and cancer. *Biochemistry (Mosc).* 1998;63(7):854-865.
25. de Wilt JH, Manusama ER, van Tiel ST, van Ijken MG, ten Hagen TL, Eggermont AM. Prerequisites for effective isolated limb perfusion using tumour necrosis factor alpha and melphalan in rats. *Br J Cancer.* 1999;80(1-2):161-166.
26. Folli S, Pelegri A, Chalandon Y, et al. Tumor-necrosis factor can enhance radio-antibody uptake in human colon carcinoma xenografts by increasing vascular permeability. *Int J Cancer.* 1993;53(5):829-836.
27. Rowlinson-Busza G, Maraveyas A, Epenetos AA. Effect of tumour necrosis factor on the uptake of specific and control monoclonal antibodies in a human tumour xenograft model. *Br J Cancer.* 1995;71(4):660-665.
28. Sacchi A, Gasparri A, Curmis F, Bellone M, Corti A. Crucial role for interferon gamma in the synergism between tumor vasculature-targeted tumor necrosis factor alpha (NGR-TNF) and doxorubicin. *Cancer Res.* 2004;64(19):7150-7155.
29. Zlotecki RA, Boucher Y, Lee I, Baxter LT, Jain RK. Effect of angiotensin II induced hypertension on tumor blood flow and interstitial fluid pressure. *Cancer Res.* 1993;53(11):2466-8.
30. Rubin K, Sjoquist M, Gustafsson AM, Isaksson B, Salvessen G, Reed RK. Lowering of tumoral interstitial fluid pressure by prostaglandin E(1) is paralleled by an increased uptake of (51)Cr-EDTA. *Int J Cancer.* 2000;86(5):636-43.
31. Boucher Y, Baxter LT, Jain RK. Interstitial pressure gradients in tissue-isolated and subcutaneous tumors: implications for therapy. *Cancer Res.* 1990;50(15):4478-4484.

32. Rohde D, Wiesner C, Graf D, Wolff J, Fuzesi L, Jakse G. Interstitial fluid pressure is increased in renal cell carcinoma xenografts. *Urol Res.* 2000;28(1):1-5.
33. Jain RK. Barriers to drug delivery in solid tumors. *Sci Am.* 1994;271(1):58-65.
34. Kelley ST, Menon C, Buerk DG, Bauer TW, Fraker DL. Acidosis plus melphalan induces nitric oxide-mediated tumor regression in an isolated limb perfusion human melanoma xenograft model. *Surgery.* 2002;132(2):252-258.
35. Skarsgard LD, Skwarchuk MW, Vinczan A, Kristl J, Chaplin DJ. The cytotoxicity of melphalan and its relationship to pH, hypoxia and drug uptake. *Anticancer Res.* 1995;15(1):219-223.
36. Chaplin DJ, Acker B, Olive PL. Potentiation of the tumor cytotoxicity of melphalan by vasodilating drugs. *Int J Radiat Oncol Biol Phys.* 1989;16(5):1131-1135.
37. Mocellin S, Provenzano M, Rossi CR, et al. Induction of endothelial nitric oxide synthase expression by melanoma sensitizes endothelial cells to tumor necrosis factor-driven cytotoxicity. *Clin Cancer Res.* 2004;10(20):6879-6886.
38. Tozer GM, Prise VE, Bell KM. The influence of nitric oxide on tumour vascular tone. *Acta Oncol.* 1995;34(3):373-377.
39. de Wilt JH, Manusama ER, van Etten B, et al. Nitric oxide synthase inhibition results in synergistic anti-tumour activity with melphalan and tumour necrosis factor alpha-based isolated limb perfusions [In Process Citation]. *Br J Cancer.* 2000;83(9):1176-82.
40. Naredi PL, Lindner PG, Holmberg SB, Stenram U, Peterson A, Hafstrom LR. The effects of tumour necrosis factor alpha on the vascular bed and blood flow in an experimental rat hepatoma. *Int J Cancer.* 1993;54(4):645-649.
41. Mocellin S, Provenzano M, Rossi CR, Pilati P, Nitti D, Lise M. Use of quantitative real-time PCR to determine immune cell density and cytokine gene profile in the tumor microenvironment. *J Immunol Methods.* 2003;280(1-2):1-11.
42. Mocellin S, Provenzano M, Lise M, Nitti D, Rossi CR. Increased TIA-1 gene expression in the tumor microenvironment after locoregional administration of tumor necrosis factor-alpha to patients with soft tissue limb sarcoma. *Int J Cancer.* 2003;107(2):317-322.
43. Brunstein F, Hoving S, Seynhaeve AL, et al. Synergistic antitumor activity of histamine plus melphalan in isolated limb perfusion: preclinical studies. *J Natl Cancer Inst.* 2004;96(21):1603-1610.
44. Hoving S, Brunstein F, aan de Wiel-Ambagtsheer G, et al. Synergistic antitumor response of IL-2 with melphalan in isolated limb perfusion in soft-tissue sarcoma bearing rats. *Cancer Res.* 2005;65(10):4300-4308.

Chapter 6

Lack of efficacy of Doxil[®] in a TNF-based isolated limb perfusion in sarcoma-bearing rats

Timo LM ten Hagen, Saske Hoving, Gisela aan de Wiel-Ambagtsheer, Sandra T van Tiel, Alexander MM Eggermont.

Department of Surgical Oncology, Erasmus MC-Daniel den Hoed Cancer Center, Rotterdam, the Netherlands

Abstract

Here we show that Doxil[®] has minimal antitumor activity in the isolated limb perfusion (ILP) setting and its activity was not enhanced by the addition of tumor necrosis factor (TNF). Doxil[®] accumulation in tumor tissue was low and also not augmented by TNF. In contrast, activity of free conventional doxorubicin was enhanced by TNF. We conclude that application of Doxil[®] in a TNF-based ILP is not a useful alternative to free conventional doxorubicin or melphalan.

Introduction

Isolated limb perfusion (ILP) provides an excellent tool in the treatment of locally advanced tumors. During ILP, high local drug concentrations are possible due to minimal leakage into the systemic circulation, and the effect on vital organs is limited, allowing high dosages to be used. We and others have demonstrated that addition of tumor necrosis factor (TNF) to an ILP with melphalan increased the tumor response dramatically as compared to melphalan alone (1,2).

Melphalan is used most commonly in ILP, but other agents have been applied with varying success in limb or organ perfusion (3-5). We observed in ILP that local toxicity was dose-limiting at suboptimal doxorubicin concentrations (6).

The formulation of doxorubicin in long-circulating liposomes (Stealth[®] liposomal doxorubicin, Doxil[®]) prolongs circulation time, decreases toxicity and augments localization in tumor tissue (7). We hypothesized that the use of Doxil[®] in ILP may reduce local toxicity while augmenting tumor accumulation and improving tumor response. In this study, we examined the efficacy of Doxil[®] in a TNF-based ILP in sarcoma-bearing rats.

Materials and Methods

Chemicals

Human recombinant TNF- α was kindly provided by Dr G Adolf (Bender Wien GmbH, Wien, Austria). Pegylated liposomal doxorubicin (Doxil[®], Caelyx[®]) was kindly provided by Dr Working (ALZA Corporation, Mountain View, CA, USA). Doxorubicin hydrochloride (adriablastina) was purchased from Pharmacia (Brussels, Belgium).

Animals and tumor model

Male inbred BN rats (soft-tissue sarcoma model, BN175) and WAG/RIJ rats (osteosarcoma model, ROS-1) were obtained from Harlan-CPB (Austerlitz, the Netherlands). Small fragments (3mm) of tumor were implanted subcutaneously in the right hindleg, as previously described (8). Tumor growth was recorded by calliper measurements, and tumor volume was calculated using the formula $0.4(A^2B)$ (where B represents the largest diameter and A the diameter perpendicular to B). All animal studies were done in accordance with

protocols approved by the Animal Care Committee of the Erasmus University Rotterdam, the Netherlands (9).

A tumor response indicates either a partial remission (PR, decrease of tumor volume between -25 and 90%) or a complete remission (CR, tumor volume less than 10% of initial volume).

Isolated limb perfusion protocol

Rat limbs were perfused as previously described (8). Tumor necrosis factor (50 µg), Doxil[®] or doxorubicin (400 µg BN175 and 200 µg ROS-1) were added as boluses to the oxygenation reservoir. Control rats were perfused with Haemaccel or placebo liposomes alone. The concentration of TNF was adapted from previous animal studies, and doxorubicin concentrations that yielded no local toxicity were used. All animal studies were approved as stated above (9).

Assessment of doxorubicin accumulation in solid tumor during ILP

Accumulation of doxorubicin in tumor and muscle was determined directly after ILP, as previously described (6,10). As the ILP included a thorough washout, there was no intravascular doxorubicin present. All animal studies were approved as stated above (9).

Statistical analysis

The results were evaluated for statistical significance using the Mann–Whitney U-test with SPSS for Windows. P-values below 0.05 were considered statistically significant.

Results

Tumor response to Doxil[®] in TNF-based ILP

Perfusion with Doxil[®], TNF or buffer alone resulted in progressive disease in all soft-tissue sarcoma-bearing rats (Figure 1A). Perfusion with Doxil[®] plus TNF resulted in a short growth delay followed by rapid outgrowth of the tumor, and all rats showed progressive disease. Application of free conventional doxorubicin resulted only in a slight inhibition of the tumor growth, and no rats showed a tumor response. Isolated limb perfusion with conventional doxorubicin combined with 50 µg TNF increased the antitumor activity with a response rate of 83% (PR and CR combined) ($p < 0.01$ compared with doxorubicin alone).

Isolated limb perfusion in osteosarcoma-bearing rats with buffer or conventional doxorubicin alone had no significant effect on tumor growth (Figure 1B). Isolated limb perfusion with TNF alone resulted in a response rate of 25%. Isolated limb perfusion with conventional doxorubicin combined with TNF further increased the tumor response to 83% ($p < 0.05$ compared with TNF alone or doxorubicin alone). Isolated limb perfusion with Doxil[®] only, induced slight tumor growth delay comparable to free conventional

doxorubicin. Strikingly, ILP with Doxil[®] plus TNF diminished the tumor response, and none of the rats showed a tumor response.

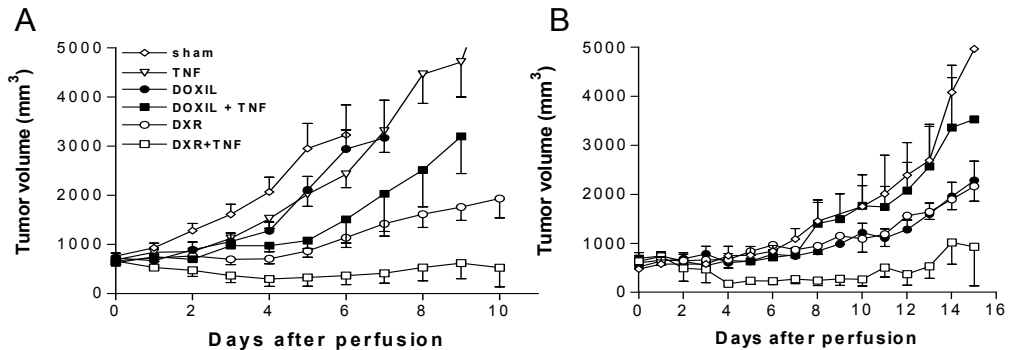


Figure 1. (A) Tumor volumes of subcutaneous implanted soft-tissue sarcoma BN175 after isolated limb perfusion with perfusate alone (n=6), 400 mg Doxil[®] (n=4), 50 mg TNF (n=6), Doxil[®] plus 50 mg TNF (n=8), 400 mg free doxorubicin (DXR) (n=7), or a combination of TNF and free DXR (n=6). (B) Tumor volumes of subcutaneous implanted osteosarcoma ROS-1 after isolated limb perfusion with perfusate alone (n=6), 200 mg Doxil[®] (n=6), 50 mg TNF (n=8), 200 mg Doxil[®] plus 50 mg TNF (n=7), 200 mg free doxorubicin (DXR) (n=6), or a combination of TNF and DXR (n=6). The mean tumor volumes are shown \pm SE.

Accumulation of doxorubicin in solid tumor after ILP

We observed that addition of TNF did not significantly augment the accumulation of Doxil[®] in soft-tissue sarcoma or osteosarcoma when compared to ILP with Doxil[®] alone (data not shown). Levels of doxorubicin were significantly increased when TNF was added to ILP with free doxorubicin (6).

Discussion

In the present study, we demonstrated that ILP treatment with Doxil[®] combined with TNF in sarcoma-bearing rats does not provide a useful alternative to free conventional doxorubicin. The lack of efficacy of Doxil[®] is not due to failure of the drug to be active at the tumor site, as dramatic synergy between Doxil[®] and TNF after systemic treatment has been shown (11). Rather, we speculate that the liposomes are unable to extravasate into the tumors during the relatively short ILP interval.

In spite of the indicated usefulness of doxorubicin in ILP for the treatment of sarcoma, we and others observed dose-limiting local toxicity after a TNF-based ILP with conventional doxorubicin (6,12). Biodistribution and pharmacokinetic studies with Doxil[®] demonstrated a favorable profile of the liposomal formulations over the free drugs, that is, circulation time was extended, toxicity reduced and tumor localization was increased (7). Therefore, we envisioned that Doxil[®] could be a good alternative to free conventional doxorubicin in

ILP. However, Doxil[®] failed to induce any response in sarcoma-bearing rats, even when applied in combination with TNF. Minimal accumulation of Doxil[®] in tumor after ILP with or without TNF was observed, whereas considerably higher levels of doxorubicin were found in tumor after ILP with free doxorubicin plus TNF. A possible explanation for the difference in accumulation between free conventional doxorubicin and liposomal doxorubicin is the particle size. Whereas distribution of a small molecule like doxorubicin is diffusion dependent, the transport of particulate matter is convection dependent (13,14). This would indicate that, during ILP, drug distribution is mostly diffusion dependent and not convection dependent.

The increased tumor localization of Doxil[®] seen after systemic administration is reportedly due to the ability of the pegylated liposomes to avoid accumulation in the liver and spleen and other parts of the mononuclear phagocytic system (MPS), which results in a long circulation time and extravasation through the leaky vasculature of tumors (7). The volume of distribution of Doxil[®] is markedly smaller than that of doxorubicin given systemically, reflecting the broad tissue distribution of the latter. The short 30-min circulation time imposed by the ILP procedure is likely inadequate for the circulation time advantage of Doxil[®] to have an effect on its distribution, and, of course, the restriction of circulation to the isolated limb obviates the value of avoiding the MPS. Thus, the rapid distribution properties of the small doxorubicin molecule makes it a better choice for ILP procedures, particularly when it is used in combination with TNF.

References

1. Eggermont AM, Schraffordt KH, Lienard D, et al. Isolated limb perfusion with high-dose tumor necrosis factor-alpha in combination with interferon-gamma and melphalan for nonresectable extremity soft tissue sarcomas: a multicenter trial. *J Clin Oncol.* 1996;14(10):2653-2665.
2. Lienard D, Ewalenko P, Delmotte JJ, Renard N, Lejeune FJ. High-dose recombinant tumor necrosis factor alpha in combination with interferon gamma and melphalan in isolation perfusion of the limbs for melanoma and sarcoma. *J Clin Oncol.* 1992;10(1):52-60.
3. Abolhoda A, Brooks A, Nawata S, Kaneda Y, Cheng H, Burt ME. Isolated lung perfusion with doxorubicin prolongs survival in a rodent model of pulmonary metastases. *Ann Thorac Surg.* 1997;64(1):181-184.
4. Rossi CR, Vecchiato A, Da Pian PP, et al. Adriamycin in hyperthermic perfusion for advanced limb sarcomas. *Ann Oncol.* 1992;3 Suppl 2:S111-S113.
5. Weksler B, Lenert J, Ng B, Burt M. Isolated single lung perfusion with doxorubicin is effective in eradicating soft tissue sarcoma lung metastases in a rat model. *J Thorac Cardiovasc Surg.* 1994;107(1):50-54.
6. van Der Veen AH, de Wilt JH, Eggermont AM, van Tiel ST, Seynhaeve AL, ten Hagen TL. TNF-alpha augments intratumoural concentrations of doxorubicin in TNF-alpha-based isolated limb perfusion in rat sarcoma models and enhances anti-tumour effects. *Br J Cancer.* 2000;82(4):973-980.
7. Gabizon A, Shmeeda H, Barenholz Y. Pharmacokinetics of pegylated liposomal Doxorubicin: review of animal and human studies. *Clin Pharmacokinet.* 2003;42(5):419-436.
8. de Wilt JH, Manusama ER, van Tiel ST, van Ijken MG, ten Hagen TL, Eggermont AM. Prerequisites for effective isolated limb perfusion using tumour necrosis factor alpha and melphalan in rats. *Br J Cancer.* 1999;80(1-2):161-166.
9. Workman P, Twentymann P, Balkwill F, et al. United Kingdom Co-ordinating Committee on Cancer Research (UKCCCR) guidelines for the welfare of animals in experimental neoplasia (second edition). *Br J Cancer.* 1988;77:1-10.

10. Mayer LD, Tai LC, Ko DS, et al. Influence of vesicle size, lipid composition, and drug-to-lipid ratio on the biological activity of liposomal doxorubicin in mice. *Cancer Res.* 1989;49(21):5922-5930.
11. ten Hagen TL, van Der Veen AH, Nooijen PT, van Tiel ST, Seynhaeve AL, Eggermont AM. Low-dose tumor necrosis factor-alpha augments antitumor activity of stealth liposomal doxorubicin (DOXIL) in soft tissue sarcoma-bearing rats. *Int J Cancer.* 2000;87(6):829-37.
12. Di Filippo F, Rossi CR, Vaglini M, et al. Hyperthermic antitumor perfusion with alpha tumor necrosis factor and doxorubicin for the treatment of soft tissue limb sarcoma in candidates for amputation: results of a phase I study. *J Immunother.* 1999;22(5):407-414.
13. Hobbs SK, Monsky WL, Yuan F, et al. Regulation of transport pathways in tumor vessels: role of tumor type and microenvironment. *Proc Natl Acad Sci U S A.* 1998;95(8):4607-12.
14. Jain RK, Stock RJ, Chary SR, Rueter M. Convection and diffusion measurements using fluorescence recovery after photobleaching and video image analysis: in vitro calibration and assessment. *Microvasc Res.* 1990;39(1):77-93.

Part III

Liposomal systemic treatment

Chapter 7

Effect of low-dose tumor necrosis factor- α in combination with Stealth[®] liposomal cisplatin (SPI-077) on soft-tissue and osteosarcoma-bearing rats

Saske Hoving, Sandra T van Tiel, Alexander MM Eggermont, Timo LM ten Hagen

Department of Surgical Oncology, Erasmus MC-Daniel den Hoed Cancer Center, Rotterdam, the Netherlands

Abstract

Cisplatin is a widely used agent for treatment of solid tumors, but its clinical utility is limited by toxicity. Preclinical studies have shown less acute toxicity when Stealth[®] liposomal cisplatin (SPI-077) is used, with antitumor effects equivalent to those of intravenously administered free cisplatin. We previously reported that systemic treatment with low-dose tumor necrosis factor- α (TNF) augments the activity of Stealth[®] liposomal doxorubicin (Doxil[®]). In this study, we examined the effect of repeated systemic applications of low-dose TNF on the antitumor activity of SPI-077 in rats with soft-tissue sarcoma or osteosarcoma. Addition of TNF to SPI-077 treatment showed an improved tumor growth delay of the soft-tissue sarcoma. The combined SPI-077/TNF treatment resulted in a more prolonged antitumor activity, whereas free cisplatin showed a better tumor response, however with a rapid outgrowth a few days after the end of therapy. In the osteosarcoma, free cisplatin did not have an antitumor effect, but addition of TNF caused a clear tumor growth delay. SPI-077 alone resulted in a tumor growth delay, but combination with TNF had no additive effect. SPI-077 yielded less systemic toxicity than cisplatin. Depending on the type of tumor, the addition of TNF to SPI-077 results in a better tumor growth delay with a prolonged antitumor effect and, in combination with the reduced toxicity of SPI-077, this combination may be preferable to cisplatin.

Introduction

Cisplatin, cis-diamminedichloroplatinum(II), is widely used in the treatment of a variety of solid tumors, particularly those in the ovary, head, neck, and lung (1-7). The drug's mechanism of action is based on direct binding of cisplatin to DNA. A major drawback of this powerful agent is its acute, dose-limiting toxicity. Administration of cisplatin is associated with nausea and vomiting, ototoxicity, nephrotoxicity, neurotoxicity and, to a lesser extent, myelosuppression (1,7,8). Other problems influencing efficacy of the agent are the rapid inactivation of the drug and the development of platinum resistance (9).

Several studies have shown that encapsulation of antineoplastic agents in liposomes can reduce systemic toxicity while retaining, or even improving, *in vivo* efficacy (10-13). SPI-077 (Stealth[®] liposomal cisplatin) is a formulation of cisplatin encapsulated in sterically stabilized, long-circulating liposomes that contain methoxy-polyethylene glycol (MPEG). Because of their small size, long circulation time and reduced interaction with formed elements of the blood, sterically stabilized liposomes tend to accumulate in tumors, presumably due to leakage through the often compromised tumor vasculature (5,10-12,14-16).

SPI-077's antitumor activity has been studied in various animal tumor models and in human xenografts. These preclinical studies demonstrated toxicity which was less acute as compared to cisplatin, and the antitumor effect was at least equivalent to that of free

cisplatin (1,5,6,17,18). In clinical studies, SPI-077 showed a markedly different pharmacokinetic profile to cisplatin. However, despite the favorable pharmacokinetic properties, enhanced antitumor activity was not observed (7,8,19,20).

We previously showed that alteration of the pharmacokinetic profile of Doxil[®] (Stealth[®] liposomal doxorubicin) by co-administration of tumor necrosis factor- α (TNF) has a strong beneficial effect. Repeated administration of Doxil[®] and low-dose TNF resulted in a pronounced tumor response in soft tissue sarcoma-bearing rats with most of the rats showing tumor regression (21,22). When Doxil[®] was administered alone, however, there was no tumor response in any of the rats. Comparable results were seen in melanoma-bearing mice (23). Administering TNF with Doxil[®] augmented accumulation of the chemotherapeutic drug in the tumor tissue and probably explains the enhanced tumor regression.

In this study, we compared placebo liposomes, free cisplatin, SPI-077, low-dose TNF, and combination therapies of cisplatin/TNF and SPI-077/TNF and evaluated the antitumor activity and side effects.

Materials and Methods

Chemicals

Human recombinant tumor necrosis factor- α (specific activity 5×10^7 IU/ml) was kindly provided by Boehringer (Boehringer Ingelheim GmbH, Austria) and stored at a concentration of 2 mg/ml. Endotoxin levels were less than 1.25 units (EU) per mg protein.

Cisplatin was purchased from Pharmachemie B.V. (Haarlem, the Netherlands) in 1 mg/ml solution ready for use. SPI-077 (Stealth[®] liposomal cisplatin) was kindly provided by ALZA Corporation (Mountain View, CA, USA). SPI-077 liposomes were comprised of hydrogenated soy phosphatidylcholine, methoxypolyethylene-glycol-distearoyl phosphatidyl-ethanolamine and cholesterol at an approximate 51:5:44 molar ratio. Briefly, preparation of the liposomes begins with dissolving the lipid components in ethanol followed by addition to an aqueous cisplatin solution. The resulting liposomes are then sized by extrusion through polycarbonate membranes and diafiltered to remove unencapsulated cisplatin. The process produces liposomes with an average particle size of 110 nm, no unencapsulated drug in the stored preparation, a final drug concentration of 1 mg/ml and a drug to lipid ratio of 0.014.

Animals and tumor model

Male inbred Brown Norway rats were used for the soft-tissue sarcoma model (BN175); WAG/RIJ rats were used for the osteosarcoma model (ROS-1). Rats were obtained from Harlan-CPB, (Austerlitz, the Netherlands), weighed 250-300 g and were fed a standard laboratory diet *ad libitum* (Hope Farms Woerden, the Netherlands).

Small fragments (3 mm) of the syngeneic BN175 or ROS-1 sarcoma were implanted subcutaneously in the right hindleg of each rat, as previously described (24). Tumor growth was recorded by caliper measurement, and tumor volume was calculated using the formula $0.4(A^2 \times B)$ (where B represents the largest diameter, and A is the diameter perpendicular to B). Rats were sacrificed when tumor diameter exceeded 25 mm or at the end of the experiment. All animal studies were done in accordance with protocols approved by the Committee on Animal Research of the Erasmus MC, Rotterdam, the Netherlands.

Treatment protocol

About 7-8 days after implantation, the tumors reached an average diameter of 9-11 mm and treatment was started. The rats were randomized into the following six groups: 1) placebo liposomes (equivalent amounts of buffer or lipids), 2) free cisplatin, 3) SPI-077, 4) low-dose TNF, 5) cisplatin/TNF and 6) SPI-077/TNF. For the BN rats concentrations of 0.1, 0.3, 1 and 3 mg/kg cisplatin or SPI-077 were used. The WAG/RIJ rats received 1 or 3 mg/kg of cisplatin or SPI-077. Both rat strains received 15 µg/kg TNF. Rats were given a total of five intravenous injections, one every four days. When the rats were treated with the combination therapies of cisplatin/TNF or SPI-077/TNF, the agents were injected separately, one shortly after the other.

Tumor response was classified as follows: progressive disease (PD) = increase of tumor volume (> 25%) over a 16-day period; no change (NC) = tumor volume equal to volume as start of treatment (in a range of -25% and +25%); partial remission (PR) = decrease of tumor volume (-25 and -90%); complete remission (CR) = tumor volume less than 10% of initial volume.

In vitro cytotoxicity assay

Cells isolated from a BN175 soft-tissue sarcoma were maintained in cell culture in RPMI 1640 supplemented with 5% fetal calf serum and 0.1% penicillin-streptomycin. The rat osteosarcoma ROS-1 cells were maintained in modified Eagle's medium supplemented with 10% fetal calf serum and 0.1% penicillin-streptomycin. Media and supplements were obtained from Life Technologies, the Netherlands.

BN175 or ROS-1 cells were added in 100-µl aliquots to 96-well, flat-bottomed, microtiter plates (Costar, Cambridge, MA, USA) at a final density of 1×10^4 cells per well and allowed to grow as a monolayer. Cells were incubated at 37°C in 5% CO₂ for 72 hours in the presence of various concentrations of TNF, cisplatin, and SPI-077. Concentrations of TNF ranged between 0 and 10 µg/ml. Concentrations of cisplatin ranged between 2.5 ng and 100 µg/ml, while those of SPI-077 were between 50 ng and 1 mg/ml. The growth of tumor cells was measured using the Sulphorhodamine-B (SRB) assay according to the method of Skehan (25). In short, cells were washed twice with phosphate buffered saline, incubated

with 10% trichloroacetic acid (1 hour, 4°C), and washed again. The cells were stained with 0.4% SRB (15-30 min), washed with 1% acetic acid and were allowed to dry. Protein-bound SRB was dissolved in TRIS (10 mM, pH 9.4). The optical density was read at 540 nm. *In vitro* tumor cell growth was calculated using the following formula: tumor cell growth = (test well/control) x 100%. The drug concentration required to reduce the absorbance to 50% of the control (IC₅₀) was determined from the growth curves. The experiments were repeated at least five times.

Nephro- and hepatotoxicity

The WAG/RIJ rats treated with 3 mg/kg cisplatin or SPI-077 were observed at regular intervals for signs of toxicity, and weight was recorded daily. Two days after every round of administration, 1 ml blood was taken from the tail vein. Levels of alanine aminotransferase (ALAT), aspartate aminotransferase (ASAT), creatinine, urea and γ -glutamyl transpeptidase (γ -GT) were measured using Granutests in order to detect renal and hepatic toxicity (Merck, Darmstadt, Germany). The principle of the creatinine measurement is the reaction of creatinine with picric acid in alkaline solution, which leads to a yellow-orange colored compound. Urea was calculated from an enzymatic reaction in conjunction with urease, where the decrease of NADH, which is needed for the reaction, was measured. Histopathological examination was performed on the kidneys and livers from another group of animals treated with 3 mg/kg cisplatin or SPI-077. The animals were autopsied at day 17 (24 hours after fifth and last treatment), the kidneys and liver were removed and fixed in 4% formaldehyde and embedded in paraffin. Tissue sections of 4 μ m were cut and stained with haematoxylin and eosin, examined on a Leica DM-RXA and photographed using a Sony DXC950 camera.

Statistical analysis

The results were evaluated for statistical significance with the Kruskal-Wallis followed by the Mann Whitney U test or the Fisher's Exact test (tumor progressors vs. non-progressors (NC + PR + CR)). P-values below 0.05 were considered statistically significant. Calculations were performed on a personal computer using GraphPad Prism v3.0 and SPSS v11.0 for Windows 2000.

Results

Effect of low-dose TNF on antitumor activity of SPI-077 in soft-tissue sarcoma- and osteosarcoma-bearing rats

BN175 soft-tissue sarcoma-bearing rats were treated with a dose range of free cisplatin or SPI-077 in combination with low-dose TNF. The highest dose of 3 mg/kg cisplatin showed severe toxicity, whereas the lower concentrations (0.1 and 0.3 mg/kg) resulted in

progressive diseases for both cisplatin and SPI-077 (data not shown). Treatment with 1 mg/kg provides the best efficacy *versus* toxicity ratio and, therefore, we chose to further evaluate the concentration of 1 mg/kg free cisplatin or SPI-077 in combination with TNF.

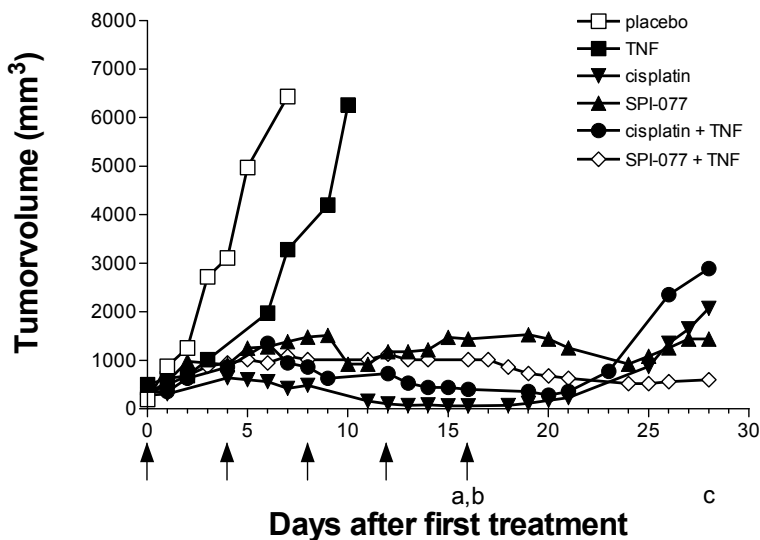


Figure 1. Growth curves of subcutaneous implanted BN-175 sarcoma after systemic treatment with SPI-077 and low-dose TNF. Rats were injected five times intravenously with an interval of 4 days between the injections with buffer alone (n=5), 15 μ g/kg TNF (n=5), 1 mg/kg cisplatin (n=3), 1 mg/kg SPI-077 (n=4), 1 mg/kg cisplatin combined with 15 μ g/kg TNF (n=3) and 1 mg/kg SPI-077 combined with 15 μ g/kg TNF (n=4). Arrows indicate injections. Median tumor volumes are shown. Statistical analysis (Mann Whitney U test): a. cisplatin vs. cisplatin + TNF ($p=0.05$), b. cisplatin vs. SPI-077 ($p=0.05$), c. cisplatin + TNF vs. SPI-077 + TNF ($p=0.05$).

Administration of 1 mg/kg SPI-077 to BN175 soft-tissue sarcoma-bearing rats resulted in pronounced growth delay of the tumor, but no regression was observed (Figure 1 and Table 1). Addition of 15 μ g/kg TNF to this regimen resulted in an improved, but not significant, tumor response. Administration of free cisplatin had a much more pronounced antitumor effect, inducing strong tumor regression, compared to SPI-077. However, in spite of the augmented antitumor activity of the combined TNF and SPI-077, the addition of low-dose TNF to the free cisplatin regimen resulted in a slightly reduced antitumor efficacy. Intravenous administration of TNF alone or placebo liposomes had no significant effect on tumor progression in any of the animals. Although tumor regression in the cisplatin treated animals was better than the combined SPI-077/TNF treatment, tumor regrowth occurred a few days after the end of therapy. The SPI-077/TNF treated animals did not show tumor outgrowth, indicating a prolonged antitumor effect.

Table 1. Tumor response in soft tissue sarcoma-bearing rats after repeated systemic treatment with Stealth[®] liposomal cisplatin (SPI-077) combined with low-dose TNF over a total period of 16 days. The animals were treated on day 0, 4, 8, 12 and 16.

Treatment	Response rate ^a			
	PD ^b	NC	PR	CR
placebo	5			
TNF (15 µg/kg)	5			
cisplatin (1 mg/kg)			3*	
SPI-077 (1 mg/kg)	4			
cisplatin (1 mg/kg) + TNF (15 µg/kg)	1	2		
SPI-077 (1 mg/kg) + TNF (15 µg/kg)	4			

^a responses were scored as described in Materials and Methods, ^b PD: progressive disease, NC: no change, PR: partial remission, CR: complete remission, * p=0.018 compared with placebo (Fisher's Exact test)

ROS-1 osteosarcoma treated animals with 3 mg/kg free cisplatin showed severe toxicity, and therefore 1 mg/kg concentration was chosen as in the BN175 experiments. In contrast to the BN175 soft tissue sarcoma, the ROS-1 osteosarcoma was not sensitive to 1 mg/kg free cisplatin with all treated animals exhibiting progressive disease (Figure 2 and Table 2).

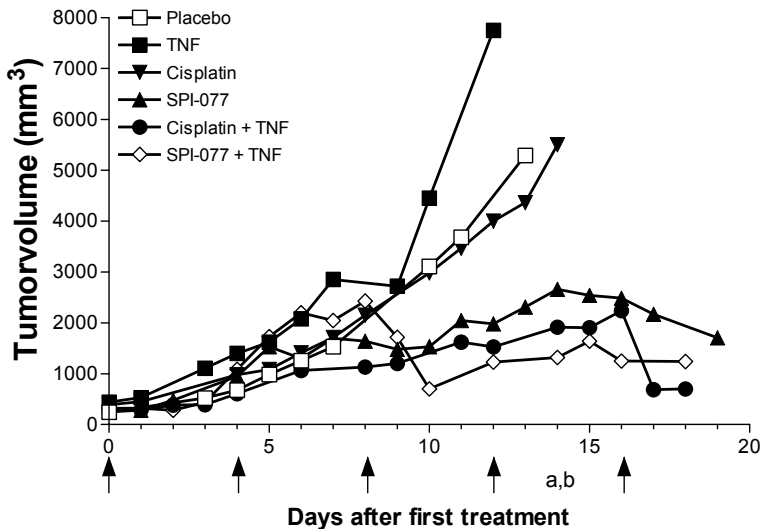


Figure 2. Growth curves of subcutaneous implanted ROS-1 osteosarcoma after systemic treatment with SPI-077 and low-dose TNF. Rats were injected five times intravenously with an interval of 4 days between the injections with buffer alone (n=5), 15 µg/kg TNF (n=5), 1 mg/kg cisplatin (n=3), 1 mg/kg SPI-077 (n=4), 1 mg/kg cisplatin combined with 15 µg/kg TNF (n=3) and 1 mg/kg SPI-077 combined with 15 µg/kg TNF (n=4). Arrows indicate injections. Median tumor volumes are shown. Statistical analysis (Mann Whitney U test): a. cisplatin vs. cisplatin + TNF (p<0.05), b. cisplatin vs. SPI-077 (p<0.05).

Administration of 15 $\mu\text{g}/\text{kg}$ TNF alone had also no effect on the tumor response. Treatment with 1 mg/kg SPI-077 resulted in progressive disease in all animals; however, these tumors did not grow as fast as those in animals treated with free cisplatin. Addition of low-dose TNF to free cisplatin improved tumor response slightly, and there were six animals with progressive disease, one no change, and one who was a complete responder (not significant compared to other treatments with Fisher's exact test). The combination of TNF with SPI-077 did not have an additive effect on the tumor response, which is in contrast with the BN175 tumor where TNF did have an additive effect.

Table 2. Tumor response in osteosarcoma-bearing rats after repeated systemic treatment with Stealth[®] liposomal cisplatin (SPI-077) combined with low-dose TNF over a total period of 16 days. The animals were treated on day 0, 4, 8, 12 and 16.

Treatment	Response rate ^a			
	PD ^b	NC	PR	CR
placebo	5			
TNF (15 $\mu\text{g}/\text{kg}$)	5			
cisplatin (1 mg/kg)	5			
SPI-077 (1 mg/kg)	7			
cisplatin (1 mg/kg) + TNF (15 $\mu\text{g}/\text{kg}$)	6	1		1
SPI-077 (1 mg/kg) + TNF (15 $\mu\text{g}/\text{kg}$)	5			

^a responses were scored as described in Materials and Methods, ^b PD: progressive disease, NC: no change, PR: partial remission, CR: complete remission

In vitro activity of cisplatin or SPI-077 combined with TNF on BN-175 and ROS-1 tumor cells

Exposure of the BN175 sarcoma cells to cisplatin caused dose-related cytotoxicity with an IC_{50} of 0.18 $\mu\text{g}/\text{ml}$ (data not shown). The cytotoxicity of cisplatin was strongly reduced upon liposomal encapsulation (IC_{50} of 59.1 $\mu\text{g}/\text{ml}$). No significant cellular toxicity could be observed when BN175 cells were exposed to TNF alone. The IC_{50} decreased to 0.14 $\mu\text{g}/\text{ml}$ when the cells were co-incubated with cisplatin and 10 $\mu\text{g}/\text{ml}$ TNF. When the cells were incubated with SPI-077 and 10 $\mu\text{g}/\text{ml}$ TNF the IC_{50} was lowered to 25.0 $\mu\text{g}/\text{ml}$ (not significant compared to cisplatin and SPI-077 alone).

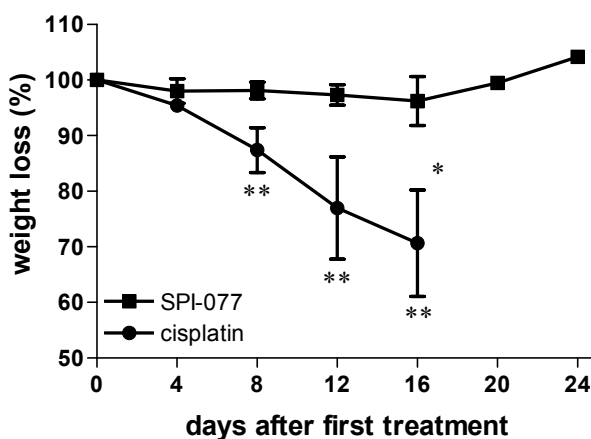
In the osteosarcoma cell line, ROS-1, liposomal encapsulation of cisplatin strongly reduced the cytotoxicity of this agent; the IC_{50} values for free cisplatin and SPI-077 were 1.24 $\mu\text{g}/\text{ml}$ and 203.4 $\mu\text{g}/\text{ml}$, respectively (data not shown). A maximal dose-dependent growth reduction of 40% was observed when ROS-1 cells were exposed to TNF concentrations up to 10 $\mu\text{g}/\text{ml}$. Although TNF had some effect on the ROS-1 cells no synergy was observed when TNF was combined with SPI-077 or free cisplatin. The IC_{50} values for free cisplatin

and SPI-077 in combination with 10 µg/ml TNF were 0.72 and 214.6 µg/ml, respectively (not significant compared to cisplatin and SPI-077 alone).

Toxicity evaluation

Weight changes during the course of the systemic treatment are presented in Figure 3. We observed that repeated administration of free cisplatin at a dose of 3 mg/kg per injection resulted in dramatic weight loss ($29\% \pm 10\%$ after day 16; $p < 0.05$) as compared to baseline in the WAG/RIJ rats. However, none of the rats treated with 3 mg/kg SPI-077 showed significant weight loss. The rats treated with free cisplatin showed general lethargy, whereas no such observation was made with animals treated with SPI-077. Addition of TNF to the cisplatin or SPI-077 treatment did not cause an extra effect on the weight loss (data not shown).

Figure 3. Weight loss of WAG/RIJ rats after systemic treatment with 3 mg/kg cisplatin (n=3) or 3 mg/kg SPI-077 (n=3). The percent of original weight \pm SE is shown. * Most of the animals in the cisplatin group were sacrificed because of severe weight loss. ** $p = 0.05$ compared with SPI-077 (Mann Whitney U test).



To determine the nephro- and hepatotoxicity in WAG/RIJ rats, serum toxicity parameters were measured. Creatinine and urea levels were elevated 1.9 and 2.5-fold, respectively, in rats treated with cisplatin, indicating renal failure (Table 3). No significant effects in these values were seen when the animals were treated with SPI-077. Both free cisplatin and SPI-077 appeared to affect liver function, as shown by elevated ALAT and ASAT levels. After treatment with cisplatin, the levels of γ -GT were 0 U/L. The levels increased up to more than 5 U/L after five treatments with SPI-077. The levels of γ -GT even continued to increase a few days after the last treatment, which is indicative of liver damage.

Histopathological examination was performed on the kidneys and livers from animals treated with 3 mg/kg cisplatin or SPI-077. The animals were autopsied 24 hours after the fifth and last treatment. The renal sections of the cisplatin-treated animals revealed remarkable degenerative changes in the proximal tubules, including cytoplasmic vacuolization, necrosis and pyknotic degeneration. Rats treated with SPI-077 showed no

damage to the kidney (Figure 4). Treatment with cisplatin or SPI-077 did not cause any obvious histologically evident liver damage, in spite of increased ALAT and ASAT levels in both groups and elevated γ -GT levels in the SPI-077 group.

Table 3. Kidney and liver toxicity and function of WAG/RIJ rats after treatment with cisplatin (3 mg/kg) or SPI-077 (3 mg/kg).

		day 2	day 6	day 10	day 14	day 18
Urea	cisplatin	8.4 ± 2.5	7.2 ± 1.1	10.4 ± 3.0	15.6 ± 6.7	22.1 ± 7.6#
	SPI-077	8.9 ± 2.1	8.5 ± 0.8	7.5 ± 0.9	8.0 ± 0.1	8.6 ± 0.4
Creatinine	cisplatin	49.0 ± 11.8	43.7 ± 8.0	56.0 ± 5.3	70.3 ± 10.7	70.0 ± 9.5#
	SPI-077	45.0 ± 18.0	43.3 ± 9.0	47.0 ± 8.5	34.0 ± 11.3	29.3 ± 6.5
ALAT	cisplatin	49.8 ± 7.1	57.8 ± 3.6	49.1 ± 3.9	48.5 ± 8.3	92.3 ± 32.4
	SPI-077	65.5 ± 9.4	80.8 ± 10.3#	90.7 ± 12.5#	88.5 *	96.2 ± 12.5
ASAT	cisplatin	82.2 ± 20.0	108.8 ± 28.8	128.2 ± 47.8	126.9 ± 26.7	140.9 ± 40.3
	SPI-077	148.0 ± 13.9#	203.3 ± 41.5#	180.2 ± 23.8	169.8 *	189.2 ± 67.3
γ -GT	cisplatin	0.0 ± 0.0	0.0 ± 0.0	0.0 ± 0.0	0.0 ± 0.0	0.0 ± 0.0
	SPI-077	0.0 ± 0.0	0.0 ± 0.0	0.4 ± 0.7	1.3 ± 1.8	4.1 ± 1.9#

note: The animals were treated on day 0, 4, 8, 12 and 16 (n=3 for both groups) with 3 mg/kg free cisplatin or SPI-077. Blood samples were taken two days after every treatment. Mean ± SD is shown. * values are missing, # p<0.05 compared to the other group at the same timepoint (Mann Whitney U test). Normal serum values: urea 8.7 ± 0.5 mmol/L, creatinine 36.7 ± 1.2 μ mol/L, ALAT: 58.5 ± 9.4 U/L, ASAT: 83.3 ± 10.2 U/L, γ -GT: 0.0 ± 0.0 U/L

Discussion

We have examined the efficacy of Stealth[®] liposomal cisplatin (SPI-077) combined with TNF in the treatment of solid tumors. We demonstrated that repeated systemic administration of SPI-077 alone to soft-tissue sarcoma-bearing rats resulted in less antitumor activity compared to free cisplatin. Combination treatment of cisplatin and low-dose TNF was less potent than cisplatin alone, but addition of TNF to a SPI-077 treatment caused a better tumor growth delay than SPI-077 alone. The combined SPI-077/TNF treatment resulted in a more prolonged antitumor activity, whereas free cisplatin showed a better tumor response, but with a rapid tumor outgrowth a few days after end of therapy.

In the ROS-1 osteosarcoma-bearing rats, free cisplatin alone had no antitumor activity, whereas treatment with a similar dose of SPI-077 resulted in a slightly improved antitumor activity. Addition of low-dose TNF improved the cisplatin treatment, but not the SPI-077 treatment. Although SPI-077 did not effect a better tumor response in the osteosarcoma compared to free cisplatin, fewer systemic side effects were detected. No weight loss, histological liver and kidney damage or lethargy were observed in the rats treated with SPI-077.

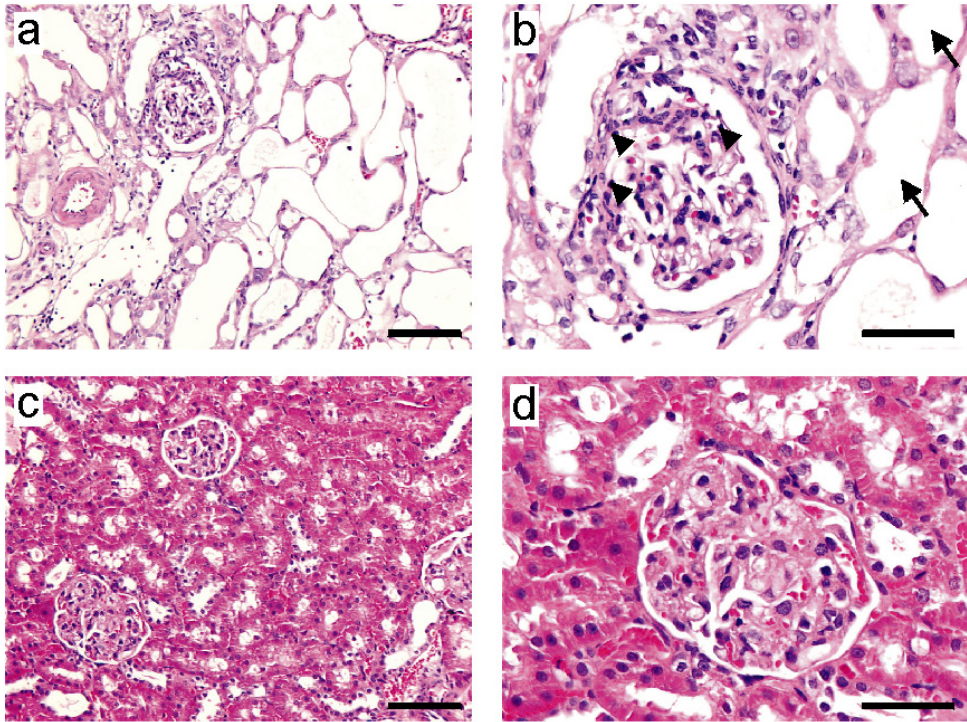


Figure 4. Paraffin sections of the kidney from osteosarcoma-bearing rats, after systemic treatment, haematoxylin-eosin stained. Overview of kidney after 5-fold treatment with 3 mg/kg cisplatin (a and b) (n=3) or 3 mg/kg SPI-077 (c and d) (n=3). Representative pictures are shown. Pycnotic degeneration (arrowheads) and cytoplasmic vacuolization (arrows) is indicated. Original magnification x16 (a and c) or x40 (b and d). Bar, 100 μ m (a and c) and 50 μ m (b and d).

In the current study, we showed that repeated administration of free cisplatin in soft-tissue sarcoma-bearing rats resulted in a pronounced antitumor effect, inducing strong tumor regression. Previously, we reported on the antitumor activity of free doxorubicin, which delayed tumor growth only slightly (22). Given that *in vitro* experiments showed comparable IC_{50} values for both drugs, the *in vivo* activity of cisplatin may be explained by pharmacokinetic differences between doxorubicin and cisplatin. It has been reported, by several investigators, that plasma levels of cisplatin decay in a biphasic mode with an initial half-life of 25 to 49 min and a secondary phase ranging from 2 to 3 days after a single intravenous administration of cisplatin (26,27). Cisplatin is nonenzymatically converted to several products (metabolites) which are not believed to be active as antitumor agents, but are highly bound to proteins in the serum, primarily to albumin. The conversion of the parent cisplatin to metabolites is rapid with a half-life of less than 2 hours (27). Doxorubicin shows a relatively rapid fall in plasma concentration, yielding an initial half-life of less than 5 minutes and an elimination half-life of about 35 hours (28-30). The longer

circulation half-life of cisplatin may enable a better accumulation at the tumor site. One reason why no antitumor activity of 1 mg/kg cisplatin was seen in the osteosarcoma-bearing rats, could be because this dose was below the effective dose for this tumor type, which is supported by our *in vitro* data showing a lower sensitivity of ROS-1 to cisplatin compared to BN175 tumor cells. Possibly the effective level of SPI-077 is being reached. A higher dose of 3 mg/kg cisplatin resulted in pronounced antitumor activity (data not shown).

The antitumor activity of SPI-077 has been studied in various animal tumor models, human xenografts and clinical studies. These studies do not give a uniform picture and cisplatin is more often more effective than SPI-077 (1,5-7,17-19). Encapsulation of a cytotoxic agent in pegylated liposomes does not always guarantee enhanced antitumor activity. Because of the low water solubility and low lipophilicity of cisplatin, the lipid formulation results in a very low drug-to-lipid ratio, which may explain its lack of efficacy. For SPI-077, the drug-to-lipid ratio is 14 µg/mg, compared with 125 µg/mg for Doxil[®]. Therefore, each Doxil[®] liposome delivers approximately nine times more drug than a SPI-077 liposome (19).

Burger and colleagues (31) described a method for efficient encapsulation of cisplatin in a lipid formulation that incorporates repeated freezing and thawing of a concentrated solution of cisplatin in the presence of the negatively-charged phospholipid, phosphatidylserine (PS). They showed a dramatic 100-fold increased cytotoxicity of the liposomal formulation compared to free drug *in vitro*. This method may be useful for generation of SPI-077 and, when combined with TNF, strong antitumor responses may be obtained.

Another explanation for the lack of efficacy of SPI-077 may be the stability of the liposome. Bandak and colleagues reported less than 10% platinum release from SPI-077 *in vitro* and concluded that the formulation had low bioavailability and slow-release kinetics, such that the drug concentration failed to exceed the threshold for therapeutic effects (1). This is supported by a study of Zamboni *et al*, where they showed that more SPI-077 distribute into tumors, but release less active platinum into tumor extracellular fluid, and form fewer platinum-DNA adducts than cisplatin (32).

In this study, we observed that TNF improved the antitumor activity of SPI-077 in the soft-tissue sarcoma, which is in agreement with the results of our earlier study of Doxil[®] and TNF (22). When rats were injected 3-times with liposomes combined with TNF, accumulation increased to 3- to 3.5 fold ($p < 0.02$) compared to liposomes alone. Currently the effect of TNF on biodistribution and distribution in tumor tissue is studied in detail. TNF probably increases the leakiness of the vasculature by increasing the gaps between the endothelial lining in the tumor, possibly explaining the augmented accumulation of liposomes (33,34). Besides a favorable effect of TNF in a systemic setting, we have also showed there was an increased accumulation of melphalan or doxorubicin when given in combination with high-dose TNF after an isolated limb perfusion (21,35).

The use of cisplatin is seriously hampered by its side effects, which include acute nausea and vomiting and chronic side effects resulting from nephrotoxicity, ototoxicity, and neurotoxicity (1,7,8). In the cisplatin-treated animals, urea and creatinine levels were elevated, cytoplasmic vacuolization was detected in kidney tissue and severe weight loss occurred. Treatment with cisplatin or SPI-077 did not cause any obvious histologically evident liver damage, although increased ALAT and ASAT levels in both groups and elevated γ -GT levels in the SPI-077 group were observed indicating liver-related toxicity. Overall, SPI-077 induced fewer side effects than cisplatin in this study. Our results are in agreement with other studies that show the majority of the administered SPI-077 dose is found in plasma, with secondary accumulation in the liver and spleen. The latter were not associated with observable increases in hepatic or splenic toxicity (1,5).

In conclusion, we demonstrated that administration of SPI-077 results in less antitumor activity than free cisplatin in soft tissue sarcoma-bearing rats. However, the addition of low-dose TNF to the SPI-077 treatment enhanced the antitumor activity. The combined treatment resulted in a prolonged antitumor effect compared to free cisplatin alone, where rapid outgrowth of the tumor occurred a few days after the end of therapy. In osteosarcoma-bearing rats, administration of SPI-077 improved the antitumor activity compared with free cisplatin. In these animals, addition of low-dose TNF improved the efficacy of free cisplatin, but not of SPI-077. The SPI-077 formulation of cisplatin yielded fewer systemic side effects than free cisplatin. Depending on the type of tumor, the therapeutic window of the liposomal formulation with the addition of TNF can be better than the free drug, especially when looking at prolonged treatment. Refinement of the lipid formulation to enhance bioavailability and increase drug-to-lipid ratios may improve the efficacy of pegylated liposomal cisplatin, and co-administration of TNF is likely to further increase the antitumor activity of the liposomal cisplatin.

Acknowledgements

We would like to thank Boehringer Ingelheim GmbH for the generous supply of rhTNF, and ALZA for SPI-077. We thank Peter Working and Bob Albra for advice and comments on the manuscript. This study was supported by a grant of the Dutch Cancer Society.

References

1. Bandak S, Goren D, Horowitz A, Tzemach D, Gabizon A. Pharmacological studies of cisplatin encapsulated in long-circulating liposomes in mouse tumor models. *Anticancer Drugs*. 1999;10(10):911-920.
2. Eroglu A, Kocaoglu H, Demirci S, Akgul H. Isolated limb perfusion with cisplatin and doxorubicin for locally advanced soft tissue sarcoma of an extremity. *Eur J Surg Oncol*. 2000;26(3):213-221.
3. Gondal JA, Preuss HG, Swartz R, Rahman A. Comparative pharmacological, toxicological and antitumoral evaluation of free and liposome-encapsulated cisplatin in rodents. *Eur J Cancer*. 1993;29A(11):1536-1542.

4. Iga K, Hamaguchi N, Igari Y, Ogawa Y, Toguchi H, Shimamoto T. Increased tumor cisplatin levels in heated tumors in mice after administration of thermosensitive, large unilamellar vesicles encapsulating cisplatin. *J Pharm Sci.* 1991;80(6):522-525.
5. Newman MS, Colbern GT, Working PK, Engbers C, Amantea MA. Comparative pharmacokinetics, tissue distribution, and therapeutic effectiveness of cisplatin encapsulated in long-circulating, pegylated liposomes (SPI-077) in tumor-bearing mice. *Cancer Chemother Pharmacol.* 1999;43(1):1-7.
6. Thamm DH, Vail DM. Preclinical evaluation of a sterically stabilized liposome-encapsulated cisplatin in clinically normal cats. *Am J Vet Res.* 1998;59(3):286-289.
7. Veal GJ, Griffin MJ, Price E, et al. A phase I study in paediatric patients to evaluate the safety and pharmacokinetics of SPI-77, a liposome encapsulated formulation of cisplatin. *Br J Cancer.* 2001;84(8):1029-1035.
8. Meerum TJ, Groenewegen G, Pluim D, et al. Phase I and pharmacokinetic study of SPI-77, a liposomal encapsulated dosage form of cisplatin. *Cancer Chemother Pharmacol.* 2002;49(3):201-210.
9. Burger KN, Staffhorst RW, de Vijlder HC, et al. Nanocapsules: lipid-coated aggregates of cisplatin with high cytotoxicity. *Nat Med.* 2002;8(1):81-84.
10. Allen TM, Newman MS, Woodle MC, Mayhew E, Uster PS. Pharmacokinetics and anti-tumor activity of vincristine encapsulated in sterically stabilized liposomes. *Int J Cancer.* 1995;62(2):199-204.
11. Lasic DD. Doxorubicin in sterically stabilized liposomes. *Nature.* 1996;380(6574):561-562.
12. Papahadjopoulos D, Allen TM, Gabizon A, et al. Sterically stabilized liposomes: improvements in pharmacokinetics and antitumor therapeutic efficacy. *Proc Natl Acad Sci U S A.* 1991;88(24):11460-11464.
13. Sparano JA, Winer EP. Liposomal anthracyclines for breast cancer. *Semin Oncol.* 2001;28(4 Suppl 12):32-40.
14. van Der Veen AH, Eggermont AM, Seynhaeve AL, van T, ten Hagen TL. Biodistribution and tumor localization of stealth liposomal tumor necrosis factor-alpha in soft tissue sarcoma bearing rats. *Int J Cancer.* 1998;77(6):901-906.
15. Gabizon A, Martin F. Polyethylene glycol-coated (pegylated) liposomal doxorubicin. Rationale for use in solid tumours. *Drugs.* 1997;54 Suppl 4:15-21.
16. Wu NZ, Da D, Rudoll TL, Needham D, Whorton AR, Dewhirst MW. Increased microvascular permeability contributes to preferential accumulation of Stealth liposomes in tumor tissue. *Cancer Res.* 1993;53(16):3765-70.
17. Harrington KJ, Rowlinson-Busza G, Syrigos KN, et al. Pegylated liposome-encapsulated doxorubicin and cisplatin enhance the effect of radiotherapy in a tumor xenograft model. *Clin Cancer Res.* 2000;6(12):4939-4949.
18. Vaage J, Donovan D, Wipff E, et al. Therapy of a xenografted human colonic carcinoma using cisplatin or doxorubicin encapsulated in long-circulating pegylated stealth liposomes. *Int J Cancer.* 1999;80(1):134-137.
19. Harrington KJ, Lewanski CR, Northcote AD, et al. Phase I-II study of pegylated liposomal cisplatin (SPI-077) in patients with inoperable head and neck cancer. *Ann Oncol.* 2001;12(4):493-496.
20. Kim ES, Lu C, Khuri FR, et al. A phase II study of STEALTH cisplatin (SPI-77) in patients with advanced non-small cell lung cancer. *Lung Cancer.* 2001;34(3):427-432.
21. van Der Veen AH, de Wilt JH, Eggermont AM, van Tiel ST, Seynhaeve AL, ten Hagen TL. TNF-alpha augments intratumoural concentrations of doxorubicin in TNF-alpha-based isolated limb perfusion in rat sarcoma models and enhances anti-tumour effects. *Br J Cancer.* 2000;82(4):973-980.
22. ten Hagen TL, van Der Veen AH, Nooijen PT, van Tiel ST, Seynhaeve AL, Eggermont AM. Low-dose tumor necrosis factor-alpha augments antitumor activity of stealth liposomal doxorubicin (DOXIL) in soft tissue sarcoma-bearing rats. *Int J Cancer.* 2000;87(6):829-37.
23. Brouckaert P, Takahashi N, van Tiel ST, et al. Tumor necrosis factor-alpha augmented tumor response in B16BL6 melanoma-bearing mice treated with stealth liposomal doxorubicin (Doxil) correlates with altered Doxil pharmacokinetics. *Int J Cancer.* 2004;109(3):442-448.
24. Manusama ER, Nooijen PT, Stavast J, Durante NM, Marquet RL, Eggermont AM. Synergistic antitumour effect of recombinant human tumour necrosis factor alpha with melphalan in isolated limb perfusion in the rat. *Br J Surg.* 1996;83(4):551-555.
25. Skehan P, Storeng R, Scudiero D, et al. New colorimetric cytotoxicity assay for anticancer-drug screening. *J Natl Cancer Inst.* 1990;82(13):1107-1112.
26. DeConti RC, Toftness BR, Lange RC, Creasey WA. Clinical and pharmacological studies with cis-diamminedichloroplatinum (II). *Cancer Res.* 1973;33(6):1310-1315.
27. Evans WE, Yee GC, Crom WR, Pratt CB, Green AA. Clinical pharmacology of bleomycin and cisplatin. *Head Neck Surg.* 1981;4(2):98-110.
28. Chan KK, Cohen JL, Gross JF, et al. Prediction of adriamycin disposition in cancer patients using a physiologic, pharmacokinetic model. *Cancer Treat Rep.* 1978;62(8):1161-1171.

29. Robert J, Bui NB, Vrignaud P. Pharmacokinetics of doxorubicin in sarcoma patients. *Eur J Clin Pharmacol.* 1987;31(6):695-699.
30. Robert J, Illiadis A, Hoerni B, Cano JP, Durand M, Lagarde C. Pharmacokinetics of adriamycin in patients with breast cancer: correlation between pharmacokinetic parameters and clinical short-term response. *Eur J Cancer Clin Oncol.* 1982;18(8):739-745.
31. Burger KN, Staffhorst RW, de Kruijff B. Interaction of the anti-cancer drug cisplatin with phosphatidylserine in intact and semi-intact cells. *Biochim Biophys Acta.* 1999;1419(1):43-54.
32. Zamboni WC, Gervais AC, Egorin MJ, et al. Systemic and tumor disposition of platinum after administration of cisplatin or STEALTH liposomal-cisplatin formulations (SPI-077 and SPI-077 B103) in a preclinical tumor model of melanoma. *Cancer Chemother Pharmacol.* 2004;53(4):329-336.
33. Brett J, Gerlach H, Nawroth P, Steinberg S, Godman G, Stern D. Tumor necrosis factor/cachectin increases permeability of endothelial cell monolayers by a mechanism involving regulatory G proteins. *J Exp Med.* 1989;169(6):1977-1991.
34. Partridge CA, Horvath CJ, Del Vecchio PJ, Phillips PG, Malik AB. Influence of extracellular matrix in tumor necrosis factor-induced increase in endothelial permeability. *Am J Physiol.* 1992;263(6 Pt 1):L627-L633.
35. de Wilt JH, ten Hagen TL, de Boeck G, van Tiel ST, de Bruijn EA, Eggermont AM. Tumour necrosis factor alpha increases melphalan concentration in tumour tissue after isolated limb perfusion. *Br J Cancer.* 2000;82(5):1000-1003.

Chapter 8

Addition of low-dose tumor necrosis factor- α to systemic treatment with Stealth liposomal doxorubicin (Doxil)[®] improved anti-tumor activity in osteosarcoma-bearing rats

Saske Hoving, Ann LB Seynhaeve, Sandra T van Tiel, Alexander MM Eggermont, Timo LM ten Hagen

Department of Surgical Oncology, Erasmus MC-Daniel den Hoed Cancer Center, Rotterdam, the Netherlands

Abstract

Improved efficacy of Doxil[®] (Stealth[®] liposomal doxorubicin) compared to free doxorubicin has been demonstrated in the treatment of several tumor types. We have shown that addition of low-dose TNF to systemic Doxil[®] administration dramatically improved tumor response in the highly vascularized rat soft-tissue sarcoma BN175. Whether a similar enhanced efficacy can be achieved in less vascularized tumors is uncertain. We therefore examined the effect of systemic administration of Doxil[®] in combination with low-dose TNF in intermediate vascularized osteosarcoma-bearing rats (ROS-1). Small fragments of the osteosarcoma were implanted s.c. in the lower limb. Treatment was started when the tumors reached an average diameter of 1 cm. Rats were treated with 5 i.v. injections at 4-day interval with Doxil[®] or doxorubicin and TNF. Systemic treatment with Doxil[®] resulted in a better tumor growth delay than free doxorubicin, but with progressive diseases in all animals. The 3.5-fold augmented accumulation of Doxil[®] compared to free doxorubicin presumably explains the enhanced tumor regression. Addition of low-dose TNF augmented the anti-tumor activity of Doxil[®], although no increased drug uptake was found compared to Doxil[®] alone. *In vitro* studies showed that ROS-1 is sensitive to TNF, but systemic treatment with TNF alone did not result in a tumor growth delay. Furthermore, we demonstrated that treatment with Doxil[®] alone or with TNF resulted in massive coagulative necrosis of tumor tissue. In conclusion, combination therapy of Doxil[®] and low-dose TNF seems attractive for the treatment of highly vascularized tumors, but also of intermediate vascularized tumors like the osteosarcoma.

Introduction

Encapsulation of anticancer agents in liposomes offers a potential means of manipulating drug distribution to improve antitumor efficacy and reduce toxicity. Stealth[®] liposomes are sterically stabilized liposomes that contain methoxy-polyethylene glycol (MPEG). Because of their small size, long circulation time, and reduced interaction with formed elements of the blood, these liposomes tend to accumulate in tumors, presumably due to leakage through the often-compromised tumor vasculature (1-8). Doxil[®] (Stealth[®] liposomal doxorubicin) is effective in the treatment of several tumor types, including advanced or metastatic soft tissue sarcoma (9), AIDS-related Kaposi's sarcoma (10), metastatic breast cancer (11) and epithelial ovarian cancer (12).

Pre-clinical and clinical studies have shown impressive improvement of the anti-tumor activity of melphalan and doxorubicin in local treatment of different tumor types when TNF was co-administered (13-18). We demonstrated that the basis for the synergy is, on one hand a significant enhancement of tumor selective melphalan and doxorubicin uptake and on the other hand the subsequent destruction of tumor vasculature caused by TNF (14,19).

Successful application of TNF for systemic treatment of tumors however is seriously hampered by its severe toxicity and therefore only low dosages can be administered (20,21). In previous studies we showed that systemic co-administration of Doxil[®] and low-dose TNF resulted in a pronounced tumor response in both rat and mice tumor models. In soft-tissue sarcoma-bearing rats systemic treatment with Doxil[®] in combination with low-dose TNF improved the anti-tumor activity dramatically resulting in a tumor response (complete or partial regression) in most of the animals. Repeated injection of Doxil[®] combined with TNF resulted in augmented accumulation of the drug in tumor tissue which could explain the observed synergistic anti-tumor effect (22). When B16BL6 melanoma-bearing mice were injected with Doxil[®] combined with TNF, also an increased drug accumulation was found compared to liposomes alone (23). TNF increases the leakiness of the vasculature by increasing the gaps between the endothelial lining in the tumor, possibly explaining the augmented accumulation after extravasation of liposomes (24,25).

We evaluate in the experiments described here whether the use of TNF in combination with Doxil[®] not only results in synergistic anti-tumor response in the highly vascularized soft-tissue sarcoma but also in the less vascularized osteosarcoma.

Materials and methods

Chemicals

Human recombinant Tumor Necrosis Factor- α (specific activity 5×10^7 IU/mg) was kindly provided by Dr. G. Adolf (Bender Wien GmbH, Wien, Austria) and stored at a concentration of 2 mg/ml at -80°C or under liquid nitrogen. Endotoxin levels (LAL) were below 0.624 EU/mg. Pegylated liposomal doxorubicin (Doxil[®]) was kindly provided by Dr. P. Working (ALZA Corporation, Mountain View, CA, USA). Doxorubicin hydrochloride (adriablastina) was purchased from Pharmacia (Brussels, Belgium).

Animals and tumor model

Male inbred WAG/RIJ rats were used for the osteosarcoma model (ROS-1). This tumor originated spontaneously in the tibia of a rat. Rats were obtained from Harlan-CPB, (Austerlitz, the Netherlands) and weighing 250-300 g. Rats were fed a standard laboratory diet *ad libitum* (Hope Farms Woerden, the Netherlands).

Small fragments (3 mm) of the syngeneic ROS-1 sarcoma or the soft-tissue sarcoma BN175 were implanted subcutaneously in the right hindleg as previously described (26). Tumor growth was recorded by caliper measurement and tumor volume calculated using the formula $0.4(A^2 \times B)$ (where B represents the largest diameter and A the diameter perpendicular to B). Rats were sacrificed if tumor diameter exceeded 25 mm or at the end of the experiments. Animal studies were done in accordance with protocols approved by the committee on Animal Research of the Erasmus MC, Rotterdam, the Netherlands.

Treatment protocol

Treatment was started when the ROS-1 tumors reached an average diameter of 9-11 mm. The rats were randomized into the following 6 groups: placebo liposomes (equivalent amounts of buffer or lipids), low dose TNF, free doxorubicin, Doxil[®], doxorubicin plus TNF and Doxil[®] plus TNF. Rats were injected five times intravenously with an interval of 4 days between the injections; first dose of 4.5 mg/kg Doxil[®] or free doxorubicin and 1.0 mg/kg for consecutive doses. TNF was given at a concentration of 15 µg/kg for all five doses. When rats were treated with doxorubicin or Doxil[®] combined with TNF, these agents were injected separately, shortly after each other.

The classification of tumor response was: progressive disease (PD) = increase of tumor volume (> 25%) over a 20 day period; no change (NC) = tumor volume equal to volume as start of treatment (in a range of - 25% and + 25%); partial remission (PR) = decrease of tumor volume (- 25 and -90 %); complete remission (CR) = tumor volume less than 10% of initial volume.

Measurement of doxorubicin accumulation in tumor tissue

The effect of TNF on Doxil[®] accumulation in ROS-1 tumors was investigated. After three injections the tumor size of rats treated with Doxil[®] in combination with TNF started to differ from the tumor size of rats in the other groups and for this reason we decided to compare doxorubicin tumor uptake not later than this time point. Rats received 3 injections of doxorubicin or Doxil[®] with or without TNF with an interval of 4 days between the injections as described in the treatment protocol. Tumors were excised 24 hours after the last injection and tissues were analyzed for doxorubicin and its fluorescent metabolites as previously described (27). Briefly, tumors were incubated in acidified isopropanol (0.075 N HCl in 90% isopropanol) for 24 hours at 4°C and after that the tumors were homogenized (PRO200 homogenizer with 10 mm generator, Pro Scientific, CT, USA), centrifuged for 30 min at 2500 rpm and supernatants were harvested. A Hitachi F4500 fluorescence spectrometer (excitation 472 nm and emission 590 nm) was used for measurement of the samples. A standard curve was prepared with known concentrations of doxorubicin diluted in acidified isopropanol. All measurements were repeated after addition of an internal doxorubicin standard.

Histology

Rats were treated with placebo liposomes, TNF, Doxil[®] or Doxil[®] + TNF. When the tumors reached an average diameter of 17±1 mm, they were excised and fixed in 4% formaldehyde and embedded in paraffin. Tissue sections of 4 µm were cut and stained with haematoxylin and eosin, examined on a Leica DM-RXA and photographed using a Sony DXC950

camera. At least three different tumors in each experimental group were subjected to blind evaluation.

Immunohistochemistry

Untreated BN175 and ROS-1 tumors with a diameter of 9-11 mm were excised and immediately frozen in liquid nitrogen. Immunohistochemical studies were performed on acetone-fixed 7 μm cryostat sections. The tumor sections were fixed for 30 min with 4% formaldehyde and after rinsing with PBS, the endogenous peroxidase activity was blocked by incubation for 5 minutes in methanol/3% H_2O_2 . The slides were incubated for 1 hour with 1:50 mouse-anti-rat-CD31 (Becton Dickinson, Alphen aan den Rijn, the Netherlands) diluted in 5% rat serum/PBS. Thereafter, sections were washed with PBS and incubated for 1 h with goat-anti-mouse peroxidase-labeled antibody (DAKO, ITK Diagnostics BV, Uithoorn, the Netherlands) diluted 1:100 in PBS with 5% rat serum. After rinsing with PBS, positive cells were revealed by immunoperoxidase reaction with DAB solution (DAB-kit, DAKO) and counterstained lightly with haematoxylin (Sigma).

The sections were examined on a Leica DM-RXA and photographed using a Sony 3CCD DXC 950 camera. The number of vessels and the area of vessels per field of interest were measured in calibrated digital images (Research Assistant 3.0, RVC, Hilversum, the Netherlands). For quantification of the microvessel density (MVD) six representative fields of interest per slide (magnification 16x), 3 slides per tumor and 4 animals per group were examined.

In vitro cytotoxicity assay

The rat osteosarcoma ROS-1 cells were maintained in modified Eagle's medium supplemented with 10% fetal calf serum and 0.1% penicilline-streptomycine. Media and supplements were obtained from Life Technologies, the Netherlands.

ROS-1 cells were added in 100 μl aliquots to 96-well flat-bottomed microtiter plates (Costar, Cambridge, MA, USA) at a final concentration of 1×10^4 cells per well and allowed to grow as a monolayer. Cells were incubated at 37°C in 5% CO_2 for 72 hours in the presence of various concentrations of TNF, doxorubicin and Doxil[®]. The range of final drug concentrations was 0.1 - 10 $\mu\text{g}/\text{ml}$ for TNF, 0.001 - 100 $\mu\text{g}/\text{ml}$ doxorubicin and 0.05 - 1000 $\mu\text{g}/\text{ml}$ Doxil[®]. Growth of tumor cells was measured using the Sulphorhodamine-B (SRB) assay according to the method of Skehan (28). In short, cells were washed twice with phosphate buffered saline, incubated with 10% trichloric acetic acid (1 hour, 4°C) and washed again. Cells were stained with 0.4% SRB (15-30 min), washed with 1% acetic acid and were allowed to dry. Protein bound SRB was dissolved in TRIS (10 mM, pH 9.4). The optical density was read at 540 nm. Tumor cell growth was calculated using the formula: cell growth = (test well/control) x 100 percent. The drug concentration reducing the cell

growth to 50% of the control (IC_{50}) was determined from the growth curves. The experiments were repeated at least 5 times.

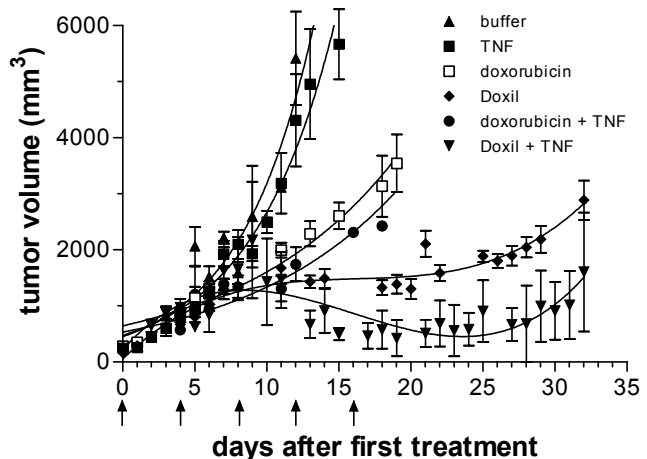
In vitro assessment of doxorubicin uptake in tumor cells

Intracellular doxorubicin levels in osteosarcoma ROS-1 cells were measured by flowcytometry to determine whether the observed *in vitro* toxicity correlated with cellular uptake of doxorubicin. ROS-1 cells were plated in 24-well plates at a final concentration of 5×10^4 cells per well and allowed to grow as a monolayer. Doxorubicin, Doxil[®] and TNF, diluted in DMEM supplement with 10 % fetal bovine serum, were added to the wells, after which cells were incubated for 10, 30, 60 and 120 min. The final drug concentration in the wells for all three drugs was 0, 0.1, 1.0 and 10 $\mu\text{g}/\text{ml}$. After incubation, cells were washed to discard non-incorporated drug and treated with trypsin-EDTA for 2 min. The cell suspensions were washed twice in DMEM supplemented with 10% FCS and resuspended in PBS. Cellular uptake was measured on a Becton Dickinson FACScan using Cell Quest software on Apple Macintosh computer. Excitation was set at 488 nm and emission at 530 nm. Fluorescence was corrected for cell size using the forward scatter (FSC) with the formula: corrected fluorescence (FLcor) = fluorescence at 530 nm (FL530) / FSC – FL530_c / FSC_c (FL530_c and FSC_c are fluorescence and forward scatter with no drug added to the cells).

Statistical analysis

Results were evaluated for statistical significance with the Mann Whitney U test. P-values below 0.05 were considered statistically significant. Calculations were performed on a personal computer using GraphPad Prism v3.0 and SPSS v10.0 for Windows 2000.

Figure 1. Growth curves of subcutaneous implanted ROS-1 osteo-sarcoma after systemic treatment with Doxil[®] and low dose TNF. Rats were injected five times intravenously with an interval of 4 days between the injections; first dose 4.5 mg/kg Doxil[®] or free doxorubicin and 1.0 mg/kg for consecutive doses and 15 $\mu\text{g}/\text{kg}$ TNF for all five doses. Buffer alone, TNF, doxorubicin, Doxil[®], doxorubicin plus TNF and Doxil[®] plus TNF. Mean tumor volumes are shown \pm SEM.



Results

Effect of low-dose TNF on anti-tumor activity of Doxil[®]

To evaluate the anti-tumor activity of Doxil[®] in combination with low-dose TNF, osteosarcoma-bearing rats were treated with a total of 5 injections of doxorubicin or Doxil[®] with or without TNF. Treatment with free doxorubicin resulted in a slight delay in tumor growth, with progressive diseases in all animals (Figure 1). Progressive disease was also seen in all animals treated with Doxil[®], but with a better tumor growth delay than free doxorubicin. Addition of TNF to the Doxil[®] treatment enhanced the anti-tumor response, resulting in a response rate of 50% (partial plus complete response). In contrast, addition of TNF to doxorubicin treatment did not improve the anti-tumor response. Treatment with TNF alone had no anti-tumor effect. No obvious systemic toxicity was observed in any of the treatments.

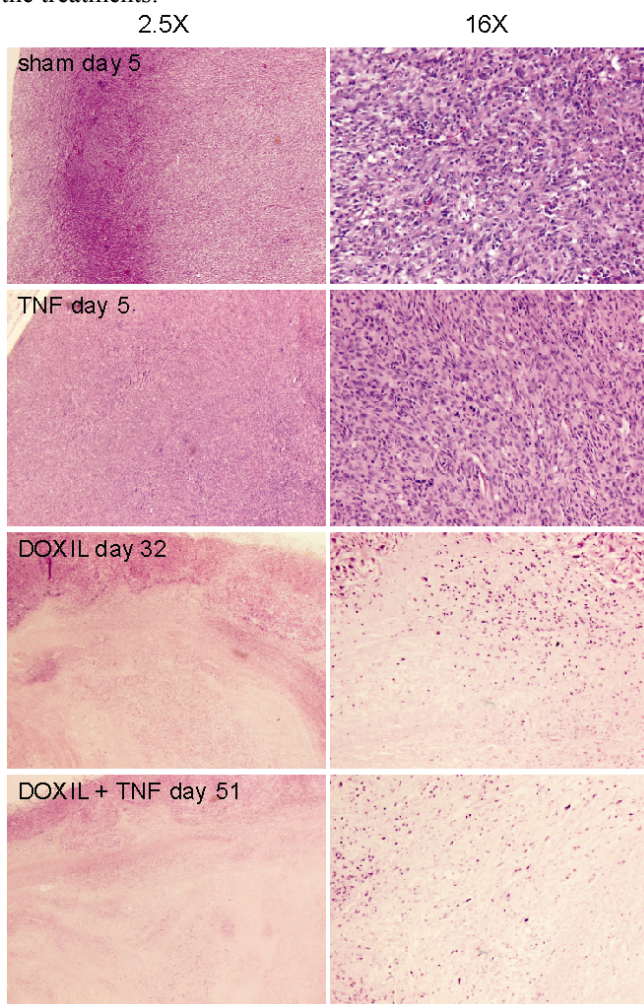
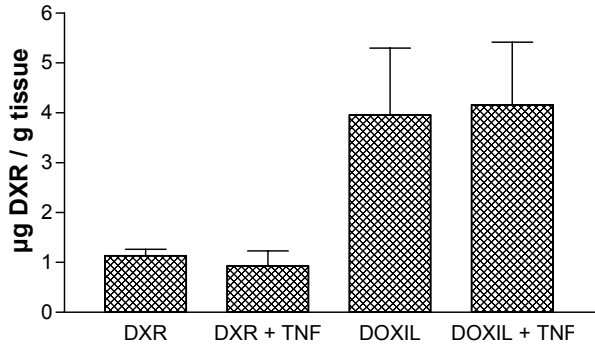


Figure 2. Paraffin sections of the rat osteosarcoma after systemic treatment, haema-toxylin-eosin stained. Rats were treated with placebo liposomes, TNF (15 µg/kg), Doxil[®] (4.5 mg/kg first dose and 1 mg/kg dose 2 to 5) or TNF combined with Doxil[®]. Representative pictures are shown. Original magnification 2.5 and 16X.

Histologic examination of anti-tumor activity of Doxil[®] in combination with TNF

Histopathological examination was performed on tumors with the same size, shortly after regrowth occurred. Treatment of the rats with Doxil[®] and Doxil[®] in combination with TNF resulted in severe tumor necrosis and extensive cell death (Figure 2). Massive coagulative necrosis of 68% of the tumor area was seen in Doxil[®] treated tumors and 40% in the Doxil[®] plus TNF treated tumors. Less necrosis was seen in rats treated with placebo liposomes or TNF (10 and 17%, respectively). In all four groups infiltrated PMN were detected.

Figure 3. Concentrations of doxorubicin in ROS-1 tumors after systemic administration of 3 injections of doxorubicin (DXR) or Doxil[®] (4.5 mg/kg first dose and 1 mg/kg dose 2 and 3) with or without TNF. Tumors were excised 24 hours after last injection. The mean of 3 to 6 rats is shown \pm SEM.



Doxil[®] and doxorubicin accumulation in tumor tissue

To investigate whether the observed beneficial effect of TNF on the Doxil[®] treatment was due to an increased liposome extravasation into tumor tissue, doxorubicin concentrations in tumors after three treatments were determined. Doxorubicin levels in tumors were 3.5-fold higher when Doxil[®] was injected compared to free doxorubicin, although not significantly (Figure 3). Addition of TNF did not induce a further accumulation of Doxil[®] and TNF had also no effect on the tumor uptake of free doxorubicin.

Microvessel density

Quantification of the microvessel density (MVD) was performed by immunohistochemical staining of endothelial cells in frozen BN175 and ROS-1 tumor sections (Figure 4A-D). The number of vessels as well as the total tumor vessel area was measured. The area per vessel is computed by dividing the total vessel area by the number of vessels. The number of vessels in the BN175 tumor was 2.9 times higher than in the ROS-1 tumor (Figure 4A)($p=0.021$), although the vessels have the same size (Figure 4B).

Direct effect of Doxil[®] combined with TNF on ROS-1 cells in vitro

In vitro experiments were performed to define whether direct cytotoxicity contributed to the improved tumor response of Doxil[®] in combination with TNF. Figure 5 shows that exposure of ROS-1 tumor cells to doxorubicin resulted in a dose dependent cell growth

inhibition, with an IC₅₀ of 3.8 µg/ml. Doxil[®] appeared to be less cytotoxic to osteosarcoma cells with an IC₅₀ of 25.7 µg/ml. ROS-1 cells were moderately sensitive to TNF with a maximum growth inhibition of 32% at 10 µg/ml TNF. Addition of TNF to doxorubicin or Doxil[®] had no effect on the cytotoxicity of the anti-tumor agents; comparable IC₅₀ values were found.

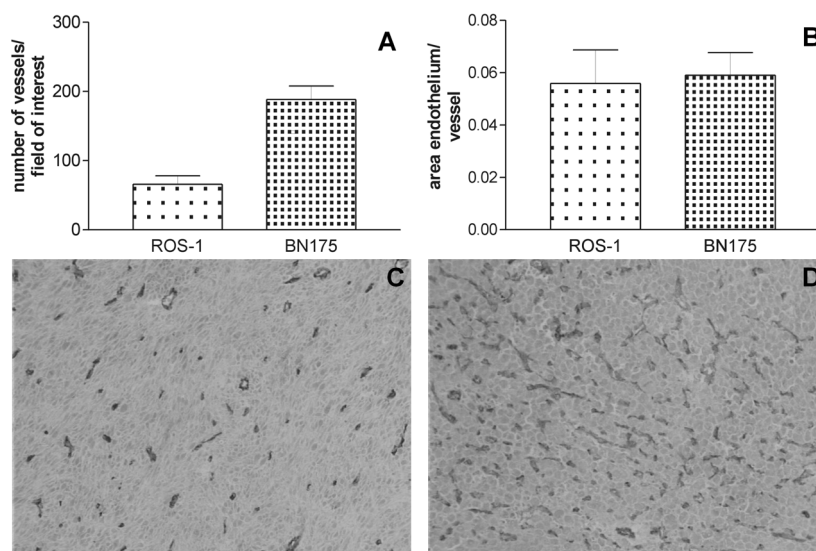


Figure 4. Microvessel density (MVD) of untreated ROS-1 and BN175 tumors of 9-11 mm in diameter was assessed by immunohistochemical staining for CD31. (A) Number of vessels per field of interest. The BN175 tumor has 2.9 times more vessels than the ROS-1 tumor ($p=0.021$) (B) area endothelium per vessel. The vessels of the BN175 and ROS-1 tumors are of the same size. Six representative fields of interest per slide (magnification 16X), 3 slides per tumor and 4 animals per group were examined. The mean \pm SEM is shown. Photographs of cryostat sections of untreated tumors of 8-10 mm in diameter stained for CD31. (C) ROS-1, (D) BN175. Representative pictures are shown. Original magnification 16X.

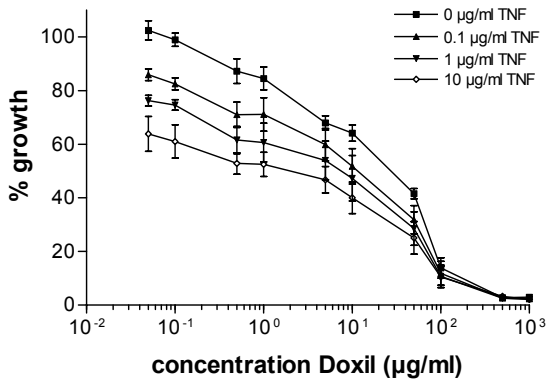
In vitro uptake of Doxil[®] or doxorubicin in tumor cells in vitro

We examined if TNF augmented the intracellular accumulation of doxorubicin or Doxil[®], which could explain the improved tumor response. Increased intracellular concentrations of doxorubicin or Doxil[®] were observed when incubated with increasing concentrations of doxorubicin or Doxil[®] (ranging 0.1 to 10 µg/ml) and increasing time (ranging 10 to 120 min). Addition of TNF up to 10 µg/ml did not result in an increased uptake of doxorubicin or Doxil[®] (data not shown).

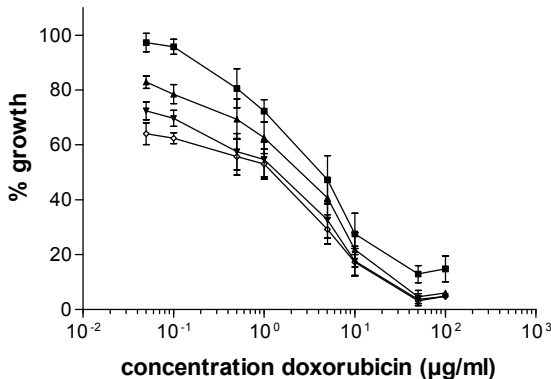
Discussion

In the present study we demonstrated that Stealth[®] liposomal doxorubicin (Doxil[®]) resulted in a better tumor growth delay than free doxorubicin in osteosarcoma-bearing rats.

However, tumor control was not achieved as progressive disease was observed in all animals. Addition of low-dose TNF augmented the anti-tumor activity of Doxil[®] resulting in a response rate of 50%. These experiments are in agreement with earlier studies where we demonstrated that TNF improved the anti-tumor activity of Doxil[®] in a rat soft-tissue sarcoma and a mouse melanoma model (22,23).



A



B

Figure 5. *In vitro* growth of the ROS-1 tumor cells as a function of the added amount of Doxil[®] (A) or doxorubicin (B) in combination with 0, 0.1, 1 and 10 µg TNF per ml. The means of at least 3 individual experiments performed in duplicate are shown ± SEM.

Transport of small drugs across the blood vessel wall involves diffusion whereas transport of macromolecules involves convection. Diffusion is the random motion of small molecules. Convection is mediated by the movement of fluid (29-32). In highly vascularized tumors more tumor cells will be reached by the chemotherapeutics. In general, tumor vessels are more permeable than normal vessels and the maximum size of particles that can cross the tumor vessel wall is called the pore cutoff size. There is a large variance in cutoff sizes in different tumor types. Vessels of some but not all primary brain tumors are nearly impermeable, while in other tumors cutoff pore sizes between 100 nm and 1.2 µm are found. Vascular permeability may depend on tumor type and microenvironment and increases with tumor size. It is believed that not the microvessel density is the limiting

factor of macromolecule drug delivery to solid tumors, but the permeability of the tumor vessels (33,34).

Several studies have shown that encapsulation of anticancer agents in liposomes can reduce systemic toxicity while retaining or even improving *in vivo* efficacy (1,4,7,35). Doxil[®] is effective in the treatment of several tumor types, including advanced or metastatic soft tissue sarcoma (9), AIDS-related Kaposi's sarcoma (10), metastatic breast cancer (11) and epithelial ovarian cancer (12). Stealth[®] liposomes have a long circulation time and tend to accumulate in tumors, presumably due to leakage through the tumor vasculature (1,3,4,6-8,36). In the present study we showed that systemic treatment with Doxil[®] resulted in a better tumor growth delay than free doxorubicin and that the 3.5-fold increased drug accumulation could explain the observed enhanced anti-tumor effect. The anti-tumor activity of Doxil[®] in the osteosarcoma model is comparable to the anti-tumor activity in the soft-tissue sarcoma BN175, although *in vitro* studies showed a clear difference. BN175 cells are 10 times more sensitive to Doxil[®] than ROS-1 cells (22). Four times more Doxil[®] is found in ROS-1 tumor tissue than in the BN175 tumor after 3 i.v. injections of Doxil[®] alone. Most likely this indicates that the tumor vessels of the ROS-1 tumor are more permeable than the vessels of the BN175 tumor.

Previously we reported on the improved anti-tumor activity of systemically injected Doxil[®] when combined with low-dose TNF in soft tissue sarcoma-bearing rats. Repeated injections of Doxil[®] plus TNF resulted in augmented tumor uptake of doxorubicin which could explain the observed enhanced anti-tumor effect (22). Also in the B16 melanoma-bearing mice an augmented accumulation of Doxil[®] is seen when combined with TNF. TNF likely increases the leakiness of the vasculature by increasing the gaps between the endothelial lining in the tumor, possibly explaining the augmented accumulation after extravasation of liposomes (24,25).

In the present study we did not observe an increased drug accumulation when Doxil[®] was combined with TNF in the osteosarcoma ROS-1 model. TNF has an effect on tumor endothelial cells and the ROS-1 tumor is less vascularized than the BN175 tumor. Although in TNF-based isolated hepatic perfusions a highly vascularized tumor results in a good tumor response and vice versa, no such effect was found in the TNF-based isolated limb perfusion (ILP). Both the BN175 and the ROS-1 tumor showed a synergistic anti-tumor response when TNF is added to the ILP (18,37).

In vitro studies demonstrated a higher sensitivity of the osteosarcoma cells for TNF as compared to the BN175 cells. The dose of TNF used in the systemic treatment is probably too low to have an effect on its own, but may switch the balance to a better response when combined with Doxil[®]. Also, administration of TNF may trigger local production of TNF and other cytokines improving tumor response when combined with Doxil[®].

We found less coagulative necrosis in tumor tissue after treatment with Doxil[®] and TNF than with Doxil[®] alone. We think this is due to the fact that the tumors were excised at the same size. As the tumors from Doxil[®] plus TNF treated rats regressed more they also regrew more to gain the same size as the Doxil[®] alone treated tumors.

We demonstrated for the first time that TNF augments the anti-tumor activity of Doxil[®] not only in highly vascularized tumors like the soft-tissue sarcoma BN175, but also in the intermediate vascularized ROS-1. These findings confirm the promising role for TNF as enhancer of systemic therapy of solid tumors with Stealth[®] liposomes.

Acknowledgements

We would like to thank Boehringer Ingelheim GmbH for the generous supply of rhTNF, and Dr. P. Working for supplying Doxil[®] (ALZA Corporation, Mountain View, CA, USA). This study was supported by grant DDHK 2000-2224 of the Dutch Cancer Society.

References

1. Allen TM, Newman MS, Woodle MC, Mayhew E, Uster PS. Pharmacokinetics and anti-tumor activity of vincristine encapsulated in sterically stabilized liposomes. *Int J Cancer*. 1995;62(2):199-204.
2. Gabizon A, Papahadjopoulos D. Liposome formulations with prolonged circulation time in blood and enhanced uptake by tumors. *Proc Natl Acad Sci U S A*. 1988;85(18):6949-6953.
3. Gabizon A, Martin F. Polyethylene glycol-coated (pegylated) liposomal doxorubicin. Rationale for use in solid tumours. *Drugs*. 1997;54 Suppl 4:15-21.
4. Lasic DD. Doxorubicin in sterically stabilized liposomes. *Nature*. 1996;380(6574):561-562.
5. Maeda H, Fang J, Inutsuka T, Kitamoto Y. Vascular permeability enhancement in solid tumor: various factors, mechanisms involved and its implications. *Int Immunopharmacol*. 2003;3(3):319-328.
6. Mayer LD, Cullis PR, and Bally MB Designing therapeutically optimized liposomal anticancer delivery systems: lessons from conventional liposomes. *In* Lasic DD and Papahadjopoulos D (eds.), *Medical Applications of Liposomes*, pp. 231-257. New York: Elsevier Science, 1998.
7. Papahadjopoulos D, Allen TM, Gabizon A, et al. Sterically stabilized liposomes: improvements in pharmacokinetics and antitumor therapeutic efficacy. *Proc Natl Acad Sci U S A*. 1991;88(24):11460-11464.
8. Wu NZ, Da D, Rudoll TL, Needham D, Whorton AR, Dewhirst MW. Increased microvascular permeability contributes to preferential accumulation of Stealth liposomes in tumor tissue. *Cancer Res*. 1993;53(16):3765-70.
9. Judson I, Radford JA, Harris M, et al. Randomised phase II trial of pegylated liposomal doxorubicin (DOXIL/CAELYX) versus doxorubicin in the treatment of advanced or metastatic soft tissue sarcoma: a study by the EORTC Soft Tissue and Bone Sarcoma Group. *Eur J Cancer*. 2001;37(7):870-877.
10. Northfelt DW, Dezube BJ, Thommes JA, et al. Pegylated-liposomal doxorubicin versus doxorubicin, bleomycin, and vincristine in the treatment of AIDS-related Kaposi's sarcoma: results of a randomized phase III clinical trial. *J Clin Oncol*. 1998;16(7):2445-2451.
11. O'Brien ME, Wigler N, Inbar M, et al. Reduced cardiotoxicity and comparable efficacy in a phase III trial of pegylated liposomal doxorubicin HCl (CAELYX/Doxil) versus conventional doxorubicin for first-line treatment of metastatic breast cancer. *Ann Oncol*. 2004;15(3):440-449.
12. Stebbing J, Gaya A. Pegylated liposomal doxorubicin (Caelyx) in recurrent ovarian cancer. *Cancer Treat Rev*. 2002;28(2):121-125.
13. Bickels J, Manusama ER, Gutman M, et al. Isolated limb perfusion with tumour necrosis factor-alpha and melphalan for unresectable bone sarcomas of the lower extremity. *Eur J Surg Oncol*. 1999;25(5):509-514.
14. Eggermont AM, Schraffordt KH, Lienard D, et al. Isolated limb perfusion with high-dose tumor necrosis factor-alpha in combination with interferon-gamma and melphalan for nonresectable extremity soft tissue sarcomas: a multicenter trial. *J Clin Oncol*. 1996;14(10):2653-2665.
15. Eggermont AM, Schraffordt KH, Klausner JM, et al. Isolated limb perfusion with tumor necrosis factor and melphalan for limb salvage in 186 patients with locally advanced soft tissue extremity sarcomas. The cumulative multicenter European experience. *Ann Surg*. 1996;224(6):756-764.

16. Lienard D, Lejeune FJ, Ewalenko P. In transit metastases of malignant melanoma treated by high dose rTNF alpha in combination with interferon-gamma and melphalan in isolation perfusion. *World J Surg.* 1992;16(2):234-240.
17. Olieman AF, Lienard D, Eggermont AM, et al. Hyperthermic isolated limb perfusion with tumor necrosis factor alpha, interferon gamma, and melphalan for locally advanced nonmelanoma skin tumors of the extremities: a multicenter study. *Arch Surg.* 1999;134(3):303-307.
18. van Der Veen AH, de Wilt JH, Eggermont AM, van Tiel ST, Seynhaeve AL, ten Hagen TL. TNF-alpha augments intratumoural concentrations of doxorubicin in TNF-alpha-based isolated limb perfusion in rat sarcoma models and enhances anti-tumour effects. *Br J Cancer.* 2000;82(4):973-980.
19. de Wilt JH, ten Hagen TL, de Boeck G, van Tiel ST, de Bruijn EA, Eggermont AM. Tumour necrosis factor alpha increases melphalan concentration in tumour tissue after isolated limb perfusion. *Br J Cancer.* 2000;82(5):1000-1003.
20. Tracey KJ, Beutler B, Lowry SF, et al. Shock and tissue injury induced by recombinant human cachectin. *Science.* 1986;234(4775):470-474.
21. Spriggs DR, Sherman ML, Michie H, et al. Recombinant human tumor necrosis factor administered as a 24-hour intravenous infusion. A phase I and pharmacologic study. *J Natl Cancer Inst.* 1988;80(13):1039-1044.
22. ten Hagen TL, van Der Veen AH, Nooijen PT, van Tiel ST, Seynhaeve AL, Eggermont AM. Low-dose tumor necrosis factor-alpha augments antitumor activity of stealth liposomal doxorubicin (DOXIL) in soft tissue sarcoma-bearing rats. *Int J Cancer.* 2000;87(6):829-37.
23. Brouckaert P, Takahashi N, van Tiel ST, et al. Tumor necrosis factor-alpha augmented tumor response in B16BL6 melanoma-bearing mice treated with stealth liposomal doxorubicin (Doxil) correlates with altered Doxil pharmacokinetics. *Int J Cancer.* 2004;109(3):442-448.
24. Brett J, Gerlach H, Nawroth P, Steinberg S, Godman G, Stern D. Tumor necrosis factor/cachectin increases permeability of endothelial cell monolayers by a mechanism involving regulatory G proteins. *J Exp Med.* 1989;169(6):1977-1991.
25. Partridge CA, Horvath CJ, Del Vecchio PJ, Phillips PG, Malik AB. Influence of extracellular matrix in tumor necrosis factor-induced increase in endothelial permeability. *Am J Physiol.* 1992;263(6 Pt 1):L627-L633.
26. Manusama ER, Nooijen PT, Stavast J, Durante NM, Marquet RL, Eggermont AM. Synergistic antitumour effect of recombinant human tumour necrosis factor alpha with melphalan in isolated limb perfusion in the rat. *Br J Surg.* 1996;83(4):551-555.
27. Mayer LD, Tai LC, Ko DS, et al. Influence of vesicle size, lipid composition, and drug-to-lipid ratio on the biological activity of liposomal doxorubicin in mice. *Cancer Res.* 1989;49(21):5922-5930.
28. Skehan P, Storeng R, Scudiero D, et al. New colorimetric cytotoxicity assay for anticancer-drug screening. *J Natl Cancer Inst.* 1990;82(13):1107-1112.
29. Boucher Y, Baxter LT, Jain RK. Interstitial pressure gradients in tissue-isolated and subcutaneous tumors: implications for therapy. *Cancer Res.* 1990;50(15):4478-4484.
30. Yuan F. Transvascular drug delivery in solid tumors. *Semin Radiat Oncol.* 1998;8(3):164-175.
31. Dvorak HF, Nagy JA, Dvorak JT, Dvorak AM. Identification and characterization of the blood vessels of solid tumors that are leaky to circulating macromolecules. *Am J Pathol.* 1988;133(1):95-109.
32. Jain RK. Transport of molecules, particles, and cells in solid tumors. *Annu Rev Biomed Eng.* 1999;1:241-263.
33. Hobbs SK, Monsky WL, Yuan F, et al. Regulation of transport pathways in tumor vessels: role of tumor type and microenvironment. *Proc Natl Acad Sci U S A.* 1998;95(8):4607-12.
34. Yuan F, Dellian M, Fukumura D, et al. Vascular permeability in a human tumor xenograft: molecular size dependence and cutoff size. *Cancer Res.* 1995;55(17):3752-3756.
35. Sparano JA, Winer EP. Liposomal anthracyclines for breast cancer. *Semin Oncol.* 2001;28(4 Suppl 12):32-40.
36. Newman MS, Colbern GT, Working PK, Engbers C, Amantea MA. Comparative pharmacokinetics, tissue distribution, and therapeutic effectiveness of cisplatin encapsulated in long-circulating, pegylated liposomes (SPI-077) in tumor-bearing mice. *Cancer Chemother Pharmacol.* 1999;43(1):1-7.
37. Manusama ER, Stavast J, Durante NM, Marquet RL, Eggermont AM. Isolated limb perfusion with TNF alpha and melphalan in a rat osteosarcoma model: a new anti-tumour approach. *Eur J Surg Oncol.* 1996;22(2):152-157.

Chapter 9

***In vivo* evaluation of drug delivery improvement by tumor vascular manipulation with TNF: an intravital microscopy study**

Saske Hoving, Ann LB Seynhaeve, Sandra T van Tiel, Gisela aan de Wiel-Ambagtsheer, Alexander MM Eggermont, Timo LM ten Hagen

Department of Surgical Oncology, Erasmus MC-Daniel den Hoed Cancer Center, Rotterdam, the Netherlands

Abstract

Adequate drug uptake at the tumor site remains a crucial problem in solid tumor therapy. Drug delivery may be improved by augmenting leakage of the tumor-associated vasculature. We and others have previously shown that combining chemotherapy with an anti-tumor vascular therapy (e.g. Tumor Necrosis factor alpha (TNF)) dramatically enhanced tumor response, which strongly correlated with increased drug concentrations in the tumor. We have used intravital microscopy to study drug distribution in solid tumor after systemic treatment with long circulating liposomes in combination with TNF. Addition of TNF to systemic injections with 100 nm liposomes improved tumor accumulation by 5 to 6-fold. Also when 400 and 800 nm liposomes were co-administered with TNF accumulation of liposomes in tumor was increased, although much less pronounced. By intravital microscopy we observed a more extensive distribution of the liposomes when TNF was co-administered. Typically, increased extravasation of liposomes was observed along the tumor vessels, with a more even distribution than without TNF. These results indicate that more tumor vessels become permeable by TNF, leading to a more homogeneous distribution of the liposomes throughout the tumor, which is crucial for an optimal tumor response.

Introduction

Successful treatment of solid tumors with chemotherapeutics requires that adequate levels of anticancer agents reach the tumor cells. Localization of drugs in solid tumors is one of the main problems faced in systemic tumor therapy and frequently responsible for failure of initially promising agents. The pathophysiology of the tumor vasculature and stromal compartment presents a major obstacle to effective delivery of agents to solid tumors (1). There are several reasons why treatment of solid tumors with anticancer drugs often fails. First, metabolism and clearance of drugs in the body results in low drug concentrations at the tumor site. Second, poor perfusion of the tumor, arterio-venous shunting and necrotic and hypoxic areas, as well as a high interstitial fluid pressure (IFP) may limit the penetration of drugs into the tumor and prevent drugs in reaching tumor cells distant from blood vessels. Finally, most anticancer drugs are also toxic towards normal cells. Hence, the dose of administrated drugs is limited by normal tissue tolerance. Inadequate drug delivery leads to poor responses and regrowth of tumors and possibly to development of drug resistant tumor cells (2).

Tumor vessels tend to exhibit an increased permeability to macromolecules when compared with normal vessels. This indicates that blood born elements, when small enough, easily cross the endothelial lining of tumor vessels (3,4). Dvorak *et al.* demonstrated that not all vessels exhibit this feature, which could explain the heterogeneous extravasation of systemically injected drugs (2).

Several studies have shown that encapsulation of anticancer agents in liposomes can reduce systemic toxicity while retaining or even improving *in vivo* efficacy (5-8). Stealth[®] liposomes are sterically stabilized liposomes that contain methoxy-polyethylene glycol (MPEG). Because of their small size, long circulation time, and reduced interaction with formed elements of the blood, these liposomes tend to accumulate in tumors, presumably due to leakage through the often-compromised tumor vasculature (7-12). Furthermore, they can target the tumor with high selectivity by taking advantage of the enhanced permeability and retention effect (EPR) (13,14).

In previous studies we showed that co-administration of Doxil[®] (Stealth[®] liposomal doxorubicin) and low-dose TNF resulted in a pronounced tumor response in both rat and murine tumor models. When B16BL6 melanoma-bearing mice were injected with Doxil[®] combined with TNF, drug accumulation increased 3-fold compared to liposomes alone (15,16). The augmented accumulation of the chemotherapeutic drug in the tumor tissue presumably explains the enhanced tumor regression. TNF likely increases the leakiness of the vasculature by increasing the gaps between the endothelial lining in the tumor, leading to augmented accumulation after extravasation of liposomes (17,18). Furthermore, TNF has been demonstrated to lower the IFP in tumors (19).

In the present study a B16BL6 mouse tumor model has been used to investigate the biodistribution of Stealth[®] liposomes of different sizes in combination with low dose TNF. Additionally we performed intravital microscopy to study tumor distribution of free and liposomal drugs in B16BL6 melanoma implanted in the mouse dorsal skin-fold chamber. Liposomes of 100 and 400 nm were used to investigate if these liposomes can cross the tumor vessel wall and if low dose TNF can cause an enhanced extravasation into the tumor tissue.

Materials and methods

Agents

Recombinant mouse Tumor Necrosis Factor- α (TNF, specific activity 3×10^7 IU/mg) was kindly provided by Dr. G. Adolf (Bender Wien GmbH, Wien, Austria) and stored at a concentration of 2 mg/mL at -80°C or under liquid nitrogen. Endotoxin levels (LAL) were below 1 EU/mg. Pegylated liposomal doxorubicin (Doxil[®]) was kindly provided by Dr. Peter Working (ALZA Corporation, Mountain View, CA, USA). Doxil[®] liposomes were labeled with DiO according to instructions (Molecular Probes, Eugene, OR, USA). Doxorubicin hydrochloride (Adriblastina[®]) was purchased from Pharmacia (Brussels, Belgium). Fluorescein isothiocyanate conjugated to bovine serum albumin (FITC-BSA; Sigma, Zwijndrecht, the Netherlands) was dissolved in phosphate buffered saline at a concentration of 10 mg/ml.

Preparation of sterically stabilized long circulation liposomes (SL)

For preparation of the liposomes the following chemicals were used: Partially Hydrogenated Egg Phosphatidyl Choline (PHEPC) was kindly provided by Lipoid GmbH and cholesterol (Chol) was obtained from Sigma (Zwijndrecht, the Netherlands). Distearoyl phosphatidylethanolamine (DSPE) is derivatized at its amino position with a MW 1900 segment of poly-(ethyleneglycol) (PEG). PEG-DSPE was kindly provided by Dr. P. Working (ALZA Corporation, Mountain View, CA, USA). Gallium⁶⁷ citrate was obtained from Nordian (Montreal, Canada) and deferoxamine mesylate (DF) from Sigma (Zwijndrecht, the Netherlands).

A mixture of PHEPC (242.5 mg), cholesterol (64.5 mg) and PEG-DSPE (67.5 mg) in a molar ratio of 1.85:1:0.15, suspended in chloroform/methanol, was evaporated to dryness in a rotary evaporator, redissolved in tertair butanol and freeze-dried overnight. The dried lipid film was resuspended in HEPES buffer (10 mM HEPES, 150 mM NaCl, pH 7.4) containing 5 mM deferoxamine mesylate (as described previously (20)). The hydrated lipidfilm was vortexed and liposomes of approximately 100 nm were brought to specific size by sonification during 10 to 15 minutes at amplitude 9 using an ultrasonic disintegrator supplied with an exponential microprobe (diameter 3.5 mm) (Soniprep 150, Sanyo, Leicester, UK). Liposomes of 400 nm and 800 nm were obtained by multiple extrusions through polycarbonate membranes (Nuclepore, Pleasanton, USA) with corresponding pore size, followed by size purification by ultra-centrifugation. Liposome size was determined by dynamic light scattering (DLS, Malvern 4700 system, Malvern, UK). The total lipid concentration was determined according to Bartlett (21) and liposomes were labeled with ⁶⁷Ga according to Gabizon *et al.* (20). 1 μmol lipid was labeled with 1 μCi ⁶⁷Ga. The amount of ⁶⁷Ga needed was diluted 1:10 in 8-hydroquinoline and incubated for 1 hour at 52°C. ⁶⁷Ga-oxine was added to the liposomes and incubated overnight at 4°C. To remove the free ⁶⁷Ga-oxine the liposomes were eluted on a sephadex G-50 (Pharmacia, Uppsala, Sweden) column and concentrated using ultra centrifugation at 60.000 rpm for 2 hours at 4°C (Beckman). The amount of lipid was determined again and the liposomes were stored at 4°C.

For the preparation of RhoPE Stealth[®] liposomes, 400 μg rhodamine-DHPE (Molecular Probes, Eugene, OR, USA) was added to the mixture of PHEPC, cholesterol and PEG-DSPE. Further preparation of 100 and 400 nm liposomes was identical as described above except for the addition of deferoxamine mesylate to the HEPES-buffer. After preparation, the amount of lipid was determined and the liposomes were stored at 4°C.

Animals and tumor model

Specific pathogen-free female C57BL/6 mice were purchased from Harlan-CPB, (Austerlitz, the Netherlands), weighing about 20 grams, and were fed a standard laboratory diet *ad libitum* (Hope Farms Woerden, the Netherlands).

The B16BL6 melanoma was used for the distribution studies. B16BL6 cells were maintained *in vitro* in DMEM supplemented with 10% FCS. Tumor was induced in donor mice by injection of 500.000 cells subcutaneously in the flank. For this purpose and experiments described below mice were anesthetized by subcutaneous injection of 150 μ l of a 1:1 (v:v) mixture of Ketamine (Alfasan, Woerden, the Netherlands) and Xylazine (Bayer AG, Leverkusen, Germany). At a tumor size of 10 mm tumor tissue was dissected under sterile conditions, cut in small pieces in sterile physiologic solution, and directly used for implantation in the window chamber or subcutaneously for the biodistribution study as described below.

All animal studies were done in accordance with protocols approved by the committee on Animal Research of the Erasmus MC, Rotterdam, the Netherlands.

Experimental procedure of tissue biodistribution of sterically stabilized liposomes

Experiments started at a tumor diameter of 10 ± 1 mm. At least 3 mice per group were injected via the tail vein with ^{67}Ga -labeled liposomes (48 $\mu\text{mol/kg}$) with or without TNF (1 $\mu\text{g}/\text{mouse}$). Mice were sacrificed 12 or 24 hours after liposome injection. Before sacrifice, blood was taken from the heart under anesthesia. Tumor, liver, spleen, lung, hart and kidney were collected, weighed, and counted in a Beckmann 8000 gamma counter.

Preparation of window chambers and tumor implantation.

The preparation of the dorsal skin-fold chamber is an adaptation from previously described procedures (22-24). Briefly, mice were anesthetized and hair was removed from the back of the animal. At one side of the skin-flap the window was outlined and a 12 mm diameter flap of skin was dissected away, leaving the fascia and opposing skin. The skin-fold on the back of mice was sandwiched between two frames, fixed with two light metal bolts and sutures. A small piece of tumor (0.1 mm^3) was transplanted in the fascia using a microsurgical microscope. On both sides the windows were closed with a 12 mm diameter microscopic cover glass of 0.13-0.16 mm thick. The mice were housed in an incubation room with an ambient temperature of 32°C and a humidity of 50%.

Experimental procedure of analysis of tumor distribution of liposomal drugs using intravital microscopy

The experiments started 10-14 days after implantation of the window chamber. The mice were anesthetized and injected via the tail vein with 4.5 mg/kg Doxorubicin, 4.5 mg/kg

Doxil[®] DiO or 48 $\mu\text{mol/kg}$ lipid 100 or 400 nm RhoPE liposomes (equals 4.5 mg/kg Doxil[®]) with or without 1 μg TNF/mouse. For intravital microscopy the mice were anesthetized and fixed to a heated microscopic stage. Injection of FITC-BSA allows visualization of functional vessels. Observations of the tumor vasculature were made with a Leica DM-RXA fluorescence microscope with the fluorescence filters for GFP (excitation 450-490 nm and emission 515 nm, long pass filter) and Rhodamine (excitation 515-560 nm and emission 590 nm, long pass filter). Images of the tumor were acquired using a Sony 3CCD DXC950 digital color video camera connected to a PC. Image acquisition and image analysis was performed with Research Assistant 3.0 for Windows 98 (RVC Visual Computing, Inc., Hilversum, the Netherlands).

For intravital confocal microscopy the mice were fixed to a Zeiss LSM 510 META confocal microscope with a heated stage. Scans were made with a 488 argon laser and 500-550 nm band pass filter (Albumin-FITC) and 543 nm laser and 560-615 nm band pass filter (Rhodamine).

In vitro uptake of (liposomal) drugs in B16BL6 cells

A circular cover glass was placed in a sterilized cell culture ring. B16BL6 cells were seeded and grown till confluency. The cells were washed and Doxil[®] or doxorubicin was added at a concentration of 5 $\mu\text{g/ml}$. The ring was placed under the Zeiss LSM 510 META confocal microscope equipped with an incubation chamber, which is maintained at 37°C with controlled CO₂-flow. Every 5 minutes scans were made using the 543 nm laser and 560-615 nm band pass filter (Rhodamine).

Statistical analysis

Results were evaluated for statistical significance with the Mann Whitney U test. P-values below 0.05 were considered statistically significant. Calculations were performed on a personal computer using GraphPad Prism v3.0 and SPSS v11.0 for Windows 2000.

Results

Tumor distribution of sterically stabilized liposomes (⁶⁷Ga-labeled)

Liposomes of 100, 400 or 800 nm with or without low-dose TNF were injected i.v. into mice bearing subcutaneous B16BL6 tumor (Figure 1A). The results show a 6.3-fold increased accumulation of 100 nm liposomes in the tumor 12 hours after co-administration with low-dose TNF compared to liposomes alone ($p < 0.02$), and a 5.5-fold increase after 24 hours ($p < 0.02$). Co-administration of TNF and 400 nm liposomes resulted in a 5.1 and 9.1-fold enhanced uptake of liposomes compared to liposomes alone (at 12 hours ($p < 0.02$) and 24 hours ($p < 0.01$), respectively). Twelve hours after treatment, TNF did not cause an increased uptake of 800 nm liposomes, but after 24 hours we saw a 12.6-fold increase in

comparison with liposomes without TNF ($p < 0.02$). Importantly, after 12 hours the uptake of 400 and 800 nm liposomes is significantly reduced compared to the 100 nm liposomes when co-administered with TNF. The same result was seen after 24 hours. There were no significant differences between 400 and 800 nm. These results indicate the beneficial properties of 100 nm liposomes as compared to the larger liposomes, even in the presence of TNF.

In conclusion, TNF is able to enhance the uptake of liposomes of 100, 400 and 800 nm and small liposomes of 100 nm localized in the tumor in a larger amount than 400 and 800 nm liposomes.

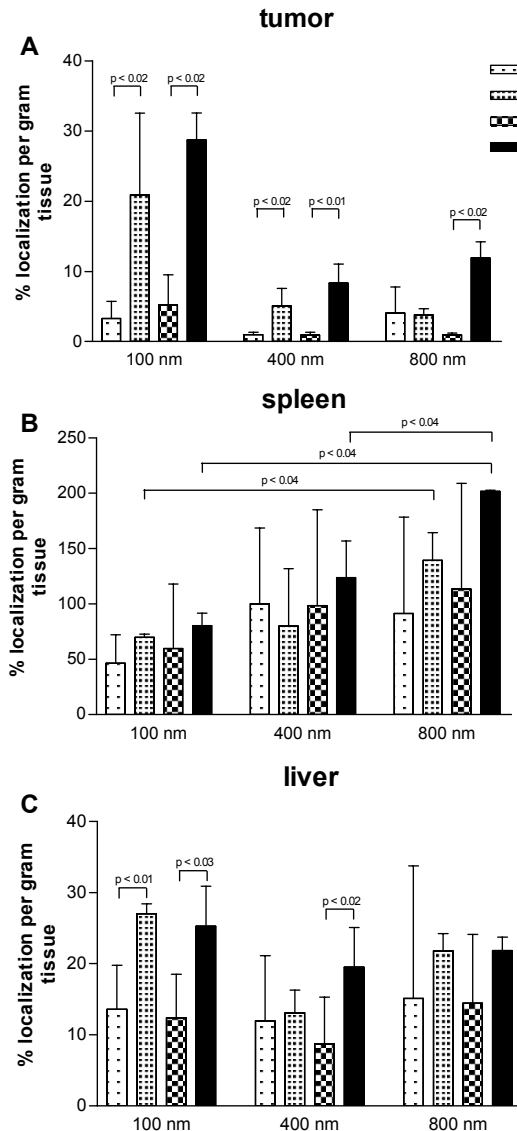


Figure 1. Accumulation of ^{67}Ga -labeled liposomes of 100, 400 or 800 nm ($48 \mu\text{mol/kg}$) with or without TNF ($1 \mu\text{g/mouse}$) in B16BL6 melanoma (a), spleen (b) and liver (c) 12 or 24 hours after injection. The mean of at least 3 mice are shown \pm SE.

Tissue distribution of sterically stabilized liposomes

Besides the tumor distribution of liposomes, also tissue distribution was investigated. In the spleen, TNF did not significantly increase uptake of all three liposome sizes, although a trend towards an increased uptake was visible (Figure 1B). Without TNF, uptake of the larger liposomes by the spleen was comparable to uptake of the 100 nm liposomes. When liposomes were co-administered with TNF, an increased uptake of the 800 nm liposomes was detected compared to the 100 nm (after 12 and 24 hours)($p < 0.04$) and the 400 nm liposomes (only after 24 hours)($p < 0.04$).

Liposome levels seemed elevated in liver tissue when TNF was added, but the increased uptake was not significant for the 800 nm liposomes at both time points and 400 nm liposomes 12 hours after injection (Figure 1C). For the 100 nm liposomes a clear increased liposome accumulation, when combined with TNF, was detected 12 and 24 hours after administration ($p < 0.01$ and $p < 0.03$, respectively) and for the 400 nm liposomes an increased accumulation after 24 hours was found ($p < 0.02$). For the liver, injection of large liposomes did not result in an increased uptake of these liposomes compared to 100 nm liposomes.

In other organs like kidney, TNF caused an augmented accumulation of liposomes, especially of the 100 and 800 nm liposomes 24 hours after injection. When co-administered with TNF, more 800 than 400 nm liposomes were taken up by the kidney, but less than 100 nm liposomes (data not shown).

Unexpectedly, levels of 100 nm liposomes in the blood circulation 24 hours after injection were increased when combined with TNF ($p < 0.03$), although this was not significant after 12 hours. TNF did not have a significant effect on the amount of large liposomes circulating in the blood. Less liposomes of 400 and 800 nm were circulating in the blood compared to 100 nm 12 hours after injection, but no differences were seen after 24 hours.

In lung and heart tissue, TNF caused an increased uptake of all three liposomes sizes 24 hours after injection. TNF enhanced the uptake of 100 nm liposomes more than 800 nm or 400 nm liposomes (data not shown).

Intratumoral distribution of liposomal drugs

Clearly, addition of a tolerable dose of TNF to systemic injection of Stealth[®] liposomes resulted in augmented accumulation of these liposomes, varying from 100 to 800 nm, in the tumor. However, insight in the intratumoral localization of the liposomes is lacking. Here we studied the effect of TNF on the intratumoral distribution of liposomal drugs with the use of intravital microscopy.

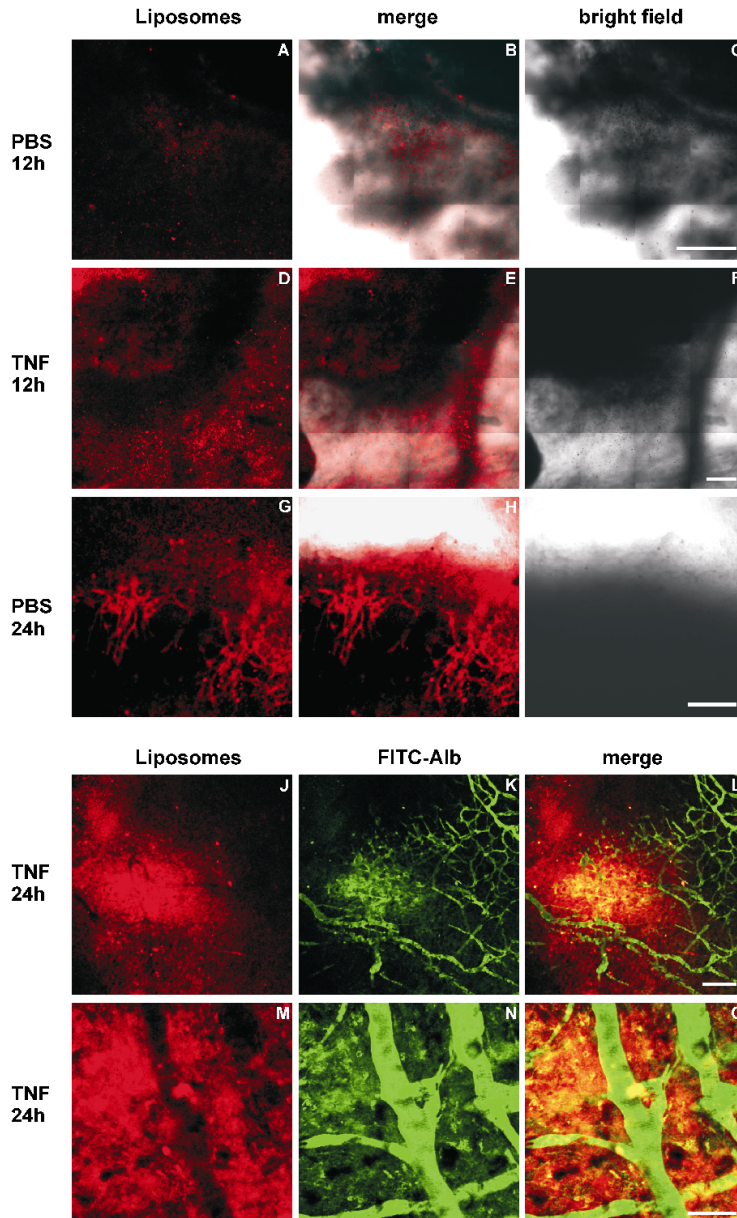


Figure 2. Extravasation and intratumoral distribution of 100 nm RhoPE liposomes in B16BL6 tumor. Injection of liposomes with PBS (PBS) or combined with 1 $\mu\text{g}/\text{mouse}$ TNF (TNF). Limited extravasation of the liposomes was observed at 12 h when no TNF was added (A-C), while most of the liposomes remained in blood vessels after 24 h (G-I). Addition of TNF to liposomal treatment resulted in massive and homogeneous extravasation of the liposomes already after 12 h (D-F). FITC-BSA was used to visualize the tumor-associated vasculature, showing extravasation of this blood marker at 24 h after injection of liposomes combined with TNF indicating prolonged vascular leakage (J-L). At higher magnification strong extravasation is observed from functional vessels at 24 h (M-O). Bar: 500 μm (A-F), 200 μm (G-L), and 50 μm (M-O).

In the 10 days after the tumor was implanted in the mouse window, it has grown approximately to a size of 4-5 mm and established its own blood supply. Unlike the normal blood vessels around the tumor, the newly formed vessels are not well organized. In the experiments FITC-BSA was injected to visualize functional blood vessels. In general it can be concluded that blood vessels in the periphery of the tumor were more functional than the vessels in the center of the tumor.

We first investigated RhoPE liposomes with a size of 100 nm. Although tumor microvessels are hyperpermeable, their permeability is very heterogeneous. In large parts of the tumor no fluorescence was detected, as shown in figures 2A-C. Most liposomes in the tumor accumulated in blood vessels at 24 hours (Figures 2G-I). Even 48 hours after injection most of the liposomes were still present in the blood vessels and did not extravasate into the tumor interstitium. Addition of TNF resulted in an abundant accumulation of liposomes in the tumor interstitium (Figure 2D-F). Only in few areas liposomes were trapped inside non-functional blood vessels. Importantly, liposomes extravasated more homogeneously throughout the tumor when TNF was co-administered. The TNF-induced permeability of the tumor vessels maintained for at least 24 h, resulting in extravasation of Albumine-FITC at that time-point at the same spot as liposomes leaked out (Figures 2J-L). At higher magnification we observed that Albumine-FITC positive vessels were quite permeable for 100 nm liposomes (Figures 2M-O). This suggests that liposomes extravasated from blood vessels that were functional. It can be concluded that the addition of TNF caused an increased extravasation of 100 nm RhoPE liposomes into the tumor interstitium in a more homogeneous way. Strikingly, less liposomes were trapped inside blood vessels when TNF was co-administered. These results indicate that administration of TNF results most likely in an increase in the number of leaky vessels.

Previous studies show that tumor vessels exhibit gaps between the endothelial cells with a cut off of approximately 400 nm (25). To investigate if TNF has a comparable effect on the intratumoral distribution of larger liposomes, RhoPE liposomes of 400 nm were injected into tumor-bearing mice. Clearly, more liposomes were trapped inside blood vessels compared to 100 nm liposomes (Figure 3). Strikingly, most of the vessels that contain liposomes were non-functional and accumulation in these blood vessels was very heterogeneous. Addition of TNF to the liposome treatment enhanced the extravasation of liposomes only slightly, mostly at the periphery of the tumor, while in the central part of the tumor liposomes appeared preferentially trapped in vessels (Figure 3). These results indicate a diminished usefulness of the 400 nm liposomes as compared to liposomes of 100 nm for the treatment of solid tumors, also in the presence of TNF.

It is known from previous studies that total drug uptake of free doxorubicin in tumor tissue is rather low compared to liposomal doxorubicin (16). In the present study we examined the tumor distribution of free doxorubicin and the long circulating liposomal form Doxil[®]

Figure 3. Diminished extravasation of 400 nm liposomes. Injection of 400 nm liposomes resulted predominantly in accumulation in tumor vessels, and remained trapped for long periods: 24 h (A-C) and 36 h (D-F). FITC-BSA was administered to visualize the functional tumor vessels. Clearly rapid extravasation of FITC-BSA was seen shortly after injection (A-C) and 12 h after FITC-BSA injection (D-F), indicating that the tumor vessels are predominantly permeable for relatively small substances. When 400 nm liposomes were co-administered with 1 μ g/ mouse TNF accumulation in tumor vessels was still observed (G-I). Detailed examination showed stasis in these vessels, even at the well-vascularized periphery. At 36 h (J-L) co-administration of TNF augmented the accumulation of 400 nm liposomes (*), although only at the outer rim of the tumor (dotted line) and in a rather heterogeneous way. FITC-BSA extravasated predominantly at the tumor periphery. Bar: 200 μ m (A-C), 500 μ m (D-F and J-L), and 100 μ m (G-I).

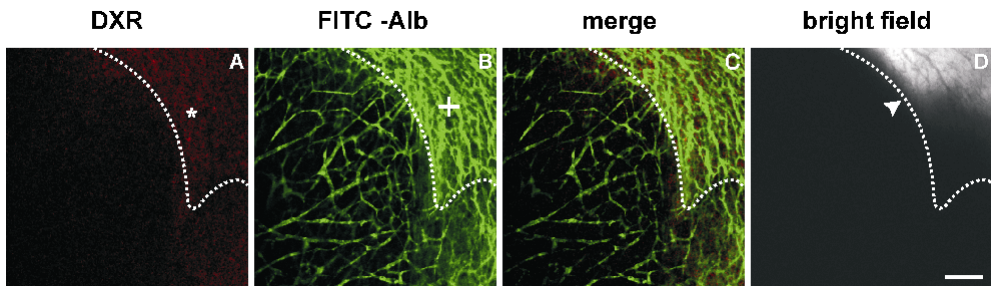
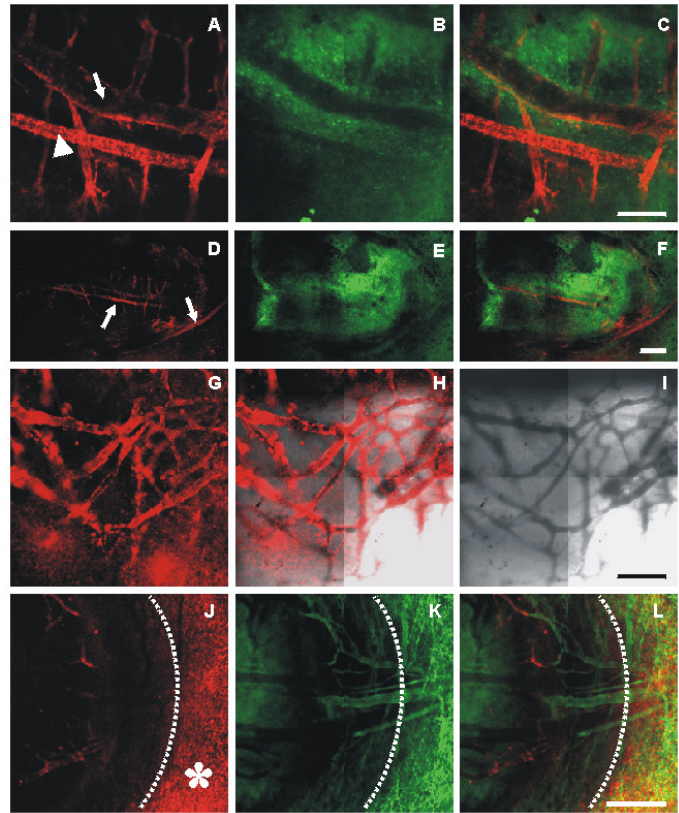


Figure 4. Tumor accumulation and intratumoral distribution of free doxorubicin in B16BL6 melanoma. After systemic injection of free doxorubicin either without or with TNF resulted in minimal drug accumulation on the B16BL6 tumor (A). Only in the periphery of the tumor (dotted line), which exhibits a high degree of vascularization (+) some accumulation of doxorubicin (*) was observed. In the more central areas of the tumor no extravasation of doxorubicin was observed. Bar, 200 μ m. While doxorubicin accumulated in low concentration in the B16BL6 tumor, either with or without TNF (B), Doxil[®] accumulation was 2.3-fold (without TNF) and 6.2-fold higher (with TNF) than free doxorubicin. Addition of TNF increased Doxil[®] accumulation 2.7-fold compared to treatment with Doxil[®] alone.

(Stealth[®] liposomal doxorubicin). Doxil[®] is labeled with DiO to distinguish between localization of the liposome (green fluorescence of the membrane-associated DiO) and doxorubicin, which is red fluorescent. When free doxorubicin was administered, either with or without TNF, hardly any drug was detectable in the tumor (Figures 4A-D). Free doxorubicin extravasated preferentially at the outer rim of the tumor, which is highly vascularized. As observed with the rhodamine-labeled liposomes, limited, focal and heterogeneous extravasation of Doxil[®] was observed especially at the tumor periphery when injected alone (data not shown). Addition of TNF dramatically enhanced the extravasation of Doxil[®] (Figure 5A-V). Although liposomes did not penetrate far into the tumor tissue, abundant extravasation could be observed already at 12 h after injection, predominantly at the rim of the tumor (Figures 5A-D). At later time-points transport of doxorubicin to the nucleus of tumor cells could be detected, while the lipid marker was only detected in the cytoplasm or interstitial space (Figures 5M-V). These results indicate that presumably most Doxil[®] liposomes are taken up intact by the cells and broken down in the cytoplasm.

In vitro uptake of (liposomal) drugs in tumor cells

When B16BL6 cells were exposed to Doxil[®] *in vitro*, accumulation of this drug in the cytoplasm was observed within a few minutes (Figure 6). Intracellular transport of the released doxorubicin to the nucleus was observed within 2 hours (Figure 6 upper panel). This in comparison with treatment with doxorubicin where the free drug was taken up directly by the nucleus within minutes after incubation (Figure 6 lower panel). Uptake by cells as well as intracellular transport of doxorubicin was not affected by TNF (data not shown).

Discussion

Here we demonstrate that administration of long circulating liposomes together with TNF results in a dramatically augmented accumulation of these liposomes in tumor tissue. Especially liposomes of 100 nm effectively home to the tumor. More precisely, intratumoral distribution studies reveal that administration of TNF results in an increased and more homogeneous distribution of the co-injected liposomes. The results indicate that TNF rendered more vessels permeable.

For a systemically injected drug to reach the tumor cell a number of hurdles have to be taken (1). Firstly, the blood volume of a solid tumor is rather low compared to the total blood volume and massive dilution of the injected drug in the bloodstream occurs. As systemic toxicity limits the dose of chemotherapeutic agents, and because of the quick clearance by liver and kidney, only low levels are present at any given moment in the tumor after systemic injection. Particles or cells are cleared by the immune system (26).

Figure 5

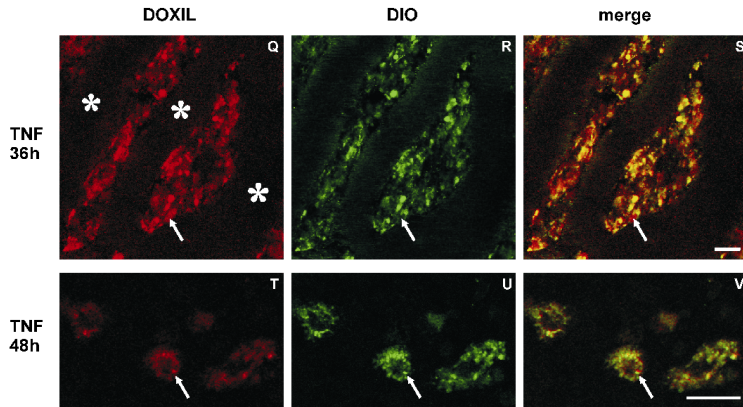
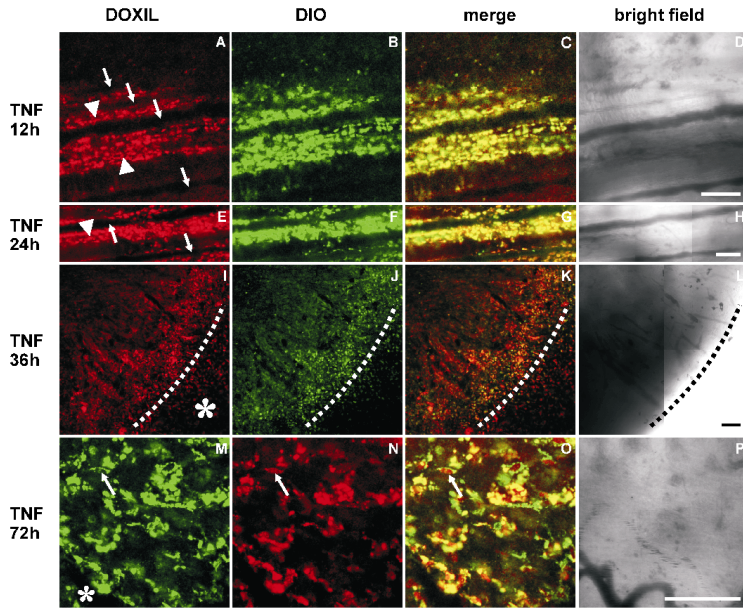


Figure 6

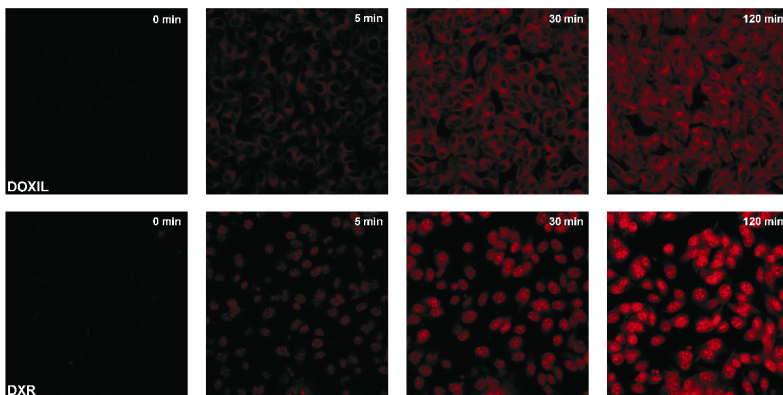


Figure 5. Intratumoral distribution of Doxil[®] in B16BL6 melanoma. The effect of TNF on the extravasation and intratumoral distribution of doxorubicin (red) released from the Doxil[®] liposomes (green) was studied by intravital microscopy. Strong and homogenous extravasation of liposomes was observed 12 and 24 h after injection (arrow, vessels and arrow head, extravasated Doxil[®])(A-H). Especially at the periphery of the tumor (dotted line) the extravasation was most abundant (I-L). At later time-points nuclear localization of doxorubicin (red) could be observed (arrow), distant from the tumor vessel (*) while the lipid marker (green) remained in the cytoplasm (M-P). Already at 36 h after injection of Doxil[®] combined with TNF nuclear localization of doxorubicin in cells (arrow) close to the tumor vessels (*) could be observed (Q-S). While concurrently doxorubicin containing liposomes (yellow in merge) could be observed in the cytoplasm of tumor cells (arrow)(T-V). Bar 100 μm (A-P) and 25 μm (Q-V).

Figure 6. *In vitro* uptake of Doxil[®] and doxorubicin in B16BL6 melanoma cells. Cells were plated in a sterilized cell culture ring and grown till confluency. The cells were incubated with 5 $\mu\text{g/ml}$ Doxil[®] (upper panel) or 5 $\mu\text{g/ml}$ doxorubicin (lower panel) and every 5 minutes scans were made using the 543 nm laser and 560-615 nm band pass filter (Rhodamine) of the Zeiss LSM 510 META confocal microscope. The original light intensities in the experiments were maintained during the experiment and were the same for both Doxil[®] and doxorubicin treatment. The experiments were repeated 3 times and representative time series are shown.

Moreover, perfusion of the tumor is heterogeneous, meaning that the drug reaches only well vascularized parts of the tumor, whereas hypoxic and necrotic parts are not targeted (27-29). Secondly, for a drug to reach the tumor cells the drug has to leave the circulation and cross the endothelial lining. Normally the endothelial lining is a closed barrier, but blood vessels supplying tumors appear permeable to macromolecules and particles, with a determined cut off of 400 nm (25). However, not all tumor vessels exhibit this feature. Dvorak *et al.* demonstrated that the leaky vessels are predominantly mature veins and venules lined by a continuous endothelium (2,30). Strikingly, immature interface vessels and tumor penetrating vessels do not leak macromolecules. Small molecules on the other hand extravasate from all tumor vessels. Thirdly, after extravasation, the anti-tumor agents embark on a third barrier, the tumor interstitium. Abundant matrix regularly present in solid tumors hinders traverse of the agent. High interstitial pressure works against the accumulation of macromolecules and particles. The accumulation of large molecules and particles is mainly convection driven, whereas small molecules distribute by diffusion (2). As solid tumors lack a normally functioning lymphatic system, fluid is driven out of the tumor at the periphery taking large molecules and particles along (31). Finally, when the drug reaches the tumor cell it has to cross the cell membrane, or when active at the DNA level, the nuclear membrane as well.

At all levels mentioned above modifications can be made to improve efficacy of the therapy. An important step forwards is to define targets closer to the injected drug, i.e. the endothelial lining, which comprise the first cells seen by an agent after intravenous or intra-arterial administration. Secondly, vascular manipulation can be used to help drugs, which act on the tumor cells, to better reach their target. Next to that tumor response would greatly

benefit from enhanced local drug levels, which can be accomplished by targeting the drug (e.g. with the aid of liposomes) or by limiting the dilution of the drug, and in the same time increasing local drug level, which can be accomplished in a so-called isolated perfusion setting.

Previously, we demonstrated that addition of TNF to an isolated perfusion with melphalan or doxorubicin dramatically improves tumor response (32-34). Moreover, also in a systemic setting addition of TNF to liposomal chemotherapy improves tumor response (15,16). This synergy is not, or at least not solely, due to a direct activity of TNF on the tumor cells and does not result from a direct destruction of the tumor-associated vasculature. However, addition of TNF, both in the perfusion setting as well as in the systemic setting, augmented the accumulation of the co-administered drug in the tumors (15,16,32-34). In other studies TNF also enhanced tumor accumulation of liposome-encapsulated adriamycin (35) and radio-antibody (36). Curnis *et al.* found that targeted delivery of TNF coupled to cyclic CNGRC peptide to tumor vessels enhances the antitumor activity of chemotherapeutic drugs and increased the penetration drugs in tumors (37). These findings led to the search for alternative agents with known vascular permeability increasing activity, such as histamine and IL-2. We have shown that these agents enhanced drug uptake in the tumor resulting in synergistic anti-tumor activity in an isolated setting (38,39) Apparently this dual approach, combination of tumor cell directed chemotherapy and tumor vasculature directed therapy, is an important principle. Although it is known that TNF, but also histamine and IL-2, are capable of increasing the permeability of an endothelial lining, the effect of TNF on tumor vessels in the tumor is largely unknown. Ruegg *et al.* showed that TNF in conjunction with IFN induced functional down-modulation of the $\alpha_v\beta_3$ integrin, resulting in detachment and anoikis of the endothelial cells (40). This possibly explains why tumor vessels, in which $\alpha_v\beta_3$ exposure is increased, are more responsive to TNF than endothelial cells from healthy vessels, which are quiescent. Important also is which tumor vessels are affected by TNF and how distribution of the chemotherapeuticum in the tumor is altered. Here we showed that TNF improves accumulation of liposomes, i.e. liposomal chemotherapeutics, by making more vessels permeable. Importantly this results in a homogeneous drug distribution and thus a homogeneous tumor cell killing.

In conclusion, we show that TNF improves drug accumulation in solid tumor by making more vessels permeable to 100 nm liposomes. As this results in a homogeneous drug distribution more tumor cells are exposed to the drug and a better tumor response is reached. Our results indicate that the dual approach with the combination of TNF and chemotherapy has strong potential for solid tumor therapy and necessitates the further development of a clinical applicable formulation.

Acknowledgement

We would like to thank Boehringer Ingelheim GmbH for the generous supply of rhTNF, and Dr. P. Working for supplying Doxil[®] (ALZA Corporation, Mountain View, CA, USA). This study was supported by grant DDHK 2000-2224 of the Dutch Cancer Society.

References

1. Jain RK. Barriers to drug delivery in solid tumors. *Sci Am.* 1994;271(1):58-65.
2. Dvorak HF, Nagy JA, Dvorak JT, Dvorak AM. Identification and characterization of the blood vessels of solid tumors that are leaky to circulating macromolecules. *Am J Pathol.* 1988;133(1):95-109.
3. Yuan F. Transvascular drug delivery in solid tumors. *Semin Radiat Oncol.* 1998;8(3):164-175.
4. Hashizume H, Baluk P, Morikawa S, et al. Openings between defective endothelial cells explain tumor vessel leakiness. *Am J Pathol.* 2000;156(4):1363-1380.
5. Allen TM, Newman MS, Woodle MC, Mayhew E, Uster PS. Pharmacokinetics and anti-tumor activity of vincristine encapsulated in sterically stabilized liposomes. *Int J Cancer.* 1995;62(2):199-204.
6. Lasic DD. Doxorubicin in sterically stabilized liposomes. *Nature.* 1996;380(6574):561-562.
7. Papahadjopoulos D, Allen TM, Gabizon A, et al. Sterically stabilized liposomes: improvements in pharmacokinetics and antitumor therapeutic efficacy. *Proc Natl Acad Sci U S A.* 1991;88(24):11460-11464.
8. Sparano JA, Winer EP. Liposomal anthracyclines for breast cancer. *Semin Oncol.* 2001;28(4 Suppl 12):32-40.
9. Gabizon A, Martin F. Polyethylene glycol-coated (pegylated) liposomal doxorubicin. Rationale for use in solid tumours. *Drugs.* 1997;54 Suppl 4:15-21.
10. Mayer LD, Cullis PR, and Bally MB Designing therapeutically optimized liposomal anticancer delivery systems: lessons from conventional liposomes. *In* Lasic DD and Papahadjopoulos D (eds.), *Medical Applications of Liposomes*, pp. 231-257. 2002.
11. Newman MS, Colbern GT, Working PK, Engbers C, Amantea MA. Comparative pharmacokinetics, tissue distribution, and therapeutic effectiveness of cisplatin encapsulated in long-circulating, pegylated liposomes (SPI-077) in tumor-bearing mice. *Cancer Chemother Pharmacol.* 1999;43(1):1-7.
12. Wu NZ, Da D, Rudoll TL, Needham D, Whorton AR, Dewhirst MW. Increased microvascular permeability contributes to preferential accumulation of Stealth liposomes in tumor tissue. *Cancer Res.* 1993;53(16):3765-70.
13. Maeda H, Fang J, Inutsuka T, Kitamoto Y. Vascular permeability enhancement in solid tumor: various factors, mechanisms involved and its implications. *Int Immunopharmacol.* 2003;3(3):319-328.
14. Torchilin VP. Drug targeting. *Eur J Pharm Sci.* 2000;11 Suppl 2:S81-91.:S81-S91.
15. Brouckaert P, Takahashi N, van Tiel ST, et al. Tumor necrosis factor-alpha augmented tumor response in B16BL6 melanoma-bearing mice treated with stealth liposomal doxorubicin (Doxil) correlates with altered Doxil pharmacokinetics. *Int J Cancer.* 2004;109(3):442-448.
16. ten Hagen TL, van Der Veen AH, Nooijen PT, van Tiel ST, Seynhaeve AL, Eggermont AM. Low-dose tumor necrosis factor-alpha augments antitumor activity of stealth liposomal doxorubicin (DOXIL) in soft tissue sarcoma-bearing rats. *Int J Cancer.* 2000;87(6):829-37.
17. Brett J, Gerlach H, Nawroth P, Steinberg S, Godman G, Stern D. Tumor necrosis factor/cachectin increases permeability of endothelial cell monolayers by a mechanism involving regulatory G proteins. *J Exp Med.* 1989;169(6):1977-1991.
18. Partridge CA, Horvath CJ, Del Vecchio PJ, Phillips PG, Malik AB. Influence of extracellular matrix in tumor necrosis factor-induced increase in endothelial permeability. *Am J Physiol.* 1992;263(6 Pt 1):L627-L633.
19. Kristensen CA, Nozue M, Boucher Y, Jain RK. Reduction of interstitial fluid pressure after TNF-alpha treatment of three human melanoma xenografts. *Br J Cancer.* 1996;74(4):533-6.
20. Gabizon A, Papahadjopoulos D. Liposome formulations with prolonged circulation time in blood and enhanced uptake by tumors. *Proc Natl Acad Sci U S A.* 1988;85(18):6949-6953.
21. Bartlett GR. Phosphorus assay in column chromatography. *J Biol Chem.* 1959;234(3):466-468.
22. Papenfuss HD, Gross JF, Intaglietta M, Treese FA. A transparent access chamber for the rat dorsal skin fold. *Microvasc Res.* 1979;18(3):311-318.
23. Leunig M, Yuan F, Menger MD, et al. Angiogenesis, microvascular architecture, microhemodynamics, and interstitial fluid pressure during early growth of human adenocarcinoma LS174T in SCID mice. *Cancer Research.* 1992;52(23):6553-6560.
24. Huang Q, Shan S, Braun RD, et al. Noninvasive visualization of tumors in rodent dorsal skin window chambers. *Nature Biotechnology.* 1999;17(10):1033-1035.

25. Yuan F, Dellian M, Fukumura D, et al. Vascular permeability in a human tumor xenograft: molecular size dependence and cutoff size. *Cancer Res.* 1995;55(17):3752-3756.
26. Gabizon A, Shmeeda H, Barenholz Y. Pharmacokinetics of pegylated liposomal Doxorubicin: review of animal and human studies. *Clin Pharmacokinet.* 2003;42(5):419-436.
27. Gillies RJ, Schornack PA, Secomb TW, Raghunand N. Causes and effects of heterogeneous perfusion in tumors. *Neoplasia.* 1999;1(3):197-207.
28. Graff BA, Kvinnsland Y, Skretting A, Rofstad EK. Intratumour heterogeneity in the uptake of macromolecular therapeutic agents in human melanoma xenografts. *Br J Cancer.* 2003;88(2):291-297.
29. Baxter LT, Jain RK. Transport of fluid and macromolecules in tumors. II. Role of heterogeneous perfusion and lymphatics. *Microvasc Res.* 1990;40(2):246-263.
30. Dvorak HF. Leaky tumor vessels: consequences for tumor stroma generation and for solid tumor therapy. *Prog Clin Biol Res.* 1990;354A:317-30.:317-330.
31. Boucher Y, Jain RK. Microvascular pressure is the principal driving force for interstitial hypertension in solid tumors: implications for vascular collapse. *Cancer Res.* 1992;52(18):5110-4.
32. de Wilt JH, ten Hagen TL, de Boeck G, van Tiel ST, de Bruijn EA, Eggermont AM. Tumour necrosis factor alpha increases melphalan concentration in tumour tissue after isolated limb perfusion. *Br J Cancer.* 2000;82(5):1000-1003.
33. Manusama ER, Stavast J, Durante NM, Marquet RL, Eggermont AM. Isolated limb perfusion with TNF alpha and melphalan in a rat osteosarcoma model: a new anti-tumour approach. *Eur J Surg Oncol.* 1996;22(2):152-157.
34. van Der Veen AH, de Wilt JH, Eggermont AM, van Tiel ST, Seynhaeve AL, ten Hagen TL. TNF-alpha augments intratumoural concentrations of doxorubicin in TNF-alpha-based isolated limb perfusion in rat sarcoma models and enhances anti-tumour effects. *Br J Cancer.* 2000;82(4):973-980.
35. Suzuki S, Ohta S, Takashio K, Nitana H, Hashimoto Y. Augmentation for intratumoral accumulation and anti-tumor activity of liposome-encapsulated adriamycin by tumor necrosis factor-alpha in mice. *Int J Cancer.* 1990;46(6):1095-1100.
36. Folli S, Pelegrin A, Chalandon Y, et al. Tumor-necrosis factor can enhance radio-antibody uptake in human colon carcinoma xenografts by increasing vascular permeability. *Int J Cancer.* 1993;53(5):829-836.
37. Curnis F, Sacchi A, Corti A. Improving chemotherapeutic drug penetration in tumors by vascular targeting and barrier alteration. *J Clin Invest.* 2002;110(4):475-482.
38. Brunstein F, Hoving S, Seynhaeve AL, et al. Synergistic antitumor activity of histamine plus melphalan in isolated limb perfusion: preclinical studies. *J Natl Cancer Inst.* 2004;96(21):1603-1610.
39. Hoving S, Brunstein F, van de Wiel-Ambagtsheer G, et al. Synergistic antitumor response of IL-2 with melphalan in isolated limb perfusion in soft-tissue sarcoma bearing rats. *Cancer Res.* 2005;65(10):4300-4308.
40. Ruegg C, Yilmaz A, Bieler G, Bamat J, Chaubert P, Lejeune FJ. Evidence for the involvement of endothelial cell integrin alphaVbeta3 in the disruption of the tumor vasculature induced by TNF and IFN-gamma. *Nat Med.* 1998;4(4):408-14.

Chapter 10

Intrinsic and TNF-induced vascular hyperpermeability of B16BL6 melanoma versus Lewis lung carcinoma determines tumor response

Saske Hoving, Ann LB Seynhaeve, Sandra T van Tiel, Gisela aan de Wiel-Ambagtsheer, Alexander MM Eggermont, Timo LM ten Hagen

Department of Surgical Oncology, Erasmus MC-Daniel den Hoed Cancer Center, Rotterdam, the Netherlands

Submitted

Abstract

Impaired drug uptake at the tumor site remains a key barrier to effective chemotherapy of solid tumors. Clinical and animal studies show strongly improved tumor response when the vasoactive agent TNF is co-administered. Whilst addition of TNF to systemic treatment with Doxil[®] strongly improved the anti-tumor response, which correlated with the enhanced drug accumulation, in the B16BL6 model, no such effect was observed in the LLC model. B16BL6 tumor appeared less vascularized than the LLC, but the tumor vessels were larger, while local VEGF levels are comparable in both tumor types. The results indicate that tumor vascular permeability, and response to TNF, may be the limiting factor involved in liposomal drug delivery rather than microvessel density.

Introduction

Physiological barriers hinder the effective delivery of drugs to tumors (1). Heterogeneous tumor perfusion and increased interstitial fluid pressure (IFP) may limit the penetration of drugs into tumor cells distant from blood vessels. Inadequate drug delivery leads to insufficient tumor cell kill and to the induction of drug resistance (1-3). It is known that tumor blood vessels exhibit heterogeneous hyperpermeability to plasma proteins and other circulating macromolecules. Vascular permeability depends on tumor type and increases with tumor size and growth rate. It may be higher in the periphery than in the central region of the tumor (1,4-8). Delivery systems have been developed to exploit vascular permeability. Long circulating liposomal drugs preferentially extravasate from these abnormal vessels and accumulate in tumor tissue (9,10). Encapsulation of anticancer drugs in liposomes results in reduced systemic toxicity while retaining or improving *in vivo* efficacy (11-14). Stealth[®] liposomes are sterically stabilized liposomes that contain methoxy-polyethylene glycol (MPEG). They have the advantage over unmodified liposomes that they are eliminated more slowly by the reticulo-endothelial system (RES) resulting in a long circulation time (9,11-13,15-17). Doxil[®] (Stealth[®] liposomal doxorubicin) is effective in the treatment of several tumor types (18-20). We showed in previous studies that co-administration of Doxil[®] and low-dose TNF resulted in a pronounced tumor response in both rat and murine tumor models. When B16BL6 melanoma-bearing mice or soft-tissue sarcoma-bearing rats were injected with Doxil[®] combined with TNF, a 3-fold increased drug accumulation in tumor tissue was found compared to treatment with liposomes alone (18,19). The increased drug uptake correlates with the synergistic antitumor response. A possible explanation for the augmented accumulation is that TNF increases the leakiness of the vasculature by increasing the gaps between the endothelial lining in the tumor (20,21).

In the present study we investigated whether addition of low-dose TNF to Doxil[®] treatment would lead to the same anti-tumor response and liposomal tumor distribution in tumors

which differed in tumor vasculature characteristics: the B16BL6 tumor and the Lewis Lung Carcinoma (LLC).

Materials and methods

Agents

Recombinant murine tumor necrosis factor- α (specific activity 3×10^7 IU/mg) was kindly provided by Dr. G. Adolf (Bender Wien GmbH, Wien, Austria) and stored at a concentration of 2 mg/mL at -80°C or under liquid nitrogen. Endotoxin levels (LAL) were below 1 EU/mg. Pegylated liposomal doxorubicin (Doxil[®]) was kindly provided by Dr. Peter Working (ALZA Corporation, Mountain View, CA, USA). Doxil[®] liposomes were labeled with DiO (Molecular Probes, Eugene, OR, USA). Doxorubicin hydrochloride (Adriablastina) was purchased from Pharmacia (Brussels, Belgium).

Preparation of sterically stabilized long circulation RhoPE liposomes

For preparation of the liposomes the following chemicals were used: Partially Hydrogenated Egg Phosphatidyl Choline (PHEPC) was kindly provided by Lipoid GmbH and cholesterol (Chol) was obtained from Sigma (Zwijndrecht, the Netherlands). Distearoyl phosphatidylethanolamine (DSPE) is derivatized at its amino position with a MW 1900 segment of poly-(ethyleneglycol) (PEG). PEG-DSPE was kindly provided by Dr. P. Working (ALZA Corporation, Mountain View, CA, USA).

A mixture of PHEPC (242.5 mg), cholesterol (64.5 mg) and PEG-DSPE (67.5 mg) in a molar ratio of 1.85:1:0.15 and 400 μg lissamine-rhodamine-phosphatidyl-ethanolamine (Rho-PE) (Molecular Probes, Eugene, OR, USA) was suspended in chloroform/methanol. The mixture was evaporated to dryness in a rotary evaporator, redissolved in tertair butanol and freeze-dried overnight. The dried lipid film was resuspended in HEPES buffer (10 mM HEPES, 150 mM NaCl, pH 7.4), as described previously (10). The hydrated lipid film was vortexed and liposomes of approximately 100 nm were brought to specific size by sonification during 10 to 15 minutes at amplitude 9 using an ultrasonic disintegrator supplied with an exponential microprobe (diameter 3.5 mm) (Soniprep 150, Sanyo, Leicester, UK). Liposome size was determined by dynamic light scattering (DLS, Malvern 4700 system, Malvern, UK). The total lipid concentration was determined according to Bartlett (22) and the liposomes were stored at 4°C .

Animals and tumor model

Specific pathogen-free female C57BL/6 mice were purchased from Harlan-CPB, (Austerlitz, the Netherlands), weighing about 20 grams, and were fed a standard laboratory diet *ad libitum* (Hope Farms Woerden, the Netherlands).

Small fragments (3 mm) of the B16BL6 melanoma or Lewis Lung Carcinoma (LLC) were implanted subcutaneously in the flank of the mice. The mice were anesthetized by subcutaneous injection of 150 μ l of a 1:1 (v:v) mixture of Ketamine (Alfasan, Woerden, Netherlands) and Xylazine (Bayer AG, Leverkusen, FRG). At a tumor size of 10 mm, tumor tissue was dissected under sterile conditions, cut in small pieces in sterile physiologic solution, and directly used for implantation in the window chamber or subcutaneously for the efficacy study and measurements of liposomal drug accumulation as described below. All animal studies were done in accordance with protocols approved by the committee on Animal Research of the Erasmus MC, Rotterdam, the Netherlands.

Treatment protocol

Treatment was started when the tumors reached an average diameter of 8-10 mm. The mice were randomized into the following 6 groups: placebo liposomes (equivalent amounts of buffer or lipids), low dose TNF, Doxil[®] and Doxil[®] plus TNF. Mice were injected five times intravenously with an interval of 4 days between the injections; first dose of 4.5 mg/kg Doxil[®] and 1.0 mg/kg for consecutive doses. TNF was given at a concentration of 1 μ g/mouse for all five doses. When mice were treated with Doxil[®] combined with TNF, these agents were injected separately, shortly after each other. Tumor growth was recorded by caliper measurement. Tumor size was expressed as tumor size index, i.e. the product of the largest perpendicular diameters. Mice were sacrificed if tumor diameter exceeded 15 mm or at the end of the experiments.

Measurement of doxorubicin accumulation in tumor tissue

The effect of TNF on Doxil[®] accumulation in tumors was investigated. Mice received a single dose of 1 mg/kg Doxil[®] with or without low dose TNF. Tumors were excised 24 hours after injection and tissues were analyzed for doxorubicin and its fluorescent metabolites as previously described (23). Briefly, tumors were incubated in acidified isopropanol (0.075 N HCl in 90% isopropanol) for 24 hours at 4°C and after that the tumors were homogenized (PRO200 homogenizer with 10 mm generator, Pro Scientific, CT, USA), centrifuged for 30 min at 2500 rpm and supernatants were harvested. A Hitachi F4500 fluorescence spectrometer (excitation 472 nm and emission 590 nm) was used for measurement of the samples. A standard curve was prepared with known concentrations of doxorubicin diluted in acidified isopropanol. All measurements were repeated after addition of an internal doxorubicin standard.

Preparation of window chambers and tumor implantation.

The preparation of the dorsal skin-fold chamber is an adaptation from previously described procedures (24-26). Briefly, mice were anesthetized and hair was removed from the back of

the animal. At one side of the skin-flap the window was outlined and a 12 mm diameter flap of skin was dissected away, leaving the fascia and opposing skin. The skin-fold on the back of mice was sandwiched between two frames, fixed with two light metal bolts and sutures. A small piece of tumor (0.1 mm³) was transplanted in the fascia using a microsurgical microscope. On both sides the windows were closed with a 12 mm diameter microscopic cover glass of 0.13-0.16 mm thick. The mice were housed in an incubation room with an ambient temperature of 32°C and a humidity of 50%.

Experimental procedure of tumor distribution of (liposomal) drugs using intra-vital microscopy

The experiments started 10-14 days after tumor implantation in the window chamber. The mice were anesthetized and injected via the tail vein with 48 µmol/kg 100 nm RhoPE liposomes (equals 4.5 mg/kg Doxil[®]) or 4.5 mg/kg Doxil[®] DiO with or without 1 µg TNF/mouse. For intravital microscopy the mice were anesthetized and fixed to a heated microscopic stage. Observations of the tumor vasculature were made with a Leica DM-RXA fluorescence microscope with the fluorescence filters for GFP (excitation 450-490 nm and emission 515 nm, long pass filter) and Rhodamine (excitation 515-560 nm and emission 590 nm, long pass filter). Images of the tumor were acquired using a Sony 3CCD DXC950 digital color video camera connected to a PC. Image acquisition and image analysis were performed with Research Assistant 3.0 for Windows 98 (RVC Visual Computing, Inc., Hilversum, the Netherlands).

Immunohistochemistry

Untreated tumors with a diameter of 8-10 mm were excised and immediately frozen in liquid nitrogen. Immunohistochemical studies were performed on acetone-fixed 5 µm cryostat sections. The tumor sections were fixed for 30 min with 4% formaldehyde and after rinsing with PBS, the endogenous peroxidase activity was blocked by incubation for 5 minutes in methanol/3% H₂O₂. The slides were incubated for 1 hour with 1:50 rat-anti-mouse-CD31 (Becton Dickinson, Alphen aan den Rijn, the Netherlands) diluted in 5% rabbit serum/PBS. Thereafter, sections were washed with PBS and incubated for 1 h with rabbit-anti-rat peroxidase-labeled antibody (DAKO, ITK Diagnostics BV, Uithoorn, the Netherlands) diluted 1:100 in PBS with 5% mouse serum. After rinsing with PBS, positive cells were revealed by immunoperoxidase reaction with DAB solution (DAB-kit, DAKO) and counterstained lightly with haematoxylin (Sigma).

The sections were examined on a Leica DM-RXA and photographed using a Sony 3CCD DXC 950 camera. The number of vessels and the area of vessels per field of interest were measured in calibrated digital images (Research Assistant 3.0, RVC, Hilversum, the

Netherlands). For quantification of the microvessel density (MVD) six representative fields of interest (magnification 16x) per tumor and 5 or 6 animals per group were examined.

In vitro cytotoxicity assay

The mouse B16BL6 melanoma and LLC cells were both maintained in DMEM supplemented with 10% fetal calf serum and 0.1% penicilline-streptomycine. Media and supplements were obtained from Life Technologies, the Netherlands.

The tumor cells were added in 100 μ l aliquots to 96-well flat-bottomed microtiter plates (Costar, Cambridge, MA, USA) at a final concentration of 6×10^3 cells per well and allowed to grow as a monolayer. *In vitro* cytotoxicity was measured using the MTT assay. The MTT assay is based on the conversion of the yellow tetrazolium salt, 3-(4,5-dimethylthiazol-2-yl)-2,5-diphenyltetrazolium bromide (MTT) to the purple colored formazan pigment by mitochondrial enzymes in viable cells. Tumor cells were incubated at 37°C in 5% CO₂ for 72 hours in the presence of various concentrations of TNF and Doxil[®]. The range of final drug concentrations was 1×10^{-6} - 10 μ g/ml for TNF and 0.001 – 5 μ g/ml Doxil[®]. After 72 hours of incubation the medium was replaced with 50 μ l of MTT (3 mg/ml in PBS) and incubated for 3 hours at 37°C in 5% CO₂. Then medium was removed and the formazan crystals were dissolved in 100 μ l DMSO and the optical density was read at 540 nm in a microtiter plate reader. Tumor cell growth was calculated using the formula: cell growth = (test well/control) x 100 percent. The drug concentration reducing the cell growth to 50% of the control (IC₅₀) was determined from the growth curves. The experiments were repeated at least 3 times in duplo.

VEGF ELISA

VEGF was measured from cell-culture supernatants by ELISA (BioSource Europe, Nivelles, Belgium). Briefly, B16BL6 and LLC tumor cells were plated in 6-wells plates at a density of $1.25 \cdot 10^5$ cells/well. After 2 days, medium was replaced by 1.5 mL of fresh medium and the cells were incubated under normoxic and hypoxic (1% O₂) conditions. After 48 hours supernatant was collected and spun down to remove cell debris. Cell numbers were counted in every well. The experiments were performed 3 times and all analyses and calibrations were carried out in duplicate. Protein levels were normalized to cell number.

Statistical analysis

Results were evaluated for statistical significance with the Mann Whitney U test. P-values below 0.05 were considered statistically significant. Calculations were performed on a personal computer using GraphPad Prism v3.0 and SPSS v11.0 for Windows 2000.

Results

Addition of low-dose TNF improves anti-tumor activity of Doxil[®] in B16BL6 melanoma but not in Lewis lung carcinoma.

To evaluate the anti-tumor activity of Doxil[®] in combination with low-dose TNF, B16BL6 and LLC-bearing mice were treated at 4 days-intervals with a total of 5 injections of Doxil[®] with or without TNF. Untreated B16BL6 tumors were growing slightly faster than untreated LLC tumors. Treatment of B16BL6 melanoma and LLC tumor with Doxil[®] alone resulted in a slight tumor growth delay in both tumor types, compared to placebo treated animals (Figure 1). Treatment with TNF alone showed a minor but visible anti-tumor effect in the B16BL6 tumor but not in the LLC tumor. In the B16BL6 tumor the combination treatment of low dose TNF and Doxil[®] proved to be more effective than Doxil[®] alone, with a prolonged tumor growth delay. These results are in contrast with the LLC tumor, where addition of low dose TNF to Doxil[®] treatment did not improve the tumor response.

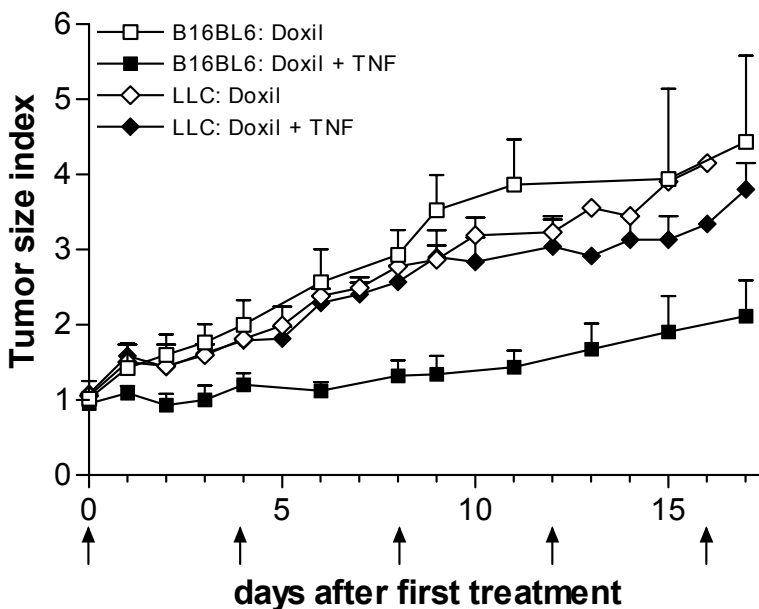


Figure 1. Combination of TNF with Doxil[®] results in synergistic response of B16BL6 melanoma, but is not found in Lewis lung carcinoma. Growth curves of subcutaneous implanted B16BL6 melanoma and Lewis Lung Carcinoma after systemic Doxil[®] treatment with or without low dose TNF. Mice were injected five times intravenously with an interval of 4 days between the injections; first dose 4.5 mg/kg Doxil[®] and 1.0 mg/kg for consecutive doses and 1 µg TNF per mouse for all five doses. Tumor size index is plotted against time (days after first treatment) and represents the mean of at least 5 mice per group \pm SEM.

TNF improves Doxil[®] accumulation in B16BL melanoma but not in Lewis lung carcinoma.

To investigate the difference in response of B16BL6 melanoma and the LLC tumor to the combination therapy of TNF and Doxil[®], accumulation of Doxil[®] in tumor tissue was measured. After a single dose of 1 mg/kg Doxil[®] the amount of drug in tumor tissue 24 hours after injection was 2.4 times higher in the B16BL6 tumor compared to the LLC tumor (Figure 2). Addition of TNF to the Doxil[®] treatment resulted in a 1.8-fold increased uptake in the B16BL6 tumor, whereas no increased uptake in the LLC tumor was found.

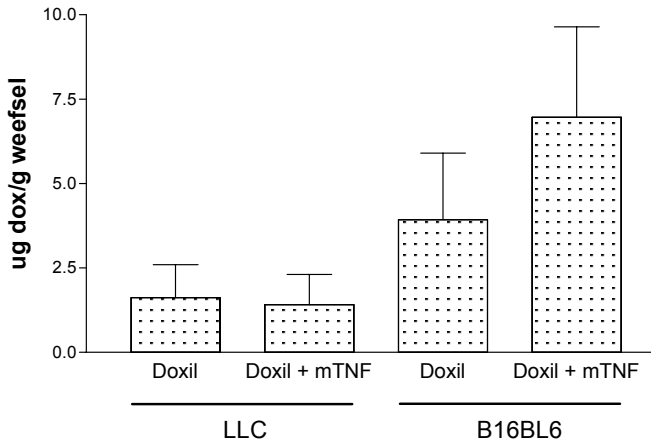


Figure 2. In contradiction to Lewis lung carcinoma addition of TNF to Doxil[®] treatment enhances drug delivery in B16BL6 melanoma. Concentration of doxorubicin in B16BL6 melanoma or LLC carcinoma after systemic treatment with Doxil[®] with or without TNF. Tumors were excised 24 hours after a single dose of 1 mg/kg Doxil[®] ± 1 µg/mouse TNF. Total doxorubicin content was determined as described in materials and methods. The results represent the mean of 3-5 rats ± SD.

Direct effect of Doxil[®] combined with TNF on tumor cells in vitro does not explain the improved activity towards B16BL6 melanoma.

In vitro experiments were performed to define whether direct cytotoxicity contributed to the improved tumor response of Doxil[®] in combination with TNF of the B16BL6 tumor. Exposure of B16BL6 or LLC cells to Doxil[®] resulted in a response curve with an IC₅₀ of 0.07 and 0.08 µg/ml respectively (Figure 3A and B). B16BL6 cells were moderately sensitive to TNF, a cell viability reduction up to 24% at 10 µg/ml was observed (p<0.01). Co-incubation of Doxil[®] and TNF slightly increased the IC₅₀ value up to 0.10 µg/ml, although this increase was not significant. When LLC cells were treated with TNF, a 65% reduced cell viability was detected at 10 µg/ml (p<0.01) and the IC₅₀ value of TNF was estimated at 4.7 ng/ml. Addition of TNF to Doxil[®] did not significantly alter the IC₅₀ of Doxil[®], a value of 0.17 µg/ml was found.

In conclusion, LLC and B16BL6 cell lines were equally sensitive to Doxil[®]. LLC cells were more sensitive to TNF than B16BL6 cells and TNF did not have a synergistic effect in either cell line.

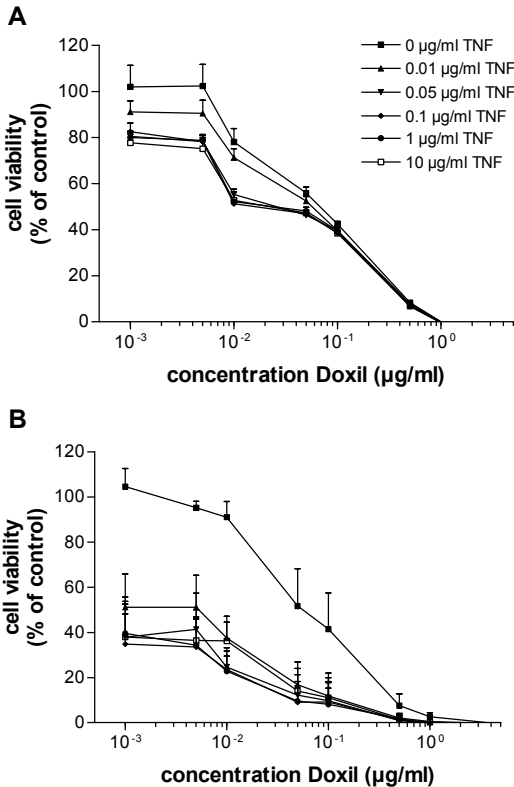


Figure 3. Lewis lung carcinoma cells exhibit increased sensitivity to TNF compared to B16BL6 melanoma cells. *In vitro* cell viability of B16BL6 (a) and LLC (b) cells exposed to Doxil[®] combined with 0, 0.01, 0.05, 0.1, 1 or 10 µg/ml TNF compared to untreated cells. The effects after 72 hours of exposure were determined by MTT assay. The results are expressed as mean ± SEM of at least three independent experiments performed in duplo.

B16BL6 and Lewis lung carcinoma exhibit comparable VEGF production in vitro

We measured the VEGF production of the B16BL6 melanoma and LLC tumor *in vitro* under normoxic and hypoxic conditions for 48 hours (Figure 4). The LLC tumor cells produced slightly more VEGF than the B16BL6 melanoma cells, namely 1.38 ng VEGF/10⁶ cell/24 hours and 1.08 ng VEGF/10⁶ cell/24 hours, respectively ($p=0.05$). Under hypoxic conditions the VEGF production is about 2.5-times higher than under normoxic conditions for both cell lines ($p=0.05$), although less than half of the cells survived.

B16BL6 melanoma tumor vascularization is lower compared to Lewis lung carcinoma.

Approximately 10 days after tumor implantation in the dorsal skin-fold chamber, tumors have grown to a size of 4-5 mm and established their own blood supply. Unlike the normal blood vessels around the tumor, the tumor microvessels are not well organized. There is a clear difference in the organization of the tumor vessels between the B16BL6 and the LLC tumor. The LLC tumor has many supplying vessels and the vessels grow from outside the tumor towards the tumor (Figure 5a and b). The B16BL6 tumor has few supplying vessels and many branches within the tumor. The vessels seem to grow from the inside of the tumor towards the tumor border (Figure 6a).

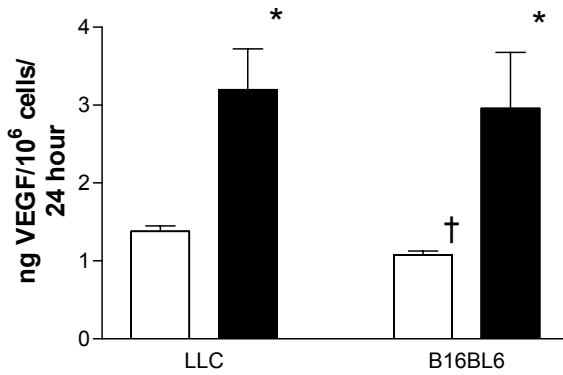


Figure 4. B16BL6 melanoma and Lewis lung carcinoma produce equivalent levels of VEGF. VEGF levels in conditioned medium of B16BL6 melanoma and Lewis Lung Carcinoma after 48 hours of incubation under normoxic (open bars) or hypoxic (1% O₂) (closed bars) conditions. The *in vitro* experiments were performed 3 times and all analyses and calibrations were carried out in duplicate. VEGF levels were normalized to cell number. The mean ± SEM is shown. † p=0.05 compared to LLC, * p=0.05 compared to normoxic conditions.

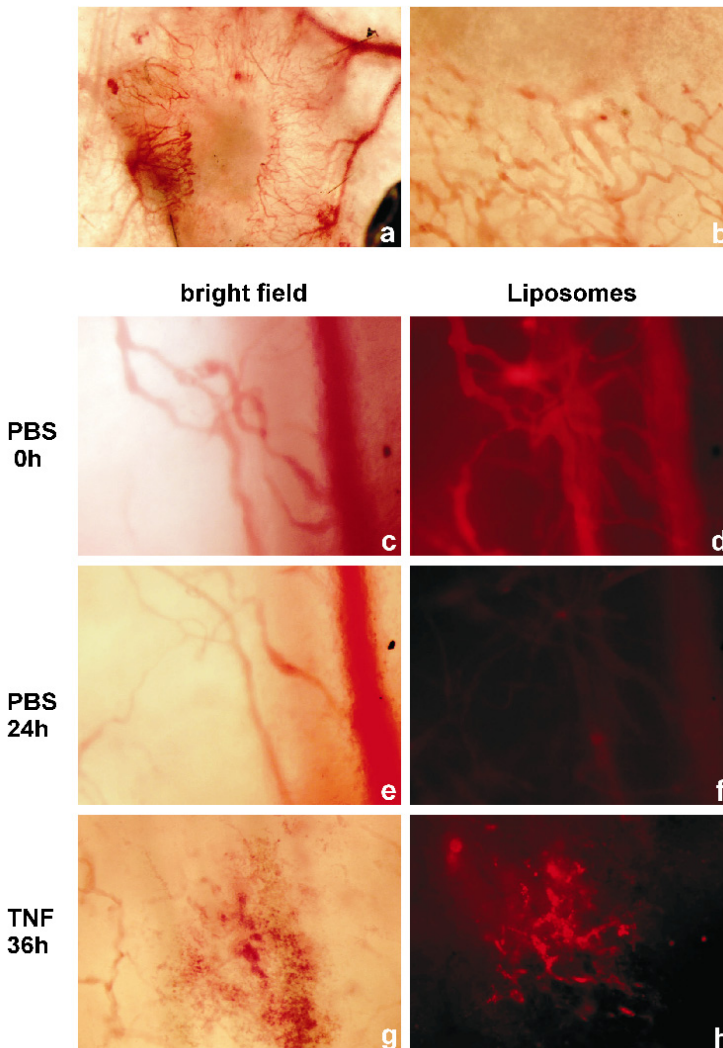


Figure 5. Tumor vascularization and liposomal distribution in Lewis Lung Carcinoma is not affected by TNF. Bright field pictures of tumor vascularization. Many supplying vessels are observed, which grow from outside the tumor towards the tumor (a,b). Directly after i.v. injection of RhoPE liposomes, liposomes were visibly circulating inside the tumor vessels (c,d). 24 hours later hardly any liposomes could be detected in the tumor tissue (e,f). Co-injection of RhoPE liposomes and TNF resulted in a slightly increased liposome accumulation mainly in haemorrhagic areas (g,h). The original light intensities in the images were maintained during the experiments and representative pictures are shown. Original magnification x2.5 (a), x10 (b,g,h) and x20 (c-f).

Quantification of the microvessel density (MVD) was performed by immunohistochemical staining of endothelial cells in frozen tumor sections (Figure 7a-d). The number of vessels as well as the total tumor vessel area was measured. The area per vessel is computed by dividing the total vessel area by the number of vessels. The number of vessels in the LLC tumor was 2.1-fold higher than in the B16BL6, although not significantly due to large standard deviations (Figure 7a). The total tumor vessel area was larger in the LLC tumor than in the B16BL6 tumor, but the area per vessel was 2.4 times higher in the B16BL6 than in the LLC tumor, although this was not significant (Figure 7b). In conclusion, B16BL6 tumor has less, but larger vessels than the LLC tumor.

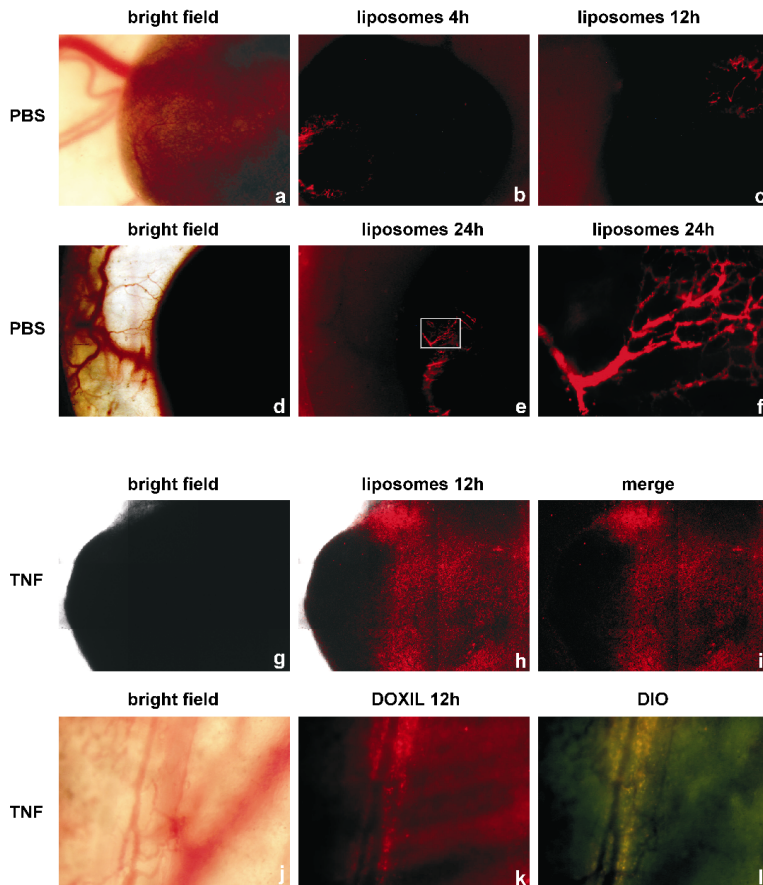


Figure 6. Addition of TNF to Doxil[®] strongly improves liposomal distribution in B16BL6 melanoma. Bright field picture of tumor vascularization. Few supplying vessels can be observed, while the new tumor vessels seem to grow mainly inside the tumor towards the tumor border (a). Heterogeneous distribution of RhoPE liposomes after 4 (b), 12 (c) and 24 hours (e). The liposomes accumulated inside blood vessels (e,f). Co-incubation with low-dose TNF resulted in extensive and homogeneous extravasation of RhoPE liposomes (g-i) and Doxil[®] DiO liposomes (j-l), 12 hours after injection. The original light intensities in the images were maintained during the experiments and representative pictures are shown. Original magnification x2.5 (a-e, g-i), x10 (j-l) and x20 (f).

Liposomal distribution is strongly augmented and more homogeneous in B16BL6 melanoma while accumulation in Lewis lung carcinoma is not affected.

Using the dorsal skin-fold chamber, we performed a series of experiments to examine liposome extravasation and content release from Stealth® liposomes in B16BL6 and LLC tumor tissue. To determine whether TNF could increase the permeability of the tumor microvasculature, we co-injected liposomes and low dose TNF.

RhoPE liposomes of 100 nm were injected i.v. and directly after injection most of the liposomes were circulating inside the blood vessels (Figure 5c and d). After 24 or 48 hours, hardly any liposomes were detected in the LLC tumor tissue (Figure 5e and f). When low-dose of TNF was co-administered liposome accumulation was observed solely in the haemorrhagic areas, but most of the liposomes were still inside the blood vessels even after 36 hours (Figure 5g and h).

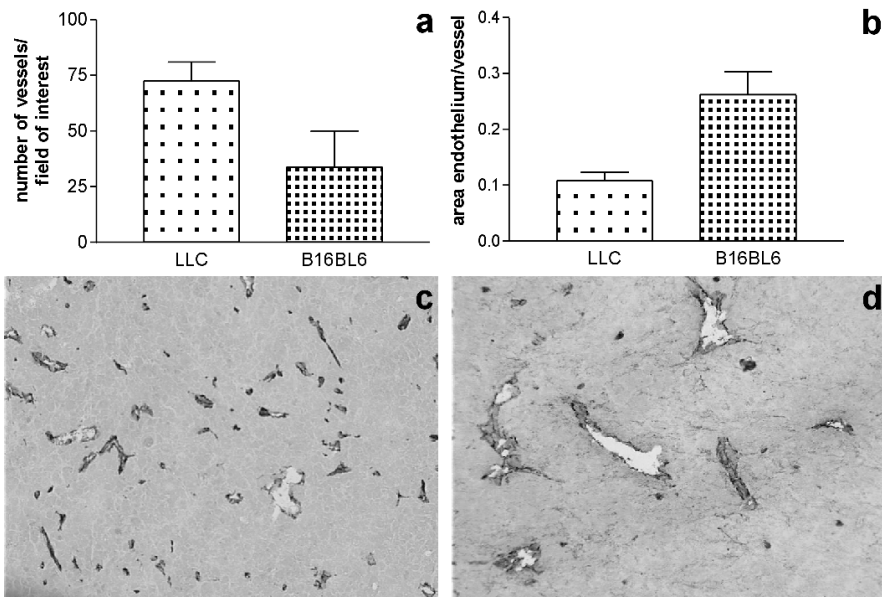


Figure 7. B16BL6 melanoma has less but larger tumor vessels compared to Lewis lung carcinoma. Microvessel density (MVD) of untreated B16BL6 and LLC tumors of 8-10 mm in diameter was assessed by immunohistochemical staining for CD31. (a) Number of vessels per field of interest, (b) area endothelium per vessel. Six representative fields of interest (magnification 16x) per tumor and 4-6 animals per group were examined. The mean \pm SEM is shown. Photographs of cryostat sections of untreated tumors of 8-10 mm in diameter stained for CD31. (c) Lewis Lung Carcinoma, (d) B16BL6 melanoma. Representative pictures are shown. Original magnification x16.

In the B16BL6 tumor, the liposomal distribution was very heterogeneous and the liposomes accumulated mostly inside blood vessels (Figure 6a-f). After 24 or 48 hours RhoPE liposomes were still trapped inside these blood vessels. Already after 12 hours, co-injection

with low-dose TNF resulted in an augmented liposome accumulation, and distribution in the tumor was more homogeneous than treatment with RhoPE liposomes alone (Figure 6g-i). Extravasation occurred more often in the peripheral part of the tumor than in the central part. Besides RhoPE liposomes also experiments with Doxil[®] were performed. Doxil[®] was labeled with DiO to distinguish between localization of the liposome itself and the doxorubicin inside. Already after 12 hours it was clear that dual treatment of TNF and Doxil[®] resulted in an augmented extravasation of liposomes into the tumor tissue and doxorubicin released from the liposomes could be observed (Figure 6j-l).

In conclusion, Stealth[®] liposomes accumulation is elevated in B16BL6 tumor compared to LLC tumor. Moreover, co-injection of low-dose TNF resulted in augmented extravasation of liposomes in the B16BL6 tumor, whereas in the LLC tumor if liposomes were present they were mainly trapped inside blood vessels.

Discussion

In the present study we show that addition of TNF to systemic Doxil[®] treatment resulted in an enhanced anti-tumor response in the B16BL6 tumor, but not in the LLC tumor. Additionally, an increased accumulation of Doxil[®] in tumor tissue was found in B16BL6 tumors systemically treated with Doxil[®] plus TNF compared to Doxil[®] alone, and no effect of TNF in the LLC tumor was found in relation to drug accumulation. These results were confirmed by intravital microscopy. First, in the B16BL6 tumor already a higher degree of liposome leakage was found compared to the LLC tumor. Second, unlike in the LLC tumor, TNF induced an augmented and more homogeneous extravasation of Stealth[®] liposomes into the B16BL6 tumor tissue.

Transport of small drugs across the blood vessel wall involves diffusion whereas transport of macromolecules involves convection. Diffusion is the random motion of small molecules and in highly vascularized tumors more tumor cells will be reached by the chemotherapeutics. Convection is mediated by the movement of fluid and may play a role in macromolecule drug delivery to especially peripheral tumor tissues, where a significant drop of the interstitial fluid pressure occurs. This pressure gradient facilitates extravasation of macromolecules in the periphery and causes extravasation of macromolecules into the tumor (2-4,7). In general, tumor vessels are more permeable than normal vessels and the maximum size of particles that can cross the tumor vessel wall is called the pore cutoff size. There is a large variance in cutoff sizes in different tumor types. Vessels of some but not all primary brain tumors are nearly impermeable and in other tumors cutoff pore sizes between 100 nm and 1.2 μm are found. Vascular permeability may depend on tumor type and microenvironment and increases with tumor size (8,27).

Liposomes have found useful applications in cancer therapy (11-14). Many studies demonstrated that long-circulating liposomes can preferentially accumulate in tumor tissue,

due to their prolonged circulation time and by taking advantage of the enhanced permeability and retention effect (EPR) (9,10,17). Because the diameters of tumor vessels readily exceed the size of liposomes, not the size of tumor microvessels is the limiting factor of drug delivery to solid tumors, but the permeability of the tumors. We showed in previous studies that the addition of low-dose TNF to Doxil[®] treatment resulted in improved anti-tumor response in soft-tissue sarcoma-bearing rats (BN175) and B16BL6 melanoma-bearing mice (18,19). Most likely the augmented accumulation of the liposomes explains the enhanced tumor response. A possible explanation for the increased drug uptake is that TNF increases the leakiness of the vasculature by enlarging the pore cutoff size in the endothelial lining of the tumor (20,21). The present study was undertaken to investigate whether or not addition of low-dose TNF to Doxil[®] treatment would have a similar effect in the Lewis lung carcinoma as in the B16BL6 melanoma model. We showed that the addition of TNF to the Doxil[®] treatment resulted in an improved anti-tumor response in the B16BL6 tumor but not in the LLC tumor. Furthermore no increased tumor drug accumulation was found in the LLC tumor, whereas in the B16BL6 a 1.8-fold increased accumulation was found. A striking difference observed between the two tumor models, was the tumor vascular architecture. The LLC tumor has more supplying vessels than the B16BL6 tumor, and the vessels grow from outside the tumor towards the tumor, whereas in the B16BL6 tumors the vessels seems to grow from the inside towards the tumor border. Although the B16BL6 had fewer blood vessels than the LLC tumor, the liposomal tumor accumulation was higher.

Vascular endothelial growth factor (VEGF) was originally discovered because of its ability to increase the permeability of microvessels, primarily postcapillary venules and small veins, to circulating macromolecules (28). Expression of VEGF is known to be an unfavorable prognostic factor in different types of tumors. Tumors with high VEGF levels have a higher vascular density, but have also more permeable blood vessels (29-31). Satchi-Fainaro *et al.* showed that the angiogenesis inhibitor TNP-470 decreased VEGF-induced vascular permeability (32), whereas Bockhorn *et al.* presented a study where vascular permeability was not significantly altered by an anti-VEGF antibody treatment (33). In our study we showed that the B16BL6 melanoma is more permeable than the LLC tumor, while LLC produced slightly more VEGF *in vitro* than B16BL6. Possibly, VEGF is not responsible for the differences in cutoff pore size in these two tumor types.

In vitro studies were performed to evaluate whether direct cytotoxicity also contributed to the improved tumor response of Doxil[®] plus TNF in the B16BL6 melanoma. The *in vitro* experiments showed that B16BL6 tumor cells were moderately sensitive to TNF, while LLC cells were quite sensitive to TNF with an IC₅₀ of 4.7 ng/ml. Although LLC cells were sensitive to TNF, systemic treatment with TNF alone did not show a tumor growth delay. Both cell lines were equally sensitive to Doxil[®] and the addition of TNF did not show an

alteration in the IC₅₀ value. This is in accordance with previous *in vitro* studies, where addition of TNF to Doxil[®] or small molecular weight drugs like doxorubicin and melphalan induced no or only an additive cytotoxic effect (19,34).

Intravital microscopy studies revealed that hardly any liposomes accumulated in LLC tumor tissue and no enhanced extravasation of these liposomes was found when co-administered with low-dose TNF. This in contrast with the B16BL6 tumor, where a clear enhanced extravasation of liposomes was found into the tumor tissue, although mainly in the periphery of the tumor. Our results, together with the data of Parr *et al.* (35) and Weissig *et al.* (36), may be considered as an indication that subcutaneous Lewis Lung carcinoma is a tumor with a small vascular pore cutoff size, which is not affected by TNF. Possibly, the lack of permeability of the tumor vessels is linked to the lack of response to TNF, which is currently under investigation. Probably treatment of less permeable tumors like LLC may be more efficient with very small long-circulating delivery systems, such as PEG-based micelles (normally between 5 and 50 nm), than with the larger long-circulating liposomes. It is possible that TNF in combination with small PEG-based micelles will result in enhanced micelle uptake in the LLC tumor.

In conclusion, addition of TNF to systemic Doxil[®] treatment resulted in an enhanced anti-tumor response and increased drug uptake in the B16BL6 tumor, but not in the LLC tumor. Likely, the subcutaneous Lewis Lung carcinoma is a tumor with a small vascular pore cutoff size. Next to that the LLC tumor vascular bed seems rather insensitive to TNF as increased leakiness was not observed. Apparently, not the microvessel density is the limiting factor of liposomal drug delivery to solid tumors, but the permeability of the tumor vessels and the responsiveness to TNF.

Acknowledgments

The authors thank Boehringer Ingelheim GmbH for the generous supply of TNF. This study was supported by grant DDHK 2000-2224 of the Dutch Cancer Society.

References

1. Jain RK. Barriers to drug delivery in solid tumors. *Sci Am.* 1994;271(1):58-65.
2. Boucher Y, Baxter LT, Jain RK. Interstitial pressure gradients in tissue-isolated and subcutaneous tumors: implications for therapy. *Cancer Res.* 1990;50(15):4478-4484.
3. Jain RK. Transport of molecules, particles, and cells in solid tumors. *Annu Rev Biomed Eng.* 1999;1:241-263.
4. Yuan F. Transvascular drug delivery in solid tumors. *Semin Radiat Oncol.* 1998;8(3):164-175.
5. Jang SH, Wientjes MG, Lu D, Au JL. Drug delivery and transport to solid tumors. *Pharm Res.* 2003;20(9):1337-1350.
6. Jain RK. Delivery of molecular and cellular medicine to solid tumors. *Adv Drug Deliv Rev.* 2001;46(1-3):149-168.
7. Dvorak HF, Nagy JA, Dvorak JT, Dvorak AM. Identification and characterization of the blood vessels of solid tumors that are leaky to circulating macromolecules. *Am J Pathol.* 1988;133(1):95-109.
8. Hobbs SK, Monsky WL, Yuan F, et al. Regulation of transport pathways in tumor vessels: role of tumor type and microenvironment. *Proc Natl Acad Sci U S A.* 1998;95(8):4607-12.

9. Wu NZ, Da D, Rudoll TL, Needham D, Whorton AR, Dewhirst MW. Increased microvascular permeability contributes to preferential accumulation of Stealth liposomes in tumor tissue. *Cancer Res.* 1993;53(16):3765-70.
10. Gabizon A, Papahadjopoulos D. Liposome formulations with prolonged circulation time in blood and enhanced uptake by tumors. *Proc Natl Acad Sci U S A.* 1988;85(18):6949-6953.
11. Allen TM, Newman MS, Woodle MC, Mayhew E, Uster PS. Pharmacokinetics and anti-tumor activity of vincristine encapsulated in sterically stabilized liposomes. *Int J Cancer.* 1995;62(2):199-204.
12. Lasic DD. Doxorubicin in sterically stabilized liposomes. *Nature.* 1996;380(6574):561-562.
13. Papahadjopoulos D, Allen TM, Gabizon A, et al. Sterically stabilized liposomes: improvements in pharmacokinetics and antitumor therapeutic efficacy. *Proc Natl Acad Sci U S A.* 1991;88(24):11460-11464.
14. Sparano JA, Winer EP. Liposomal anthracyclines for breast cancer. *Semin Oncol.* 2001;28(4 Suppl 12):32-40.
15. Gabizon A, Martin F. Polyethylene glycol-coated (pegylated) liposomal doxorubicin. Rationale for use in solid tumours. *Drugs.* 1997;54 Suppl 4:15-21.
16. Newman MS, Colbern GT, Working PK, Engbers C, Amantea MA. Comparative pharmacokinetics, tissue distribution, and therapeutic effectiveness of cisplatin encapsulated in long-circulating, pegylated liposomes (SPI-077) in tumor-bearing mice. *Cancer Chemother Pharmacol.* 1999;43(1):1-7.
17. Mayer LD, Cullis PR, and Bally MB Designing therapeutically optimized liposomal anticancer delivery systems: lessons from conventional liposomes. *In* Lasic DD and Papahadjopoulos D (eds.), *Medical Applications of Liposomes*, pp. 231-257. 2002.
18. Brouckaert P, Takahashi N, van Tiel ST, et al. Tumor necrosis factor-alpha augmented tumor response in B16BL6 melanoma-bearing mice treated with stealth liposomal doxorubicin (Doxil) correlates with altered Doxil pharmacokinetics. *Int J Cancer.* 2004;109(3):442-448.
19. ten Hagen TL, van Der Veen AH, Nooijen PT, van Tiel ST, Seynhaeve AL, Eggermont AM. Low-dose tumor necrosis factor-alpha augments antitumor activity of stealth liposomal doxorubicin (DOXIL) in soft tissue sarcoma-bearing rats. *Int J Cancer.* 2000;87(6):829-37.
20. Brett J, Gerlach H, Nawroth P, Steinberg S, Godman G, Stern D. Tumor necrosis factor/cachectin increases permeability of endothelial cell monolayers by a mechanism involving regulatory G proteins. *J Exp Med.* 1989;169(6):1977-1991.
21. Partridge CA, Horvath CJ, Del Vecchio PJ, Phillips PG, Malik AB. Influence of extracellular matrix in tumor necrosis factor-induced increase in endothelial permeability. *Am J Physiol.* 1992;263(6 Pt 1):L627-L633.
22. Bartlett GR. Phosphorus assay in column chromatography. *J Biol Chem.* 1959;234(3):466-468.
23. Mayer LD, Tai LC, Ko DS, et al. Influence of vesicle size, lipid composition, and drug-to-lipid ratio on the biological activity of liposomal doxorubicin in mice. *Cancer Res.* 1989;49(21):5922-5930.
24. Papenfuss HD, Gross JF, Intaglietta M, Treese FA. A transparent access chamber for the rat dorsal skin fold. *Microvasc Res.* 1979;18(3):311-318.
25. Leunig M, Yuan F, Menger MD, et al. Angiogenesis, microvascular architecture, microhemodynamics, and interstitial fluid pressure during early growth of human adenocarcinoma LS174T in SCID mice. *Cancer Res.* 1992;52(23):6553-6560.
26. Huang Q, Shan S, Braun RD, et al. Noninvasive visualization of tumors in rodent dorsal skin window chambers. *Nat Biotechnol.* 1999;17(10):1033-1035.
27. Yuan F, Dellian M, Fukumura D, et al. Vascular permeability in a human tumor xenograft: molecular size dependence and cutoff size. *Cancer Res.* 1995;55(17):3752-3756.
28. Dvorak HF, Brown LF, Detmar M, Dvorak AM. Vascular permeability factor/vascular endothelial growth factor, microvascular hyperpermeability, and angiogenesis. *Am J Pathol.* 1995;146(5):1029-1039.
29. Hoang BH, Dyke JP, Koutcher JA, et al. VEGF expression in osteosarcoma correlates with vascular permeability by dynamic MRI. *Clin Orthop Relat Res.* 2004;(426):32-38.
30. Gasparini G. Prognostic value of vascular endothelial growth factor in breast cancer. *Oncologist.* 2000;5 Suppl 1:37-44.:37-44.
31. Salven P, Ruotsalainen T, Mattson K, Joensuu H. High pre-treatment serum level of vascular endothelial growth factor (VEGF) is associated with poor outcome in small-cell lung cancer. *Int J Cancer.* 1998;79(2):144-146.
32. Satchi-Fainaro R, Mamluk R, Wang L, et al. Inhibition of vessel permeability by TNP-470 and its polymer conjugate, caplostatin. *Cancer Cell.* 2005;7(3):251-261.
33. Bockhorn M, Tsuzuki Y, Xu L, Frilling A, Broelsch CE, Fukumura D. Differential vascular and transcriptional responses to anti-vascular endothelial growth factor antibody in orthotopic human pancreatic cancer xenografts. *Clin Cancer Res.* 2003;9(11):4221-4226.
34. van Der Veen AH, ten Hagen TL, Seynhaeve AL, Eggermont AM. Lack of cell-cycle specific effects of tumor necrosis factor-alpha on tumor cells in vitro: implications for combination tumor therapy with doxorubicin. *Cancer Invest.* 2002;20(4):499-508.

35. Parr MJ, Masin D, Cullis PR, Bally MB. Accumulation of liposomal lipid and encapsulated doxorubicin in murine Lewis lung carcinoma: the lack of beneficial effects by coating liposomes with poly(ethylene glycol). *J Pharmacol Exp Ther.* 1997;280(3):1319-1327.
36. Weissig V, Whiteman KR, Torchilin VP. Accumulation of protein-loaded long-circulating micelles and liposomes in subcutaneous Lewis lung carcinoma in mice. *Pharm Res.* 1998;15(10):1552-1556.

Part IV

General discussion and summary

Chapter 11 -

General discussion: Current status and future perspectives of isolated limb perfusion: role for vasoactive drugs

Abstract

Isolated limb perfusion is a technique that involves cannulation of the major artery and vein, connection to an oxygenated extracorporeal circuit, ligation of collateral vessels and application of a tourniquet. Once isolation is secured, drugs can be injected into the perfusion circuit. Regional drug concentrations 15-25 times higher than those reached after systemic administration can be achieved by ILP without systemic side effects. Addition of high-dose TNF to melphalan-based ILP results in impressive enhancement of the response rates and this treatment is currently one of the therapies available for patients with advanced bulky melanoma and sarcoma of the limbs. The anti-tumor effects are indirectly mediated through an increased drug uptake in the tumor and damage of the tumor-associated vasculature. Unfortunately, not all patients respond to this therapy and other agents that can further improve the response rates must be identified. The purpose of this article is to review existing treatment modalities and recent advances for development of novel therapeutic strategies using vasoactive drugs.

Introduction

Various treatment options can be used in the management of locally advanced extremity soft tissue sarcomas (STS) or multiple in-transit melanoma metastases, like surgery, radiotherapy, chemotherapy or eventually amputation. Treatment modalities that guarantee preservation of the extremity as well as good limb function have become important, because amputation does not necessarily improve the survival rate (1,2). To eradicate tumors with chemotherapy, lethal concentration of anticancer drugs must reach the tumor cells. Unfortunately, inadequate drug delivery leads to regrowth of tumors and possible development of resistant cells. Furthermore, the dose of administered drugs is limited by normal tissue tolerance (3-7). Methods for improving drug delivery are therefore of great clinical interest. To achieve higher intratumoral drug concentration with limited systemic toxicity, an isolated limb perfusion (ILP) can be performed. Secondly, agents can be co-administered which favorably manipulate the tumor pathophysiology resulting in improved tumor response. These options will be discussed here.

Isolated limb perfusion

Isolated limb perfusion with chemotherapeutic agents was first introduced by Creech *et al.* in 1958 (8). In an ILP the circulation of a limb can be isolated from the rest of the body, while tissues of the isolated limb are kept viable with a perfusate, which is oxygenated by a bubble oxygenator. The advantage of ILP is the 15 to 25 times higher concentrations of chemotherapeutic agents which can be reached locally, while limiting the systemic side effects (9). The technique was modified in 1969 by Stehlin to include hyperthermia, which was expected to increase the antitumor effect of most antineoplastic agents (10). Since then,

hyperthermic ILP with the alkylating cytotoxic agent melphalan (L-phenyl-alaninemustard) has been used for the treatment of patients with advanced extremity melanoma. A mean complete remission rate of about 54% can be obtained (reviewed in (11)). Several chemotherapeutic agents have been used alternative to, or combined with melphalan. These include imidazole carboxamide, nitrogen mustard, thiotepa, fotemustine in combination with systemic chemosensitization (DTIC), none of which appeared to provide a better tumor response compared to melphalan alone (12-14). The response rates of ILP with cisplatin were comparable to those of melphalan, but with severe locoregional toxicity (15,16).

Melphalan has also been used in the treatment of (nonresectable) extremity soft tissue sarcoma (STS). Because sarcomas are big in contrast to the relatively small melanomas, results have been quite poor. Besides melphalan, other cytotoxic drugs such as doxorubicin, dactinomycin and cisplatin have been used and low clinical response rates have been reported (17-21).

TNF-based isolated limb perfusion

Combination therapy with melphalan

Tumor necrosis factor- α (TNF), named for its ability to cause haemorrhagic necrosis in subcutaneous sarcoma in mice (22), has shown anti-tumor activity in some murine and human tumors *in vivo* (23-25) and *in vitro* (26). The results from animal studies raised high expectations concerning the clinical trials. However, systemic TNF therapy proved ineffective with a lack of tumor response and severe side effects (hypotension and organ failure). The maximum tolerated dose was 10-50 times lower than the estimated effective dose (27-31). Importantly, such concentrations can be achieved by ILP. The application of TNF (plus interferon- γ (IFN)) and melphalan in ILP was pioneered by Lejeune and Lienard in 1988 in patients with melanoma in-transit metastases and advanced STS showing impressive results (32). TNF-based ILP has been reported in a European multicenter trial with response rates greater than 80% and limb salvage rates above 70% in advanced soft tissue sarcoma (33,34) and advanced extremity melanoma (35,36). Addition of IFN had only a marginal effect on the outcome (32,35,36). These studies led to the approval of TNF by the European Medicine Evaluation Agency (EMA) in 1998 (37).

Mechanism of TNF-based therapies

To improve the current response rate and for the further development of combination therapy, it is imperative to understand the mechanism by which TNF enhances the tumor response so dramatically. TNF has some anti-tumor activity in certain tumors, but the majority of the tumor cells appear insensitive to TNF. It was speculated that the anti-tumor effects are indirectly mediated through damage of the tumor associated vasculature (22-25).

The selective destructive effects of high dose TNF in ILP have been illustrated in pre- and post perfusion angiographies. Angiographic studies revealed that 1 or 2 weeks after ILP all tumor-associated vessels had disappeared, and that normal blood vessels were still intact (38,39). It is important to note that in contrast to high doses of TNF (1-5 μg), low doses of TNF (0.01-1 ng) induce angiogenesis (40).

To gain better insight in the working mechanism of TNF we developed TNF-based isolated limb perfusion models in rats, with similar results compared to the clinical setting. Directly after perfusion with TNF and melphalan or doxorubicin softening of the tumor tissue and significantly enhanced drug accumulation in tumor tissue specifically were observed (41-43). Kristensen *et al.* showed that TNF caused a reduction in the interstitial fluid pressure (IFP) in human melanoma xenografts, what could lead to enhanced uptake of large molecules (44). In our experiments we did not see an effect of TNF on the IFP and we concluded that the enhanced drug uptake in the ILP setting was not due to a lowering of IFP. Furthermore, application of TNF did not seem to affect local pH, indicative that degree of hypoxia is not altered within the ILP time-frame. Although scattered extravasation of erythrocytes was observed shortly after TNF ILP, accompanied by few apoptotic endothelial cells, ILP with TNF alone is not capable of inducing any tumor response (45). Ruegg *et al.* showed that inhibition of the $\alpha_v\beta_3$ -mediated endothelial cell adhesion results in apoptosis and finally disruption of the tumor vasculature induced by TNF and IFN, but in this study tumor biopsies were examined 24 hours after ILP (46). More important, we observed an increased permeability of an endothelial layer within 30 minutes after exposure to TNF, which was enhanced by IFN and the presence of polymorphonuclear leukocyte (PMN) (45). The results indicate a subtle early effect of TNF on the tumor vasculature favoring augmented accumulation of the co-administered drug.

At the histopathological level shortly after ILP the effects of TNF in a melphalan-based ILP starts with intratumoral endothelial cell activation followed by over-expression of adhesion molecules. Early PMN infiltrates were seen 2 to 3 hours after TNF-based ILP and lasted for at least 7 days (47). Homing of PMNs led to endothelium injury and finally coagulative and haemorrhagic necrosis. The tumors became infiltrated with T-lymphocytes, macrophages and B-lymphocytes after 1 to 3 weeks, indicating the induction of a secondary cellular and humoral immune response (48,49).

Other combination therapies with TNF

In Italy, TNF-based ILPs in combination with doxorubicin have been performed in patients with STS. Similar results were seen, although with significantly more regional toxicity in the healthy tissue (50). We also showed in our rat sarcoma ILP models that local toxicity was dose-limiting at sub-optimal doxorubicin concentrations (43). To decrease toxicity, the formulation of doxorubicin in long-circulating liposomes (Stealth[®] liposomal doxorubicin,

Doxil[®]) can be used. Another advantage is that Doxil[®] liposomes have a prolonged circulation time and that tumor accumulation is augmented (51-53). However, when Doxil[®] was used in the rat ILP model, minimal antitumor activity was found and its activity was not enhanced by TNF. No augmented accumulation of Doxil[®] was found compared to doxorubicin and the short circulation time during ILP is like inadequate for the circulation time advantage of Doxil[®] to have an effect on the distribution (54). This is in contrast with a study of Di Filippo *et al.*, where a favorable response with Doxil[®] was demonstrated (55). While, transport of small drugs, like doxorubicin, across the blood vessel wall involves diffusion, transport of macromolecules, like liposomes, involves convection. In tumor tissue the IFP is elevated and inhibits extravasation of macromolecules (56,57). However, we showed that the elevated IFP in tumors is even more enhanced due to the ILP procedure and therefore probably resulting in less accumulation of Doxil[®] in tumor tissue (45).

It is well known that TNF enhances the activity of actinomycin D (58,59) and therefore the combination of TNF and actinomycin D is evaluated in our rat soft-tissue sarcoma model. We showed that this combination therapy led to a synergistic anti-tumor response, but is accompanied with dramatic local toxicity and should therefore not be explored in a clinical setting (60).

Some studies showed that administration of TNF resulted in a reduced blood flow, whereas others saw no effect of TNF on tumor blood flow (61-63). Initial reduction of tumor blood flow limits the delivery of any further external agent. However, if antivasular events are generated within the tumor tissue, the rate of drug removal is impaired while leaving more drug entrapped in the tumor.

High levels of NO results in vasodilatation, a higher blood flow and could therefore have an beneficial effect on drug delivery (64). On the other side reduction of the local NO level impairs blood flow as well as subsequent washout. Moreover, tumor cells may suffer from the lack of oxygen and nutrient delivery. De Wilt *et al.* demonstrated a much better tumor response when the NO inhibitor L-NAME was added to the synergistic combination of melphalan and TNF (response rate increased up to 100%) (65). To obtain further insight into the mechanism underlying the effect of TNF on tumor blood flow, more research has to be performed.

Disadvantages of TNF-based ILP

Currently, TNF-based ILP is the standard treatment for patients with multiple in transit melanoma metastases and non-resectable extremity sarcomas. TNF is approved and registered in Europe and clinical trials are ongoing in the United States. An important disadvantage is the costs involved in TNF-based ILP.

Despite the good tumor responses found in patients treated by ILP with TNF plus melphalan, still about 20% of the patients do not respond to this treatment therapy. Other

agents that can further improve the response rates must be identified. Furthermore, TNF-based ILP is a considerable surgical procedure with a risk of regional and systemic complications. Accurate and real-time monitoring of systemic leakage is needed with the aim of avoiding severe systemic TNF mediated toxicity. Regional toxicity can cause long-term impaired extremity function, and the risk of a shock-like syndrome is considerable if >10% leakage of TNF to the systemic circulation during ILP occurs (36,66).

Vasoactive drugs in combination with isolated limb perfusion

As we observed that TNF mainly improves drug accumulation in tumor tissue which results from an enhanced permeability of the tumor-associated vasculature, other agents were sought and tested which are known for their vasoactive behavior.

Interleukin-2

In different animal models interleukin-2 (IL-2), as a single agent, has been shown to have antitumor activity (67,68). Clinical studies have been carried out mainly in patients with renal cell cancer and melanomas. High doses and multiple dosing are needed, which is associated with serious systemic toxicity with hypotension, massive vascular leakage syndrome and multiple organ failure leading to death (69-72). Response rates and survival benefits of current systemic treatments are disappointing. We hypothesized that IL-2 could be a good candidate to be used in an isolated limb perfusion. IL-2 is known not to have direct antitumor activity, but we speculated that IL-2 could well impact on the tumor pathophysiology in a similar way as TNF.

We demonstrated for the first time that ILP with the combination of IL-2 and melphalan in the BN175 tumor resulted in a strong synergistic tumor response. The tumor response (PR and CR combined) of 67% was much higher than the tumor response of melphalan alone (17%), while progressive disease was seen in all animals treated with IL-2 alone. We showed that IL-2 caused a 3.7-fold augmented accumulation of melphalan specifically in tumor tissue, which correlated closely with the enhanced tumor responses. This increase could very well explain the improved efficacy, as ILP with IL-2 alone did not induce any tumor response. Furthermore, a redistribution of macrophages was seen and increased levels of TNF mRNA were found in tumors treated with IL-2 plus melphalan (73). These observations indicate a potentially important role for macrophages in the IL-2-based perfusion, as activated macrophages produce several cytokines (like TNF) and free radicals which can have a cytotoxic effect on tumor cells (74-77).

More research has to be done to investigate whether IL-2-based ILP gives comparable results in other tumor types, like osteosarcoma and melanoma and the novel combination of IL-2 and melphalan should be explored in a clinical ILP setting. IL-2 is already used in a systemic clinical setting and is a potentially safer drug than TNF and therefore a useful

alternative for ILP with TNF. Importantly, the lack of toxicity of IL-2 warrants its use in loco-regional therapy of organs such as the liver in which the application of TNF is strongly impaired.

Histamine

Another vasoactive drug we tested is histamine. The interest in histamine as a potential anti-neoplastic agent originated in the late 1970s from mouse studies in which passive induction of local anaphylaxis reduced the size of established, chemically induced fibrosarcomas (78). Antitumor effects have also been seen in Leydig cell sarcoma (79), chemically induced gut tumor (80), colorectal carcinoma (81) and melanoma (82). The mechanisms for the anti-tumoral effects of histamine are largely unknown, but it is suggested that both histamine receptor 1 and 2 (H₁-R and H₂-R) are involved (81-83).

Histamine is causing edema in fine vessels by increasing the flow of lymph and lymph proteins into the extracellular space and also by promoting the formation of gaps between endothelial cells (84). Therefore, it is suggested that the same mechanism that causes edema in fine vessels could potentially be used to increase drug concentration in tumor tissues.

We showed the synergistic effect of histamine plus melphalan in ILP for the treatment of rat soft-tissue sarcoma. Tumor regression was seen in 66% of the animals treated with histamine and melphalan compared to 17% after treatment with histamine or melphalan alone. No systemic toxicity was observed in rats treated with histamine and melphalan. Histamine showed to have a direct cytotoxic effect on both tumor cells and tumor-associated vasculature. Very importantly, addition of histamine led to a two-fold increased melphalan uptake in tumor tissue, whereas a reduced melphalan concentration in muscle tissue was found. After ILP with histamine and melphalan, most of the tumor vessels were severely damaged and massive haemorrhage was observed (85).

In conclusion, histamine plus melphalan in ILP seems to be a promising alternative to TNF and should be further evaluated in preclinical tumor models and eventually in a clinical setting for both limb as well as organs.

IL-2 + histamine

One of the proposed limitations of IL-2-based therapy involves inactivation of peritumoral and intratumoral cytotoxic T and NK cells. Reactive oxygen species (ROS) generated by monocytes/macrophages (MO) may inhibit cytotoxic activity within the tumor. Cytokine-based immunotherapy could be more effective if the generation of ROS were inhibited. Histamine is a potent inhibitor of ROS formation through interaction with the H₂-R receptor on phagocytic cells. Experimental data indicate that histamine and IL-2 act synergistically to activate NK cell cytotoxicity (86,87). Inhibition of tumor growth and angiogenesis in malignant glioma is found after systemic treatment with IL-2 and histamine (88). Use of

histamine as an adjuvant to IL-2 is associated with a statistically significant prolongation of survival compared to IL-2 alone in metastatic melanoma patients with liver involvement (89).

We have shown that the synergy between histamine and IL-2 seen in the systemic treatment is lost in the regional setting, with a 30% decrease in the tumor response rate, as compared to each drug alone plus melphalan. Tumor accumulation of melphalan after ILP with the triple combination of histamine, IL-2 and melphalan is very similar to the levels obtained after ILP with histamine or IL-2 plus melphalan. However, less haemorrhagic necrosis was found after the triple therapy compared to ILP with histamine plus melphalan (90).

In conclusion, the combination of histamine and IL-2 in the melphalan-based ILP setting diminished the tumor response compared to melphalan ILP with either drug alone and should not be further explored in a clinical setting.

Conclusions

Isolated limb perfusion is an important treatment option in the management of locally advanced extremity soft tissue sarcoma and in-transit melanoma metastases. The addition of TNF to the melphalan-based ILP greatly improved the response rates. The majority of the anti-tumor effects are indirectly mediated through damage of the tumor-associated vasculature leading to haemorrhagic necrosis. Importantly, addition of TNF to the perfusate results in an increased drug uptake in the tumor. Despite the good tumor responses, still about 20% of the patients do not respond to this treatment therapy. We recently showed the importance of vasoactive drugs in combination with melphalan in an isolated limb perfusion setting. ILP with histamine or IL-2 in combination with melphalan showed similar response rates compared to TNF plus melphalan. In both treatment modalities an effect on the tumor-associated vasculature is found leading to increased drug uptake in the tumor. These findings emphasize the importance of altering the tumor pathophysiology that leads to improved tumor drug uptake and the potential that this approach has to improve efficacy of various standard agents.

References

1. Lejeune FJ, Pujol N, Lienard D, et al. Limb salvage by neoadjuvant isolated perfusion with TNF α and melphalan for non-resectable soft tissue sarcoma of the extremities. *Eur J Surg Oncol*. 2000;26(7):669-678.
2. Mann GB, Lewis JJ, Brennan MF. Adult soft tissue sarcoma. *Aust N Z J Surg*. 1999;69(5):336-343.
3. Dvorak HF, Nagy JA, Dvorak JT, Dvorak AM. Identification and characterization of the blood vessels of solid tumors that are leaky to circulating macromolecules. *Am J Pathol*. 1988;133(1):95-109.
4. Jain RK. Barriers to drug delivery in solid tumors. *Sci Am*. 1994;271(1):58-65.
5. Jain RK. Delivery of molecular medicine to solid tumors: lessons from in vivo imaging of gene expression and function. *J Control Release*. 2001;74(1-3):7-25.
6. Jang SH, Wientjes MG, Lu D, Au JL. Drug delivery and transport to solid tumors. *Pharm Res*. 2003;20(9):1337-1350.
7. Yuan F. Transvascular drug delivery in solid tumors. *Semin Radiat Oncol*. 1998;8(3):164-175.

8. Creech O, Kremenz ET, Ryan RF, Winblad JN. Chemotherapy of cancer: regional perfusion utilizing an extracorporeal circuit. *Ann Surg.* 1958;148(4):616-632.
9. Benckhuijsen C, Kroon BB, van Geel AN, Wieberdink J. Regional perfusion treatment with melphalan for melanoma in a limb: an evaluation of drug kinetics. *Eur J Surg Oncol.* 1988;14(2):157-163.
10. Stehlin JS. Hyperthermic perfusion with chemotherapy for cancers of the extremities. *Surg Gynecol Obstet.* 1969;129(2):305-308.
11. Vrouenraets BC, Nieweg OE, Kroon BB. Thirty-five years of isolated limb perfusion for melanoma: indications and results. *Br J Surg.* 1996;83(10):1319-1328.
12. Ariyan S, Poo WJ, Bologna J. Regional isolated perfusion of extremities for melanoma: a 20-year experience with drugs other than L-phenylalanine mustard. *Plast Reconstr Surg.* 1997;99(4):1023-1029.
13. Pontes L, Lopes M, Ribeiro M, Santos JG, Azevedo MC. Isolated limb perfusion with fotemustine after chemosensitization with dacarbazine in melanoma. *Melanoma Res.* 1997;7(5):417-419.
14. Shiu MH, Knapper WH, Fortner JG, et al. Regional isolated limb perfusion of melanoma intransit metastases using mechlorethamine (nitrogen mustard). *J Clin Oncol.* 1986;4(12):1819-1826.
15. Hoekstra HJ, Schraffordt KH, de Vries LG, van Weerden TW, Oldhoff J. Toxicity of hyperthermic isolated limb perfusion with cisplatin for recurrent melanoma of the lower extremity after previous perfusion treatment. *Cancer.* 1993;72(4):1224-1229.
16. Thompson JF, Gianoutsos MP. Isolated limb perfusion for melanoma: effectiveness and toxicity of cisplatin compared with that of melphalan and other drugs. *World J Surg.* 1992;16(2):227-233.
17. Abe S, Tokizaki T, Miki Y, et al. Hyperthermic isolated regional perfusion with CDDP for bone and soft-tissue sarcoma of the lower limb: pharmacokinetics, thermal dose, toxicity, and feasibility. *Cancer Chemother Pharmacol.* 2005;.
18. Eroglu A, Kocaoglu H, Demirci S, Akgul H. Isolated limb perfusion with cisplatin and doxorubicin for locally advanced soft tissue sarcoma of an extremity. *Eur J Surg Oncol.* 2000;26(3):213-221.
19. Hoekstra HJ, van Ginkel RJ. Hyperthermic isolated limb perfusion in the management of extremity sarcoma. *Curr Opin Oncol.* 2003;15(4):300-303.
20. Rossi CR, Vecchiato A, Da Pian PP, et al. Adriamycin in hyperthermic perfusion for advanced limb sarcomas. *Ann Oncol.* 1992;3 Suppl 2:S111-S113.
21. Schraffordt KH, Eggermont AM, Lienard D, et al. Hyperthermic isolated limb perfusion for the treatment of soft tissue sarcomas. *Semin Surg Oncol.* 1998;14(3):210-214.
22. Carswell EA, Old LJ, Kassel RL, Green S, Fiore N, Williamson B. An endotoxin-induced serum factor that causes necrosis of tumors. *Proc Natl Acad Sci U S A.* 1975;72(9):3666-3670.
23. Palladino MA, Jr., Shalaby MR, Kramer SM, et al. Characterization of the antitumor activities of human tumor necrosis factor-alpha and the comparison with other cytokines: induction of tumor-specific immunity. *J Immunol.* 1987;138(11):4023-4032.
24. Sohmura Y, Nakata K, Yoshida H, Kashimoto S, Matsui Y, Furuichi H. Recombinant human tumor necrosis factor--II. Antitumor effect on murine and human tumors transplanted in mice. *Int J Immunopharmacol.* 1986;8(3):357-368.
25. Watanabe N, Niitsu Y, Umeno H, et al. Toxic effect of tumor necrosis factor on tumor vasculature in mice. *Cancer Res.* 1988;48(8):2179-2183.
26. Nakano K, Abe S, Sohmura Y. Recombinant human tumor necrosis factor--I. Cytotoxic activity in vitro. *Int J Immunopharmacol.* 1986;8(3):347-355.
27. Spriggs DR, Sherman ML, Michie H, et al. Recombinant human tumor necrosis factor administered as a 24-hour intravenous infusion. A phase I and pharmacologic study. *J Natl Cancer Inst.* 1988;80(13):1039-1044.
28. Blick M, Sherwin SA, Rosenblum M, Gutterman J. Phase I study of recombinant tumor necrosis factor in cancer patients. *Cancer Res.* 1987;47(11):2986-2989.
29. Feinberg B, Kurzrock R, Talpaz M, Blick M, Saks S, Gutterman JU. A phase I trial of intravenously-administered recombinant tumor necrosis factor-alpha in cancer patients. *J Clin Oncol.* 1988;6(8):1328-1334.
30. Chapman PB, Lester TJ, Casper ES, et al. Clinical pharmacology of recombinant human tumor necrosis factor in patients with advanced cancer. *J Clin Oncol.* 1987;5(12):1942-1951.
31. Sherman ML, Spriggs DR, Arthur KA, Imamura K, Frei E, III, Kufe DW. Recombinant human tumor necrosis factor administered as a five-day continuous infusion in cancer patients: phase I toxicity and effects on lipid metabolism. *J Clin Oncol.* 1988;6(2):344-350.
32. Lienard D, Ewalenko P, Delmotte JJ, Renard N, Lejeune FJ. High-dose recombinant tumor necrosis factor alpha in combination with interferon gamma and melphalan in isolation perfusion of the limbs for melanoma and sarcoma. *J Clin Oncol.* 1992;10(1):52-60.
33. Eggermont AM, Schraffordt KH, Lienard D, et al. Isolated limb perfusion with high-dose tumor necrosis factor-alpha in combination with interferon-gamma and melphalan for nonresectable extremity soft tissue sarcomas: a multicenter trial. *J Clin Oncol.* 1996;14(10):2653-2665.

34. Eggermont AM, Schraffordt KH, Klausner JM, et al. Isolated limb perfusion with tumor necrosis factor and melphalan for limb salvage in 186 patients with locally advanced soft tissue extremity sarcomas. The cumulative multicenter European experience. *Ann Surg.* 1996;224(6):756-764.
35. Olieman AF, Lienard D, Eggermont AM, et al. Hyperthermic isolated limb perfusion with tumor necrosis factor alpha, interferon gamma, and melphalan for locally advanced nonmelanoma skin tumors of the extremities: a multicenter study. *Arch Surg.* 1999;134(3):303-307.
36. Vrouenraets BC, Eggermont AM, Hart AA, et al. Regional toxicity after isolated limb perfusion with melphalan and tumour necrosis factor- alpha versus toxicity after melphalan alone. *Eur J Surg Oncol.* 2001;27(4):390-395.
37. Eggermont AM, Koops HS, Klausner JM, et al. Limb salvage by isolation limb perfusion with tumor necrosis factor alpha and melphalan for locally advanced extremity soft tissue sarcomas: results of 279 perfusions in 246 patients. *Proc Am Soc Clin Oncol.* 1999;11:497.
38. Eggermont AM, Schraffordt KH, Klausner JM, et al. Isolation limb perfusion with tumor necrosis factor alpha and chemotherapy for advanced extremity soft tissue sarcomas. *Semin Oncol.* 1997;24(5):547-555.
39. Eggermont AM, de Wilt JH, ten Hagen TL. Current uses of isolated limb perfusion in the clinic and a model system for new strategies. *Lancet Oncol.* 2003;4(7):429-437.
40. Fajardo LF, Kwan HH, Kowalski J, Prionas SD, Allison AC. Dual role of tumor necrosis factor-alpha in angiogenesis. *Am J Pathol.* 1992;140(3):539-544.
41. de Wilt JH, ten Hagen TL, de Boeck G, van Tiel ST, de Bruijn EA, Eggermont AM. Tumour necrosis factor alpha increases melphalan concentration in tumour tissue after isolated limb perfusion. *Br J Cancer.* 2000;82(5):1000-1003.
42. Manusama ER, Stavast J, Durante NM, Marquet RL, Eggermont AM. Isolated limb perfusion with TNF alpha and melphalan in a rat osteosarcoma model: a new anti-tumour approach. *Eur J Surg Oncol.* 1996;22(2):152-157.
43. van Der Veen AH, de Wilt JH, Eggermont AM, van Tiel ST, Seynhaeve AL, ten Hagen TL. TNF-alpha augments intratumoural concentrations of doxorubicin in TNF-alpha-based isolated limb perfusion in rat sarcoma models and enhances anti-tumour effects. *Br J Cancer.* 2000;82(4):973-980.
44. Kristensen CA, Nozue M, Boucher Y, Jain RK. Reduction of interstitial fluid pressure after TNF-alpha treatment of three human melanoma xenografts. *Br J Cancer.* 1996;74(4):533-6.
45. Hoving S, Seynhaeve AL, van Tiel ST, et al. Early changes in tumor pathophysiology during TNF-based isolated limb perfusion determines response. Submitted.
46. Ruegg C, Yilmaz A, Bieler G, Bamat J, Chaubert P, Lejeune FJ. Evidence for the involvement of endothelial cell integrin alpha β 3 in the disruption of the tumor vasculature induced by TNF and IFN-gamma. *Nat Med.* 1998;4(4):408-14.
47. Renard N, Lienard D, Lespagnard L, Eggermont A, Heimann R, Lejeune F. Early endothelium activation and polymorphonuclear cell invasion precede specific necrosis of human melanoma and sarcoma treated by intravascular high-dose tumour necrosis factor alpha (rTNF alpha). *Int J Cancer.* 1994;57(5):656-663.
48. Nooijen PT, Manusama ER, Eggermont AM, et al. Synergistic effects of TNF-alpha and melphalan in an isolated limb perfusion model of rat sarcoma: a histopathological, immunohistochemical and electron microscopical study. *Br J Cancer.* 1996;74(12):1908-1915.
49. Nooijen PT, Eggermont AM, Schalkwijk L, Henzen-Logmans S, De Waal RM, Ruiter DJ. Complete response of melanoma-in-transit metastasis after isolated limb perfusion with tumor necrosis factor alpha and melphalan without massive tumor necrosis: a clinical and histopathological study of the delayed-type reaction pattern. *Cancer Res.* 1998;58(21):4880-4887.
50. Rossi CR, Foletto M, Di Filippo F, et al. Soft tissue limb sarcomas: Italian clinical trials with hyperthermic antitlastic perfusion. *Cancer.* 1999;86(9):1742-1749.
51. Gabizon A, Shmeeda H, Barenholz Y. Pharmacokinetics of pegylated liposomal Doxorubicin: review of animal and human studies. *Clin Pharmacokinet.* 2003;42(5):419-436.
52. Gabizon AA. Selective tumor localization and improved therapeutic index of anthracyclines encapsulated in long-circulating liposomes. *Cancer Res.* 1992;52(4):891-6.
53. Judson I, Radford JA, Harris M, et al. Randomised phase II trial of pegylated liposomal doxorubicin (DOXIL/CAELYX) versus doxorubicin in the treatment of advanced or metastatic soft tissue sarcoma: a study by the EORTC Soft Tissue and Bone Sarcoma Group. *Eur J Cancer.* 2001;37(7):870-877.
54. ten Hagen TL, Hoving S, Ambagtsheer G, van Tiel ST, Eggermont AM. Lack of efficacy of Doxil in TNF-alpha-based isolated limb perfusion in sarcoma-bearing rats. *Br J Cancer.* 2004;90(9):1830-1832.
55. Di Filippo F, Cavaliere F, Anza M, et al. Liposomal doxorubicin in the perfusional treatment of advanced soft tissue limb sarcoma. *J Chemother.* 2004;16 Suppl 5:66-9.:66-69.
56. Boucher Y, Baxter LT, Jain RK. Interstitial pressure gradients in tissue-isolated and subcutaneous tumors: implications for therapy. *Cancer Res.* 1990;50(15):4478-4484.

57. Jain RK. Transport of molecules, particles, and cells in solid tumors. *Annu Rev Biomed Eng.* 1999;1:241-263.
58. Alexander RB, Nelson WG, Coffey DS. Synergistic enhancement by tumor necrosis factor of in vitro cytotoxicity from chemotherapeutic drugs targeted at DNA topoisomerase II. *Cancer Res.* 1987;47(9):2403-2406.
59. Alexander RB, Isaacs JT, Coffey DS. Tumor necrosis factor enhances the in vitro and in vivo efficacy of chemotherapeutic drugs targeted at DNA topoisomerase II in the treatment of murine bladder cancer. *J Urol.* 1987;138(2):427-429.
60. Seynhaeve AL, de Wilt JH, van Tiel ST, Eggermont AM, ten Hagen TL. Isolated limb perfusion with actinomycin D and TNF-alpha results in improved tumour response in soft-tissue sarcoma-bearing rats but is accompanied by severe local toxicity. *Br J Cancer.* 2002;86(7):1174-1179.
61. Naredi PL, Lindner PG, Holmberg SB, Stenram U, Peterson A, Hafstrom LR. The effects of tumour necrosis factor alpha on the vascular bed and blood flow in an experimental rat hepatoma. *Int J Cancer.* 1993;54(4):645-649.
62. Pimm MV, Gribben SJ, Morris TM. Influence of recombinant tumour necrosis factor alpha on blood flow and antibody localisation in human tumour xenografts in nude mice. *J Cancer Res Clin Oncol.* 1991;117(6):543-548.
63. Folli S, Pelegrin A, Chalandon Y, et al. Tumor-necrosis factor can enhance radio-antibody uptake in human colon carcinoma xenografts by increasing vascular permeability. *Int J Cancer.* 1993;53(5):829-836.
64. Tozer GM, Prise VE, Bell KM. The influence of nitric oxide on tumour vascular tone. *Acta Oncol.* 1995;34(3):373-377.
65. de Wilt JH, Manusama ER, van Etten B, et al. Nitric oxide synthase inhibition results in synergistic anti-tumour activity with melphalan and tumour necrosis factor alpha-based isolated limb perfusions [In Process Citation]. *Br J Cancer.* 2000;83(9):1176-82.
66. Laurenzi L, Natoli S, Di Filippo F, et al. Systemic and haemodynamic toxicity after isolated limb perfusion (ILP) with TNF-alpha. *J Exp Clin Cancer Res.* 2004;23(2):225-231.
67. Baselmans AH, Koten JW, Battermann JJ, Van Dijk JE, Den Otter W. The mechanism of regression of solid SL2 lymphosarcoma after local IL-2 therapy. *Cancer Immunol Immunother.* 2002;51(9):492-498.
68. Den Otter W, De Groot JW, Bernsen MR, et al. Optimal regimes for local IL-2 tumour therapy. *Int J Cancer.* 1996;66(3):400-403.
69. Atkins MB. Interleukin-2: clinical applications. *Semin Oncol.* 2002;29(3 Suppl 7):12-17.
70. Epstein AL, Mizokami MM, Li J, Hu P, Khawli LA. Identification of a protein fragment of interleukin 2 responsible for vasopermeability. *J Natl Cancer Inst.* 2003;95(10):741-749.
71. Siegel JP, Puri RK. Interleukin-2 toxicity. *J Clin Oncol.* 1991;9(4):694-704.
72. Winkelhake JL, Gauny SS. Human recombinant interleukin-2 as an experimental therapeutic. *Pharmacol Rev.* 1990;42(1):1-28.
73. Hoving S, Brunstein F, aan de Wiel-Ambagtsheer G, et al. Synergistic antitumor response of IL-2 with melphalan in isolated limb perfusion in soft-tissue sarcoma bearing rats. *Cancer Res.* 2005;65(10):4300-4308.
74. Economou JS, McBride WH, Essner R, et al. Tumour necrosis factor production by IL-2-activated macrophages in vitro and in vivo. *Immunology.* 1989;67(4):514-519.
75. Maekawa H, Iwabuchi K, Nagaoka I, Watanabe H, Kamano T, Tsurumaru M. Activated peritoneal macrophages inhibit the proliferation of rat ascites hepatoma AH-130 cells via the production of tumor necrosis factor-alpha and nitric oxide. *Inflamm Res.* 2000;49(10):541-547.
76. Albina JE, Reichner JS. Role of nitric oxide in mediation of macrophage cytotoxicity and apoptosis. *Cancer Metastasis Rev.* 1998;17(1):39-53.
77. Bonnotte B, Larmonier N, Favre N, et al. Identification of tumor-infiltrating macrophages as the killers of tumor cells after immunization in a rat model system. *J Immunol.* 2001;167(9):5077-5083.
78. Lynch NR, Salomon JC. Passive local anaphylaxis: demonstration of antitumor activity and complementation of intratumor BCG. *J Natl Cancer Inst.* 1977;58(4):1093-1098.
79. Rizell M, Hellstrand K, Lindner P, Naredi P. Monotherapy with histamine dihydrochloride suppresses in vivo growth of a rat sarcoma in liver and subcutis. *Anticancer Res.* 2002;22(4):1943-1948.
80. Tatsuta M, Iishi H, Ichii M, Noguchi S, Yamamura H, Taniguchi H. Inhibitory effects of tetragastrin and histamine on carcinogenesis in the small intestines of W rats by N-methyl-N'-nitro-N-nitrosoguanidine. *J Natl Cancer Inst.* 1986;76(2):277-281.
81. Suonio E, Tuomisto L, Alhava E. Effects of histamine, H1, H2 and Hic receptor antagonists and alpha-fluoromethylhistidine on the growth of human colorectal cancer in the subrenal capsule assay. *Agents Actions.* 1994;41 Spec No:C118-20.:C118-C120.
82. Hellstrand K, Asea A, Hermodsson S. Role of histamine in natural killer cell-mediated resistance against tumor cells. *J Immunol.* 1990;145(12):4365-4370.

83. Burtin C, Scheinmann P, Salomon JC, Lespinats G, Canu P. Decrease in tumour growth by injections of histamine or serotonin in fibrosarcoma-bearing mice: influence of H1 and H2 histamine receptors. *Br J Cancer*. 1982;45(1):54-60.
84. Garison JC Histamine, bradykinin, 5-hydroxytryptamine and their antagonists. *In* Goodman Gilman A, Rall TW, Nie AS, and Taylor P (eds.), *The pharmacological basis of therapeutics*, 8th ed, pp. 575-599. Elmsford (NY): Pergamon Press, 1990.
85. Brunstein F, Hoving S, Seynhaeve AL, et al. Synergistic antitumor activity of histamine plus melphalan in isolated limb perfusion: preclinical studies. *J Natl Cancer Inst*. 2004;96(21):1603-1610.
86. Agarwala SS, Sabbagh MH. Histamine dihydrochloride: inhibiting oxidants and synergising IL-2-mediated immune activation in the tumour microenvironment. *Expert Opin Biol Ther*. 2001;1(5):869-879.
87. Hellstrand K, Hermodsson S. Synergistic activation of human natural killer cell cytotoxicity by histamine and interleukin-2. *Int Arch Allergy Appl Immunol*. 1990;92(4):379-389.
88. Johansson M, Henriksson R, Bergenheim AT, Koskinen LO. Interleukin-2 and histamine in combination inhibit tumour growth and angiogenesis in malignant glioma. *Br J Cancer*. 2000;83(6):826-832.
89. Agarwala SS, Glaspy J, O'Day SJ, et al. Results from a randomized phase III study comparing combined treatment with histamine dihydrochloride plus interleukin-2 versus interleukin-2 alone in patients with metastatic melanoma. *J Clin Oncol*. 2002;20(1):125-133.
90. Brunstein F, Hoving S, Abbas AK, de Boeck G, Eggermont AM, ten Hagen TL. Lack of synergy between histamine and IL-2 in the melphalan-based isolated limb perfusion. Submitted.

Chapter 12

General discussion: Bringing liposomal antitumor therapy to a new level

Introduction

Successful treatment of solid tumors with chemotherapeutics requires that adequate levels of anticancer agents reach the tumor cells. Physiological barriers hinder the effective delivery of drugs to tumors and are frequently responsible for failure of initially promising agents. Inadequate drug delivery could lead to regrowth of tumors and possible development of resistance cells. It is quite difficult to achieve adequate concentrations of anticancer agents at the tumor site because: 1) After the drug enters the bloodstream, massive dilution occurs. 2) Most anticancer drugs are also toxic towards normal cells and therefore the dose of administered drugs is limited by normal tissue tolerance. 3) Heterogeneous tumor perfusion of the tumor, arterio-venous shunting and necrotic and hypoxic areas, as well as a high interstitial fluid pressure (IFP) may limit the penetration of drugs into the tumor and prevent drugs in reaching tumor cells distant from blood vessels (1-7). Methods for improving drug delivery and penetration in tumor tissues are therefore of great clinical interest. There are two general directions within drug delivery to improve therapy, namely site-specific delivery and site-specific triggering. By incorporating an active and site-specific release mechanism into liposomes release and therapeutic efficacy of the carried drug may be dramatically increased. This review concentrates on the use of site-specific targeting.

(Stealth[®]) Liposomes

Liposomes were discovered in 1965 (8) and soon after that their potential as vehicles for the delivery of cytotoxic drugs to tumors was explored (9-11). However, the use of these so-called conventional liposomes was limited due to rapid recognition and removal from the circulation by the mononuclear phagocyte system (MPS) represented by the primary organs liver, spleen and lung. In the late eighties, liposome surface coating with polyethylene glycol (PEG), a synthetic hydrophilic polymer, was introduced. The PEG headgroup serves as a barrier preventing interactions with plasma opsonins as a result of the concentration of highly hydrated groups that sterically inhibit hydrophobic and electrostatic interactions of a variety of blood components with the liposome surface. These PEG-coated liposomes are referred to as sterically stabilized or Stealth[®] liposomes (12-14). Stealth[®] liposomes have a long circulation time because of their small size and reduced interaction with formed elements of the blood. Selective targeting of liposomes to tumor tissue is believed to be achieved through the so-called EPR (enhanced permeability and retention) effect. Normally the endothelial lining is a closed barrier, but it is known that tumor blood vessels exhibit heterogeneous hyperpermeability to plasma proteins and other circulating macromolecules. Within the tumor several vascular permeability factors are produced, including vascular endothelial growth factor (VEGF) and TNF. Vascular permeability depends on tumor type, increases with tumor size and rate and is higher in the periphery compared to the central

region of the tumor. Furthermore, poor lymphatic drainage leads to long-term retention of liposomes in tumor tissue (15-20).

The use of Stealth[®] liposomes as drug carriers for chemotherapeutic agents offers a potential means of manipulating drug distribution to improve antitumor efficacy and reduce toxicity. A well known liposomal formulation is Doxil[®] (Stealth[®] liposomal doxorubicin). Doxil[®] is approved in the United States and Europe for the treatment of AIDS-associated Kaposi's sarcoma (21) and ovarian cancer (22) and is also effective in the treatment of advanced or metastatic soft tissue sarcoma (23) and metastatic breast cancer (24). Also other anticancer drugs encapsulated in sterically stabilized liposomes have been tested in preclinical and clinical studies, like SPI-077 (Stealth[®] liposomal cisplatin) and vincristine (25-27). Despite advances with prolonged circulation and liposome accumulation in the tumor, antitumor efficacy of these formulations is still not sufficient.

Tumor cell targeting of liposomes

Liposomal drug delivery is based on 'passive' targeting to tumor tissue. It's the natural fate of long circulating particles (such as Stealth[®] liposomes) to extravasate at site with increased capillary leakage. However, these carriers do not directly target tumor cells, tumor vascular endothelial cells or other possible targets. The efficacy of liposomes as a drug delivery system could be increased dramatically if it were possible to selectively deliver their contents to the particular tumor sites. The next generation of liposomes features direct molecular targeting of cancer cells via antibody-mediated or other ligand-mediated interactions.

Immunoliposomes

Immunoliposomes are developed to combine monoclonal antibody technology with the pharmacokinetic and drug delivery advantages of long circulating liposomes and represent a novel strategy for tumor-targeted drug delivery. The antibody can be coupled either to the lipid head group or PEG distal end.

The HER-2 oncogene (also named neu or c-erbB-2) is a readily accessible transmembrane tyrosine kinase receptor with extensive homology to the epidermal growth factor receptor. HER-2 is overexpressed in 20-30% of breast and ovarian cancers and overexpression is associated with poor prognosis. Overexpression also occurs frequently in other carcinomas like lung, gastric and oral cancers. Immunoliposomes containing Fab' or scFv fragments against Her-2 were used to deliver doxorubicin, resulting in potent and selective antitumor activity in a number of animal models (28,29). The efficacy of immunoliposomes containing doxorubicin was superior compared with free drug, non-targeted liposomal doxorubicin or non-targeted liposomal doxorubicin plus free anti-Her-2 Mab .

Immunoliposomes can also be used for targeting antigens. The human antibody GAH binds to cell surface antigens expressed in human gastric, colorectal and mammary cancer tissues, while normal tissues such as liver, lung or uterine do not show any significant reactivity with GAH. MCC-465 is an immunoliposome-encapsulated doxorubicin tagged with PEG and the F(ab')₂ fragment of the human antibody GAH. The immunoliposome accumulates in tumor tissue by utilizing the EPR effect, binds to the cancer cell surface, and is internalised by GAH-antigen interaction (30). MCC-465 showed strong antitumor activity against gastrointestinal cancers (30,31).

Nam *et al.* reported that doxorubicin encapsulated in anti-G(M3) immunoliposomes was able to reduce *in vivo* tumor growth and metastasis of B16BL6 mouse melanoma cells more greatly than non-targeted drugs (32).

Ligand-directed liposomes

Receptor-mediated endocytosis pathways can be exploited for specific targeting of liposomes and intracellular delivery of liposome contents (33). Liposomes conjugated to a ligand, that is directed to an over-expressed receptor in tumor cells and that normally undergoes endocytosis, is a strategy that can improve selectivity and facilitate access of liposomes to the intracellular compartment.

Folic acid is a well-studied targeting ligand and cell surface receptors for this vitamin are overexpressed in many human tumors (34,35). Macromolecules coupled to folic acid are successfully recognized by folate receptors and internalized into cells via folate receptor mediated endocytosis (36,37). Several studies showed that folate receptor targeted liposomes are effective for *in vitro* and *in vivo* delivery of anticancer drugs and have potential application in the treatment of folate receptor positive solid tumors (36-40).

Transferrin receptor-mediated endocytosis is a normal physiological process by which transferrin delivers iron to the cells. The transferrin receptor concentration on tumor cells is much higher than on normal cells. The glycoprotein transferrin has been employed as a targeting ligand to direct liposomal drugs to various types of cancer *in vivo*. Several studies reported that transferrin-conjugation to PEG-liposome is useful for intracellular uptake in tumor cells *in vitro* and *in vivo* (41-43).

Vascular targeting of liposomes

Vascular targeting has become a focus of interest, since cells of the vasculature are the first to be encountered by systemically injected drugs or drug carriers. Especially, targeting for tumor angiogenic vessels seems promising for cancer treatment since these vessels express several proteins that are absent or barely detectable in established blood vessels, including integrins and receptors for certain angiogenic growth factors (44,45).

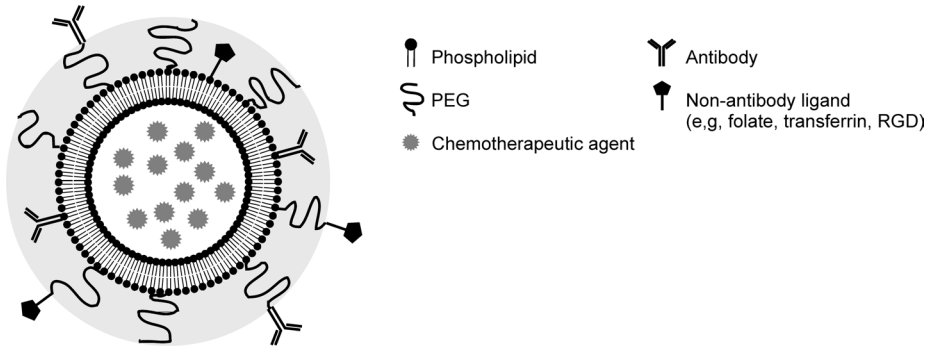


Figure 1. Schematic representation of different liposome types. Stealth[®] liposomes are conventional liposomes coated with polyethyleneglycol (PEG). Antibodies or ligands can be coupled to the lipid head group or PEG distal end.

Integrin targeting

Targeting of small peptides towards integrins was investigated by phage display library selection of peptides targeting to tumor blood vessels. The peptide sequence showing efficient binding to the $\alpha_v\beta_3$ and $\alpha_v\beta_5$ -integrin receptor was the Arg-Gly-Asp (RGD) tripeptide (46). By coupling cyclic RGD-peptides to the distal end of Stealth[®] liposomes a superior anti-tumor activity in a murine C26 colon carcinoma model was found when compared to non-targeted Stealth[®] liposomes (47).

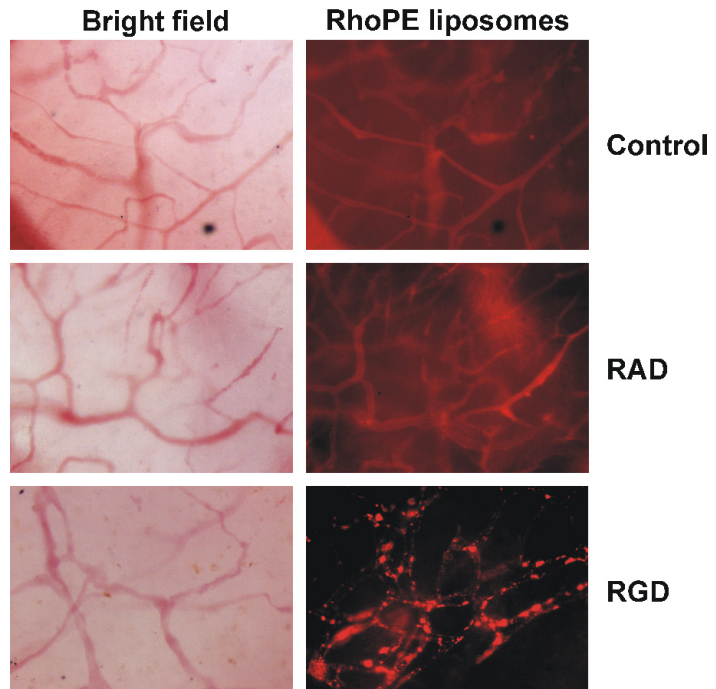


Figure 2. Intravital microscopy image of localization of RhoPE liposomes couples with RAD or RGD peptides. Pictures are taken 45 minutes after in-jection.

Maeda *et al.* suggested that Ala-Pro-Arg-Pro-Gly (APRPG) is a useful probe for targeting to angiogenic vessels, although the target molecule of APRPG is unknown. They showed that adriamycin-encapsulated liposomes modified with APRPG-PEG were more effective than adriamycin-encapsulated liposomes modified with PEG alone in Colon 26 carcinoma-bearing mice. This difference was achieved in spite of quite similar accumulation of both types of liposomes in the tumor (48).

Pastorino and coworkers reported anti-angiogenic chemotherapy by use of NGR peptide-modified long-circulating liposomes encapsulating doxorubicin targeting aminopeptidase N. They showed not only drastic therapeutic efficacy against tumor-bearing mice, but also pronounced destruction of the tumor vasculature by use of the angiogenic endothelial cell-targeted liposomal anti-cancer drug (49).

Endoglin (CD105) is a component of the transforming growth factor β receptor complex and elevated levels of endoglin were detected in the vasculature of different tumors (50-52). *In vitro* studies showed increased binding and internalization of the anti-endoglin liposomes (ILA5) and the endothelial cell-specific immunoliposomes may be useful in cancer therapy (53).

Another vascular target is membrane type-1 matrix metalloproteinase (MT1-MMP). MT1-MMP is expressed specifically on angiogenic endothelium as well on tumor cells, and liposomes modified with MT1-MMP targeted peptide were able to induce tumor growth suppression by damaging angiogenic endothelial cells (54).

TNF-based liposomal therapy

In many studies is shown that addition of high-dose TNF to a melphalan-based isolated limb perfusion (ILP) results in excellent antitumor effects against melanoma (55), large soft tissue sarcomas (56,57) and various other tumors in the clinical setting (58-60). We have previously shown that the basis for the synergy is, on one hand a significant enhancement of tumor selective melphalan uptake and on the other hand destruction of tumor vasculature (61-64). Unfortunately, the systemic application of high-dose TNF is hampered by severe toxicity, suggesting that only low dosages can be applied (65,66).

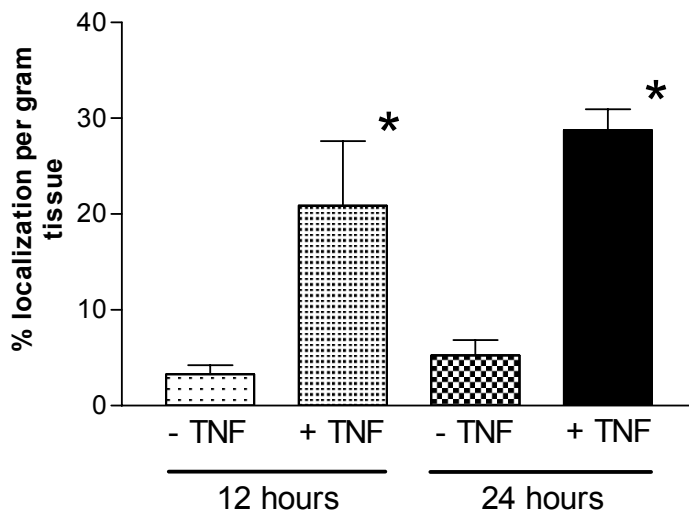
The first systemic treatments we performed with low-dose TNF were in the highly vascularized rat soft tissue sarcoma BN175. We showed that co-administration of Doxil[®] and low-dose TNF resulted in a pronounced tumor response and augmented accumulation of the chemotherapeutic drug in tumor tissue (67). In addition, combination therapy of Doxil[®] and low-dose TNF seems attractive for the treatment of the intermediate vascularized rat osteosarcoma (68). However, when Doxil[®] was used in the ILP, minimal antitumor activity was found in both tumor models and its activity was not enhanced by TNF. Accumulation of Doxil[®] was not augmented compared to doxorubicin. We

hypothesized that the short circulation time during ILP is likely inadequate for the circulation time advantage of Doxil[®] to have an effect on the distribution (69).

Also another cytotoxic agent encapsulated in pegylated liposomes was tested, SPI-077. Addition of TNF to a SPI-077 treatment resulted in a better tumor growth delay in the BN175 sarcoma than treatment with SPI-077 alone and a more prolonged antitumor activity was detected, but no such effect was seen in the rat osteosarcoma (70). A major difference between Doxil[®] and SPI-077 is the drug-to-lipid ratio. For SPI-077, the drug-to-lipid ratio is 14 $\mu\text{g}/\text{mg}$, compared with 125 $\mu\text{g}/\text{mg}$ for Doxil[®]. Therefore, each Doxil[®] liposome delivers approximately nine times more drug than a SPI-077 liposome, which will have an important effect on activity (26).

In murine tumor models similar results were seen. When B16BL6 melanoma-bearing mice were injected with Doxil[®] combined with TNF a pronounced tumor response was found (71). A more than 5-fold increased tumor drug uptake was found when liposomes of 100 nm were combined with TNF (Figure 3). TNF was also able to enhance the uptake of larger liposomes of 400 and 800 nm, although liposomes of 100 nm were localized in the tumor in a larger amount than 400 and 800 nm liposomes (72).

Figure 3. Accumulation of ⁶⁷Ga-labeled liposomes of 100 nm (48 $\mu\text{mol}/\text{kg}$) with or without TNF (1 $\mu\text{g}/\text{mouse}$) in B16BL6 mouse melanoma. The tumors were excised 12 or 24 hours after i.v. injection. The mean of at least 3 mice are shown \pm SE. * $p < 0.02$.



However, insight in the intratumoral localization of the liposomes is lacking. Therefore we studied the effect of TNF on the intratumoral distribution of liposomal drugs with the use of intravital microscopy. Addition of TNF resulted in an abundant accumulation of liposomes in the tumor interstitium and the liposomes extravasated more homogeneously throughout the tumor. Less liposomes were trapped inside blood vessels when TNF was co-administered and these results indicate that TNF likely increases the leakiness of the vasculature by increasing the gaps between the endothelial lining in the tumor, leading to

augmented accumulation after extravasation of liposomes (72-74). In figure 4, increased extravasation of liposomes nearby blood vessels is shown in the B16BL6 melanoma (72) and similar effects were seen in the rat soft tissue sarcoma BN175 (Figure 5).

In other studies TNF also caused an augmented tumor accumulation of liposome-encapsulated adriamycin (75) and radio-antibody (76). Curnis *et al.* found that targeted delivery of TNF coupled to cyclic CNGRC peptide to tumor vessels enhances the antitumor activity of chemotherapeutic drugs and increased the penetration drugs in tumors (77). Kristensen *et al.* showed that TNF caused a reduction in the IFP in human melanoma xenografts, what could lead to enhanced uptake of large molecules (78). Also other compounds that reduce IFP are associated with improved tumor uptake (79).

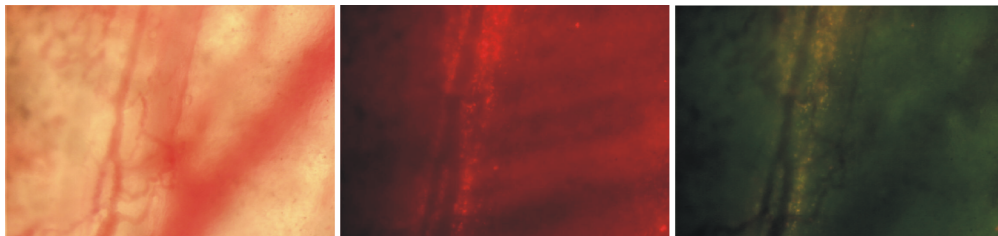


Figure 4. Intravital microscopy image of localization of Doxil[®] DiO in tumor vasculature en B16BL6 melanoma 24 hours after injection of liposomes and 1 µg/mouse TNF. Green: DiO, red: doxorubicin.

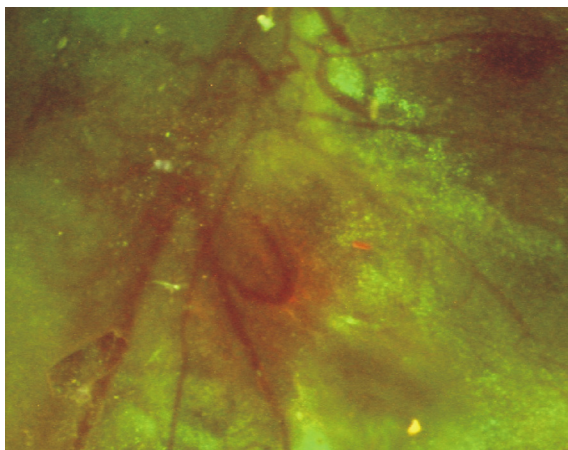


Figure 5. Intravital microscopy image of local-ization of Doxil[®] DiO in tumor vasculature of BN175 soft-tissue sarcoma 4 days after injection of liposomes and 15 µg/kg TNF. Green: DiO, red: doxorubicin.

In general, tumor vessels are more permeable than normal vessels and the maximum size of particles that can cross the tumor vessel wall is called the pore cut-off size. Vascular permeability may depend on tumor type and microenvironment and increases with tumor size. It is believed that not the microvessel density is the limiting factor of macromolecule drug delivery to solid tumors, but the permeability of the tumor vessels (20,80). In our experiments we saw clear differences between two mouse tumor models, B16BL6 and Lewis Lung Carcinoma (LLC). In the B16BL6 tumor already a higher degree of liposome

leakage was found compared to the LLC tumor and TNF did not induce an augmented accumulation or extravasation of liposomes in the LLC tumor. A striking difference observed between the two tumor models was the tumor vascular architecture. The B16BL6 had fewer blood vessels and produced also slightly less VEGF than LLC (81). In general, tumors with high VEGF levels have a higher vascular density, but have also more permeable blood vessels (82-84). Our results, together with the data of Parr *et al.* (85) and Weissig *et al.* (86), may be considered as an indication that subcutaneous Lewis Lung carcinoma is a tumor with a small vascular pore cut-off size. Possibly, VEGF is not responsible for the differences in cut-off pore size in these two tumor types.

Conclusions

It is well known that the use of Stealth[®] liposomes as drug carriers for chemotherapeutic agents improve antitumor efficacy and reduce toxicity. The pegylated liposomes are long circulating and accumulate significantly in tumors due to a leaky vasculature. Several attempts are made to further improve drug targeting. Molecular targeting of cancer cells via antibody-mediated or other ligand-mediated liposomes have shown increased efficacy. Besides targeting tumor cells, also the tumor vasculature can be targeted since injected drugs first meet blood vessels before they extravasate into the tumor interstitium. Liposomes can be coupled to small peptides that target integrins or endothelial cell markers. We have shown in several experiments that addition of TNF to different liposomal formulation in diverse tumor models improved the antitumor activity and caused enhanced tumor drug accumulation. These experiments have led to new perspectives in systemic treatment of solid tumors.

References

1. Jain RK. Barriers to drug delivery in solid tumors. *Sci Am.* 1994;271(1):58-65.
2. Dvorak HF, Nagy JA, Dvorak JT, Dvorak AM. Identification and characterization of the blood vessels of solid tumors that are leaky to circulating macromolecules. *Am J Pathol.* 1988;133(1):95-109.
3. Jain RK. Delivery of molecular and cellular medicine to solid tumors. *Adv Drug Deliv Rev.* 2001;46(1-3):149-168.
4. Jang SH, Wientjes MG, Lu D, Au JL. Drug delivery and transport to solid tumors. *Pharm Res.* 2003;20(9):1337-1350.
5. Yuan F. Transvascular drug delivery in solid tumors. *Semin Radiat Oncol.* 1998;8(3):164-175.
6. Gillies RJ, Schornack PA, Secomb TW, Raghunand N. Causes and effects of heterogeneous perfusion in tumors. *Neoplasia.* 1999;1(3):197-207.
7. Baxter LT, Jain RK. Transport of fluid and macromolecules in tumors. II. Role of heterogeneous perfusion and lymphatics. *Microvasc Res.* 1990;40(2):246-263.
8. Bangham AD, Standish MM, Watkins JC. Diffusion of univalent ions across the lamellae of swollen phospholipids. *J Mol Biol.* 1965;13(1):238-252.
9. Gregoriadis G. The carrier potential of liposomes in biology and medicine (second of two parts). *N Engl J Med.* 1976;295(14):765-770.
10. Gregoriadis G. The carrier potential of liposomes in biology and medicine (first of two parts). *N Engl J Med.* 1976;295(13):704-710.
11. Gregoriadis G, Wills EJ, Swain CP, Tavill AS. Drug-carrier potential of liposomes in cancer chemotherapy. *Lancet.* 1974;1(7870):1313-1316.
12. Lasic DD. Doxorubicin in sterically stabilized liposomes. *Nature.* 1996;380(6574):561-562.

13. Papahadjopoulos D, Allen TM, Gabizon A, et al. Sterically stabilized liposomes: improvements in pharmacokinetics and antitumor therapeutic efficacy. *Proc Natl Acad Sci U S A*. 1991;88(24):11460-11464.
14. Sparano JA, Winer EP. Liposomal anthracyclines for breast cancer. *Semin Oncol*. 2001;28(4 Suppl 12):32-40.
15. Gabizon A, Papahadjopoulos D. Liposome formulations with prolonged circulation time in blood and enhanced uptake by tumors. *Proc Natl Acad Sci U S A*. 1988;85(18):6949-6953.
16. Maeda H, Fang J, Inutsuka T, Kitamoto Y. Vascular permeability enhancement in solid tumor: various factors, mechanisms involved and its implications. *Int Immunopharmacol*. 2003;3(3):319-328.
17. Wu NZ, Da D, Rudoll TL, Needham D, Whorton AR, Dewhirst MW. Increased microvascular permeability contributes to preferential accumulation of Stealth liposomes in tumor tissue. *Cancer Res*. 1993;53(16):3765-70.
18. Gabizon AA. Liposomal drug carrier systems in cancer chemotherapy: current status and future prospects. *J Drug Target*. 2002;10(7):535-538.
19. Dvorak HF, Brown LF, Detmar M, Dvorak AM. Vascular permeability factor/vascular endothelial growth factor, microvascular hyperpermeability, and angiogenesis. *Am J Pathol*. 1995;146(5):1029-1039.
20. Hobbs SK, Monsky WL, Yuan F, et al. Regulation of transport pathways in tumor vessels: role of tumor type and microenvironment. *Proc Natl Acad Sci U S A*. 1998;95(8):4607-12.
21. Northfelt DW, Dezube BJ, Thommes JA, et al. Pegylated-liposomal doxorubicin versus doxorubicin, bleomycin, and vincristine in the treatment of AIDS-related Kaposi's sarcoma: results of a randomized phase III clinical trial. *J Clin Oncol*. 1998;16(7):2445-2451.
22. Stebbing J, Gaya A. Pegylated liposomal doxorubicin (Caelyx) in recurrent ovarian cancer. *Cancer Treat Rev*. 2002;28(2):121-125.
23. Judson I, Radford JA, Harris M, et al. Randomised phase II trial of pegylated liposomal doxorubicin (DOXIL/CAELYX) versus doxorubicin in the treatment of advanced or metastatic soft tissue sarcoma: a study by the EORTC Soft Tissue and Bone Sarcoma Group. *Eur J Cancer*. 2001;37(7):870-877.
24. O'Brien ME, Wigler N, Inbar M, et al. Reduced cardiotoxicity and comparable efficacy in a phase III trial of pegylated liposomal doxorubicin HCl (CAELYX/Doxil) versus conventional doxorubicin for first-line treatment of metastatic breast cancer. *Ann Oncol*. 2004;15(3):440-449.
25. Allen TM, Newman MS, Woodle MC, Mayhew E, Uster PS. Pharmacokinetics and anti-tumor activity of vincristine encapsulated in sterically stabilized liposomes. *Int J Cancer*. 1995;62(2):199-204.
26. Harrington KJ, Lewanski CR, Northcote AD, et al. Phase I-II study of pegylated liposomal cisplatin (SPI-077) in patients with inoperable head and neck cancer. *Ann Oncol*. 2001;12(4):493-496.
27. Meerum TJ, Groenewegen G, Pluim D, et al. Phase I and pharmacokinetic study of SPI-77, a liposomal encapsulated dosage form of cisplatin. *Cancer Chemother Pharmacol*. 2002;49(3):201-210.
28. Park JW, Hong K, Kirpotin DB, et al. Anti-HER2 immunoliposomes: enhanced efficacy attributable to targeted delivery. *Clin Cancer Res*. 2002;8(4):1172-1181.
29. Park JW, Kirpotin DB, Hong K, et al. Tumor targeting using anti-her2 immunoliposomes. *J Control Release*. 2001;74(1-3):95-113.
30. Hosokawa S, Tagawa T, Niki H, Hirakawa Y, Nohga K, Nagaike K. Efficacy of immunoliposomes on cancer models in a cell-surface-antigen-density-dependent manner. *Br J Cancer*. 2003;89(8):1545-1551.
31. Hamaguchi T, Matsumura Y, Nakanishi Y, et al. Antitumor effect of MCC-465, pegylated liposomal doxorubicin tagged with newly developed monoclonal antibody GAH, in colorectal cancer xenografts. *Cancer Sci*. 2004;95(7):608-613.
32. Nam SM, Kim HS, Ahn WS, Park YS. Sterically stabilized anti-G(M3), anti-Le(x) immunoliposomes: targeting to B16BL6, HRT-18 cancer cells. *Oncol Res*. 1999;11(1):9-16.
33. Sapro P, Allen TM. Internalizing antibodies are necessary for improved therapeutic efficacy of antibody-targeted liposomal drugs. *Cancer Res*. 2002;62(24):7190-7194.
34. Toffoli G, Cernigoi C, Russo A, Gallo A, Bagnoli M, Boiocchi M. Overexpression of folate binding protein in ovarian cancers. *Int J Cancer*. 1997;74(2):193-198.
35. Weitman SD, Lark RH, Coney LR, et al. Distribution of the folate receptor GP38 in normal and malignant cell lines and tissues. *Cancer Res*. 1992;52(12):3396-3401.
36. Sudimack J, Lee RJ. Targeted drug delivery via the folate receptor. *Adv Drug Deliv Rev*. 2000;41(2):147-162.
37. Lu Y, Low PS. Folate-mediated delivery of macromolecular anticancer therapeutic agents. *Adv Drug Deliv Rev*. 2002;54(5):675-693.
38. Gabizon A, Horowitz AT, Goren D, Tzemach D, Shmeeda H, Zalipsky S. In vivo fate of folate-targeted polyethylene-glycol liposomes in tumor-bearing mice. *Clin Cancer Res*. 2003;9(17):6551-6559.
39. Pan XQ, Wang H, Lee RJ. Antitumor activity of folate receptor-targeted liposomal doxorubicin in a KB oral carcinoma murine xenograft model. *Pharm Res*. 2003;20(3):417-422.

40. Gabizon A, Shmeeda H, Horowitz AT, Zalipsky S. Tumor cell targeting of liposome-entrapped drugs with phospholipid-anchored folic acid-PEG conjugates. *Adv Drug Deliv Rev.* 2004;56(8):1177-1192.
41. Ishida O, Maruyama K, Tanahashi H, et al. Liposomes bearing polyethyleneglycol-coupled transferrin with intracellular targeting property to the solid tumors in vivo. *Pharm Res.* 2001;18(7):1042-1048.
42. Eavarone DA, Yu X, Bellamkonda RV. Targeted drug delivery to C6 glioma by transferrin-coupled liposomes. *J Biomed Mater Res.* 2000;51(1):10-14.
43. Inuma H, Maruyama K, Okinaga K, et al. Intracellular targeting therapy of cisplatin-encapsulated transferrin-polyethylene glycol liposome on peritoneal dissemination of gastric cancer. *Int J Cancer.* 2002;99(1):130-137.
44. Bloemendal HJ, Logtenberg T, Voest EE. New strategies in anti-vascular cancer therapy. *Eur J Clin Invest.* 1999;29(9):802-809.
45. Ruoslahti E. Drug targeting to specific vascular sites. *Drug Discov Today.* 2002;7(22):1138-1143.
46. Arap W, Pasqualini R, Ruoslahti E. Cancer treatment by targeted drug delivery to tumor vasculature in a mouse model. *Science.* 1998;279(5349):377-380.
47. Schiffelers RM, Koning GA, ten Hagen TL, et al. Anti-tumor efficacy of tumor vasculature-targeted liposomal doxorubicin. *J Control Release.* 2003;91(1-2):115-122.
48. Maeda N, Takeuchi Y, Takada M, Sadzuka Y, Namba Y, Oku N. Anti-neovascular therapy by use of tumor neovascular-targeted long-circulating liposome. *J Control Release.* 2004;100(1):41-52.
49. Pastorino F, Brignole C, Marimpietri D, et al. Vascular damage and anti-angiogenic effects of tumor vessel-targeted liposomal chemotherapy. *Cancer Res.* 2003;63(21):7400-7409.
50. Fonsatti E, Altomonte M, Arslan P, Maio M. Endoglin (CD105): a target for anti-angiogenic cancer therapy. *Curr Drug Targets.* 2003;4(4):291-296.
51. Wikstrom P, Lissbrant IF, Stattin P, Egevad L, Bergh A. Endoglin (CD105) is expressed on immature blood vessels and is a marker for survival in prostate cancer. *Prostate.* 2002;51(4):268-275.
52. Burrows FJ, Derbyshire EJ, Tazzari PL, et al. Up-regulation of endoglin on vascular endothelial cells in human solid tumors: implications for diagnosis and therapy. *Clin Cancer Res.* 1995;1(12):1623-1634.
53. Volkel T, Holig P, Merdan T, Muller R, Kontermann RE. Targeting of immunoliposomes to endothelial cells using a single-chain Fv fragment directed against human endoglin (CD105). *Biochim Biophys Acta.* 2004;1663(1-2):158-166.
54. Kondo M, Asai T, Katanasaka Y, et al. Anti-neovascular therapy by liposomal drug targeted to membrane type-1 matrix metalloproteinase. *Int J Cancer.* 1993;108(2):301-306.
55. Lienard D, Lejeune FJ, Ewalenko P. In transit metastases of malignant melanoma treated by high dose rTNF alpha in combination with interferon-gamma and melphalan in isolation perfusion. *World J Surg.* 1992;16(2):234-240.
56. Eggermont AM, Schraffordt KH, Lienard D, et al. Isolated limb perfusion with high-dose tumor necrosis factor-alpha in combination with interferon-gamma and melphalan for nonresectable extremity soft tissue sarcomas: a multicenter trial. *J Clin Oncol.* 1996;14(10):2653-2665.
57. Eggermont AM, Schraffordt KH, Klausner JM, et al. Isolated limb perfusion with tumor necrosis factor and melphalan for limb salvage in 186 patients with locally advanced soft tissue extremity sarcomas. The cumulative multicenter European experience. *Ann Surg.* 1996;224(6):756-764.
58. Bickels J, Manusama ER, Gutman M, et al. Isolated limb perfusion with tumour necrosis factor-alpha and melphalan for unresectable bone sarcomas of the lower extremity. *Eur J Surg Oncol.* 1999;25(5):509-514.
59. Eggermont AM, de Wilt JH, ten Hagen TL. Current uses of isolated limb perfusion in the clinic and a model system for new strategies. *Lancet Oncol.* 2003;4(7):429-437.
60. Olieman AF, Lienard D, Eggermont AM, et al. Hyperthermic isolated limb perfusion with tumor necrosis factor alpha, interferon gamma, and melphalan for locally advanced nonmelanoma skin tumors of the extremities: a multicenter study. *Arch Surg.* 1999;134(3):303-307.
61. Nooijen PT, Manusama ER, Eggermont AM, et al. Synergistic effects of TNF-alpha and melphalan in an isolated limb perfusion model of rat sarcoma: a histopathological, immunohistochemical and electron microscopical study. *Br J Cancer.* 1996;74(12):1908-1915.
62. de Wilt JH, ten Hagen TL, de Boeck G, van Tiel ST, de Bruijn EA, Eggermont AM. Tumour necrosis factor alpha increases melphalan concentration in tumour tissue after isolated limb perfusion. *Br J Cancer.* 2000;82(5):1000-1003.
63. Manusama ER, Stavast J, Durante NM, Marquet RL, Eggermont AM. Isolated limb perfusion with TNF alpha and melphalan in a rat osteosarcoma model: a new anti-tumour approach. *Eur J Surg Oncol.* 1996;22(2):152-157.
64. van Der Veen AH, de Wilt JH, Eggermont AM, van Tiel ST, Seynhaeve AL, ten Hagen TL. TNF-alpha augments intratumoural concentrations of doxorubicin in TNF-alpha-based isolated limb perfusion in rat sarcoma models and enhances anti-tumour effects. *Br J Cancer.* 2000;82(4):973-980.
65. Tracey KJ, Beutler B, Lowry SF, et al. Shock and tissue injury induced by recombinant human cachectin. *Science.* 1986;234(4775):470-474.

66. Spriggs DR, Sherman ML, Michie H, et al. Recombinant human tumor necrosis factor administered as a 24-hour intravenous infusion. A phase I and pharmacologic study. *J Natl Cancer Inst.* 1988;80(13):1039-1044.
67. ten Hagen TL, van Der Veen AH, Nooijen PT, van Tiel ST, Seynhaeve AL, Eggermont AM. Low-dose tumor necrosis factor- α augments antitumor activity of stealth liposomal doxorubicin (DOXIL) in soft tissue sarcoma-bearing rats. *Int J Cancer.* 2000;87(6):829-37.
68. Hoving S, Seynhaeve AL, van Tiel ST, Eggermont AM, ten Hagen TL. Addition of low-dose tumor necrosis factor- α to systemic treatment with Stealth liposomal doxorubicin (Doxil) improved anti-tumor activity in osteosarcoma-bearing rats. *Anticancer Drugs.* 2005;16(6):667-74.
69. ten Hagen TL, Hoving S, Ambagtsheer G, van Tiel ST, Eggermont AM. Lack of efficacy of Doxil in TNF- α -based isolated limb perfusion in sarcoma-bearing rats. *Br J Cancer.* 2004;90(9):1830-1832.
70. Hoving S, van Tiel ST, Eggermont AM, ten Hagen TL. Effect of low-dose tumor necrosis factor- α in combination with STEALTH liposomal cisplatin (SPI-077) on soft-tissue- and osteosarcoma-bearing rats. *Anticancer Res.* 2005;25(2A):743-750.
71. Brouckaert P, Takahashi N, van Tiel ST, et al. Tumor necrosis factor- α augmented tumor response in B16BL6 melanoma-bearing mice treated with stealth liposomal doxorubicin (Doxil) correlates with altered Doxil pharmacokinetics. *Int J Cancer.* 2004;109(3):442-448.
72. Hoving S, Seynhaeve AL, van Tiel ST, aan de Wiel-Ambagtsheer G, Eggermont AM, ten Hagen TL. In vivo evaluation of drug delivery improvement by tumor vascular manipulation with TNF: an intravital microscopy study. Submitted.
73. Brett J, Gerlach H, Nawroth P, Steinberg S, Godman G, Stern D. Tumor necrosis factor/cachectin increases permeability of endothelial cell monolayers by a mechanism involving regulatory G proteins. *J Exp Med.* 1989;169(6):1977-1991.
74. Partridge CA, Horvath CJ, Del Vecchio PJ, Phillips PG, Malik AB. Influence of extracellular matrix in tumor necrosis factor-induced increase in endothelial permeability. *Am J Physiol.* 1992;263(6 Pt 1):L627-L633.
75. Suzuki S, Ohta S, Takashio K, Nitana H, Hashimoto Y. Augmentation for intratumoral accumulation and anti-tumor activity of liposome-encapsulated adriamycin by tumor necrosis factor- α in mice. *Int J Cancer.* 1990;46(6):1095-1100.
76. Folli S, Pelegrin A, Chalandon Y, et al. Tumor-necrosis factor can enhance radio-antibody uptake in human colon carcinoma xenografts by increasing vascular permeability. *Int J Cancer.* 1993;53(5):829-836.
77. Curnis F, Sacchi A, Corti A. Improving chemotherapeutic drug penetration in tumors by vascular targeting and barrier alteration. *J Clin Invest.* 2002;110(4):475-482.
78. Kristensen CA, Nozue M, Boucher Y, Jain RK. Reduction of interstitial fluid pressure after TNF- α treatment of three human melanoma xenografts. *Br J Cancer.* 1996;74(4):533-6.
79. Salnikov AV, Iversen VV, Koisti M, et al. Lowering of tumor interstitial fluid pressure specifically augments efficacy of chemotherapy. *Faseb J.* 2003;17(12):1756-1758.
80. Yuan F, Dellian M, Fukumura D, et al. Vascular permeability in a human tumor xenograft: molecular size dependence and cutoff size. *Cancer Res.* 1995;55(17):3752-3756.
81. Hoving S, Seynhaeve AL, van Tiel ST, aan de Wiel-Ambagtsheer G, Eggermont AM, ten Hagen TL. Intrinsic and TNF-induced vascular hyperpermeability of B16BL6 melanoma versus Lewis lung carcinoma determines tumor response. Submitted.
82. Hoang BH, Dyke JP, Koutcher JA, et al. VEGF expression in osteosarcoma correlates with vascular permeability by dynamic MRI. *Clin Orthop Relat Res.* 2004;(426):32-38.
83. Gasparini G. Prognostic value of vascular endothelial growth factor in breast cancer. *Oncologist.* 2000;5 Suppl 1:37-44.:37-44.
84. Salven P, Ruotsalainen T, Mattson K, Joensuu H. High pre-treatment serum level of vascular endothelial growth factor (VEGF) is associated with poor outcome in small-cell lung cancer. *Int J Cancer.* 1998;79(2):144-146.
85. Parr MJ, Masin D, Cullis PR, Bally MB. Accumulation of liposomal lipid and encapsulated doxorubicin in murine Lewis lung carcinoma: the lack of beneficial effects by coating liposomes with poly(ethylene glycol). *J Pharmacol Exp Ther.* 1997;280(3):1319-1327.
86. Weissig V, Whiteman KR, Torchilin VP. Accumulation of protein-loaded long-circulating micelles and liposomes in subcutaneous Lewis lung carcinoma in mice. *Pharm Res.* 1998;15(10):1552-1556.

Chapter 13

Summary and conclusions

Samenvatting en conclusies

Summary

Adequate drug uptake at the tumor site remains a crucial problem in solid tumor therapy. Physiological barriers hinder the effective delivery of drugs to tumors and are frequently responsible for failure of initially promising agents. Metabolism and clearance of drugs in the body result in low drug concentrations at the tumor site and heterogeneous tumor perfusion and increased interstitial fluid pressure (IFP) may limit the penetration of drugs into the tumor.

Isolated limb perfusion is an important treatment option in the management of locally advanced extremity soft tissue sarcoma and in-transit melanoma metastases. The addition of TNF to the melphalan-based ILP greatly improved the response rates. Despite the good tumor responses, still about 20% of the patients do not respond to this treatment therapy. New treatment modalities are therefore of great clinical interest.

Encapsulation of anticancer agents in Stealth[®] liposomes can reduce systemic toxicity while retaining or even improving *in vivo* efficacy. In previous studies we showed that co-administration of Doxil[®] (Stealth[®] liposomal doxorubicin) and low-dose TNF resulted in enhanced tumor response in rat and murine tumor models.

The aim of this thesis was to further improve local and systemic chemotherapy by changing the pathophysiology of solid tumors in different animal models. We tried to gain more insight in the mechanism of TNF in both ILP and systemic liposomal treatment. The enhanced tumor uptake of different cytotoxic agents due to addition of TNF to ILP prompted us to investigate a number of vasoactive drugs for similar effects. In this thesis the use of IL-2 and/or histamine in melphalan-based ILP was explored.

In **chapter 1** an overview is given of the history and application of TNF, IL-2 and histamine in cancer treatment. Previous work with ILP and systemic treatment with liposomes is described and the aim of the thesis is explained.

In **chapter 2** the synergistic antitumor activity of the combination of IL-2 and melphalan in ILP in soft-tissue sarcoma-bearing rats is shown, which is without any local or systemic toxicity. IL-2 significantly enhanced melphalan uptake in tumor tissue. Although scattered extravasation of erythrocytes was detected in the IL-2 plus melphalan treated animals, no signs of tumor vascular damage were seen. Clear differences were seen in the localization of macrophages and additionally increased levels of TNF mRNA in tumor tissue were found, indicating a potentially important role for macrophages in the IL-2-based ILP. The results in this study indicate that the novel combination of IL-2 and melphalan in ILP may be an alternative for ILP with TNF and melphalan.

In **chapter 3** another vasoactive drug was tested in our preclinical soft-tissue sarcoma model. A synergistic antitumor effect was found when histamine and melphalan were combined in the ILP. In comparison with TNF and IL-2, histamine alone did cause some

tumor regression as was seen with treatment with melphalan alone. The strong effect of histamine-based ILP with melphalan was explained by direct cytotoxicity to both tumor cells and tumor-associated vasculature and an indirect effect through histamine-mediated increased melphalan concentration in the tumor. Therefore, the combination of histamine and melphalan in ILP seems to be a promising alternative to TNF and should be evaluated in the clinical setting in both limb and organ perfusions.

Based on the potential synergistic effects of IL-2 and histamine in the systemic setting, the combination of these drugs in the melphalan-based ILP was evaluated (**chapter 4**). A 30% decrease in response rate was found compared to each drug alone plus melphalan, although there was a similar melphalan accumulation in the tumor. In the different pharmacokinetic scenarios the combination of the two drugs lead to a down regulation of their action and consequently to the lost in efficacy.

Addition of high-dose TNF to melphalan-based ILP enhances anti-tumor effects impressively, but the mechanism of action of TNF is still under debate. In **chapter 5** effects of TNF on the tumor microenvironment and on secondary immunological events during and shortly after ILP in soft-tissue sarcoma-bearing rats are discussed. The TNF-induced augmentation of drug accumulation was the key explanation for the observed synergistic anti-tumor response, whereas it was too early for an immune response related to TNF to be detected. The augmented accumulation of melphalan was not due to an altered IFP, but most likely results from an increased permeability of the tumor vasculature.

In **chapter 6** the use of Doxil[®] in the ILP setting was explored. Doxil[®] had minimal antitumor activity, its activity was not enhanced by the addition of TNF and drug accumulation in tumor tissue was low. The application of Doxil[®] in an isolated setting is not a useful alternative for doxorubicin or melphalan.

In **chapter 7** the effects of systemic treatment with low-dose TNF in combination with liposomal cisplatin (SPI-077) in soft-tissue or osteosarcoma-bearing rats are reported. Depending on the type of tumor, the addition of TNF to SPI-077 resulted in a better tumor growth delay with a prolonged antitumor effect and in combination with the reduced toxicity of SPI-077, this combination may be preferable to cisplatin.

The efficacy of Doxil[®] in combination with low-dose TNF in the intermediate vascularized osteosarcoma ROS-1 is reported in **chapter 8**. Not only in highly vascularized tumors TNF enhanced the systemic Doxil[®] treatment, but also in less vascularized tumors, although no increased drug uptake was found. Presumably the improved response when TNF was added resulted from a direct activity of this cytokine on the ROS-1 cells.

Drug delivery and distribution in the B16BL6 mouse melanoma is studied in **chapter 9** by intravital microscopy. A more homogeneous tumor distribution and increased extravasation of liposomes along tumor vessels was found when liposomal therapy was combined with

low-dose TNF, which is crucial for an optimal tumor response. The results indicated that more tumor vessels become more permeable by TNF.

Whilst addition of TNF to systemic treatment with Doxil[®] enhanced drug accumulation and strongly improved the anti-tumor response in the B16BL6 model, no such effect was observed in the LLC model (**chapter 10**). B16BL6 tumor appeared less vascularized than the LLC, but the tumor vessels were larger, while local VEGF levels were comparable in both tumor types. The results of this study suggest that not the tumor microvessel density but the tumor vascular permeability, and response to TNF, may be the limiting factor involved in liposomal drug delivery.

The purpose of **chapter 11** is to review existing ILP treatment modalities and recent advances for development of novel therapeutic strategies using vasoactive drugs.

Chapter 12 is an overview of the use of liposomes in cancer treatment. Different ways of site-specific targeting to tumors are described.

Conclusions

- ILP with IL-2 in combination with melphalan results in synergistic antitumor activity.
- Addition of histamine to melphalan-based ILP improves the tumor response dramatically.
- Combination of IL-2 and histamine leads to diminished efficacy in melphalan-based ILP.
- TNF-induced augmented drug uptake in ILP is the key explanation for the observed anti-tumor response.
- Application of Doxil[®] in ILP is not a useful alternative for doxorubicin.
- Encapsulation of cisplatin results in reduced toxicity and in combination with TNF may be preferable to free cisplatin.
- TNF not only improves systemic Doxil[®] treatment in highly vascularized tumors, but also in intermediate vascularized tumors.
- Increased number of tumor vessels become more permeable by TNF.
- Tumor vascular permeability and not microvessel density is the limiting factor for liposomal drug delivery.

Samenvatting

Een van de essentiële problemen bij de behandeling van solide tumoren is een onvoldoende opname van chemotherapeutica in het tumorweefsel. Fysiologische barrières verhinderen de effectieve opname van geneesmiddelen in de tumor en zijn dikwijls verantwoordelijk voor het falen van oorspronkelijk veelbelovende therapieën. Metabolisme en eliminatie van chemotherapeutica zorgen voor een lage concentratie van de chemotherapeutica in het tumorweefsel. Door de heterogene perfusie en de verhoogde interstitiële vloeistof druk (IFP) in de tumor penetreren chemotherapeutica niet ver in het tumorweefsel.

Geïsoleerde extremitetsperfusie (ILP) is een belangrijke klinische toepassing bij de behandeling van lokaal vergevorderde weke delen sarcomen en in transit melanoma metastasen. Toevoeging van tumor necrose factor- α (TNF) aan ILP met melfalan resulteert in een sterk verbeterde tumor respons. Ondanks de goede tumor respons, reageert 20% van de patiënten niet op deze behandelingsmethode en nieuwe therapieën zijn daarom van groot klinisch belang.

Inkapseling van chemotherapeutica in Stealth[®] liposomen kan leiden tot een verminderde systemische toxiciteit terwijl de *in vivo* werkzaamheid van het geneesmiddel gelijk blijft of zelfs verbetert. In eerdere studies hebben wij laten zien dat de combinatie therapie van Doxil[®] (Stealth[®] liposomaal doxorubicine) en een lage dosis TNF leidt tot een verbeterde tumor response in rat en muis tumor modellen.

Onderzoek beschreven in dit proefschrift is gericht op de verbetering van lokale en systemische chemotherapieën door middel van verandering van de pathofysiologie van solide tumoren. Dit werd onderzocht in verschillende dier modellen. We hebben geprobeerd een beter inzicht te krijgen in het mechanisme van TNF in zowel ILP als systemische liposomale behandeling. De verhoogde opname van chemotherapeutica in tumorweefsel door toevoeging van TNF heeft geleid tot het onderzoeken van andere vasoactieve stoffen die mogelijk een zelfde effect hebben. In dit proefschrift is het gebruik van IL-2 en/of histamine in geïsoleerde extremitetsperfusies met melfalan getest.

Hoofdstuk 1 is een overzicht van de geschiedenis en het gebruik van TNF, IL-2 en histamine bij de behandeling van kanker. Eerder gepubliceerde onderzoeken over geïsoleerde extremitetsperfusies en het gebruik van liposomen bij systemische behandelingen zijn beschreven. Het doel van de in dit proefschrift beschreven studies wordt uiteengezet.

In **hoofdstuk 2** wordt beschreven dat de combinatie therapie van IL-2 en melfalan in geïsoleerde extremitetsperfusies leidde tot een synergistische antitumorale werking bij rat weke delen sarcomen, zonder dat er lokale of systemische toxiciteit optreedt. IL-2 zorgde voor een verhoogde opname van melfalan in het tumor weefsel. Verspreide uittrekking van rode bloedcellen werd waargenomen bij de dieren die zijn behandeld met de combinatie

therapie IL-2 en melfalan, maar er was geen schade zichtbaar aan de tumor vaatwand. Echter, duidelijke verschillen in de verdeling van macrofagen in het tumorweefsel werden gezien en tevens werd een verhoogde expressie van TNF mRNA in het tumorweefsel gedetecteerd. Dit zou een mogelijk belangrijke rol voor macrofagen kunnen betekenen bij de perfusie met IL-2. De resultaten van deze studie geven aan dat de nieuwe combinatie van IL-2 en melfalan in geïsoleerde perfusies een goed alternatief kan zijn voor TNF en melfalan.

In **hoofdstuk 3** is een andere vasoactieve stof getest in ons preklinisch weke delen sarcoom model. De combinatie therapie van histamine en melfalan in ILP zorgde voor een synergistische antitumor activiteit. In vergelijking met TNF en IL-2, resulteerde perfusie met histamine in tumor regressie zoals ook werd gezien met melfalan alleen. Het effect van ILP met histamine en melfalan kan worden verklaard door de directe cytotoxiciteit op zowel tumor cellen als de tumor vasculatuur en door een indirect effect, namelijk de verhoogde opname van melfalan in het tumorweefsel door histamine. De combinatie therapie van histamine en melfalan is mogelijk een goed alternatief voor TNF en zal daarom verder getest moeten worden in de klinische setting in zowel extremiteit als orgaan perfusies.

Aangezien IL-2 en histamine voor een synergistisch effect zorgen in de systemische setting, is deze combinatie getest in ILP met melfalan (**hoofdstuk 4**). Echter een afname van 30% in de tumor respons is gevonden in vergelijking met IL-2 of histamine plus melfalan. De opname van melfalan in de tumor is echter wel gelijk gebleven. Door verschillende werkingsmechanismen van de twee stoffen is een goede tumor respons verloren gegaan.

Toevoeging van hoge dosis TNF aan ILP met melfalan resulteert in een goede antitumorale werking, maar het precieze mechanisme is nog niet geheel bekend. In **hoofdstuk 5** zijn de effecten van TNF op het lokale tumor micromilieu en de secundaire immunologische gevolgen tijdens en kort na perfusie onderzocht. De door TNF geïnduceerde verhoogde melfalan opname in tumorweefsel was de belangrijkste verklaring voor de synergistische antitumor respons. Op dit tijdstip is het te vroeg om een immuun response gerelateerd aan TNF te detecteren. De verhoogde tumorale opname van melfalan is niet het gevolg van een verandering in IFP, maar hoogst waarschijnlijk door een verhoogde permeabiliteit van de tumor vasculatuur.

Hoofdstuk 6 presenteert het gebruik van Doxil[®] in de geïsoleerde extremiteitsperfusie. Doxil[®] had echter minimale antitumor activiteit en toevoeging van TNF had geen effect op de opname van doxorubicine in tumorweefsel en de antitumorale werking werd ook niet verbeterd. Het gebruik van Doxil[®] in ILP is geen goed alternatief voor doxorubicine.

De effecten van lage dosis TNF in combinatie met liposomaal cisplatin (SPI-077) in ratten met weke delen sarcomen of osteosarcomen zijn beschreven in **hoofdstuk 7**. Afhankelijk van het type tumor, zorgde de toevoeging van TNF aan SPI-077 voor een groei vertraging

van de tumor met een langdurig effect. Aangezien inkapseling van cisplatin tevens leidde tot een verminderde toxiciteit, is de combinatie van SPI-077 en TNF verkiesbaar boven cisplatin.

In eerdere studies is aangetoond dat TNF zorgt voor een verbetering van de behandeling met Doxil[®] in goed gevasculariseerde tumoren. In **hoofdstuk 8** is deze combinatie therapie getest in een minder goed gevasculariseerde rat osteosarcoom. Wederom werd een verbetering van de tumor response gevonden, alhoewel geen verhoogde opname van doxorubicine in de tumor is gedetecteerd. Vermoedelijk is de verbetering van de tumor response toe te schrijven aan een direct effect van TNF op de tumorcellen.

De opname en distributie van (liposomale) chemotherapeutica in het muis melanoom model is onderzocht met behulp van intravitaal microscopie (**hoofdstuk 9**). Wanneer liposomale therapie werd gecombineerd met een lage dosis TNF, werd een meer homogene tumor verdeling en een betere penetratie van liposomen in het tumorweefsel gevonden. De verhoogde en verbeterde opname van chemotherapeutica in de tumoren is cruciaal voor een optimale tumor response. De resultaten in deze studie laten zien dat meer bloedvaten in de tumor permeabel worden door TNF.

Terwijl toevoeging van TNF aan de systemische behandeling met Doxil[®] zorgt voor een verhoogde tumorale opname van doxorubicine en de antitumor activiteit sterk is verbeterd in het B16BL6 muis melanoom model, werden deze effecten niet waargenomen in de Lewis Long Carcinoom (LLC) (**hoofdstuk 10**). B16BL6 is een minder goed gevasculariseerde tumor dan LLC, maar de bloedvaten zijn groter en de lokale productie van VEGF is vergelijkbaar. In deze studie wordt gesuggereerd dat niet de mate van tumor vascularisatie, maar de permeabiliteit van de vasculatuur de beperkende factor is bij de opname van liposomen.

In **hoofdstuk 11** wordt een overzicht gegeven van bestaande ILP behandelmethoden en nieuwe ontwikkelingen door het gebruik van vasoactieve stoffen.

In **hoofdstuk 12** wordt het gebruik van liposomen bij de behandeling van kanker beschreven. Diverse mogelijkheden om de opname van liposomen specifiek in tumorweefsel te verbeteren worden uiteengezet.

Conclusies

- Geïsoleerde extremitetsperfusie met IL-2 en melfalan resulteert in een synergistische antitumor activiteit.
- Toevoeging van histamine aan ILP met melfalan verbetert de tumor respons drastisch.
- De combinatie van IL-2 en histamine leidt tot een verminderde antitumor activiteit van geïsoleerde extremitetsperfusies met melfalan.
- De door TNF verhoogde intratumorale concentratie van chemotherapeutica is waarschijnlijk de belangrijkste verklaring voor de anti-tumor activiteit.

- Het gebruik van Doxil[®] in geïsoleerde extremitetsperfusies is geen goed alternatief voor doxorubicine.
- Liposomale inkapseling van cisplatin resulteert in een verminderde toxiciteit en in combinatie met TNF kan dit de voorkeur geven boven cisplatin.
- TNF zorgt niet alleen voor een verbetering van de systemische Doxil[®] behandeling in goed gevasculariseerde tumoren, maar ook in minder gevasculariseerde tumoren.
- TNF zorgt voor een toename in het aantal permeabele bloedvaten in tumorweefsel.
- De permeabiliteit van het tumor vaatbed en niet de mate van vascularisatie is de beperkende factor voor opname van liposomen in tumorweefsel.

Dankwoord

Het is nu bijna vijf jaar geleden dat ik ben begonnen aan dit promotie-onderzoek, waaraan ik al die tijd met veel plezier heb gewerkt en ik ben dan ook erg blij met het eindresultaat. De studies beschreven in dit proefschrift zouden niet mogelijk zijn geweest zonder de inzet en steun van vele anderen, direct of indirect, bewust of onbewust. Graag wil ik er een aantal in het bijzonder noemen.

Allereerst Dr. T.L.M. ten Hagen, beste Timo: bedankt voor de altijd openstaande deur en de mogelijkheid om alle experimenten te doen die ik wilde doen. Tevens wil de waardering uiten dat ik dankzij jou naar veel internationale congressen ben geweest. Fantastisch hoe jij in een korte tijd een mooi lab hebt opgebouwd met zeer veel geavanceerde technieken. De eerste high impact papers zijn gepubliceerd en mogen er nog vele volgen. Nogmaals bedankt voor alle steun.

Prof. dr. A.M.M. Eggermont, beste Lex: ondanks dat je niet zo veel aanwezig was in het lab, ben ik erg blij om bij jou te promoveren. In het bijzonder heb ik goede herinneringen overgehouden aan de jaarlijkse Lab-science day: de snelheid waarbij jij de resultaten onthoudt is indrukwekkend en je enthousiasme voor de wetenschap werkt aanstekend.

Mijn dank gaat ook uit naar de leden van de leescommissie, Prof. dr. J. Verweij, Prof. dr. G. Storm en Prof. dr. B.B.R. Kroon: bedankt dat jullie bereid waren het proefschrift te beoordelen en zitting te nemen in de kleine commissie.

Prof dr. Ernst de Bruijn, Gert de Boeck en Gunther Guetens: bedankt voor de melphalan bepalingen die jullie hebben uitgevoerd.

Sandra en Gisela: jullie hebben mij de afgelopen jaren ondersteund bij het uitvoeren van de vele perfusies, window experimenten en celkweek proefjes. De tijdstippen van de dierexperimenten (12, 24, 36 en 48 uur) waren niet om jullie te pesten. Bedankt voor de hoeveelheid werk die jullie mij uit handen hebben genomen.

Verder wil ik de rest van de mensen op het lab bedanken die de dagelijkse sfeer op de werkvloer hebben bepaald. Vooral de lab-uitjes en de vrijdagmiddag borrels met frituur waren erg gezellig!

De mede-AIO's Remco, Ann, Lucy en Flavia: de literatuur besprekingen en alle andere formele en informele gesprekken zijn nuttig en vooral gezellig geweest. Jullie nog veel succes met het afronden van jullie proefschrift.

Natuurlijk wil ik de stagiaires Marien en Cindy bedanken voor de experimenten die zij voor mij hebben gedaan. Cindy: het spijt me dat je zo veel coupes moest scoren dat je er 's nachts zelfs over moest dromen.

Tevens wil ik alle vrienden bedanken die de afgelopen jaren voor de nodige afleiding hebben gezorgd in de vorm van tennissen, volleyballen en heerlijke etentjes. Marloes, bedankt dat ik jou altijd kon bellen voor een kopje thee en om samen te lunchen. Ik vind het geweldig dat je mijn paranimf wil zijn.

Beste collega's van het NKI: bedankt voor de afleiding van de afgelopen maanden. Fiona: vanaf nu kan ik mijn volledig aandacht richten op het *grote vaten project*. Ik heb er zin in! Martijn: wanneer is jouw boekje klaar?

Natuurlijk wil ik ook mijn ouders bedanken die altijd achter me hebben gestaan en belangstelling hebben getoond. Op de vraag: "Schiet het een beetje op?" Heb ik nu eindelijk een antwoord: "Ja, het is af!".

Mijn lieve zus Janneke, bedankt voor je vrolijke aanwezigheid tijdens mijn weekendjes in het noorden. Jammer dat je aan de andere kant van het land woont. Ik vind het heel erg leuk dat je mijn paranimf wil zijn.

En als laatst natuurlijk Eltjo, bedankt voor je vertrouwen, relativeringsvermogen en vooral je liefde. Zal ik vanaf nu maar weer eens gaan koken?

Saske Hoving werd op 5 mei 1977 geboren te Musselkanaal. In 1995 behaalde zij het VWO diploma aan scholengemeenschap Dr. Nassau College te Assen en begon in datzelfde jaar aan de opleiding Voeding en Gezondheid aan de Wageningen Universiteit. Haar eerste afstudeervak werd bij de leerstoelgroep Toxicologie uitgevoerd onder begeleiding van Ir. Ilonka Meerts en Prof. dr. Ir. Bram Brouwer waarbij gekeken is naar de (anti-)oestrogene werking van gebromeerde vlamvertragers. Tevens werkte zij 5 maanden als onderzoeksassistent bij dezelfde leerstoelgroep. Bij Numico Research te Wageningen deed ze haar tweede afstudeervak onder begeleiding van Dr. Irma Meijerman en Dr. Mirian Lansink waarbij onderzoek is gedaan naar *in vitro* modellen om de rol van angiogenese bij colon kanker te onderzoeken. Haar buitenlandse stage werd uitgevoerd in het Andrus Gerontology Center aan de University of Southern California, waarbij onder begeleiding van Prof. Caleb Finch gekeken is naar de effecten van hormoonvervangende therapieën op hersencellen. In september 2000 behaalde zij haar doctoraaldiploma (met lof) en begon zij haar promotieonderzoek bij de afdeling Experimentele Chirurgische Oncologie aan de Erasmus Universiteit onder begeleiding van Dr. Timo ten Hagen en Prof. dr. Lex Eggermont. Sinds juni 2005 is zij werkzaam als postdoc bij de afdeling Experimentele Therapie van het Nederlands Kanker Instituut.

List of publications

Hoving S, Seynhaeve AL, van Tiel ST, Eggermont AM, ten Hagen TL. Addition of low-dose tumor necrosis factor-alpha to systemic treatment with STEALTH liposomal doxorubicin (Doxil) improved anti-tumor activity in osteosarcoma-bearing rats. *Anticancer Drugs*. 2005;16(6):667-74.

Hoving S, Brunstein F, aan de Wiel-Ambagtsheer G, van Tiel ST, de Boeck G, de Bruijn EA, Eggermont AM, ten Hagen TL. Synergistic antitumor response of IL-2 with melphalan in isolated limb perfusion in soft-tissue sarcoma bearing rats. *Cancer Res*. 2005;65(10):4300-8.

Hoving S, van Tiel ST, Eggermont AM, ten Hagen TL. Effect of low-dose tumor necrosis factor-alpha in combination with STEALTH liposomal cisplatin (SPI-077) on soft-tissue- and osteosarcoma-bearing rats. *Anticancer Res*. 2005;25(2A):743-50.

Brunstein F, **Hoving S**, Seynhaeve AL, van Tiel ST, Guetens G, de Bruijn EA, Eggermont AM, ten Hagen TL. Synergistic antitumor activity of histamine plus melphalan in isolated limb perfusion: preclinical studies. *J Natl Cancer Inst*. 2004;96(21):1603-10.

ten Hagen TL, **Hoving S**, Ambagtsheer G, van Tiel ST, Eggermont AM. Lack of efficacy of Doxil in TNF-alpha-based isolated limb perfusion in sarcoma-bearing rats. *Br J Cancer*. 2004;90(9):1830-2.

Other publications

Meerts IA, Lilienthal H, **Hoving S**, van den Berg JH, Weijers BM, Bergman A, Koeman JH, Brouwer A. Developmental Exposure to 4-Hydroxy-2,3,3',4',5-Pentachlorobiphenyl (4-OH-CB107): Long Term Effects on Brain Development, Behavior and Brain Stem Auditory Evoked Potentials in Rats. *Toxicol Sci*. 2004; 82(1):207-18.

Meerts IA, **Hoving S**, Van Den Berg JH, Weijers BM, Swarts HJ, van der Beek EM, Bergman A, Koeman JH, Brouwer A. Effects of in Utero Exposure to 4-Hydroxy-2,3,3',4',5-Pentachlorobiphenyl (4-OH-CB107) on Developmental Landmarks, Steroid Hormone Levels and Female Estrous Cyclicity in Rats. *Toxicol Sci*. 2004;82(1):259-67.

Rozovsky I, **Hoving S**, Anderson CP, O'Callaghan J, Finch CE. Equine estrogens induce apolipoprotein E and glial fibrillary acidic protein in mixed glial cultures. *Neurosci Lett*. 2002;323(3):191-4.

Meerts IA, Letcher RJ, **Hoving S**, Marsh G, Bergman A, Lemmen JG, van der Burg B, Brouwer A. In vitro estrogenicity of polybrominated diphenyl ethers, hydroxylated PDBEs, and polybrominated bisphenol A compounds. *Environ Health Perspect.* 2001;109(4):399-407.

Abstracts

Hoving S, van Tiel ST, Seynhaeve AL, aan de Wiel-Ambagtsheer G, Eggermont AM, ten Hagen TL. The role of TNF in changing pathophysiology of solid tumors that leads to enhanced uptake of Stealth liposomal chemotherapeutics. 8th Liposome Research Days Conference: "Beyond The Impossible" 21 -24 May 2002, Berlin, Germany.

Hoving S, aan de Wiel-Ambagtsheer G, van Tiel ST, Eggermont AM, ten Hagen TL. Lack of efficacy of Doxil[®] in TNF-alpha-based isolated limb perfusion in sarcoma-bearing rats. Sixth International Conference, Liposome Advances, Progress in Drug and Vaccine Delivery, 15-19 December 2003, London.

Hoving S, aan de Wiel-Ambagtsheer G, Eggermont AM, ten Hagen TL. Tumorinfiltration of macrophages, CD4 and CD8 cells after TNF-alpha-based isolated limb perfusion in a rat model. AACR, 95th Annual Meeting, 27 - 31 March 2004, Orlando, USA.

Hoving S, van Tiel ST, aan de Wiel-Ambagtsheer G, Seynhaeve AL, Eggermont AM, ten Hagen TL. Modulation of tumor permissiveness for liposomal formulation by Tumor Necrosis Factor alpha. 10th International TNF Superfamily Conference, 29 September - 2 October 2004, Lausanne, Switzerland.

Hoving S, van Tiel ST, aan de Wiel-Ambagtsheer G, Eggermont AM, ten Hagen TL. Manipulation of tumor vasculature with tumor necrosis factor- improves local and systemic treatment of solid tumors with anticancer agents. 15th Endothelial Cell Research Symposium 2004, 23 November 2004, Maastricht.

Hoving S, Brunstein F, van Tiel ST, aan de Wiel-Ambagtsheer G, Eggermont AM, ten Hagen TL. IL-2 and histamine as possible alternatives for TNF-alpha in isolated limb perfusion. 9th Molecular Medicine Day, 9 February 2005, Rotterdam, the Netherlands.

Abbreviations

BN	Brown Norway
BSA	Bovine serum albumin
CD	Cluster of Differentiation (as in CD4)
cDNA	Complementary deoxyribonucleic acid
CR	Complete response
EPR	Enhanced permeability and retention system
FCS	Fetal calf serum
FITC	Fluorescein isothiocyanate
Hi	Histamine
HUVEC	Human umbilical vein endothelial cells
IFN	Interferon
IFP	Interstitial fluid pressure
IL	Interleukin (as in Il-2)
ILP	Isolated limb perfusion
LLC	Lewis lung carcinoma
LPS	Lipopolysaccharide
MCP	Monocyte chemotactic protein
MIP	Macrophage inflammatory protein
MPS	Mononuclear phagocytic system
mRNA	Messenger ribonucleic acid
MTT	3-(4,5-dimethylthiazol-2-yl)-2,5-diphenyltetrazolium bromide
NC	No change
PBS	Phosphate buffered saline
PD	Progressive disease
PEG	Polyethylene glycol
PMN	Polymorphonuclear leukocytes
PR	Partial response
ROS	Reactive oxygen species
ROS-1	Rat osteosarcoma-1
RT-PCR	Reverse transcriptase-polymerase chain reaction
SD	Standard deviation
SEM	Standard error of the mean
SRB	Sulphorhodamine-B
TGF	Transforming growth factor
TNF	Tumor Necrosis Factor- α
VEGF	Vascular endothelial growth factor

